TESIS DE LA UNIVERSIDAD DE ZARAGOZA

2024

400

David Rupérez Cebolla

On the road to sustainability: food safety of biobased packaging materials and new active packaging solutions

Director/es

Almeida E Silva, Filomena Augusta

Nerín De La Puerta, María Consolación Cristina

ISSN 2254-7606

Prensas de la Universidad Universidad Zaragoza

Universidad de Zaragoza
Servicio de Publicaciones

ISSN 2254-7606

Universidad Zaragoza
1542

Tesis Doctoral

ON THE ROAD TO SUSTAINABILITY: FOOD SAFETY OF BIOBASED PACKAGING MATERIALS AND NEW ACTIVE PACKAGING SOLUTIONS

Autor

David Rupérez Cebolla

Director/es

Almeida E Silva, Filomena Augusta
Nerín De La Puerta, María Consolación Cristina

UNIVERSIDAD DE ZARAGOZA
Escuela de Doctorado

Programa de Doctorado en Ciencia Analítica en Química

2024

Universidad Zaragoza
1542

Instituto Universitario de Investigación de Ingeniería de Aragón
Universidad Zaragoza

Tesis Doctoral

On the road to sustainability: food safety of bio-based packaging materials and new active packaging solutions

David Rupérez Cebolla

Directoras:

Cristina Nerín de la Puerta

Filomena Augusta Almeida e Silva

2024

GOBIERNO DE ESPAÑA
MINISTERIO DE CIENCIA E INNOVACIÓN

AGENCIA ESTATAL DE INVESTIGACIÓN

Esta tesis ha sido financiada gracias a una ayuda del Fondo Social Europeo para contratos predoctorales para la formación de Doctores (PRE2019-088628) del Ministerio de Ciencia e Innovación.

Y por el proyecto LMP49_18 “Envases activos para mejorar la seguridad alimentaria utilizando nanomateriales bifuncionales antimicrobianos y antioxidantes” del Gobierno de Aragón y financiado por el Fondo Europeo de Desarrollo Regional (FEDER) de la Unión Europea.

La **Dra. Cristina Nerín de La Puerta**, catedrática emérita del Departamento de Química Analítica de la Universidad de Zaragoza y la **Dra. Filomena Almeida e Silva**, investigadora sénior de la Fundación Agencia Aragonesa para la Investigación y Desarrollo (ARAID) en la Facultad de Veterinaria e Instituto de Investigación en Ingeniería de Aragón de la Universidad de Zaragoza,

CERTIFICAN:

Que la presente Memoria, titulada: **"On the road to sustainability: food safety of bio-based packaging materials and new active packaging solutions"** presentada por **D. David Rupérez Cebolla** para optar al grado de Doctor con Mención Internacional, ha sido realizada bajo nuestra codirección en el Instituto de Investigación en Ingeniería de Aragón y el departamento de Química Analítica de la Universidad de Zaragoza. Por tanto, autorizamos su presentación para proseguir con los trámites oportunos y proceder a su calificación por el tribunal correspondiente.

En Zaragoza, a 26 de abril de 2024,

Dra. Cristina Nerín de la Puerta

Dra. Filomena Augusta Almeida e Silva

During this PhD thesis, a series of contributions have been made, as author or co-author, towards the following publications:

Title: Mechanochemically Scaled-Up Alpha Cyclodextrin Nanosponges: Their Safety and Effectiveness as Ethylene Scavenger

Authors: David Rupérez, Nicolás Gracia-Vallés, Eva Clavero, Filomena Silva, Cristina Nerín

Status: Published in *Nanomaterials* (Basel). 2022 Aug 23;12(17):2900. doi: 10.3390/nano12172900.

Title: Controlling beef microbial spoilage with diacetyl-based active packaging sachet

Authors: David Rupérez, Cristina Nerín, Filomena Silva

Status: Submitted to *Food Packaging and Shelf Life*, under review.

Title: Synthesis and quantification of oligoesters migrating from starch-based food packaging materials

Authors: David Rupérez, Matthieu Rivière, Jacques Lebreton, Margarita Aznar, Filomena Silva, Arnaud Tessier, Ronan Cariou, Cristina Nerín

Status: Draft prepared, to be submitted to *Journal of Hazardous Materials*

Title: Synthesis, biodegradation, and application of starch-based nanosponges in hard water treatment

Authors: David Rupérez, Eduardo Fioravanti, Danielle dalla Pria, Filomena Silva, Cristina Nerín, Francesco Trotta, Adrián Matencio

Status: Draft in preparation

Moreover, the work herein developed has been presented, as poster or oral presentations, in a range of scientific conferences:

Title: Nanomateriales y seguridad alimentaria

Authors: David Rupérez, Héctor Soria

Format: Oral presentation

Event: 'Nuevos conceptos y riesgos emergentes en restauración colectiva' Antequera, Spain, March 2021.

Title: Innovative eco-friendly active packaging approach for ethylene removal

Authors: David Rupérez, Nicolás Gracia-Vallés, Filomena Silva, Cristina Nerín

Format: Oral presentation

Event: '3rd International Congress Advances in the Packaging Industry: Sustainability, product and processes', online, November 2021.

Title: Innovative, eco-friendly, biodegradable and non-toxic: an active packaging based on cyclodextrin nanosponges for ethylene removal

Authors: David Rupérez, Nicolás Gracia-Vallés, Filomena Silva, Cristina Nerín

Format: Oral presentation

Event: 'Total Food 2022: maximizing value from the food chain' Nottingham, United Kingdom, July 2022.

Title: Synthesis, Biodegradation and Application of Biopolymers Derived from Starch in the Treatment of Hard Water

Authors: Adrián Matencio, Edoardo Fioravanti, **David Rupérez**, Filomena Silva, Danielle dalla Pria, Francesco Trotta

Format: E-poster

Event: 'Materials Science and Manufacturing' Istanbul, Turkey, November 2023.

Title: Exploring starch-derived biopolymers: synthesis, biodegradation and applications in hard water treatment

Authors: Adrián Matencio, Edoardo Fioravanti, **David Rupérez**, Filomena Silva, Danielle dalla Pria, Francesco Trotta

Format: Poster

Event: 'Simposio de investigación en ciencias experimentales de la Universidad de Almería' Almería, Spain, November 2023.

Title: Risk assessment of plastic breastmilk bags. Evaluation of non-volatile migrants.

Authors: Margarita Aznar, **David Rupérez**, María López, Cristina Nerín

Format: Poster

Event: '41th International Conference on Environmental & Food Monitoring' in Amsterdam, The Netherlands, November 2023.

Title: Control of microbial spoilage of fresh beef meat with a diacetyl-based active packaging sachet

Authors: David Rupérez, Cristina Nerín, Filomena Silva

Format: Oral presentation

Event: '11th Shelf Life International Meeting'Reggio Emilia, Italy, May 2024.

Title: Synthesis, identification, and quantification of non-volatile migrant oligoesters from starch-based food packaging materials

Authors: David Rupérez, Matthieu Rivière, Jacques Lebreton, Margarita Aznar, Filomena Silva, Arnaud Tessier, Ronan Cariou, Cristina Nerín

Format: Oral presentation / Poster

Event: 'XXIV Reunión de la Sociedad Española de Química Analítica', Zaragoza, Spain, July 2024.

Agradecimientos

Caminante, son tus huellas el camino y nada más;

caminante, no hay camino, se hace camino al andar.

Al andar, se hace camino, y al volver la vista atrás,

se ve la senda que nunca se ha de volver a pisar.

Caminante, no hay camino, sino estelas en la mar.

Antonio Machado (1875-1939)

'Proverbios y cantares', *Campos de Castilla*, 1912

Y es que de caminos va la cosa, pues este camino que ha sido la tesis ha estado lleno de huellas. Huellas más anchas, más pequeñas, más profundas, más firmes, pero huellas al fin y al cabo. Por eso, las primeras líneas de este trabajo van dedicadas a todas aquellas personas que en algún momento han recorrido el camino a mi lado.

En primer lugar, a mis directoras, Cristina y Filomena. Si vuestras personalidades fueran la base de un cóctel, saldría una bebida con marcadas notas de esfuerzo y trabajo, determinación, valentía y, sobre todo, mucho carácter. Os agradezco enormemente que rescatarais a este expatriado de Reino Unido y le acogierais en el grupo GUIA. Cristina, gracias por siempre estar. Siempre he sentido que podía entrar a tu despacho a pedirte consejo, y siempre has estado dispuesta a ayudar en todo lo que he necesitado. Gracias. Filomena, no sé por dónde empezar. Según nuestras conversaciones de WhatsApp, nos hemos dado las gracias 259 veces. Has sido para mí jefa, madre, compañera, y amiga. Jefa por tener la capacidad de llamarme siempre cuando estoy en el baño, madre por la paciencia infinita que nos

hemos tenido, compañera por siempre ofrecerte a echarme una mano en el trabajo cuando lo he necesitado, y amiga, por razones evidentes.

En segundo lugar, al resto del grupo GUIA. Me habéis hecho sentir en casa tanto en micro como en químicas. Espero no haberos distraído mucho con mis tonterías y mis capazos. Por mi parte, agradeceros el haber encontrado siempre en vosotros una sonrisa y compartiros que sin duda habéis hecho que estos cuatro años hayan sido una experiencia inolvidable.

A mi compi de despacho Pilar, que me debe una merienda en Escatrón. Me ha dado vida sentarme enfrente tuyo, me has hecho reír muchísimo (bah!). Tus historias, miradas, y las situaciones por las que hemos pasado no las cambio por nada. Siento que hemos compartido mucho más que trabajo, y eso ya sabes que me llena. A mi otra recién incorporada compi de despacho, Silvia. Posiblemente la más sensiblona de todas, pero una amiga con la que bromear y a la que pedir ayuda (o un refrán), pues si está en su mano te la va a dar. Nuestras risas y miradas cómplices lo dicen todo.

Seguimos con las de arriba, Paula y Elena, dos currantas y luchadoras siempre dispuestas a echar una mano y con las que no me he podido reír más. Os merecéis lo mejor y os agradezco el haber sido un ejemplo de dedicación por el trabajo bien hecho. Paula, queda pendiente una borrachera por Ayerbe, y te adelanto cómo terminará la noche: yo cantando jotas y tú bailándolas.

A Marga, CEO fundadora de Uber Chemicals y una gran anfitriona en Ciencias. Gracias infinitas por haberme ayudado siempre que has podido y por haber contado conmigo para nuevos proyectos. Al fin y al cabo, esa co-dirección de TFG nos unió mucho. A Celia, la estilosa navarrosoriana afincada en Zaragoza, gracias por esas infinitas conversaciones. Ah, y por el chorizo.

A Raquel, gracias por haberme ayudado tanto en mis periplos por microbiología, respondiendo a mis múltiples preguntas con tanta paciencia. Has sido un ejemplo de dedicación y saber hacer. También a Marinelly y especialmente a Sandy, la morrita del laboratorio que donde la manden, allá está.

A mis Filomenos y químicos renegados, Laura y Nico. Hemos vivido una extraña mezcla de buenos y malos momentos durante la tesis. Nico, fue una grata sorpresa encontrarme con una cara conocida (detrás de una mascarilla) al empezar. Múltiples litros de cerveza han bajado por nuestras gargantas desde entonces, e incluso te has mudado *intramuros*. Gracias por tomarte tu trabajo como doctorando senior tan en serio. Los dos lo teníamos claro, ante la imposibilidad de conseguir título nobiliario, habríamos de conformarnos con el de Doctor. Laura, gracias por ser un ejemplo de lucha y tesón, y por siempre ayudarme en micro cuando lo he necesitado. Poco a poco, tu horizonte se despeja, así que acelera, que seguro que el coche responde.

A mis nuevos doctorandos Carlos y Estela. Me quedo muy tranquilo pues la sangre nueva es buena. Carlos, ten fe: vales mucho y vas a ser un Doctor de los pies a la cabeza. Que la calidad siempre te acompañe. Estela, incluso siendo kapoper, menuda suerte hemos tenido, vas a brillar mucho, y sé que vas a acoger a todo el mundo maravillosamente, aunque sea para que te acompañen a por bubble tea.

A los demás integrantes del grupo GUIA que en algún momento han compartido unas risas conmigo: Magda, Jesús, Carlos, Berta y Araceli. También a todos aquellos que han pasado por aquí dejando su huella: Jorge, Suki, Leonardo, Leticia, Lidia, Robert, Phanwippa, Nils, Adrián, Alejandro, María, Andrei, César, María, Javi, Azem, Luis, Mario, y los que me dejo.

Este trabajo no hubiera sido el mismo sin la oportunidad de realizar una estancia de investigación en Nantes. Hubo momentos duros, pero la vida me regaló grandes personas en el destino, à commencer par mes responsables du séjour, Ronan et Arnaud. Merci beaucoup de m'avoir donné cette opportunité, et de vous soucier de moi à tout moment. Vous êtes de grands professionnels à admirer. Surtout, merçi à mon pote Matthieu, qui, en plus d'avoir une patience infinie avec moi, a pris la peine de m'apprendre non seulement la synthèse, mais aussi l'argot. Merçi aussi à Jacques, Monique, Muriel, Mathilde, Margaux, Luca, Vincent, Lawrence, Kevin, Debora, Lars et Julie.

Francia no está mal, pero mejora si te encuentras con hispanohablantes. En ese aspecto, mis señoras, Dimitri y Magda, fueron una luz en el campus. Me acogieron desinteresadamente, sabiendo que yo pronto partiría, y su alegría, abrazos, planes, borracheras, cafés y descansos fueron un pilar fundamental y por eso, siempre estaré en deuda con ellos. También a mi pareja de valencianos, Jordi y Judith, que como si de su hijo se tratara, cuidaron de mí y evitaron que estuviera solo, llevándome de excursión y parando cuando sentía una urgencia inexplicable de comprar brioche en medio de La Vendée.

Si nos remontamos en el camino, hay que empezar por los de siempre: Guille, Amelia, Tania, Marina y Paricio. Y es que siempre han estado, y por lo que a mí respecta, estarán. No hay nada que me haga más feliz que seguir compartiendo nuestros éxitos y viéndonos crecer. Os quiero muchísimo.

No me olvido de mis tenores Ignacio, Alex y Jorge. Cuatro adolescentes que coincidieron en unos campus científicos de verano y que en vez de planear botellones organizaban escapadas para ver el convento de las Carmelitas Descalzas. Estoy muy orgulloso y agradecido de que podamos seguir manteniendo nuestra amistad. Cada uno a vuestra manera me inspiráis mucho.

A mis grandes amigos de la carrera; Raquel, Miriam, Arturo, Pablo y Héctor. Cada vez nos vemos menos, pero aunque nos falte la física, la química prevalece. Con vosotros he compartido momentos increíbles que nos arrancan risas cada vez que nos vemos. De todos, no podía perder la oportunidad de dedicarle a Héctor unas palabras. Has sido desde el primer momento un amigo, y te has convertido poco a poco en una inspiración como científico y persona. Nada me hacía más feliz al volver de Londres que encontrarme contigo por los pasillos. Junto con Maria, espero que no nos faltéis y seguir contando con vosotros muchos años.

Dicen que un amigo es aquel que está en las buenas y en las malas, y mis amigos del pueblo lo han sido. Muchas gracias Dani, Sergio, Diego, Antonio, Javi, Leire y David por haber sido un refugio en lo que últimamente ha sido para mí tierra hostil.

Nos quedan muchos años de torreznos, casillo, caballo y castillo bajo las estrellas de Pinares.

Durante mi paso por Londres tuve la suerte de coincidir con brillantes científicas que fueron las que realmente me inspiraron a hacer el doctorado, Milena y Kate. Nada me dolió más que rechazar esa oferta del King's College y hacer un giro en el camino. A mis bitches, Luise, Lucia and Christelle, we shall rule the world in due time. Gracias por cuidarme tanto durante esa pandemia en el exilio, con Bushy park como testigo. También a Josh y Rhian, dos amigos que surgieron sin querer, y formaron parte de la London experience.

Afecto, comprensión, compromiso, responsabilidad, comunicación y tolerancia son las características que definen a una familia, y la mía las tienen todas. Que existan lazos de sangre es algo más que secundario. A mi padrino Isidro, que con su marcado carácter siempre me ha enseñado que la familia es lo primero. A mi tío Nacho, el otro químico de la familia, por servirme de inspiración. A Gloria, por ser otra madre. Podría seguir uno por uno, pero esto no terminaría nunca, y ya sabéis lo importantes que sois para mí. Montse, Víctor, Alba, Consuelo, Felisa, Alicia, Marcial, Angelita, Diego, Rosa, Jose Antonio, Jose, Marisa, Enrique, y Laura; gracias.

Durante estos años de tesis también me ha aumentado la familia (legalmente hablando). Tengo la inmensa suerte de haber sido acogido en una familia increíble, a la que lo único que se les puede echar en cara es lo que les cuesta despedirse cada vez que nos juntamos. A Susana y a Juan Carlos, gracias por apoyarnos siempre, y por darme ese cariño de padres desde el principio. A Alberto, casi un hermano, el verte crecer y alcanzar la felicidad me llena de alegría; te quiero muchísimo. Al resto de talegueros, Pili, Espe, Sandra, Jose, Adriana, Natalia, Iñi, Santi, por no haberme metido al pilón nunca, también en el sentido figurado de la palabra. También a los Gracia, en especial a Pili, David, Joaquín y Ángela, por ese cariño y abrazos que siempre me han dado.

De mis abuelos podría escribir otra tesis. No puedo concebir vuestros nombres sin la palabra abuelo o abuela delante. Eso sí que es un título y no el de Doctor. A mi

abuela Vitor, que se ha ido durante esta tesis, gracias por decirme siempre que sí. A mi abuela Mari Luz, que está sin estar, y a la que más echo de menos, ojalá pudieras haber compartido mucho más conmigo, tu 'nieto querido'. A mi abuelo Manuel, ejemplo y referencia de padre, abuelo y marido. Los límites de tu sabiduría solo se superan por los de tu amor. Aun siendo un hombre sencillo, de campo, siempre lo has tenido claro; 'tú estudia, que más vale un duro en estudios que cinco en trabajo'.

A mis padres, que me lo han dado todo y nunca han reparado en mi formación, esta tesis también es vuestra. Papá, tus formas siempre han sido muy sutiles; 'si no estudias, siempre te quedará el huerto', pero supongo que han funcionado. Espero que estés tan orgulloso de mí como yo lo estoy de ti. Mamá, mi hada madrina, la relación que tenemos no la cambio por nada. Gracias por tu paciencia, por aguantar mi genio, por sentarte conmigo a hacer los deberes y por enseñarme el amor por la ciencia y las matemáticas. Nos quedan muchas borracheras, lloros, y fiestas juntos. Papá, mamá; os quiero.

Pocas personas en mi vida han ocupado tanto mis pensamientos como la bebé, mi hermana María. Probablemente la persona más buena y sensible que conozco. Como hermano mayor, siempre sentí que debía ser un ejemplo a seguir para ti. Sin embargo, ahora soy yo el que aprendo de la mujer responsable, por la que por todos se preocupa, en la que te has convertido. Gracias por ser la mejor hermana que uno pueda desear.

Y por último, pero no por ello menos importante, a Alejandro. Desde aquella noche que me diste tu móvil, has ocupado y llenado mi corazón. Me has dado fuerzas para seguir el camino cuando las he necesitado, siendo a la vez bastón, refugio y hogar. Durante estos años, hemos crecido juntos y construido un hogar y una familia. Fíjate dónde estábamos hace 10 años y dónde estamos ahora. En fin, que me muero de ganas de ver dónde nos lleva la vida. A mí, siempre que sea a tu lado, no me importa.

‘La fantasía abandonada de la razón produce monstruos,

pero unida a ella es la madre de las artes’

Francisco de Goya y Lucientes

‘… y de las ciencias’

David Rupérez Cebolla

Table of contents

Abbreviations

AA: Adipic acid

ABS: Acrylonitrile butadiene styrene

ADMET: Absorption, distribution, metabolism, excretion, and toxicity

AGC: Automatic gain control

ASAP: Atmospheric solids analysis probe

ATR: Attenuated total reflectance

BCE: Before the Christian Era

BD: 1,4-Butanediol

BET: Brunauer–Emmett–Teller

BHI: Brain Heart Infusion

BSE: Bovine spongiform encephalopathy

CD: Cyclodextrin

CDI: N,N'-Carbonyl diimidazole

CE: Collision cell energy

CECT: Spanish Type Culture Collection

CFU: Colony forming units

COSY: Homonuclear correlation spectroscopy

DAD: Diode array detector

DEG: Diethylene glycol

DLS: Dynamic light scattering

EC: European Commission

EFSA: European Food Safety Authority

EG: Ethylene glycol

EO: Essential oil

ESI: Electrospray ionization

EU: European Union

EVA: Ethylene vinyl acetate

EVOH: Ethylene vinyl alcohol

FAO: Food and Agriculture Organization

FCM: Food contact material

FDA: Food and Drug Administration

FID: Flame ionization detector

FTIR: Fourier transform infrared

GC: Gas chromatography

GRAS: Generally recognized as safe

HDPE: High density polyethylene

HNP: High nitrile polymers

HPLC: High performance liquid chromatography

HRMS: High resolution mass spectrometry

HS: Headspace

HSQC: Heteronuclear single quantum coherence

IAS: Intentionally added substances

ICH: International Conference on Harmonization

iPA: Isophthalic acid

LA: Lactic acid

LD: Lethal dose

LDPE: Low density polyethylene

LOD: Limit of detection

LOQ: Limit of quantification

MAP: Modified atmosphere packaging

MHA: Mueller–Hinton agar

MHB: Mueller–Hinton broth

MIC: Minimal inhibitory concentration

MS: Mass spectrometry

NaSt: Sodium stearate

NIAS: Non-intentionally added substances

NMR: Nuclear magnetic resonance

NS: Nanosponges

PA: Polyamide

PAA: Primary aromatic amines

PBA: Poly(1,4-butylene adipate)

PBAT: Poly(butylene adipate-co-terephtalate)

PBT: Poly(butylene terephthalate)

PC: Polycarbonate

PE: Polyethylene

PEF: Poly(ethylene furanoate)

PET: Poly(ethylene terephthalate)

PG: Propylene glycol

PLA: Poly(lactic acid)

PM: Planetary mill

PP: Polypropylene

PS: Polystyrene

PTFE: Poly(tetrafluoroethylene)

PU: Polyurethane

PVA: Poly(vinyl alcohol)

PVC: Poly(vinyl chloride)

QC: Quality control

QTOF: Quadrupole time of flight

ROS: Reactive oxygen species

RSD: Relative standard deviation

SA: Sebacic acid

SB: Styrene butadiene

SD: Standard deviation

SDG: Sustainable development goal

SPME: Solid phase micro extraction

TGA: Thermogravimetric analyses

TLC: Thin layer chromatography

TMP: Trimethyl propane

TPA: Terephthalic acid

TPA: Texture profile analysis

TPS: Thermoplastic starch

TTC: Threshold of toxicological concern

UPLC: Ultra performance liquid chromatography

WHO: World Health Organization

XRD: X-ray diffraction

List of figures

List of tables

Summary

Throughout human evolution, food has been a central milestone for not only survival, but also for social cohesion and cultural identity. However, the complexity of modern food systems has posed new challenges for which society is not as prepared as it should be. For example, we have never produced as much food as today, yet a significant percentage of the population suffers from malnutrition, while thousands of tons of food are lost or wasted throughout the food chain. Moreover, ensuring food safety is a pivotal challenge for our globalized and interconnected society, as the only role that food should have is to provide enough nutrients for the population, and not to cause illnesses or, in the worst-case scenario, death. In this context, food packaging serves not only to preserve freshness and quality of products but also as barrier against contamination. At the heart of food packaging innovation lies active food packaging which, with tailored solutions to specific preservation challenges, can reduce food losses and waste and contribute towards food safety. However, decades of unsustainable plastic management and production have risen environmental alarms on the use of conventional plastic as food packaging materials, for which bio-based polymers have emerged as an eco-friendly and more sustainable alternative. Nevertheless, as consumers rightfully demand foods free from harmful substances, new packaging materials and solutions must meet the necessary standards to ensure they do not compromise food safety.

Food safety has been the main focus of this PhD work, which was tackled by the development of new active packaging solutions to target food losses and waste while, at the same time, studying and ensuring the safety of new bio-based packaging materials. This PhD thesis has explored the application of nanostructured molecules as ethylene scavengers, the antimicrobial activity of a volatile organic compound (VOC)-based active packaging solution, and the safety of new starch-based packaging materials. For the first time, the scalability by mechanochemical means of food-grade α-cyclodextrin nanosponges (α-CD-NS) and their use as ethylene scavenger has been attempted. Moreover, the application

of an active packaging solution based on diacetyl as antimicrobial VOC was explored. Finally, the migration profile and safety compliance of starch-based food packaging materials was studied.

Early ripening of fruits, vegetables, and other horticultural products affects their quality and increases susceptibility to fungal contamination. The ripening process is mainly controlled by ethylene, a phytohormone produced by fruits, vegetables, and ornamental flowers that, even at $\mu L\ L^{-1}$ concentrations, contribute towards food senescence and spoilage. Commercial solutions to control ethylene levels involve the use of potassium permanganate, an effective but toxic and difficult to discard alternative. To address this problem, the application of food-grade α-CD-NS as a greener ethylene scavenger was explored. First, a solvent-free synthesis of α-CD-NS was successfully scaled up through mechanochemical means using N,N'-carbonyldiimidazole as crosslinker, by varying the rotation frequency of a planetary ball mill. Then, the validation of a fast and sensitive HPLC-DAD method allowed to optimize a washing protocol to monitor imidazole, a toxic reaction subproduct, yielding food-grade α-CD-NS. Their absorbent capacity was evaluated through BET isotherms and ethylene absorption experiments using gas chromatography (GC) coupled to a flame ionization detector (FID). When compared to other absorbents (zeolite and bentonite), α-CD-NS showed the highest ethylene removal capacity (93 $\mu L\ h^{-1}\ kg_{adsorbent}^{-1}$), opening the doors for a greener and safer sachet-shaped ethylene removal active packaging solution.

Antimicrobial active packaging solutions are also an active food packaging category of high relevance, as pathogenic microorganisms such as *Salmonella enterica* and *Listeria monocytogenes*, commonly found in fresh meat products, continue to be responsible for serious illnesses and food safety outbreaks. The antimicrobial activity of diacetyl, an antimicrobial VOC produced by lactic acid bacteria during fermentation, was tested *in vitro* against *S. enterica* and *L. monocytogenes*. Having verified a higher diacetyl antimicrobial susceptibility in vapor phase towards *S. enterica,* this bacterium was selected as the model strain for the following experiments. Then, to entrap the volatile component, a diacetyl-based sodium stearate (NaSt) gel formulation was developed by balancing its antimicrobial and

rheological properties, as determined by texture profile analysis. The gel was also supported onto the previously developed food-grade α-CD-NS, forming a diacetyl-based α-CD-NS-NaSt composite, with view to increase its surface area and potential release. Both active materials displayed similar *in vitro* anti-*Salmonella* activity. However, diacetyl quantification by GC-FID showed that stearate gels released 1.12 ± 0.09 milligrams per gram of material while the α-CD-NS composites were able to release 2.97 ± 0.07 milligrams per gram of material, confirming that the α-CD-NS-NaSt composite displayed a superior release behavior. Next, the antimicrobial efficacy of both materials in the form of sachets was tested *in vivo* against a packaged fresh beef meat artificially inoculated with *Salmonella enterica* under refrigerated storage. The composite showed higher inhibition of *Salmonella* (77%) when compared to the gel (33%). Likewise, both materials demonstrated comparably strong inhibitory effects against common beef meat microbiota, including total viable counts, pseudomonads, and lactic acid bacteria, ranging from 93% to nearly complete (99%) inhibition.

Following the quest towards a safe and sustainable food packaging sector, bio-based polymers such as starch-based films, must comply with food safety regulations if destined to be in contact with food. Thus, the chemical risk assessment of three starch-based food packaging films was evaluated according to directive EU 10/2011. Migration experiments using three different food simulants (Tenax®, 3% *v/v* Acetic acid and 10% *v/v* Ethanol) revealed the migration of a large number of cyclic and linear oligomer combinations of adipic acid, 1,4-butanediol, propylene glycol, isophthalic acid and lactic acid monomers, among others, as determined by UPLC-MS(QTOF). Oligomers are low molecular weight molecules that can migrate from a food contact material into foodstuffs. As newly discovered compounds, they lack reference standards available for the necessary toxicological risk assessment and analytical studies. To this end, a stepwise synthesis approach was used to synthesize and isolate, for the first time, eleven cyclic and linear oligoester standard combinations using adipic acid, 1,4-butanediol, propylene glycol, and isophthalic acid monomers. This stepwise synthesis protocol allowed to obtain the desired oligoester standards with good overall yields ranging from 18 to

52 %. Then, standards were characterised by ^{1}H and ^{13}C NMR as well as UPLC-MS(Orbitrap) and demonstrated an overall purity over 98 %. Next, the synthesized standards were used to unequivocally identify the migrant oligoesters by their UPLC profile and MS/MS spectra. Finally, according to their threshold of toxicological concern concept, quantification results using the standards deemed safe only one of the three assessed bio-based polymer films.

In conclusion, this PhD thesis evaluated the ethylene removal efficacy and the antimicrobial activity of two new active packaging solutions, offering new alternatives to control food safety and food waste. Moreover, it also contributed towards the food safety of bio-based packaging materials by providing this series of synthesized oligoester standards to unequivocally identify and quantify migrant oligomers in emergent bio-based polymers.

Resumen

A lo largo de la evolución humana, la comida ha sido un eje central no solo para la supervivencia, sino también para la cohesión social y la identidad cultural. Sin embargo, la complejidad de la actual cadena alimentaria ha planteado nuevos desafíos para los cuales la sociedad no está tan preparada como debería. Por ejemplo, nunca hemos producido tanta comida, y sin embargo, un porcentaje significativo de la población sufre de desnutrición mientras que miles de toneladas de alimentos se pierden o desperdician a lo largo de la cadena alimentaria. Además, garantizar la seguridad alimentaria es un desafío crucial para la globalizada e interconectada sociedad en la que vivimos, puesto que el único papel que debería tener la comida es el de proporcionar suficientes nutrientes para la población, y no el de causar enfermedades o, en el peor de los casos, la muerte. En este contexto, el envasado de alimentos sirve no solo para preservar la frescura y la calidad de los productos, sino también como barrera contra una posible contaminación externa. En el centro de la innovación en envasado alimentario se encuentran los envases activos que, con soluciones adaptadas a desafíos específicos de conservación, pueden reducir las pérdidas y el desperdicio alimentario y contribuir así a la seguridad alimentaria. Sin embargo, décadas de insostenible gestión y producción de plásticos han hecho sonar alarmas medioambientales sobre el uso de plásticos convencionales en el envasado alimentario. Como consecuencia, los materiales biobasados se han posicionado como una alternativa más ecológica y sostenible. No obstante, a la vez que los consumidores demandan alimentos más seguros y libres de sustancias dañinas, los nuevos materiales y soluciones de envase han de cumplir también con los estándares necesarios para garantizar que no comprometan la seguridad alimentaria.

De hecho, la seguridad alimentaria ha sido el enfoque principal de esta tesis doctoral, que ha abordado el desarrollo de nuevas soluciones de envase activo para combatir las pérdidas y el desperdicio alimentario, al mismo tiempo que ha estudiado y contribuido a la seguridad de nuevos biomateriales de envase. En esta

tesis doctoral se ha explorado la aplicación de moléculas nanoestructuradas como captadores de etileno, la actividad antimicrobiana de una solución de envase activo basada en un compuesto orgánico volátil (VOC) y la seguridad de nuevos biomateriales de envase con base de almidón. Por primera vez, se ha intentado escalar por métodos mecanoquímicos la síntesis nanoesponjas de alfa-ciclodextrina (α-CD-NS) de grado alimenticio, así como su aplicación como captadores de etileno. Además, se ha explorado la aplicación de una solución de envase activo antimicrobiano basada en diacetilo como agente activo. Finalmente, se estudió el perfil de migración y el cumplimiento de la seguridad de materiales de envasado alimentario con base de almidón.

La maduración precoz de frutas, verduras y otros productos hortícolas afecta directamente a su calidad y aumenta la susceptibilidad de los mismos a la contaminación fúngica. El proceso de maduración está principalmente controlado por el etileno, una fitohormona producida por frutas, verduras y flores ornamentales que, incluso en concentraciones de μL L^{-1}, contribuye al deterioro y el desperdicio alimentario. Las soluciones comerciales existentes para controlar los niveles de etileno implican el uso de permanganato potásico, una alternativa efectiva pero tóxica y difícil de desechar. Para abordar este problema, se ha explorado la aplicación de α-CD-NS de grado alimenticio como una alternativa más ecológica de captadores de etileno. Primero, se escaló con éxito una síntesis 'verde' sin disolventes de α-CD-NS mediante métodos mecanoquímicos utilizando N,N'-carbonyldiimidazol como agente reticulante, variando la frecuencia de rotación de un molino de bolas planetario. Luego, la validación de un método HPLC-DAD rápido y sensible permitió optimizar un protocolo de lavado para monitorear el imidazol, un subproducto tóxico de la reacción, obteniendo así las α-CD-NS de grado alimenticio. Su capacidad captadora de etileno fue evaluada a través de isotermas BET y experimentos de retirada de etileno utilizando cromatografía de gases (GC) acoplada a un detector de ionización de llama (FID). En comparación con otros adsorbentes (zeolita y bentonita), las α-CD-NS mostraron mayor capacidad de eliminación de etileno (93 μL h^{-1} $kg_{adsorbente}^{-1}$), abriendo así las puertas a una solución

de envase activo para eliminación de etileno más ecológica y segura en formato de sachet.

Las soluciones de envase activo antimicrobiano son también una categoría de envase activo alimentario de alta relevancia, ya que microorganismos patógenos como *Salmonella enterica* y *Listeria monocytogenes*, comúnmente encontrados en productos cárnicos frescos, continúan siendo responsables de enfermedades y brotes de seguridad alimentaria. La actividad antimicrobiana del diacetilo, un VOC antimicrobiano producido por bacterias ácido-lácticas durante la fermentación, fue evaluada *in vitro* frente a *S. enterica* y *L. monocytogenes*. Tras comprobar una mayor susceptibilidad antimicrobiana del diacetilo en fase de vapor hacia *S. enterica*, esta bacteria fue seleccionada como especie modelo para los siguientes experimentos. Con el objetivo de retener el componente volátil, se desarrolló una formulación de gel de estearato de sodio (NaSt) basada en diacetilo, equilibrando sus propiedades antimicrobianas y reológicas. El gel también se soportó en las α-CD-NS de grado alimenticio previamente desarrolladas, formando un compuesto α-CD-NS-NaSt basado en diacetilo, con el objetivo de aumentar su área superficial y su potencial liberación. Ambos materiales activos mostraron una actividad *in vitro* similar. Sin embargo, la medición de diacetilo por GC-FID demostró que el gel de estearato liberó 1,12 ± 0,09 miligramos por gramo de material mientras que el compuesto de α-CD-NS-NaSt liberó 2,97 ± 0,07 miligramos por gramo de material, confirmando así una liberación superior del compuesto de α-CD-NS-NaSt. A continuación, se probó la eficacia antimicrobiana de ambos materiales en forma de sachets *in vivo* frente a carne envasada de ternera fresca artificialmente inoculada previamente con *Salmonella entérica,* bajo refrigeración. El compuesto de α-CD-NS-NaSt mostró una mayor inhibición de *Salmonella* (77%) en comparación con el gel (33%). De igual forma, ambos materiales demostraron similares efectos inhibitorios frente a microbiota presente en carne de ternera, como los recuentos totales, *pseudomonas* y bacterias ácido lácticas, que oscilaron entre inhibiciones del 93% y casi totales (99%).

Continuando el objetivo hacia un sector de envase alimentario seguro y sostenible, los bioplásticos como los films con base de almidón han de cumplir con las

regulaciones de seguridad alimentaria si están destinados a entrar en contacto con alimentos. Por ello, se evaluó el riesgo químico de tres films de envase de alimentario con base de almidón de acuerdo con la directiva de la UE 10/2011. Los experimentos de migración utilizando tres simulantes alimentarios diferentes (Tenax, ácido acético al 3% *v/v* y etanol al 10% *v/v*) revelaron la migración de una gran cantidad de combinaciones de oligómeros cíclicos y lineales de ácido adípico, 1,4-butanodiol, propilenglicol, ácido isoftálico y monómeros de ácido láctico, entre otros, tal y como fue determinado por UPLC-MS (QTOF). Los oligómeros son compuestos de bajo peso molecular que pueden migrar de un material a los alimentos. Como compuestos emergentes, carecen de los estándares de referencia necesarios para su evaluación toxicológica y los correspondientes estudios analíticos. Con el fin de contribuir a su disponibilidad, se utilizó un enfoque de síntesis por etapas para sintetizar y aislar, por primera vez, once combinaciones estándar es de oligoésteres cíclicos y lineales utilizando como monómeros ácido adípico, 1,4-butanodiol, propilenglicol y ácido isoftálico. Este protocolo de síntesis por etapas permitió obtener los estándares de oligoésteres deseados con buenos rendimientos generales que fueron desde el 18 al 52%. Luego, los estándares fueron caracterizados por RMN de ^{1}H y ^{13}C, así como por UPLC-MS (Orbitrap), demostrando una pureza general superior al 98%. A continuación, los estándares sintetizados se utilizaron para identificar y cuantificar inequívocamente los oligoésteres migrantes mediante su perfil de UPLC y sus espectros MS/MS. Finalmente, según el concepto de umbral de preocupación toxicológica (TTC concept), los valores de cuantificación obtenidos utilizando los estándares consideraron seguros solamente uno de los tres films de biomateriales de almidón evaluados.

En conclusión, en esta tesis doctoral se ha evaluado la eficacia de eliminación de etileno y la actividad antimicrobiana de dos nuevas soluciones de envase activo, ofreciendo nuevas alternativas para controlar la seguridad alimentaria y el desperdicio de alimentos. Además, también se ha contribuido a la seguridad alimentaria de nuevos biomateriales de envase sintetizando una serie de

estándares de oligoésteres con los que identificar y cuantificar inequívocamente los oligómeros migrantes en biomateriales emergentes.

Section I: Introduction

1. Food safety

In 1969, the Food and Agriculture Organization of the United Nations (FAO) defined food safety as the 'assurance that food will not cause adverse health effects to the consumer when prepared or eaten', establishing the first global efforts towards food hygiene (FAO, 2023a). However, the oldest known food safety regulations date back to the Babylonian Code of Hammurabi, ca. 1772 BCE. Back in the day, the code included actions related to food safety and hygiene, such as penalties for selling spoiled or adulterated food, stressing the importance of ensuring the quality and safety of food for public health and well-being (Prince, 1904).

In the interconnected global landscape we live in, food safety has become more than ever paramount due to the intricate network of food production, distribution, and consumption spanning across countries and continents. The increased complexity of the supply chains and the globalization of food trade, lead to potential hazards such as contamination, adulteration, and improper handling that can occur at any stage, posing significant risks to human health and economic stability. As the standard of living improves, it is expected that so will food security. However, despite all efforts, a recent study showed that the number of severely food insecure people has done nothing but increase from 560 to 900 million in the period from 2015 to 2023, being Asia and Africa the most affected regions (FAO, 2023b). In fact, it is estimated that 600 million people, almost 1 in 10 people in the world, will fall ill after eating contaminated food at least once in a lifetime (WHO, 2022). Moreover, unsafe food disproportionally affects vulnerable groups of people such as the elderly, infants and children with a major incidence in low- and middle-income countries (WHO, 2015). Apart of the invaluable impact on human health, the losses related to productivity, trade-related and medical care can account for as much as 110 billion US dollars per year (WHO, 2022).

Food safety incidents occur on a daily basis to varying degrees. However, historically, there have been several chemically, biologically and environmentally related food safety tragedies and challenges, that due to their impact and repercussion have remained in the collective memory (Fung et al., 2018). One of the

most notorious was the so-called Minamata disease, which happened twice, in 1956 and 1965, in Niigata Prefecture in Japan (Eto, 2000). In this disease, discharges of mercury oxide in Minamata bay and its bioconversion to methyl mercury, caused bioaccumulation of the neurotoxic compound in sea life that later appeared in the local fish and seafood food chain. As a result, over 900 people died and millions suffered from neurological problems such as sensory disturbance, narrowing of the visual field, and hearing and speech disturbances (Shimohata et al., 2015). One particularly unfortunate case of food adulteration happened in China in 2008, when infant formula was adulterated with melamine. As a result, tens of thousands of infants were hospitalised as they produced kidney stones with some resulting in renal failure (Gossner et al., 2009).

Apart from the impact on human health and the economy, foodborne outbreaks can have great social implications. For example, the so-called mad cow disease, which originated in the United Kingdom in 1996 and soon affected other neighbouring countries, threatened the future of European integration. In the outbreak, the transmission of the degenerative bovine spongiform encephalopathy (BSE) infection to humans through the ingestion of beef meat led to symptoms like those of Creutzfeldt-Jakob disease, that fatally affected the brain and spinal cord (FDA, 2020). Positively, the social concerns derived from this crisis deeply impacted regulatory harmonization and policies of a newly formed European Union (Köckerling et al., 2017).

Foodborne pathogens have also been responsible for a great number of food outbreaks. In 2011, Germany experienced a large outbreak of entero-haemorrhagic *Escherichia coli* (EHEC) considered by the World Health Organisation (WHO) as the largest in Europe at the time (Köckerling et al., 2017). Thousands of people across Europe were hospitalized due to a new *E. coli* strain, *E. coli* O104:H4 in contaminated bean sprouts which lead to widespread illness and hospitalizations. One example where globalisation played a big part on the food outbreak was the 2009 scandal associated to the Peanut Corporation of America, a major peanut product provider. As a result of the distribution of *Salmonella Typhimurium*

contaminated peanut paste, a salmonellosis outbreak quickly spread through 46 states and Canada (CDC, 2009).

Table 1. Major examples of world-wide foodborne outbreaks.

Event	Agent	Region	Effects
Minamata disease (1956 & 1965)	Methyl mercury	Japan	900 people died and 2 million suffered neurological health problems (Eto, 2000; Shimohata et al., 2015)
Melamine in infant formula (2008)	Melamine	China	6 death and 300,000 affected infants (Gossner et al., 2009)
Mad cow disease (1996)	Bovine spongiform encephalopathy (BSE)	Europe	Degenerative until fatal, 223 human victims (FDA, 2020)
E. coli outbreak (2011)	*E. coli* O104:H4	Europe	53 people died, 3,842 suffered symptoms (Yeni et al., 2016)
Peanut Corporation of America (2009)	*Salmonella Typhimurium*	United States	9 deaths and 714 infected persons (CDC, 2009)

Due to the global implications, and in addition to national food safety initiatives, the WHO has been promoting international and national cooperation by setting and addressing a food safety agenda. The first Global Food Safety Strategy was published in 2002 and aimed to safeguard public health and facilitate international trade by ensuring the safety and quality of food products worldwide, promoting comprehensive food safety systems at national and international levels (WHO, 2002). The plan was later updated in 2013 to strengthen surveillance mechanisms, risk assessment and management practices between not only governments, but also industries and international organizations, focussing on foodborne illnesses, and specially in zoonoses (WHO, 2013). The actual strategy (WHO, 2022) builds up upon the two previous initiatives to address emerging challenges and evolving food safety concerns. This strategy emphasizes a more holistic approach towards food safety, considering not only microbial but also chemical and physical hazards, as well as issues related to antimicrobial resistance and environmental sustainability.

The current WHO Global strategy for food safety underlies five major strategic priorities (WHO, 2022):

- Strategic priority 1: Strengthening national food control systems – competent authorities can establish and strengthen national food control systems by evaluating and improving key components that will contribute to reducing the burden of foodborne diseases.
- Strategic priority 2: Identifying and responding to food safety challenges resulting from global changes and food systems transformation – national governments can identify and proactively respond to global changes and transformations to food systems, as well as to the movement of foods that have the potential to impact food safety.
- Strategic priority 3: Improving the use of food chain information, scientific evidence and risk assessment in making risk management decisions – resources to strengthen national food systems are allocated through an evidence and risk-based approach.
- Strategic priority 4: Strengthening stakeholders (regulators, academia, food industry, consumers) engagement and risk communication – food safety stakeholders adapt a food safety culture and encourage the acceptance of their individual and collective responsibility for food safety.
- Strategic priority 5: Promoting food safety as an essential component in domestic, regional and international food trade – economic success of national food production in domestic, regional and international trade is promoted by national food systems which act as a safety warrant of food products.

This strategy also aligns food safety and the strategic priorities with the Sustainable Development Goals (SDGs) and the 2030 agenda (WHO, 2022). The SDGs are a call for action by 193 countries to collectively achieve 17 objectives that would promote prosperity while protecting the planet (UN General Assembly, 2015). As such, food safety is fundamental to SDG 1, 2, 3, 6, 8, 12 and 17 (Figure 1).

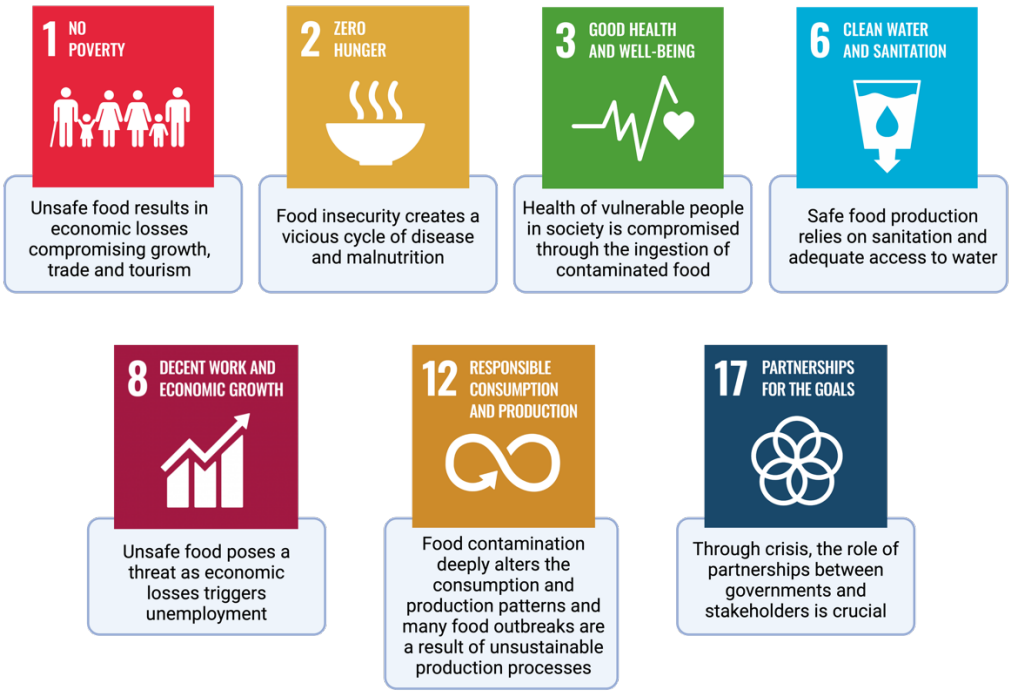

Figure 1. Aligment of food safety with the Sustainable Development Goals

2. Packaging materials and food chemical risk

2.1. Food packaging materials

Food is exposed to a series of physical, chemical, and microbiological agents during the storage, distribution, and commercialization stages. Historically, the way humans stored food remained unchanged practically until 100 years ago, when new materials and manufacturing techniques came into place (Risch, 2009). Nowadays, food packaging is an essential part of the food chain not only by providing protection, but also by helping to maintain food quality and extending food shelf-life. As such, food packaging has three primary roles (protection, utility, and communication) in three different environments: physical, atmospheric, and human. In consequence, an ideal food package should effectively serve its three functions in all three environments (Risch, 2009).

Nowadays, the number of food packages could be as big as the number of food products, as the market has adapted to cover any specific needs. As seen in figure 2, the most used materials by market share are plastics (45 %), cardboard and paper (33 %), metals (12 %) and glass (6 %) (Cameron, 2020). That been said, food packages are usually multi-layer materials instead of mono-materials to gather a combination of the necessary properties that ensure the best preservation of the packaged food product. The most common example of a multilayer material is Tetra Brick®, a combination of laminated paper, aluminium foil and plastic (low density polyethylene, LDPE). The combination of these three materials gives the packaging materials structural support (paper), aroma and light barrier properties (aluminium), and sealing, adhesion and ink support (LDPE), (Georgiopoulou et al., 2021).

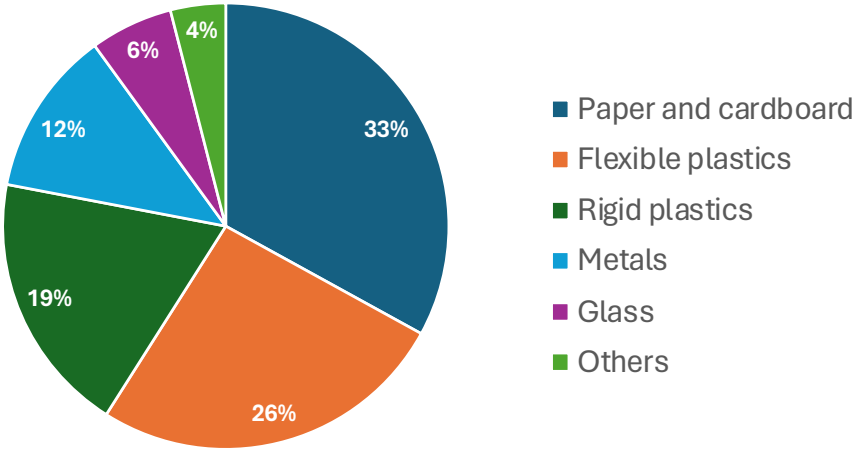

Figure 2. Market share of food packaging materials. Adapted from Cameron, 2020.

Despite being relatively new, plastics represent the most used materials in food packaging mainly due to their unique properties as they are mouldable, generally chemically inert, cost effective, lightweight, and provide multiple choices in terms of transparency, heat resistance, sealability, and barrier properties (Kirwan et al., 2011). Moreover, many of them are recyclable. Table 2 showcases the types of plastics used in food packaging.

Table 2. Types of plastics used in food packaging and their acronyms.

Type of plastic (Acronym)	
Polyethylene (PE)	Polyvinyl chloride (PVC)
Polypropylene (PP)	Polystyrene (PS)
Polyethylene terephthalate (PET)	Styrene butadiene (SB)
Polybutylene terephthalate (PBT)	Ethylene vinyl alcohol (EVOH)
Polycarbonate (PC)	Polyvinyl acetate (PVA)
Ethylene vinyl acetate (EVA)	Polyamides (PA)
Polymethyl pentene (TPX)	High nitrile polymers (HNP)
Fluoropolymers (PCTFE/PTFE)	Acrylonitrile butadiene styrene (ABS)

As food packaging materials, low- and high-density polyethylene (LDPE and HDPE respectively) are the most used with over 50 % by market weight, with PP, PET, PS and PVC accounting for most of the remaining bulk (Kirwan et al., 2011).

However, the large use of this type of polymers together with their long degradation rates have posed significant environmental challenges. Despite efforts set by environmental goals, factors such as economics, politics, and society play an important role on plastic packaging recycling. Recycling can be defined as the processing of material waste for its original purpose or for other purposes. However, when it comes to plastic food packaging, materials need first to be accurately sorted, washed and successfully decontaminated which, together with the technical feasibility associated to each material, make the process often not viable (Dainelli, 2008).

The environmental concerns outlined above, together with legislation efforts, have increased the interest for the development of new materials for food packaging applications. Even though bio-based polymers only account for 1 % of plastics produced annually, they represent an important part of the food packaging industry as most of them are destined for food packaging applications (Torres-Giner et al., 2021). Bio-based polymers consist of a whole family of materials with distinct properties and applications and can be categorised as 'bio-based', 'biodegradable', or both. Bio-based polymers encompass any polymer produced from renewable resources, comprising both naturally occurring polymers and synthetic ones synthesized using monomers derived from biological sources (Ashter, 2016). They offer the advantage of using biomass that regenerates annually and the potential for carbon neutrality. On the other side, biodegradable polymers are those capable of decomposing rapidly by microorganisms under natural conditions through aerobic or anaerobic processes to carbon dioxide, methane, water, or biomass (Laycock et al., 2017). As such, bio-based polymers can be biodegradable but not all biodegradable polymers are bio-based.

Grujić et al. divided bio-based polymers according to their origin and production methods into four fundamental classes (Grujić et al., 2017).

- Class 1- those obtained from biomass such as polysaccharides (starch, chitosan, cellulose, etc.) and proteins (collagen, gluten, casein, etc.).

- Class 2- bio-based polymers produced through usual chemical pathways but from bio-based monomers often obtained from fermentation of carbohydrates, such as chemically synthesized poly lactic acid or bio-polyesters.
- Class 3- bio-based polymers produced by microorganism activity such as polyhydroxyalkanoates (PHAs) and bacterial cellulose.
- Class 4- as in class 2, bio-based polymers produced through usual chemical pathways but from a combination of bio-based and conventional, petroleum-based monomers. Examples include polybutylene succinate (PBS), bio-based terephthalic acid (TPA), bio-based PP and PE, etc.

A non-exhaustive list of the most important bio-based polymer materials trends for food packaging applications and their properties can be found in table 3.

Table 3. Bio-based polymer materials trends for food packaging applications and their class according to their origin and production method and their properties.

Bio-based polymer	Source	Properties	References
Polylactide (PLA) Class 2	Corn, sugarcane	Formed of lactic acid units. Similarly to PET, PS and PC, the most relevant characteristics of this bio-based polymer are high rigidity, good transparency, heat sealability, printability, and melt processability. No oxygen or water barrier. Biodegradable under industrial composting conditions.	(Garlotta, 2001)
Poly(3-hydroxybutyrate) (PHB) Class 3	Microorganism activity	Made of 3-hydroxybutarate units, PHB is the most common type of polyhydroxyalkanoate. It has similar properties to polyolefins and can be processed by all common methods. Good water stability but poor impact-strength resistance. Biodegradable under domestic composting conditions, soil, and in the marine environment.	(Yeo et al., 2018)

Poly(butylene adipate-co-terephtalate) (PBAT) Class 4	Corn, sugarcane + petroleum	Bio-polyester from 1,4-butanediol, adipic acid and terephthalic acid. Ductility and thermomechanical properties comparable to LDPE but low mechanical strength and water barrier properties. Biodegradable under composting and under certain soil and marine conditions.	(G. Li et al., 2015)
Bio-polybutylene succinate (bioPBS) Class 2	Corn, sugarcane	Bio-polyester from 1,4-butanediol and succinic acid. Balanced mechanical and processing properties comparable to PP but with higher rigidity. Biodegradable under composting and under certain soil and marine conditions.	(Rafiqah et al., 2021)
Poly(ethylene furanoate) (PEF) Class 2	Corn, sugarcane	This polymer from bio-based 2,5-furandicarboxylic acid and bio-monoethylene glycol has excellent mechanical strength and oxygen and water barrier properties outperforming those of PET. Not biodegradable.	(Kasmi et al., 2018)
Thermoplastic starch (TPS) Class 1	Cassava, corn	Starch based with moderate oxygen barrier but poor moisture and mechanical properties. It is mixed with plasticizers to increase its processability. Biodegradable with suitable microbial activity conditions.	(F. Zhu, 2015)
Cellulose derivatives Class 1	Wood	Unsuitable for film production, neat cellulose is chemically modified and mixed with plasticizers to achieve good mechanical properties. Bad gas and moisture barrier properties and not water stable. Biodegradable in nature under suitable microbial activity conditions.	(Petersen et al., 1999)
Proteins Class 1	Wheat, animal skins, bones	Protein-based films from gelatine, wheat gluten, soy, corn zein, or milk. These films have high cohesiveness and good barrier properties against oxygen	(Andrade et al., 2015; Azevedo et al., 2015)

	and aroma. They have however high water vapor permeability. Biodegradable in nature under suitable microbial activity conditions.

Despite all the research involved in developing bio-based packaging materials, there are ethical discussions surrounding the use of biomass and potential food and feed resources towards material production. Consequently, parallel research on utilizing non-edible by-products as the primary source for bio-based plastics is now one of the main focuses for sustainable packaging development. This involves significant quantities of cellulosic by-products and waste materials like straw, corn stover or bagasse (Torres-Giner et al., 2021). Consequently, the ongoing trend in the development of the next generation of bio-based plastics is primarily driven by the shift towards traditional polymers derived from renewable sources that are not intended for human consumption.

2.2. Food safety of packaging materials

2.2.1. Legislation

Food packaging plays a crucial role in ensuring the safety of food products as well as their handling and transportation. Diverse materials such as plastic, glass, metal, paper, and their combination are employed for safeguarding food from chemical contamination and extending its shelf-life. Nevertheless, the growing health awareness among consumers has raised concerns regarding the potential transfer of harmful substances from packaging materials to food products.

To address these potential hazards, a series of national and European Union regulations have been implemented. At the Union level, the European Commission (EC) provides a harmonised legal EU framework regarding materials intended to come into contact with food during its production, processing, storage, preparation and serving (Table 3). Regulation EC 1935/2004 sets out the principles for FCMs such as requirements of not releasing their constituents into food at levels that are

harmful to human health and not changing food in composition, taste and odour in an unacceptable way. Moreover, it provides a framework for compliance documentation and traceability of materials as well as labelling instructions for FCMs (EC, 2004). Likewise, commission regulation EC 2023/2006 ensures that the manufacturing process of a FCM is well controlled so that it remains compliant with the legislation (EC, 2006).

Apart from the general legislation mentioned above, specific EU measures apply to certain harmonized FCMs of interest due to their varied nature such as plastics (EU, 2011) and recycled plastics (EU, 2022), active and intelligent materials (EC, 2009), ceramics (EEC, 1984), and regenerated cellulose films (EC, 2007). For other non-harmonized FCMs not covered by EU specific legislation such as adhesives, cork, rubbers, glass, metals, paper and board, printing inks, silicones, textiles, etc., the International Life Sciences Institute (ILSI) has recently published a series of recommendations, based on specific national level legislations, regarding their testing conditions (Oldring, 2023).

Regulation EU 10/2011 is the most comprehensive of all regulations due to the broad use of plastics as FCMs. It covers rules on the composition of plastic FCMs and limits the substances that can be used for their production, setting out restrictions for the compliance of plastic materials and articles (EU, 2011). This include FCMs made of conventional plastics and also bio-based polymers that, without a specific legislation, also reside under the same regulation. The evolving nature of plastics along with parallel research on their safety has forced regulation EU 10/2011 to be amended quite regularly over the last 13 years, making it paramount to work on the consolidated version, now containing 17 amendments. Furthermore, regulation EU 2022/1616 exists to control the recycling and decontamination processes of recycled plastic FCMs (EU, 2022). Nevertheless, FCMs manufactured with recycled plastics must still comply with EU 10/2011. Likewise, regulation EC 450/2009 exempts active and intelligent FCMs to follow the inertness stated by EC 1935/2004 so that they can address their specific purpose by, for example, absorbing and releasing substances that will extend the shelf-life or improve the condition of packaged food (EC, 2009). Finally, directive 84/500/EEC

and 2007/42/EC cover the rules on ceramic articles (EEC, 1984) and regenerated cellulose film materials and articles (EC, 2007) intended to come into contact with foods, respectively.

Table 4. Major European regulations on food contact materials (FCM).

General FCM regulations	
Regulation EC 1935/2004 on materials and articles intended to be in contact with food	
Regulation EC 2023/2006 on good manufacturing practices	
Specific FCM regulations	
Plastic	Regulation EU 10/2011 (as 04/2024)
Active and intelligent materials	Regulation EC 450/2009
Recycled plastic materials	Regulation EU 2022/1616
Ceramics	Directive 84/500/EEC
Regenerated cellulose film	Directive 2007/42/EC
Other regulations	
Regulation EU 2018/213 restricting the use of bisphenol A in varnishes and coatings of FCMs	
Regulation EC 1895/2005 restricting the use of certain epoxy derivatives in FCMs	
Directive 93/11/EEC regulating the release of N-nitrosamines and N-nitrosatable substance from rubber teats and soothers	
Regulation EU 284/2011 setting out import procedures for polyamide and melamine plastic kitchenware from China and Hong Kong	

Other EU regulations regarding food contact materials address the use of substances such as bisphenol A, epoxy derivatives, and nitrosamines to ensure consumer safety. Bisphenol A (BPA), known for its potential health risks, is subjected to strict controls under EU regulation 2018/213, with bans on its use in certain products like baby bottles and restrictions on its presence in other food contact materials in the form of varnishes and coatings (EU, 2018). Similarly, epoxy derivatives, which may contain BPA, are subject to regulation EC 1895/2005 to limit their migration into food (EC, 2005). Also, nitrosamines, known carcinogens, are strictly regulated through Directive 93/11/EEC to prevent their presence in rubber teats and soothers (EEC, 1993). Furthermore, the EU implemented specific procedures for monitoring polyamide and melamine products imported from China

or Hong Kong to ensure compliance with EU safety standards, given the importance of these materials in food packaging and plastic kitchenware (EC, 2011).

Overall, these regulations, together with the European Food Safety Authority (EFSA) and ILSI recommendations, underscore the EU's commitment to safeguarding public health and ensuring the safety of food contact materials in the European market.

2.2.2. Migration phenomena: intentionally added substances (IAS) and non-intentionally added substances (NIAS)

While one of the main purposes of food packaging is to preserve foods from chemical hazards, interaction of FCMs with food matrices can result in the transfer of chemical substances, having significant implications for food safety and public health. This complex phenomenon receives the name of migration and can occur through various mechanisms, including diffusion, partitioning, and adsorption-desorption processes (Arvanitoyannis et al., 2014). Over the last years, extensive research has been performed on migration processes (Aznar et al., 2011; Canellas et al., 2015d, 2017, 2019, 2020; Nerín et al., 2022a; Oldring, 2023; Vera et al., 2018, 2019; Wrona & Nerín, 2020) due to their complexity and varied migration scenarios. Some factors that can have a direct influence over migration extent and rate are:

- The nature of the food: the choice of food simulant directly influences the migration processes observed. The use of a fatty food simulant would likely result in higher migration levels compared to the use of an aqueous or acidic simulant due to the greater solubility of substances in fats (Coltro et al., 2014; Urbelis & Cooper, 2021).
- The type of contact: numerous studies suggest that the degree of migration correlates with the type of contact (direct or indirect). Evidence indicates an increase in migration levels when direct contact with food occurs (Alamri et al., 2021; Eicher et al., 2015).
- The time and temperature of contact: as demonstrated by Arvanitoyannis et al., the concentration of the migrating compound is directly proportional to

the square root of the contact time (Arvanitoyannis & Kotsanopoulos, 2014; Guan et al., 2023). Likewise, higher temperatures lead to higher migration rates.

- The nature of the packaging material: packaging characteristics such as thickness have a great influence on the migration level. For example, thinner packages are subject to higher migration rates (Nerín et al., 2007; Ramírez Carnero et al., 2021).
- The characteristics and the amount of migrant: for example, highly volatile migrants show a higher migration rate. Likewise, high molecular weight (>1,200 Da) substances present lower migration levels when compared to low molecular weight molecules (Triantafyllou et al., 2007). Moreover, higher concentrations of migrant in the FCMs will inevitably lead to a higher transfer onto the food matrix due to the difference in the concentration gradient and Fickian diffusion phenomena (Kato & Conte-Junior, 2021).

Depending on their origin, we can classify migrating substances into two big groups: intentionally added substances (IAS) and non-intentionally added substances (NIAS). As indicated by their names, IAS are substances deliberately incorporated into FCMs during production, processing, or packaging to fulfil specific functions such as improving the material's properties, enhancing performance, or providing aesthetic qualities. For plastic FCMs, they include plasticizers, antioxidants and stabilizers, colorants, flame retardants, adhesives and coatings and UV stabilizers (Arvanitoyannis et al., 2014). Table 5 gathers some examples of common IAS migrating from plastic FCMs. Common plasticizers belong to the group of esters of phthalic acid and adipic acid (Alp & Yerlikaya, 2020). Due to their stability and excellent oxidation resistance, phenolic compounds such as butylated hydroxyanisole (BHA), butylated hydroxytoluene (BHT) and tert-butylhydroquinone (TBHQ) are some of the most used antioxidants in plastic FCMs (Ousji & Sleno, 2020; W. Zhu et al., 2023). Flame retardants such as brominated and organophosphate compounds are also often added to reduce the flammability of plastic FCMs (Paseiro-Cerrato et al., 2021). Adhesives and coatings such of acrylic and PU origin, are used to bond different material layers together to improve

sealability and barrier properties of the final material and can also be transferred into the food matrix (Aznar et al., 2011; Canellas et al., 2015a, 2015b, 2015c, 2017; Félix et al., 2012; Isella et al., 2013; Jaén et al., 2022; Vera et al., 2011, 2012, 2013). Migration of commercial families of compounds such as Tinuvin, Irganox, Irgafos, etc., that are UV stabilizers added to protect FCMs from degradation caused by UV radiation, can also occur (Monteiro et al., 1999; Reinas et al., 2012). Finally, an interesting case is that of bisphenol A (BPA). BPA is typically considered an IAS as it is deliberately incorporated into the production of certain plastics, such as polycarbonate plastics and epoxy resins to impart specific properties, including transparency and durability. However, BPA can also be considered a NIAS if it is detected in FCMs unintentionally (Dreolin et al., 2019; López-Cervantes & Paseiro-Losada, 2003).

Table 5. Examples of common IAS migrating from plastic FCMs.

IAS	Origin/Role	Packaging material	References
di(2-ethylhexyl) phthalate (DEHP) diisononyl phthalate (DINP) diisodecyl phthalate (DIDP)	Plasticizer	PVC	(Alp & Yerlikaya, 2020; Su, Vera, Nerín, et al., 2021)
butylated hydroxyanisole (BHA) butylated hydroxytoluene (BHT) tert-butylhydroquinone (TBHQ)	Antioxidants and stabilizers	PE, PP, PS, PET	(Ousji & Sleno, 2020; Su, Vera, Salafranca, et al., 2021; W. Zhu et al., 2023)
2,4,6-tribromophenol (TBP), 3,3',5,5'-tetrabromobisphenol A (TBBPA)	Flame retardants	PC, PU, PE	(Paseiro-Cerrato et al., 2021)
9,10-dihydroanthracene retene	Adhesives and coatings	Multilayer materials	(Canellas et al., 2021; Clemente, Aznar, Nerín, et al., 2016; Domeño et al., 2017; Salafranca et al., 2015; Vera et al., 2011)

Tinuvin, Irganox, Cyanox, Irgafos	UV stabilizer	PE, PP, PET	(Aznar et al., 2023; Reinas et al., 2012)
Bisphenol A (BPA)	Production	PC, epoxy resins	(Dreolin et al., 2019; López-Cervantes & Paseiro-Losada, 2003)

On the other hand, NIAS are chemicals that are present in FCMs but were not intentionally added during its manufacturing. The source of NIAS in plastic FCMs is very broad and can include impurities from primary materials, contaminants from recycled components, degradation by-products from the polymer matrix and/or its additives, and compounds resulting from reactions between polymer constituents or its interactions with food (Wrona & Nerín, 2020). As a result, most NIAS are unknown and can vary a lot from sample to sample, making it compulsory to perform non-targeted analysis to determine all possible migrants through high-resolution mass spectrometry (HR-MS). HR-MS allows finding molecular weights of migrants to several decimal figures, allowing to determine the exact molecular formula of the compound being analysed. However, qualitative analysis of NIAS through HR-MS can be very difficult and challenging due to the complexity of puzzling out chromatographic and spectrum results and a usual lack of information about composition of a material (Nerin et al., 2013; Nerín et al., 2022b).

Two important terms that should not be mistaken are overall migration and specific migration. Overall migration is a measure of inertness of a material and refers to the total amount of migrant substances released from packaging per unit area under specific predetermined conditions, often including substances whose identities are not always known. In contrast, specific migration relates to every single substance released by the packaging material (Robertson, 2016). In Europe, both IAS and NIAS in plastic FCMs are controlled by Commission Regulation No 10/2011 (EU, 2011), which specifies specific migration limits for some substances. For not listed substances, migration should not be higher than 0.01 mg kg^{-1} (ratio 6:1) of food or food simulant (EU, 2011). This limit is established for the concept of functional

barrier, but in practice, this value is applied to non listed substances, once provided that they are non carcinogenic, mutagenic or reprotoxic (CMR). Moreover, for substances without a toxicity assessment, a procedure of toxicity determination can be assessed by application of the threshold of toxicological concern (TTC), a theoretical approach of toxicity based on chemical structure, where analytes are classified into three Cramer classes (Younes et al., 2022). This is the system currently applied in Europe, although there is not an official regulation around it.

Plastic FCMs migration tests are commonly carried out using different food simulants: liquid (e.g., 95% (*v/v*) ethanol, 3% (*v/v*) acetic acid) and/or solid (Tenax®). Temperature and time of migration tests depend on the intended application and worst-case scenario of the FCM is recommended for the tests (EU, 2011). The most common migrants are organic analytes, which can be differentiated into two big groups: volatile and non-volatile compounds, determining the analytical procedure for their detection and quantification. Nerín et al. recently published a guidance for selecting the appropriate method for the identification and quantification of NIAS in FCMs (Nerín et al., 2022a). Volatile analytes will likely be analysed by gas chromatography whereas non-volatile ones will be separated by liquid chromatography. In both cases, chromatography will be coupled to different kinds of mass spectrometry detectors, changing only the injection mode according to the matrix of the migration extract (Nerin et al., 2013; Nerín et al., 2022a; Wrona & Nerín, 2020). Thus, as illustrated in Table 6, different analytical approaches have been developed to analyse the migration of these extracts.

Table 6. Examples of analytical procedures for different food simulants. Adapted *from* Wrona & Nerín, 2020. *SPME*-GC-MS, solid phase microextraction gas chromatography coupled to mass spectrometry (MS) detector; HS, headspace; UPLC-HR-MS, ultra-high performance liquid chromatography coupled to a high-resolution mass spectrometry detector (eg. quadruple time-of-flight, orbitrap).

Food simulant	Description	Analytical procedure
A	Ethanol 10% (*v/v*)	SPME-GC-MS either by HS or total immersion mode. Direct injection for UPLC-HR-MS
B	Acetic acid 3% (*v/v*)	SPME-GC-MS either by HS or total immersion mode. Direct injection for UPLC-HR-MS
C	Ethanol 20% (*v/v*)	SPME-GC-MS either by HS or total immersion mode. Direct injection for UPLC-HR-MS
D1	Ethanol 50% (*v/v*)	SPME-GC-MS either by HS or total immersion mode, but previously diluting the migration extract 5 times. Direct injection for UPLC-HR-MS
D2	Any vegetable oil containing less than 1% unsaponifiable matter. Can be replaced by 95% (*v/v*) ethanol and isooctane	HS- SPME-GC-MS for direct oil analysis. For liquid injection in a GC-MS or UPLC-HR-MS system, oil needs first to be extracted. When using 95% ethanol and isooctane, direct injection can occur in both GC-MS and UPLC-HR-MS
E	poly(2,6-diphenyl-p-phenyleneoxide) known as Tenax®, particle size 60-80 mesh, pore size 200 nm	Tenax® needs to be extracted with some organic solvent (eg. ethanol or methanol) and then concentrated under nitrogen stream. Then, direct injection can occur in both GC-MS and UPLC-HR-MS

2.2.3. Unaddressed risks: oligomers

As structurally diverse compounds coming from incomplete polymerisation or polymer degradation, oligomers have already surpassed the number of polymers. Being low molecular weight polymers, they constitute one of the primary forms of NIAS (Shi et al., 2023). Due to their low molecular weight (generally below 1,000 Da) they can migrate from the material matrix into the food and are often disregarded by polymer scientists, which concentrate their attention into the 10^4 to 10^6 Da range (Shi et al., 2023).

Oligomers have been found across all kinds of plastic FCMs. PET oligomers are of special interest due to the growing popularity of recycled PET, as recycling processes can trigger polymer degradation which leads to oligomers formation (Alberto Lopes & Tsochatzis, 2023a; Barnard et al., 2021; Cho et al., 2016; Ubeda et al., 2018). Oligomers content can represent an important part of a material, with some studies reporting PET FCMs to contain up to 1.2% w/w of oligomers (Hoppe et al., 2018). Migrating oligomers have also being found in PE (Biedermann-Brem et al., 2011; Coulier et al., 2007), PP (Coulier et al., 2007) and PS (Choi et al., 2005; Z. Tian et al., 2020). In another case study, oligomers coming from PU are able to migrate from lamination adhesives of multilayer materials (Ubeda et al., 2020; N. Zhang et al., 2018). Moreover, the increasing popularity of bio-based polymers, usually manufactured by mixing various monomers and materials to enhance their properties, has multiplied the numbers of oligomeric combinations. As a result, various cyclic and linear oligoester combinations of PLA (Aznar et al., 2019; Burgos et al., 2014) have been found, as well as numerous monomer combinations of diacids (e.g. phthalic acid, adipic acid, sebacic acid) and diols (e.g. 1,4-butanediol, ethylene glycol, propylene glycol, diethylene glycol, 1,6-hexanediol, neopentyl glycol) used in bio-based polymer manufacturing (Aznar et al., 2019; Cariou et al., 2022; E.L. Bradley, 2010; Omer et al., 2018; Ubeda et al., 2021).

The lack of isolated oligoester standards results in an analytical challenge for the identification and quantification of NIAS (Nerin et al., 2013; Nerín et al., 2022a). Moreover, it limits the capability to perform toxicological risks assessments that would shed some light into the human and environmental exposure as well as the Absorption, Distribution, Metabolism, Excretion and Toxicity (ADMET) of oligoesters, as very few studies have been performed regarding the toxicity of oligomers. Wang et al. proved that PLA oligomers can potentially induce acute intestinal and colon inflammation in mice (M. Wang et al., 2023). Moreover, there is evidence that PS oligomers cause human endocrine disruption (Ohyama et al., 2001). Hence, in recent years, synthetic efforts have been made by independent research groups to contribute towards the availability of migrant oligoesters (Cariou et al., 2022; Paseiro-Cerrato et al., 2016; Pietropaolo et al., 2018; Úbeda et al., 2017).

Nevertheless, urging to fill oligomers knowledge gaps, the need for reference standards is rapidly increasing (Nerín et al., 2022a).

3. Biological risks and active packaging

Food spoilage poses a significant challenge to global food security, affecting both developed and developing nations alike. Inadequate storage and transportation infrastructure contribute to substantial losses of perishable goods, provoking food insecurity issues. Active packaging technologies have emerged as a promising solution to prevent food spoilage and foodborne diseases transmission by incorporating active agents with antimicrobial activity into packaging materials (Yildirim & Röcker, 2018).

3.1. Food spoilage and insecurity

All food eventually spoils. Deterioration can happen through physiological, biochemical, microbiological, or environmental processes, which contribute to changes in the nutritional value, texture, flavour, and overall quality of the food product (Hammond et al., 2015). Moreover, food spoilage has social, economic, and political implications, such as the waste of valuable resources and the unnecessary contribution to carbon emissions when food ends up in a landfill (Busetti & Pace, 2022; Hammond et al., 2015).

3.1.1. Senescence

According to the Food Authority Organisation (FAO), an estimated 17% of global food production is wasted (FAO, 2021), with fresh products such as fruits and vegetables being the main contributors (Blanke, 2015). This is directly linked with the availability of food across the world, with regions such as Africa suffering from hunger, which leads to sickness and premature death (James & Zikankuba, 2017). In an attempt to overcome these challenges, it is needed to target the causes of deterioration. In fruits and vegetables, they include early ripening (Pech et al., 2018), moulds and bacterial contamination (Giannakourou & Tsironi, 2021), and

mechanical injuries caused during processing (Yousuf et al., 2018). In other fresh food products such as meat, oxidation of lipids and proteins, as well as microorganism deterioration, either by post-harvest contamination or by foodborne pathogens, are the main factors of spoilage (Soladoye et al., 2015).

Early ripening is one of the main causes of fruits and vegetables senescence (Kader et al., 2003). Ripening is mainly controlled by the phytohormone ethylene, also known as the plant growth hormone, which is produced by fruits and vegetables themselves. In climacteric fruits, increasing concentrations of ethylene accelerates their ripening and senescence processes (Golden et al., 2014). The impacts differ for each fruit and vegetable, but among the most prevalent are decay, russet spotting, yellowing, odour, wilting, and scalding(Kader, 2013).

Oxidation is also another important factor that contributes significantly to the deterioration of quality and shelf-life of food. When food is exposed to oxygen, reactive oxygen species (ROS) are generated, initiating a cascade of oxidative reactions that lead to the degradation of essential nutrients, such as vitamins (A, D, E and K), proteins, and lipids (S. Tian et al., 2013) . ROS comprise a series of molecules such as singlet oxygen (O_2^1), oxygen superoxide (O_2^-), hydrogen peroxide (H_2O_2) and hydroxyl radicals ($OH^\cdot$), being the latter the most reactive of all (Meitha et al., 2020). It is a radical reaction, where free hydroxyl radicals are the initiators. This oxidative stress manifests through various visible changes, including discoloration, generation of off-flavors, and texture alterations, and can produce inflammatory and carcinogen compounds, contributing to food insecurity (F. Silva, Becerril, et al., 2019). Additionally, oxidation accelerates the breakdown of cellular structures and membranes, accelerating senescence processes such as enzymatic browning and lipid rancidity (M. Hossain et al., 2020). Understanding the mechanisms of ripening and oxidation in food senescence is crucial for developing effective preservation strategies to maintain quality and extend the shelf-life of perishable fresh food products (Nerín, 2010).

3.1.2. Microbial spoilage

As mentioned previously, the prevalence of foodborne diseases generates direct social, economic, and human health consequences as they contribute towards food spoilage, and waste, and can cause illnesses. As such, we can differentiate between food spoilage and pathogenic microorganisms. Food spoilage microorganisms mainly affect the quality and appearance of food, making it unappetizing but not necessarily harmful, while pathogenic microorganisms can cause illness or disease when consumed in contaminated food (Tropea, 2022). In fact, according to the World Health Organization (WHO), the annual global burden of foodborne diseases exceeds 600 million cases and nearly 420,000 deaths (WHO, 2015). Table 7 summarises the impact of some foodborne pathogens and microbial toxins in human health.

Table 7. Major foodborne diseases caused by pathogenic microorganisms and food toxins in 2010. Adapted from WHO, 2015.

Threat	Disease	No. of cases	No. of deaths
Virus			
Hepatitis A (HAV)	Hepatitis	13,709,836	27,731
Norovirus	Gastroenteritis	124,803,946	34,929
Bacteria			
Campylobacter spp.	Gastroenteritis	95,613,970	21,374
E. coli spp.	Gastroenteritis/haemolytic uraemic syndrome	111,476,873	63,375
Salmonella spp.	Salmonellosis	88,018,798	123,694
Vibrio cholerae	Cholera	763,451	24,649
Shigella spp.	Shigellosis	51,014,050	15,156
Listeria monocytogenes	Listeriosis	14,169	3,175
Toxins			
Aflatoxin	Aflatoxicosis	21,757	19,455

Moulds and bacteria are, by far, the most important food spoilage and pathogenic microorganisms. Moulds are often more related to food deterioration, with a special affection towards fruits and vegetables, causing large pre-harvest losses and post-

harvest waste in both household and shops (Alegbeleye et al., 2022). Moreover, consumption of mould-contaminated food can result in serious food poising if the mould has produced dangerous compounds for humans, such as mycotoxins (Table 8). Mycotoxins are secondary metabolites with diverse chemical structures and mechanisms of toxicity produced by various fungi, predominantly those belonging to the genera *Aspergillus*, *Penicillium*, and *Fusarium*. The most common mycotoxins are aflatoxins (produced by *Aspergillus* spp.), which are potent carcinogens and can lead to liver damage, ochratoxin A (produced by both *Aspergillus* and *Penicillium* spp.), associated with nephrotoxicity and immunosuppression, and deoxynivalenol (produced by *Fusarium* spp.), that is known to cause gastrointestinal disturbances and immunomodulation (Bennett & Klich, 2003). Additionally, some of these toxins and spores can survive high temperatures and pressures, posing significant challenges in food manufacturing (Tropea, 2022).

Table 8. Examples of contaminating moulds on fruit and vegetables, the infection caused, and the produce affected. *mycotoxin producer. Adapted from Alegbeleye et al., 2022.

Mould	Infection caused	Affected produce
Botrytis cinerea	Grey rot	Pectin rich fruits (eg. strawberries, kiwi, grapes, pears, peaches, plums) and leafy crucifiers (eg. lettuce, peas, beans, asparagus, pumpkin)
*Aspergillus niger**	Black rot	Citrus fruits, apples, tomatoes, peaches, grapes
Penicillium italicum	Blue rot	Citrus fruits
*Penicillium expansum**	Blue-green rot	Apple, pears
Byssochlamys spp.*	Rot	Canned fruits and vegetables, fruits juices, purees and concentrates
Rhizopus stolonifer	Soft rot	Strawberries, grapes, tomatoes, peaches, melons
Alternaria spp.	Stem-end rot, black rot	Tomatoes, potatoes, citrus, apples, carrots
Fusarium spp.*	Brown rot	Corn, tomatoes, potatoes, cucurbits, onions

Regarding pathogenic bacteria, the last EFSA zoonoses data reports the largest number of food related deaths (Table 9) in the last 10 years, mainly caused by *L. monocytogenes* and to a lesser degree by *Salmonella* spp., *Campylobacter*, and Shiga toxin-producing *Escherichia coli* (EFSA, 2023). Overall, there was a 43.9% increase of foodborne outbreaks. The presence of *Salmonella* in eggs and other egg products was the food/agent pair causing most outbreaks across all EU member states. However, despite causing lower outbreaks and illnesses, *L. monocytogenes* was responsible for the largest number of deaths due to its high mortality rate (CDC et al., 2018).

Table 9. Principal foodborne pathogenic bacteria, the number of associated outbreaks, illnesses and deaths, their yearly increase and outbreak vehicles (EFSA, 2023).

Species	Outbreaks Illnesses Deaths	Yearly increase	Outbreak vehicles
Campylobacter	255 1,097 34	2.4 % 4.4 % 30.8 %	Broiler meat, mixed foods, bovine meat, poultry meat
Salmonella	1,014 65,208 81	31.2 % 8.6 % 14.1 %	Egg and egg products, mixed food, pig meat products, sweets and chocolate, bakery products
L. monocytogenes	35 2,738 286	52.2 % 25.4 % 45.9 %	Pig products, fish products, mixed food, vegetables and juices, dairy products
Shiga toxin-producing *Escherichia coli*	71 7,117 28	229 % 17.0 % 55.6 %	Bovine meat and products thereof
Mycobacterium tuberculosis	0 130 16	0 % 17 % 60 %	-
Brucella	0 198 0	-100 % 22.2 % 0 %	-

3.2. Active food packaging

Traditional packaging can be considered inert towards the produce, by only providing protection against external physical, chemical, and microbiological

factors. Active packaging is a solution that provides the previously mentioned protection, and additionally, an interaction takes place between the packaging, the environment, and the produce (Wyrwa & Barska, 2017). Through a series of interactions, active food packaging aims to increase food shelf-life, decrease food spoilage and waste, resulting in an overall reduction of food insecurity. As a new FCMs category that interact with the food product, it follows specific requirements established by the EU regulation 450/2008: it must be effective for its intended use, not release any component that might be harmful for humans, not cause any compositional or nutritional change, not produce unacceptable taste or odour to the food, and not mislead consumers through its packaging or labelling (EC, 2009). Interactions occur through added substances, designated as active agents, that intervene in the processes that affect food shelf-life. These comprise physiological (e.g. breathing of fruits and vegetables) and chemical (e.g. oxidation of fats) processes as well as microbiological changes (Yildirim & Röcker, 2018).

The great potential economic benefits of the use of active packaging systems in the food chain have triggered the development of multiple commercial products of different nature and forms (Table 10). For example, by the development of O_2 scavengers and antioxidants, unwanted oxidation is reduced, as well as the growth of aerobic microorganisms, thus inhibiting rancidity, discoloration and mould development (Norouzbeigi et al., 2021). Free radical scavengers are usually more efficient than oxygen scavengers, as by inhibiting the initiation of the oxidation reaction, effectively act as strong antioxidants (Wrona et al., 2021). As for CO_2 emitters, they can also decrease the microbial growth by reducing their metabolic rate, contributing towards food safety (Ahmed et al., 2022). By reducing ethylene concentration, usually through an oxidation reaction using potassium permanganate supported onto a porous network, ethylene scavengers reduce ripening and deterioration of fruits, vegetables and other horticultural products, extending their shelf-life (Sadeghi et al., 2021). Likewise, by reducing humidity inside the package, moisture scavengers can control microbial growth (Inthamat et al., 2022). Finally, antimicrobial systems target the growth of microorganisms through the release of antimicrobial compounds from the packaging or their incorporation

onto the polymer matrix for their later release (Gracia-Vallés et al., 2022; Silva et al., 2019).

Table 10. Different commercially available active packaging products. Adapted from Gaikwad et al., 2020 and Wyrwa & Barska, 2017.

Type	Form	Application	Commercial product
O_2 scavengers	Sachets, labels, film, masterbach	Moisture and lipidic foods, refrigerated and frozen goods, bakery products, cooked rice, snacks, dried fruits, cured meats, fish.	ActiTUF™ Ageless® Celox™ FreshPax® OMAC® OxyGuard®
CO_2 emitters	Pads, box system with CO_2 emitters	Ground coffee, snacks, nuts, bakery products, fresh meat and fish	CO_2® FreshPads UltraZap® Xtenda Pak pads SUPERFRESH
Ethylene scavengers	Sachets, film	Fruits, vegetables and other horticultural products	Bio-fresh Ethysorb Retarder® PEAKfresh® EvertFresh Green Bags®
Moisture scavengers	Sachets, absorbent pads and trays, microwavable film	Fresh feats and meats, poultry, snacks, cereals, dried foods, fruits, vegetabkes, sandwiches	MoistCatch MeatGuard Dri-Loc® Fresh-R-Pax® TenderPac®
Antimicrobial	Sheets, labels, films, masterbatch, coatings, interleavers	Fresh fruits and vegetables, meat products, cheese, bakery products	Biomaster® Irgaguard® IonPure® d2p® Bactiblock® SANICO®
Antioxidants	Film coating, multilayer	Cereal products, coffee, chips, meat, chocolate, salads	ATOX GOGLIO pack (green tea) SAMTACK (nanoSe)

3.2.1. Antimicrobial packaging

Antimicrobial active packaging is a type of packaging technology that inhibit microbial growth and preserve the quality and food safety of the product by releasing antibacterial or antifungal agents (Wyrwa & Barska, 2017). The number of antimicrobial agents is continuously evolving and can be divided in different categories (Table 11), such as organic acids, bacteriocins, biopolymers, essential oils (EOs), volatile organic compounds (VOCs) or metal nanoparticles (Becerril et al., 2013, 2020; Manso et al., 2011, 2013, 2015). Organic acids and their salts, such as benzoic, sorbic and lactic acid, have been used for decades as preservatives and are considered to be GRAS (Generally Recognised As Safe) by the FDA (Sullivan et al., 2020). Bacteriocins are peptides of microbial origin, which form pores in microbial membranes, resulting in cell death (Mousavi Khaneghah et al., 2018). Additionally, some biopolymers such as chitosan or pectin, have inherent antimicrobial properties, which make them ideal to form bio-based antimicrobial films (Bhowmik et al., 2022a; Inthamat et al., 2022; Zimet et al., 2019). EOs are mixtures of biologically active volatile compounds normally obtained by distillation of natural materials such as herbs and spices. As complex mixtures made of terpenoids, esters, aldehydes and other antimicrobial volatile organic compounds, the use of EOs in the food industry has been widely studied (Clemente, Aznar, Silva, et al., 2016; Garzoli et al., 2019; Mukurumbira et al., 2022; F. Silva, Caldera, et al., 2019a). Finally, metal nanoparticles have also been widely used due to their thermal stability and broad antimicrobial spectrum, allowing the processing of materials at high temperatures (Gold et al., 2018).

Of special interests are the application of volatile organic compounds (VOCs). VOCs can be isolated molecules of natural origin, being part of EOs (Wrona et al., 2023), or part of the molecules produced by some microbes as defense mechanisms against antagonistic microorganisms (Zhao et al., 2022). Due to their volatile properties, not requiring direct contact with food, the application of VOCs as active agents in food packaging is currently being widely studied (Camele et al., 2023; Kreuzenbeck et al., 2023; Vanmathi Mugasundari & Anandakumar, 2022; Vayachuta et al., 2021).

Table 11. Main antimicrobials categories and agents. Adapted from Becerril et al., 2020.

Antimicrobial category	Antimicrobial agent	Reference
Organic acids and their salts	Lactic acid	(Smulders et al., 2013)
	Sodium benzoate, citric acid	(Birck et al., 2016)
	Potassium sorbate	(Liang et al., 2019)
Bacteriocins	Sakacin A	(Barbiroli et al., 2017)
	Nisin	(Zimet et al., 2019)
	Pediocin	(Meira et al., 2017)
	Bacteriocin-produced by living bacteria	(Espitia et al., 2016)
Biopolymers	Chitosan	(Kildeeva et al., 2020)
	Pectin	(Corkovi´ccorkovi´c et al., 2021)
	Hydroxyethyl cellulose	(Şen & Kahraman, 2018)
Essential oils	Cinnamon oil	(Simionato et al., 2019)
	Oregano oil	(Becerril et al., 2007)
	Rosemary oil	(Alizadeh-Sani et al., 2021)
	Thyme oil	(Sharma et al., 2020)
Volatile organic compounds	Carvacrol	(Wrona et al., 2023)
	Diacetyl	(Williams-Campbell & Jay, 2002)
	Butanal	(Camele et al., 2023)
	Ethanol	(Vayachuta et al., 2021)
Metal nanoparticles	Zinc oxide	(Marra et al., 2016)
	Silver	(Manso et al., 2021)
	Titanium oxide	(Kaewklin et al., 2018)

3.2.2. Incorporation of active agents

Antimicrobial agents can take various forms within active packaging systems, which will depend upon the active agent stability, mechanism of action, and other properties such as volatility. A comprehensive depiction of potential forms of antimicrobial food packaging scenarios is presented in Figure 3. For instance, an antimicrobial agent might be integrated into the polymer or a coating, subsequently

released into the surrounding atmosphere if it is volatile, or onto the surface of the food if it lacks volatility. Alternatively, the active agent could be enclosed within a sachet or a pad along with food-grade components capable of enclosing the agent and regulating its release into the surrounding environment (Limbo & Khaneghah, 2015).

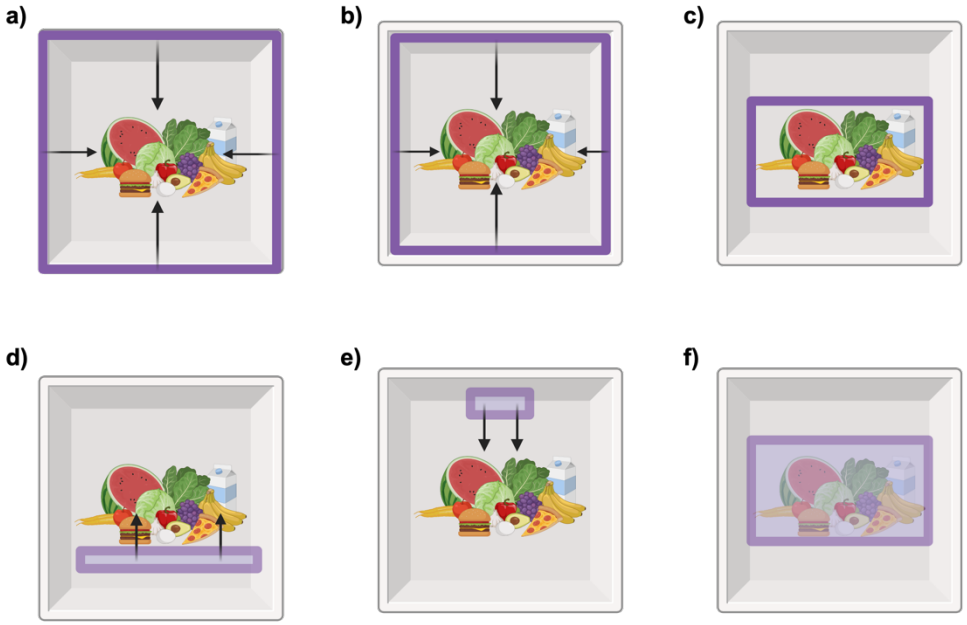

Figure 3. Possible methods and mode of actions for incorporating active agents in active packaging. a) From the polymer to the food through headspace, b) from a coating to the food through headspace, c) from a coating to the food through direct contact, d) from a pad to the food through direct contact, e) from a sachet to the food through headspace, f) from an edible film to the food through direct contact.

As the preferred method for packaging manufacturing, extrusion is often applied for the incorporation of active agents (Gómez-Estaca et al., 2014). In this case, the active agent is incorporated as an additive alongside the melted polymer material and moulded. However, this method poses a significant challenge as the active agent can degrade due to the high temperatures and pressures used (Nerin et al., 2016). To solve this stability challenge and also the incompatibility of some agents with the polymer matrix, either the coating method or the encapsulation of the active agent can be used. For coating preparation, the active agent is dissolved in a surface-compatible solution and spread onto the material. Then the solvent is left

to evaporate, leaving an immobilised active agent onto the surface (Becerril et al., 2023). For edible polymers such as chitosan, direct incorporation of the agent in the food through direct contact can also be an option (Umaraw et al., 2020). Alternatively, added elements such as sachets and pads can be used to incorporate active agents into the packaging. The difference is that pads require direct food contact (F. Silva et al., 2018), whereas sachets can easily be placed anywhere and in many forms of packaging material and interact with the packaging atmosphere. The use of sachets in the food packaging industry has become a popular active packaging strategy (Table 12).

Table 12. Examples of active food packaging strategies using sachets to incorporate active agents.

Active agent	Function	Food	Reference
Peppermint EO	Antimicrobial	Strawberry	(Amiri et al., 2022)
Thymol EO, $KMnO_4$	Antifungal, ethylene scavenger	Cherry tomatoes	(Álvarez-Hernández et al., 2021)
Oregano EO	Antimicrobial	Sliced bread	(Passarinho et al., 2014)
Ethanol	Antimicrobial	Shallots	(Utto et al., 2018)
2- nonanone	Antimicrobial	Strawberry	(Almenar et al., 2009)
Ethanol	Antimicrobial	Mulberry	(Choosung et al., 2019)
Ascorbic acid	Oxygen scavenger	Raw meatloaf	(J. Lee et al., 2018)

However, for most active agents, especially for volatile molecules (EOs, VOCs), encapsulation might be required to provide a more efficient packaging material. In this case, encapsulation systems protect volatile active agents from degradation and volatilisation, improve their availability and material compatibility and contribute towards a more sustained and controlled release. Encapsulation strategies include emulsions, and the use of encapsulating agents such as core-shell nanofibers, cyclodextrins, halloysite nanotubes (HNTs), and liposomes, among others (Becerril et al., 2020). Low particle size emulsions of two immiscible liquids offer great stability and bioavailability of active agents by forming vesicles similar to those of liposomes (Lei et al., 2019). Electrospinning of polymers at high

voltages is used to produce core-shell morphology nanofibers containing the active agent in their inner core, thus maximising its stability (C. Zhang et al., 2018). Cyclodextrins are starch-based molecules that can form inclusion complexes by accommodating hydrophobic substances through non-covalent interactions in their non-polar cavity (Caldera et al., 2017). Finally, HNTs are naturally occurring minerals that thanks to their tubular shape can be used to load and slowly release active agents (Kumar et al., 2024). Examples on active agents encapsulation for food applications can be found in Table 13.

Table 13. Examples of different encapsulation strategies used in active food packaging applications.

Active agent	Encapsulation strategy	Food	Reference
Oregano EO	Emulsion with Tween 80	Coated low-fat cheese	(Artiga-Artigas et al., 2017)
Thyme-oregano EO mixture	Emulsion with Lecithin and Tween 80	Packaged rice	(F. Hossain et al., 2019)
Angellica EO	Gelatine nanofibers	Blueberries	(Y. Zhou et al., 2020)
Cinnamon EO	β-cyclodextrin	Pork fillets	(Wen et al., 2016)
Thymol	γ-cyclodextrin	Not tested	(Aytac et al., 2017)
Carvacrol	HNTs	Cherry tomatoes	(Alkan Tas et al., 2019)
Lysozyme	HNTs	Chicken slices	(Bugatti et al., 2018)
Nisin	Lecithin and cholesterol	Coated cheese	(Cui et al., 2016)

Section II: Objectives

Objectives

The main objectives of this PhD thesis are the study and development of active packaging solutions targeting food safety and spoilage, as well as the evaluation of the chemical safety of new bio-based packaging materials. To achieve these goals, the following general objectives were set:

1. Mechanochemically synthesis, scale-up, and characterisation food-grade alpha cyclodextrin nanosponges (α-CD-NS) and evaluate their ethylene scavenging capacity.

2. Development of an antimicrobial volatile organic compound packaging solution based on diacetyl as active agent, and the evaluation of its *in vitro* and *in vivo* activity in fresh meat.

3. Assessment of the migration profile of new starch-based food packaging materials in food simulants.

4. Implementation of a stepwise synthesis approach to produce cyclic and linear migrant oligoesters based on adipic acid, 1,4-butanediol, isophthalic acid and propylene glycol.

5. Evaluation of the chemical risk of the starch-based materials by unequivocally identifying and quantifying their migrant oligomers using the synthesized oligoester standards.

Section III: Experimental part

Chapter 1:

Mechanochemically scaled-up alpha cyclodextrin nanosponges: their safety and effectiveness as ethylene scavenger

1. Introduction

In an increasingly globalized world, good resource management is of paramount importance. When it comes to food waste, figures can be alarming. The last Food Authority Organisation (FAO) report [1] pointed out that an estimated 17 percent of global food production is wasted, with fruits and vegetables being the main contributors (Blanke, 2015) mainly due to early ripening and the consequent product loss (Kader et al., 2003). The ripening process is mainly controlled by ethylene, also known as the plant growth hormone, which is a molecule responsible for numerous effects on the growth, development, and storage of fresh produces. It is produced by fruits, vegetables, and ornamental flowers and it can have detrimental effects on their shelf-life even at $\mu l\ l^{-1}$ concentrations (Saltveit, 1999). The effects vary for each product but some of the most common include decay, russet spotting, yellowing, odor, wilting and scalding, among others (Kader, 2013). Therefore, new strategies to improve fruit and vegetables shelf-life are in demand, with extensive research taking place in the food packaging sector (Enderle et al., 2022).

Since ethylene was known as plant growth regulator just over 50 years ago (Abeles et al., 1992), efforts have been made towards an effective ethylene removal approach. Several mechanisms have been studied, including adsorption on clays, zeolites and different activated carbon nanoforms (S. I. Kim et al., 2005; Liu et al., 2006; Ooka et al., 2004), oxidation using transition metals (Forsyth et al., 2011), photo-oxidation using UV lamps (Lawton, 1991) and chemical gaseous inhibitors such as 1-methylcyclopropene (Sisler, 2006). However, the most studied and used approach consists of chemical oxidation by means of potassium permanganate impregnated on high surface area materials such as clays (Zagory, 1995). This solution for ethylene removal is already being commercialized in the form of sachets but, due to the toxic nature of potassium permanganate, these sachets are very difficult to dispose. Hence, new alternatives with safer and eco-friendlier ethylene removal compounds are needed.

Cyclodextrins (Del Valle, 2004) are enzymatically bio-synthetized from starch and can be defined as cyclic glucopyranose oligomers that have the ability of including a wide range of compounds such as antimicrobials, essential oils and gases within their cone-shaped lipophilic cavity (Duarte et al., 2015; F. Silva, Caldera, et al., 2019b; F. Silva et al., 2014). Cyclodextrin nanosponges (CD-NS) are a virtually non-toxic novel type of cross-linked cyclodextrin with improved properties over cyclodextrin monomers because their higher stability over a wide pH range (1-10) and temperatures of up to 130ºC (Caldera et al., 2017).

Traditionally, CD-NS synthesis involves the use of high amounts of both energy and organic solvents (Trotta et al., 2012). Pedrazzo et al. (Pedrazzo et al., 2020) proposed a green synthesis using mechanochemistry, that eliminates the use of organic solvents and uses only water for the washing step. Mechanochemistry is a solvent-free synthesis that relies on mechanical forces such as friction to transfer energy and form chemical bonds, reducing the energy requirements and aligning with the Green Chemistry Principles (Anastas & Warner, 1998). Nevertheless, a washing step is often necessary to remove any contaminants or subproducts that may be formed during the process. One of the benefits of mechanochemical synthesis is that it can be easily scalable. However, scaling up mechanochemical organic synthesis is still at an early age as the main industry focus of this technique has been in inorganic processes that are generally less temperature dependent (Colacino et al., 2021).

Trying to address the issue of food waste due to early ripening of fruit and vegetables, the applicability of α-CD-NS for ethylene removal was studied. In this work, we aim to scale-up the synthesis of a bio-based α-CD-NS, ensuring their food safety by validating an HPLC-DAD method to monitor imidazole, a toxic sub-product from the synthesis, and assessing the ethylene removal capacity of the final product by means of gas chromatography.

2. Objectives

The main objective of this chapter is to assess the scalability by mechanochemical means of α-CD-NS and their production as food-grade materials. Moreover, the evaluation of their ethylene scavenging capacity against other common adsorbents will be performed. Thus, this study aims to validate the synthesis of α-CD-NS at a large scale and their use as ethylene scavengers as a green alternative to combat food spoilage of fruits and vegetables (Figure 1.1).

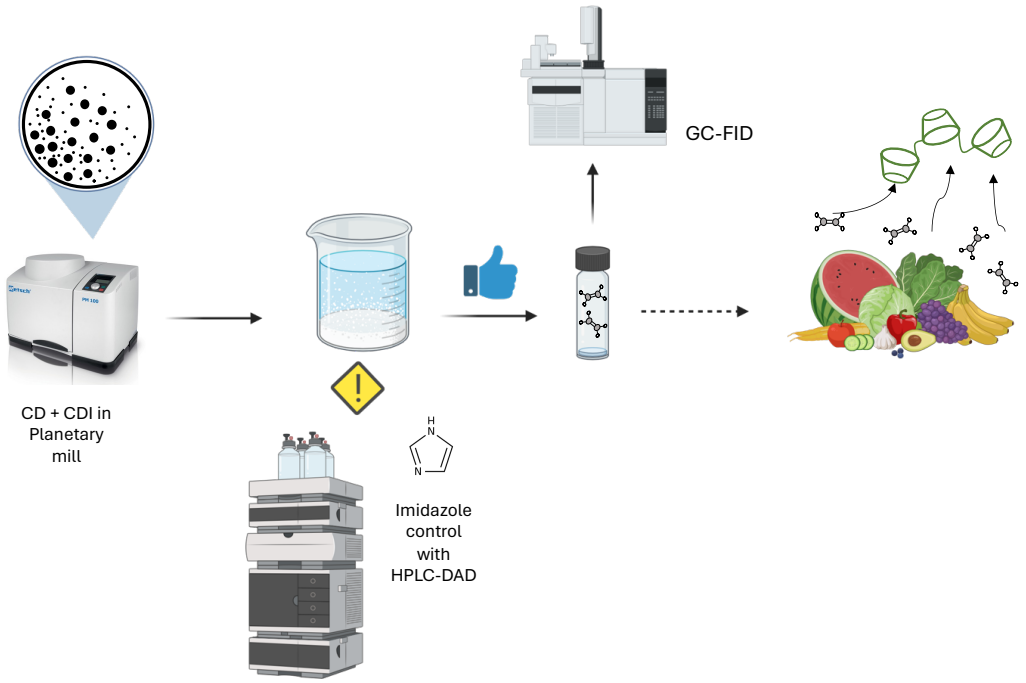

Figure 1.1. Process for the synthesis of food-grade α-CD-NS and the evaluation of their ethylene removal capacity, aiming at the development of a safe ethylene scavenger for fruits and vegetables.

3. Materials and methods

3.1. Materials

Alpha-cyclodextrin, carbonyldiimidazole (CDI), imidazole and ammonium dihydrogen phosphate were purchased from Sigma Aldrich (St. Louis, Missouri, U.S.). Milli Q water was generated using an Ultramatic Wasserlab purification

system (Navarra, Spain). For pH adjustment, 37 % hydrochloric acid and 85 % ortho-phosphoric acid (Scharlab, Spain) were used. Analytical grade acetonitrile was purchased from Honeywell (Charlotte, North Carolina, U.S.). Bentonites and zeolites were kindly provided by Nurel S.A. (Zaragoza, Spain).

3.2. Synthesis and characterization of α-CD-NS

3.2.1. Small scale synthesis

Following the synthesis described by Pedrazzo et al. (Pedrazzo et al., 2020), α-CD was dried in an oven at 100ºC until constant weight. The one step, solvent free synthesis was performed using a Retsch PM100 planetary ball mill (Haan, Germany) and CDI as cross-linking agent in a 50 mL zirconium oxide jar with 10 zirconium oxide balls of 10 mm. The amount of α-CD and CDI to achieve the chosen 1:4 molar ratio was 3.38 and 2.25 g, respectively. After 3 h of 600 rpm sun wheel speed rotation, changing the direction of rotation every 15 min, the synthesis was completed. Once washed, the product was filtered on a Buchner funnel using a 0.2 μm mixed cellulose ester Whatman membrane filter (Maidstone, U.K.). Then, it was left to dry in an oven at 50 ºC until constant weight was achieved. Afterwards, the dried CD-NS were stored in a desiccator to prevent moisture uptake.

3.2.2. Synthesis scale-up

The synthesis was scaled up from a 50 mL to a 500 mL zirconium oxide jar. The diameter of the balls was kept at 10 mm but the number of balls was increased to 100. The 1:4 α-CD and CDI ratio was identical and the quantities used were 33.8 and 22.5 g of each, respectively. Different sun wheel speed rotation frequencies (310, 350 and 400 rpm) were tested, changing the rotation direction every 15 min. From here, the washing, filtering, and drying was performed identically as above.

3.2.3. CD-NS characterization

α-CD-NS characterization was performed using Fourier Transform Infrared - Attenuated Total Reflectance (FTIR-ATR), Dynamic Light Scattering (DLS), thermogravimetric analysis (TGA) and X-ray diffraction (XRD). Prior to analysis, all

samples were powdered and dried at 100 ºC until constant weight so that a consistent relative humidity between samples can be assumed. FTIR-ATR spectroscopy was performed on a Jasco FT-IR 4100 (Madrid, Spain) and samples were measured without further preparation. Spectrum was taken with 32 scans at 4 cm^{-1} resolution in a wavenumber range of 500–4000 cm^{-1}. DLS analysis was carried out to obtain hydrodynamic diameter and polydispersity index (PDI) of the washed α-CD-NS using a Brookhaven 90Plus DLS instrument (Holtsville, New York, U.S.). All measurements were done in Milli Q water at a concentration of 0.1 mg CD-NS mL^{-1} at 25ºC. A total of 10, 45 seconds runs were done for each analysis. Thermogravimetric analyses were carried out on a Q5000SA analyzer from TA instruments (New Castle, Delaware, U.S.). Parameters were as follows: 50 mL min^{-1} synthetic air flow and ramp rate of 10 ºC min^{-1} from room temperature to 800 ºC. Powder X-ray diffraction was performed on Panalytical Empyrean X-ray diffractometer from Malvern Panalytical (Malvern, United Kingdom). CuKα radiation (λ = 1.5419 Å) was used to scan the diffraction angles (2θ) between 5° and 60° at a speed of 4°/minute.

3.3. CD-NS washing

3.3.1. Influence of pH

The product of a small scale α-CD-NS synthesis was divided in half and placed in two beakers containing 40 mL of deionized Milli Q water. Under constant stirring and temperature (25 ºC), pH was monitored every hour using a Mettler Toledo pH meter (Greifensee, Switzerland). For one of the samples, concentrated hydrochloric acid was added when necessary, to ensure the pH was kept below pKa of imidazole (6.95). After eight hours, the solution was filtered and the product characterized as described in 3.2.3.

3.3.2. CD-NS washing optimization

The same amount of product was washed under different conditions; 40 ºC and 70 ºC under constant stirring and ultrasonic extraction with different washing times (2, 4, 6 and 8 h) and two (14:1 and 28:1) water to CD-NS ratios.

To perform the experiments, 0.14 g of product were initially rinsed with 10 mL of Milli Q water to dissolve the unreacted CDI. The solution was then centrifuged at 4350 rpm using a VWR Mega Star 600R centrifuge (Radnor, Pennsylvania, U.S.) and the supernatant was taken for further analysis. Then, the product was washed changing only one of the above conditions at a time. At every time point, the solution was centrifuged using the same conditions as above and the supernatant and pellet were kept for HPLC-DAD and nitrogen content analysis, respectively. The pellet was dried at 50 ºC until a constant weight was obtained and its nitrogen content was determined via elemental analysis on a Perkin Elmer 2400 Series II CHNS/O Organic Elemental Analyzer (Waltham, Massachusetts, U.S.) using optimum burning conditions and pure oxygen atmosphere.

3.4. HPLC-DAD for imidazole quantification

3.4.1. Method validation

An HPLC method for the determination of imidazole in the washing solution was developed based on the one described by You Zhu et al. (Y. Zhu et al., 2015). Quantification was performed using an HPLC Waters 2695 Separations Module equipped with a Waters 2996 Photodiode Array Detector. Isocratic separation was performed using an Acquity UPLC BEH HILIC column (1.7 µm, 2.1 x 100 mm) from Waters (Milford, Massachusetts, U.S.). The composition of the mobile phase was a mixture of acetonitrile and 5 mM ammonium dihydrogen phosphate (80:20, v/v), adjusted with orto-phosphoric acid at pH 5. The mobile phase was filtered under vacuum using an Albet 0.2 µm nylon membrane filter (Dassel, Germany) and degassed for 30 min in an ultrasonic bath before use. An isocratic flow of 0.4 mL was applied and the column oven was maintained at 35ºC. Standards were prepared gravimetrically using mobile phase as dilution solution. The run time was 5 min and the wavelength defined to monitor imidazole at the retention time of 1.14 min was 215 nm. This method was validated according to the guidelines provided by the Food and Drug Administration (FDA) [25] and International Conference on harmonization (ICH) [26] and the parameters studied were linearity, intermediate, intra- and inter-

day precision and accuracy. Empower Pro software was used for HPLC data analysis.

3.4.2. Sample quantification

After validation, imidazole was quantified in the supernatant samples (n=3) from the different time points and conditions used in the washing optimization (see section 2.3.2. for further details). When required, samples were diluted using mobile phase to fit within the method's linear range and were analysed as described above.

3.5. Evaluation of ethylene absorption capacity of α-CD-NS and other absorbents

3.5.1. Brunauer-Emmett-Teller (BET) surface area análisis

N_2 adsorption and desorption isotherms were recorded at -196 ºC in an ASAP 2020 Micromeritics apparatus (Norcross, Georgia, U.S.). Prior to analysis, the synthesized α-CD-NS were degassed at 110 ºC under vacuum.

3.5.2. GC-FID method for the determination of ethylene

A method for ethylene analysis was developed by slightly modifying the one described by A. C. Guerreiro et al. (Guerreiro et al., 2017). Ethylene was measured using an Agilent 8860 gas chromatography system (Santa Clara, California, U.S.) fitted with a TG-BOND Alumina (Na2SO4) column (0.53 mm internal diameter, 30 m length and 10 µm film thickness) from Thermo Scientific (Waltham, Massachusetts, U.S.) and coupled to a flame ionization detector (FID) Separation was carried out in isocratic mode with a constant oven temperature of 60 ºC. Inlet and detector temperatures were both 150 ºC and the run time was 5 min with ethylene reaching the detector at 3.5 min. Helium gas was used as carrier at a flow of 3.5 mL min^{-1}. Gas samples were manually injected into the GC-FID using a Trajan 1 mL air-tight syringe fitted with a 50 mm length 0.63 mm OD side hole luer lock needle (Ringwood, Victoria, Australia). A certified 10.29 µL L^{-1} gas mixture of ethylene balanced in synthetic air (Nippon gas, Belgium) was injected using different volumes (0.1-1 mL)

on Splitless mode to achieve linear instrument response. OpenLab CDS ChemStation software was used for data analysis.

3.5.3. Ethylene removal experiments

All ethylene removal experiments were carried out at room temperature (25ºC) and for a period of eight days. A series of absorbent compounds were tested for ethylene removal capacity: previously synthetized α-CD-NS and commercial bentonites and zeolites. After drying at 100 ºC for 18 h, 0.3 g of each compound were placed inside 20 mL vials and closed with N 24 PP screw caps fitted with a 3.2 mm Mackerey-Nagel Silicone/PTFE septum (Allentown, Philadelphia, U.S.). Three replicates of a control vial without absorbent compound were also considered for every time point. Then, the inner atmosphere of the vials was replaced using the certified 10.29 µL L^{-1} ethylene gas mixture. For every time point replicate (24, 48, 72, 96 and 192 h), 0.5 mL were withdrawn through the septum using the air-tight syringe, injected manually, and analysed using the method conditions described in 2.5.1. Experiments were conducted in triplicate.

3.6. Statistics

Data analysis was performed using Microsoft Excel software, version 16.58. For variables with 3 or more categories, statistical analysis was performed using one-way ANOVA. A *p* value indicating the probability of significance of <0.05 was used to indicate statistically significant differences.

4. Results and discussion

4.1. Synthesis scale-up and characterization

Apart from the chemistry, there is a number of factors affecting the success of ball-milled organic synthesis (Stolle et al., 2011) such as, by order of importance, rotation frequency, time, type and size of milling material, number of milling balls and mode of operation.

CD-NS synthesis scale-up was performed using α-CD and carbonyldiimidazole as a crosslinker with a 1:4 molar ratio in a 500 mL zirconium oxide jar with 100 10mm diameter balls and 33.8 g of α-CD and 22.5 g of CDI. The reaction time was kept constant to focus on varying only the rotation frequency.

Three different rotation frequencies were tested: 310, 350 and 400 rpm. Above 400 rpm, jar temperature increased dramatically, which led to product degradation and, therefore, rotations above 400 rpm were not tested.

The crosslinked α-CD-NS polymers were insoluble in a range of solvents such as water, diethyl ether, dimethylformamide, petroleum ether and dimethyl sulfoxide or ethanol, agreeing with previously reported data (Pedrazzo et al., 2020; Trotta et al., 2012). Figure 1.2 shows the FTIR spectra of α-CD compared to the synthesized α-CD-NS. The band present at around 1740 cm^{-1} indicated the presence of a carbonyl bond within the structure, which is indicative of an effective crosslinking between cyclodextrin hydroxyl groups.

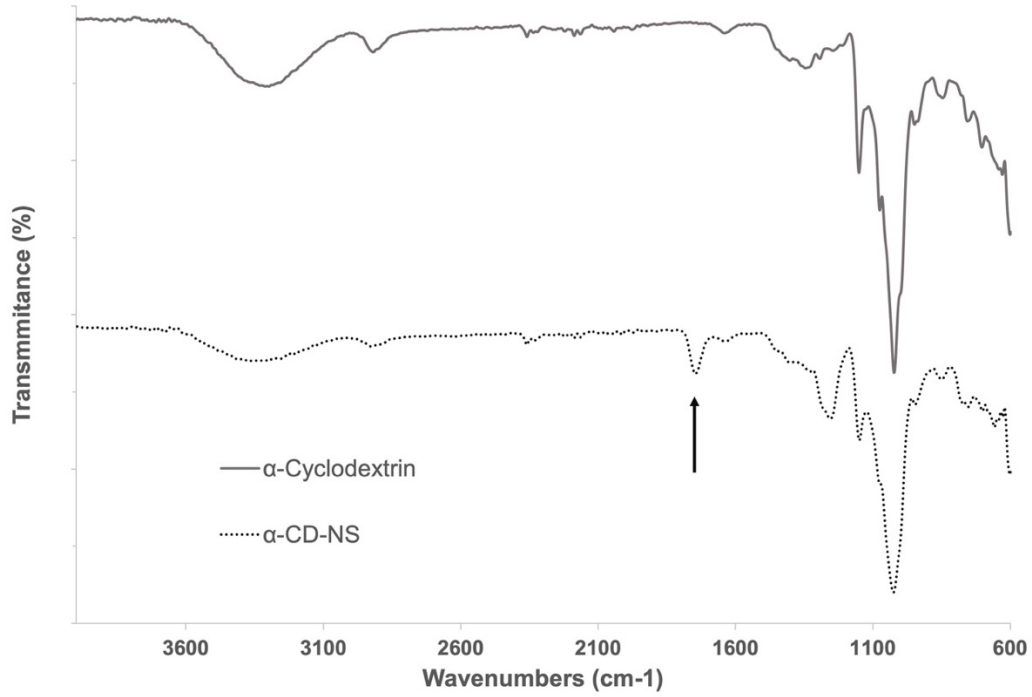

Figure 1.2. FTIR analyses of α-cyclodextrin and washed α-CD-NS. Arrow indicates the band of interest at around 1750 cm-1 assignable to the carbonyl group of the ester bond formed.

As expected for mechanochemical synthesis (Jicsinszky et al., 2017; G. W. Wang, 2013), high yields (>95 %) calculated by comparing the weight of the dry product against the sum of α-CD and one C=O bridge per cyclodextrin unit were obtained for all three frequencies tested. As can be seen by the thermogravimetric mass-loss curves and the corresponding derivative curves produced by all three rotation speeds (Figure 1.3), the synthesized polymers exhibited very close degradation paths with a relative maximum at 315 ºC and, as a result, the same molecular structure was expected for them. It is worth to point out that the three samples had very similar adsorbed water amounts, which was calculated to be 8.59 ± 0.56 %.

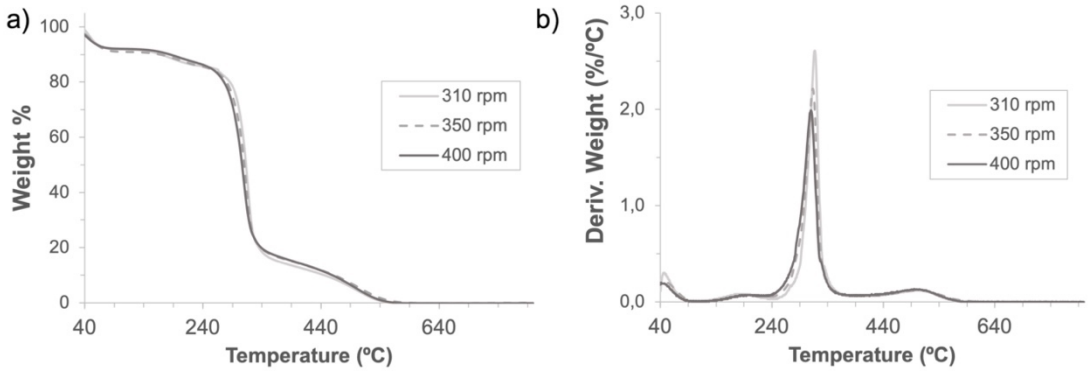

Figure 1.3. Thermogravimetric analyses (a) and their derivatives (b) of α-CD-NS obtained through 3 hours of mechanochemical (ball mill) synthesis at 310, 350 and 400 rpm using a 500 mL zirconia jar.

The comparative analysis of XRD diffraction patterns (Figure 1.4) was used to observe the differences in the spectra of α-cyclodextrin and the crosslinked α-cyclodextrin nanosponges. α-CD showed clearly defined reflections with sharp peaks, which confirmed its crystalline structure. However, diffractogram of α-CD-NS had two wide peaks with the maxima at 13.9º and 20.7º which corresponded to an amorphous polymer structure. This phenomena, which further characterizes α-CD-NS, has been observed for similar materials (W. Li et al., 2019).

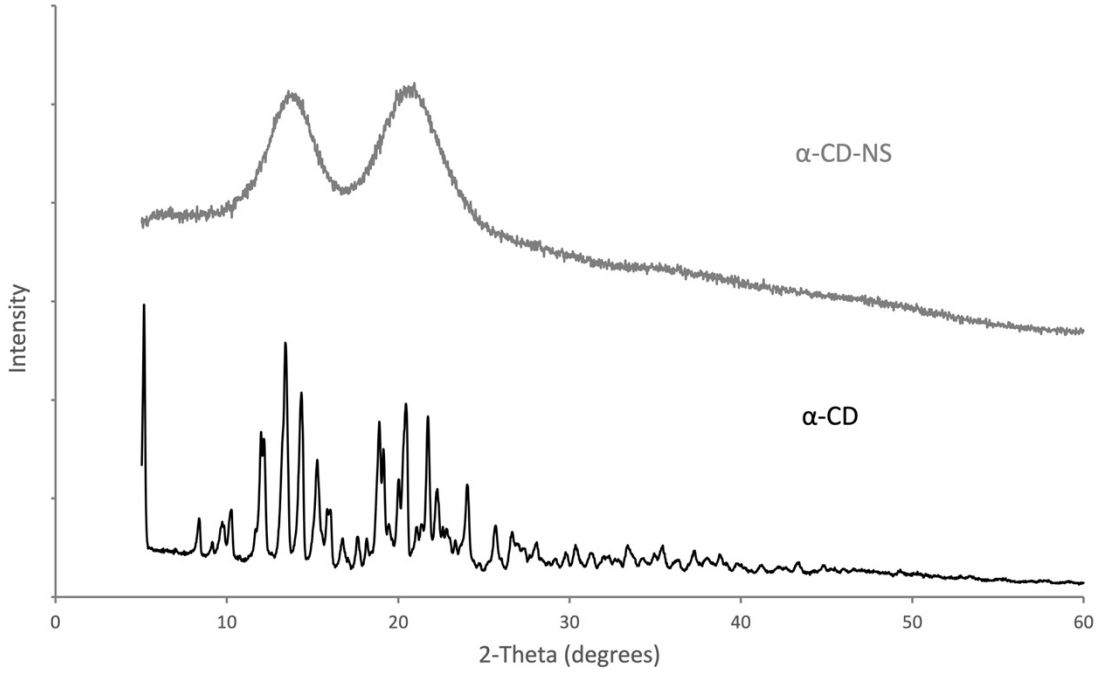

Figure 1.4. X-ray diffraction spectra for pure α-CD and the synthesized α-CD-NS.

After washing, particle size of the crosslinked cyclodextrins (figure 1.5) was around 400 nm as determined by DLS, having a polydispersity index of 0.222 ± 0.015, which is in line with what has been previously reported for cyclodextrin-based complexes after a wet milling cycle using a planetary ball mill (Calvo et al., 2011). In the case of cyclodextrin polymers that did not undergo a ball milling process, similar size measurements could only be achieved on the supernatant of a centrifuged dispersion (Ansari et al., 2011).

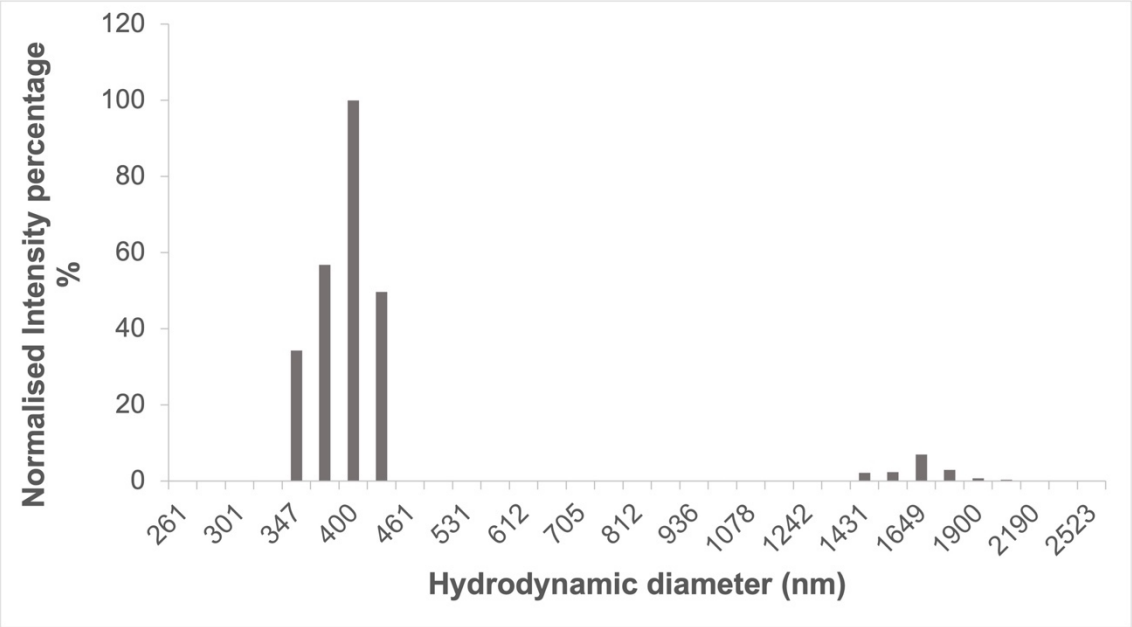

Figure 1.5. Size distribution of ball mill synthesized α-CD-NS after washing determined by dynamic light scattering (DLS).

Figure 1.6a shows the FTIR spectra performed on the scaled up α-CD-NS at the different rotations. As TGA curves exhibited similar adsorbed water for all three samples, and to semi-quantitatively compare the intensity of the carbonyl band, hence determining differences on the crosslinking degree, the ratio of the area of carbonyl band at 1740 cm^{-1} and the water bending band at 1640 cm^{-1} was calculated. Figure 1.6b shows the different ratios obtained for the rotation frequencies tested when compared to the ratio corresponding to the synthesis described by Pedrazo et al. (Pedrazzo et al., 2020) performed in a 50 mL jar at 600 rpm. We could observe that at 350 rpm, the carbonyl to water ratio was relatively higher than at 310 and 400 rpm. This could potentially mean a lower cross-linking degree at 310 rpm and some temperature-affected cross-linking degradation occurring at 400 rpm due to the sudden increase in reaction temperature.

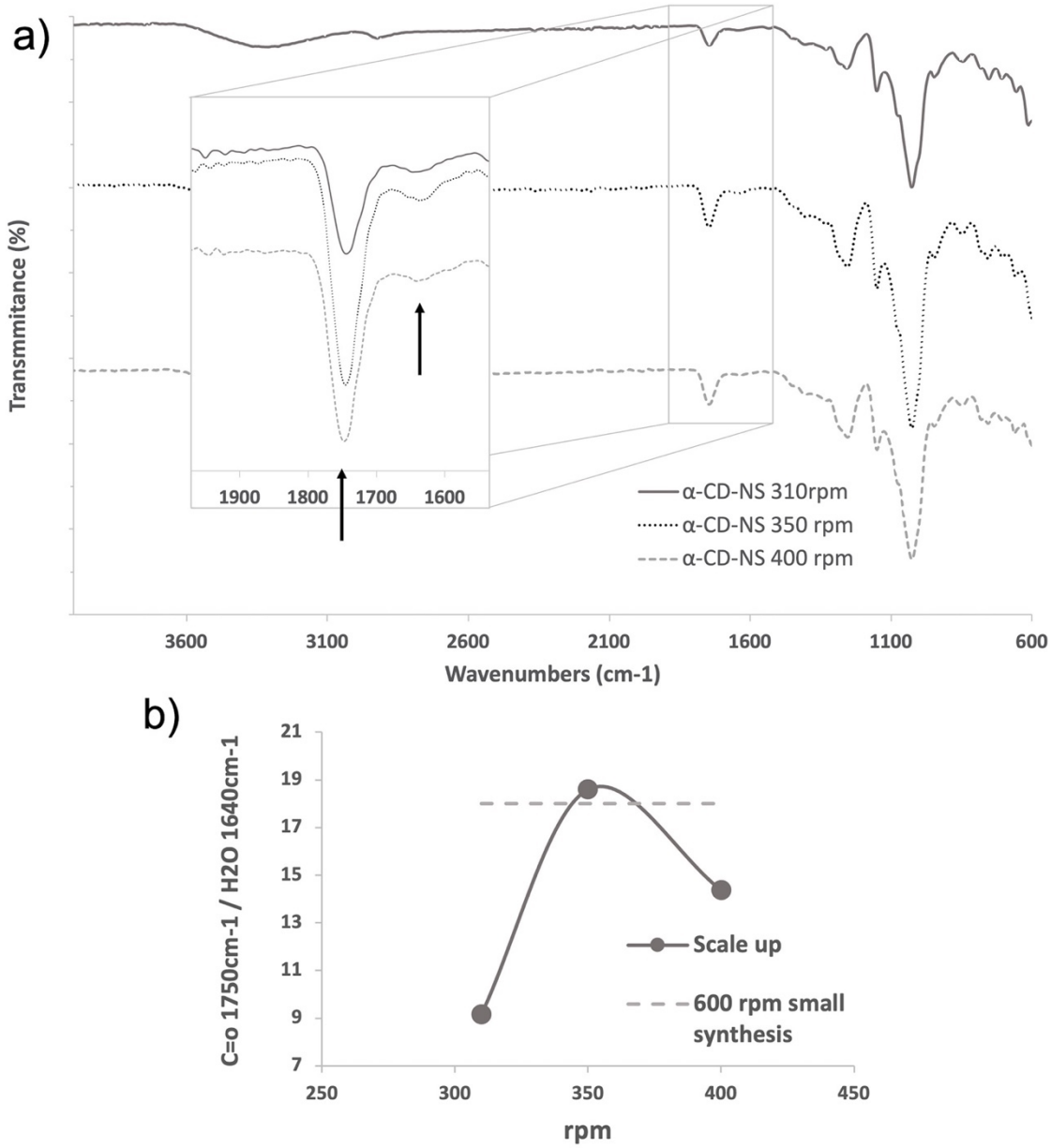

Figure 1.6. Analysis of CD-NS mechanochemical (ball mill) synthesis scale-up at 310, 350 and 400 rpm using a 500 mL zirconia jar: (a) FTIR analyses of α-CD-NS obtained with arrows indicating the band of interest at around 1750 cm-1 assignable to the carbonyl group of the ester bond and the band at 1640 cm-1 assignable to bending of the adsorbed water. (b) Carbonyl band (1750 cm-1) and water bending band (1640 cm-1) area ratio.

Considering the high yield, TGA similarities and the carbonyl to water ratio signal from FTIR, it could be stated that 350 rpm rotation frequency produced an identical α-CD-NS product to the one obtained in the small scale synthesis (Pedrazzo et al., 2020) and that the scale-up was successfully performed. Our results showed that the scale-up process cannot be performed by just proportionally increasing ball

milling parameters and that a close monitoring of the optimization is needed to ensure that the same final product is achieved, while maintaining the yields.

4.2. HPLC-DAD method validation

Several methods have been reported for the determination of imidazole derivatives using a different range of analytical techniques. However, none of them focus on just the determination of free imidazole. Zhu and collaborators reported an UV method for the determination of imidazole and two imidazole derivatives using high performance liquid chromatography (Y. Zhu et al., 2015). Considering this method as a starting point, we aimed at developing a faster, cheaper, more easily accessible and precise method that would allow imidazole monitoring in CD-NS, even at very low concentrations using high performance liquid chromatography (HPLC) coupled to a Diode Array Detector. In this way, the validated method will allow us not only to analyze imidazole in the synthetized CD-NS, but also to evaluate a possible residual imidazole release when the CD-NS are applied as ethylene scavengers in contact with foods. The method was validated in terms of linearity, intermediate, intra- and interday precision and accuracy, following a 5-day validation protocol according to FDA and ICH guidelines. The described chromatographic conditions produced a peak eluting at 1.48 min (Figure 1.7a). To evaluate the method's linearity, five replicates of eight evenly distributed calibration standards ranging 0.1 to 10 μg g^{-1} were prepared gravimetrically and analysed as described above. For intermediate precision evaluation, three quality control (QC) samples at low (LQC: 2 μg g^{-1}), medium (MQC: 4 μg g^{-1}) and high (HQC: 6 μg g^{-1}) concentrations (n=3) were also analysed each day. Calibration curves were obtained by plotting peak area against concentration. The acceptance criteria involved a Pearson coefficient of at least 0.999 and the calibration standards' accuracy within ± 10 %. To generate the best data for the chosen calibration range, six weighing factors ($1/\sqrt{x}$, 1/x, 1/x2, $1/\sqrt{y}$, 1/y, 1/y2) were evaluated. Linearity data can be found in Figure 1.7b. The weighting factor 1/x was chosen since the sum of relative errors was smaller while still presenting a mean R^2 value of at least 0.999. The limit of detection and quantification were calculated using a 25 ng g^{-1} standard and were 3.07 ng g^{-1} and 10,24 ng g^{-1}

respectively, which is considerably lower than previously reported (Y. Zhu et al., 2015), meaning that very low concentrations of imidazole contaminant can be effectively detected in the finished product.

Interday precision and accuracy (Figure 1.7c) were evaluated at eight concentrations ranging from 0.1 to 10 μg g^{-1}. The calculated relative standard deviations (RSD) were lower than 6 % for all concentration levels, while accuracy was within a ± 10 % interval from the target concentration. Intra-day precision and accuracy (Figure 1.7c) were assessed at 4 different concentration levels (0,1, 1, 5 and 10 μg g^{-1}) using six replicates for each concentration. The obtained RSDs were lower than 5 % for all concentrations, presenting an accuracy within a ± 10 % interval. Moreover, intermediate precision and accuracy (Figure 1.6c) were assessed at 3 concentrations (2, 4 and 6 μg g^{-1}) performed in triplicate over the 5-day validation protocol (n=15). The results showed RSDs lower than 3 % and the relative error in terms of accuracy being within a ± 2 % interval.

a)

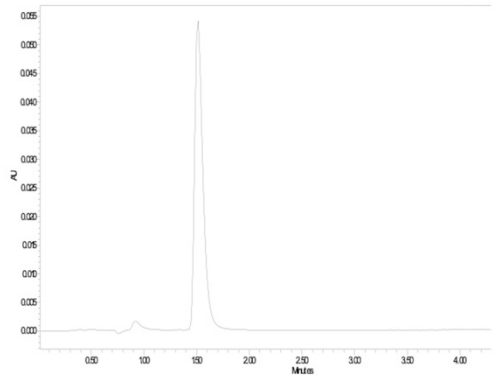

b)

Weight	Linearity	Slope	Intercept	R2
1/x	0.1-10	54545.60 ± 1303.41	1394.12 ± 987.53	0.9996 ± 0.0003

c)

	Theoretical concentration (μg/g)	Measured (μg/g)	RSD (%)	Relative Error (%)
Inter-day n=5	0.1	0.11 ± 0.01	5.64	5.95
	0.25	0.23 ± 0.01	4.11	-8.38
	0.5	0.54 ± 0.01	1.91	3.64
	1	0.98 ± 0.03	2.74	-3.46
	2.5	2.50 ± 0.03	1.02	-0.49
	5	5.08 ± 0.07	1.28	0.79
	7.5	7.55 ± 0.08	0.99	0.25
	10	10.03 ± 0.11	1.10	-0.24
Intra-day n=6	0.1	0.12 ± 0.01	3.25	9.35
	1	1.00 ± 0.02	1.58	-0.93
	5	5.30 ± 0.14	2.55	4.92
	10	10.72 ± 0.29	2.68	6.16
Intermediate n=15	2	2.08 ± 0.05	2.64	-0.10
	4	4.05 ± 0.10	2.43	0.61
	6	6.07 ± 0.09	1.55	1.12

Figure 1.7. HPLC-DAD imidazole quantification linearity and validation data: (a) typical HPLC-DAD chromatogram at λ=215 nm. (b) Imidazole linearity data (n=5) (c) Inter-day (n=5), intra-day (n=6) and intermediate (n=15) precision and accuracy. All concentrations are in μg/g. RSD, relative standard deviation. When applicable, values are presented as mean values ± standard deviation.

Overall, since RSDs and accuracy for all criteria were lower than 15 %, the HPLC-DAD method was successfully validated, allowing for a robust and sensitive quantification of imidazole within 5 min.

4.3. α-CD-NS washing optimization

N-N carbonyldiimidazole (CDI) is a commonly used reagent in peptide synthesis for coupling amino acids and in organic chemistry for the formation of ester and amide bonds. In this work, CDI has been used to crosslink α-cyclodextrin units by means of ester formation via mechanochemical synthesis. After the reaction, a washing step is necessary to eliminate free imidazole generated in the reaction and to wash the unreacted CDI and the imidazoyl carbonyl groups still present within the nanosponges network. Due to imidazole's acute toxicity (LD_{50} rat 960 mg kg^{-1} bw) (ECHA, 2012), the optimization of the washing step with water is needed to ensure its complete removal from the new material.

During the cross-linking reaction, CDI generates two molecules of imidazole which are known to be able to catalyze the hydrolysis of ester bonds at different rates when being in its neutral form (imidazole pH=pKa) (Kirsch & Jencks, 2002). To determine a possible negative influence of pH in imidazole-induced hydrolysis of CD-NS, two washing protocols (8 hours at 40 ºC under constant stirring) at pH=pKa (neutral, reactive) and pH<pKa (protonated, unreactive) were compared. Two identical amounts of synthesized product were washed, and their pH was monitored every hour. One of the washing solutions was maintained at a constant pH of 6.9, equal to imidazole's pKa. To the other solution, concentrated hydrochloric acid was added when necessary to keep a constant pH of 6.0. After filtering and drying, the same yields (99.5 %) were obtained. FTIR and TGA analysis of the two washed products (Figure 1.8 & 1.9) did not reveal any differences between the ratio of the area of the carbonyl band at 1740 cm^{-1} and the water bending band at 1640 cm^{-1}, as well as in the thermogravimetric kinetics of the samples. This indicates that no molecular structure differences were produced during both washes at pH=pKa and pH<pKa, and, therefore, pH control is not required through the washing step.

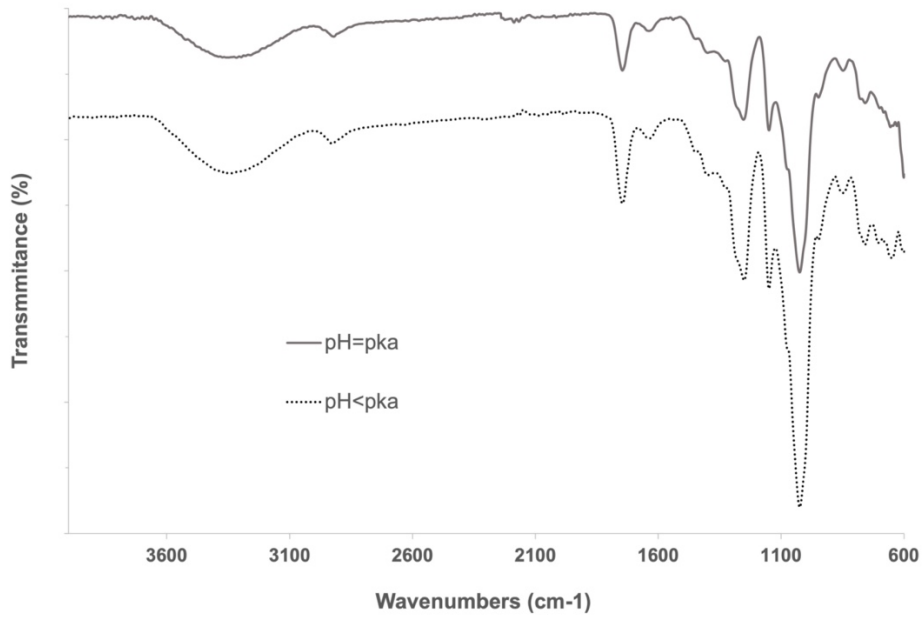

Figure 1.8. FTIR analyses of α-CD-NS washed at pH 6.9 (solid line) and pH 6.0 (dotted line). The band of interest at around 1750 cm-1 assignable to the carbonyl group was visible in both samples.

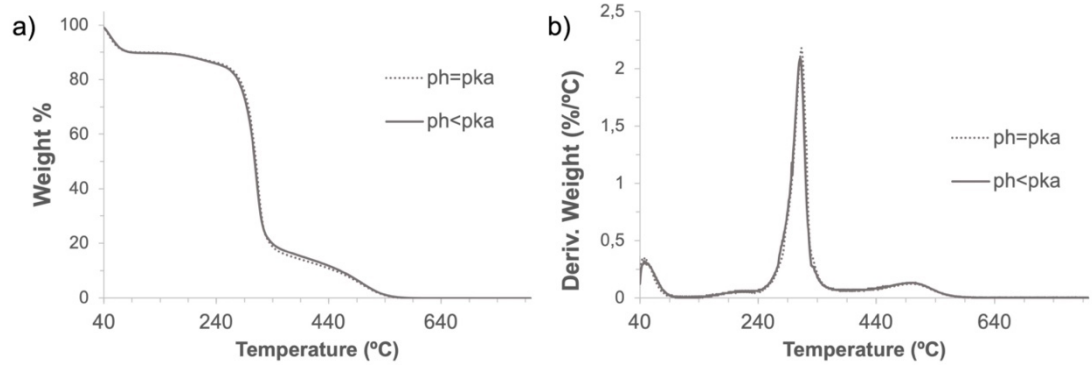

Figure 1.9. Thermogravimetric analyses (a) and their derivatives (b) of α-CD-NS washed at pH 6.9 and 6.0.

The results obtained showed that there was no statistical difference (p=0.05) among the different water to solute (CD-NS) ratios used. Figure 1.10 shows the imidazole extracted at different time points and conditions, plotted against the theoretical imidazole present in the sample. Different letters show significant differences (p≤0.05) between populations. We can observe that extraction by stirring at 70 ºC gave the highest extraction efficiency, extracting up to 110 % of the theoretical imidazole, which is within the method's accuracy limits. However, after drying, a

crystallized yellow product was obtained instead of the normal white powder (Figure 1.11).

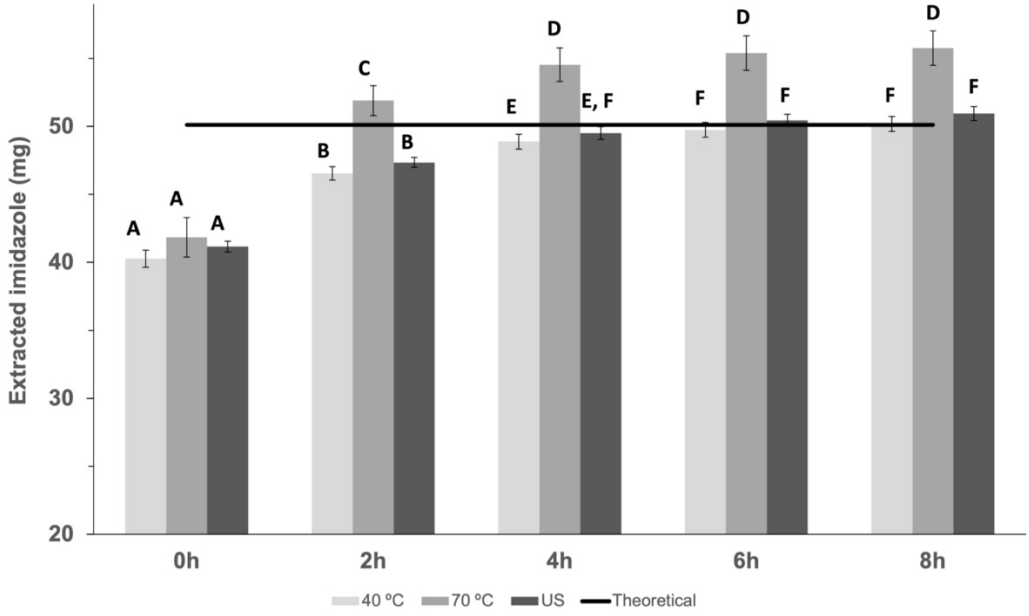

Figure 1.10. Results of the amount of imidazole extracted across time at 40 ºC and 70 ºC under constant stirring and ultrasonic extraction. Mean ± SD of three replicates is shown and compared against the theoretical imidazole in the samples. Different letters show significant differences (p=0.05) between samples.

As the CD-NS washed at 70 ºC looked like a crystalized powder, an X-ray diffraction analysis was performed on α-CD-NS washed at 40 ºC and 70 ºC (Figure 1.11). Both diffractograms showed a disordered crystal structure corresponding to an amorphous structure. However, a subtle shift could be observed in the maximum of both broad peaks, suggesting a significant change within the amorphous structure, as the shifts were not all unidirectional.

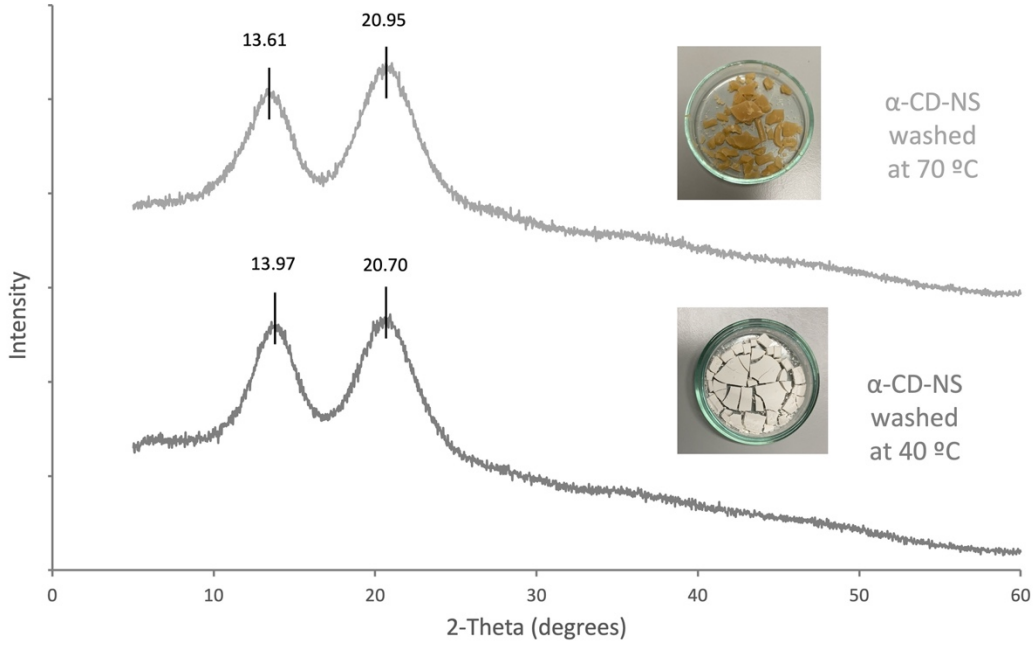

Figure 1. 11. X-ray diffraction spectra α-CD-NS washed at 40 ºC and at 70 ºC.

As α-cyclodextrin is known to be present in different hydrate forms (Georg et al., 2005; Granero-García et al., 2012), we hypothesize that a type of cross-linked α-cyclodextrin hydrate is formed during washing at 70 ºC, although more efforts are needed to fully characterize and understand these changes in the CD-NS structure.

According to our results, extraction efficiency at 4 hours cannot be considered significantly different ($p<0.05$) between stirring at 40 ºC or applying ultrasonic extraction. However, whereas for ultrasonic extraction maximum efficiency (99.39 ± 0.96 % imidazole extraction) was reached at 4 hours, stirring at 40 ºC only reached a maximum of extraction (99.39 ± 1.32 %) at 6 hours. Despite requiring longer processing times, a washing step for six hours at 40 ºC under constant stirring was selected as the preferred washing conditions, based on its easier scalability when compared to ultrasonic extraction. This was further confirmed by performing an elemental analysis of the washed product targeting carbon, hydrogen and nitrogen content, where a signal within the detection limit of the technique (± 0.3 % of Nitrogen) was considered negligible. Altogether, the described washing methodology allows for a faster washing step, with the potential to cut down energy costs.

4.4. α-CD-NS ethylene removal capacity

As CD-NS are formed by either the inner cavities of alpha-cyclodextrin and the outer cavities of the crosslinked network, we evaluated CD-NS porosity in an attempt to understand how ethylene could be absorbed by CD-NS. The porosities and pore sizes of α-CD-NS were examined by their N_2 adsorption/desorption isotherms (Figure 1.12). The isotherms displayed a typical type II profile corresponding to an unrestricted monolayer-multilayer adsorption expected for non-porous or macroporous adsorbent materials. The specific surface area was 3.90 $m^2 g^{-1}$ and the average pore diameter 10.46 nm. The pore volume of pores less than 98 nm width was 0.010 $cm^3 g^{-1}$. This high surface area matches what has been previously reported for other cyclodextrin monomers (K. Zhou et al., 2018) suggesting polymerization does not have an effect on surface area increase. Moreover, the data suggests that the presence of macropores (>50 nm) within the cyclodextrin polymeric network would likely impede α-CD-NS to outperform their monomer counterparts as ethylene scavengers if not by their higher physical and chemical stability and water insolubility, which is a major concern when developing products intended to be in contact with fruit, as they require high humidity environments (≥90% relative humidity).

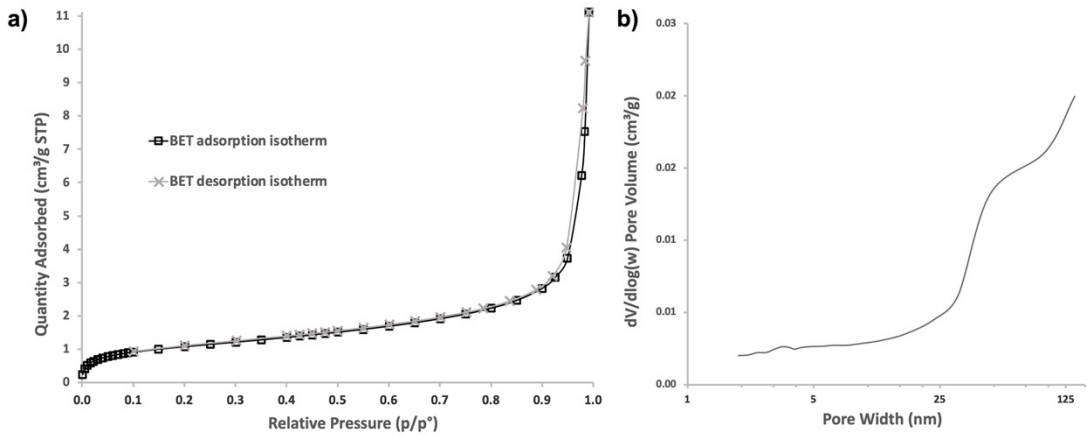

Figure 1.12. N_2 adsorption/desorption isotherms (a) and pore size distribution (b) of α-CD-NS.

Linear response using the GC-FID method described above was obtained and the amount of ethylene inside the vials was successfully quantified by integrating the

area under the ethylene peak. To evaluate ethylene removal capacity, the ethylene ratio between each replicate and the control for each time point was calculated.

Figure 1.13 shows the ethylene removal behavior of the different absorbent compounds tested. In the case of zeolites, the concentration inside the vial tended to increase throughout the assay and, as a result, negative ethylene removal percentages ranging from -44 % to -124 % were obtained. As zeolites adsorption capacity increases very rapidly with pressure (Sarker et al., 2017), the results obtained can be due to the fact that zeolites already removed some ethylene during the vial filling process, which could later be released during the assay, meaning a fast, yet weak ethylene removal capacity. With ethylene removal percentages ranging from -22 % to 11 %, bentonites showed no clear behavior that could demonstrate any potential ethylene removal capacity. However, α-CD-NS showed a clear tendency as an effective ethylene removal across time. Analysis of variance ($p>0.05$) showed that there was no difference between ethylene removed on day 3 and day 8 meaning that, after 72 hours, the maximum α-CD-NS ethylene removal capacity was reached. Furthermore, ethylene concentration inside the vial was maintained until day 8, suggesting no release of the removed ethylene back into the vial's atmosphere, which could indicate that an equilibrium state was reached (Trotta et al., 2011). At day 3, α-CD-NS ethylene removal capacity was calculated as 18 mL of ethylene per kilogram of α-CD-NS (18 mL kg^{-1} of adsorbent), which corresponds to 93 µL of ethylene h-1 kg $adsorbent^{-1}$. As most climacteric fruits and vegetables produce ethylene within the range of 0.1-10 µL kg-1 h-1 (Keller et al., 2013), α-CD-NS can be considered a suitable ethylene removal agent as it can remove more ethylene than what is produced by the fruit. When compared to permanganate-based ethylene scavengers, CD-NS ethylene removal performance, together with its non-toxic and organic, biodegradable nature, makes a reliable and effective ethylene removal alternative. Additionally, the fact that alpha-CD-NS does not react directly with ethylene, makes it possible to develop a strategy to recover empty CD-NS and reuse this material, which cannot be done in the case of permanganate-based ethylene scavengers, as permanganate readily reduces when in contact with ethylene.

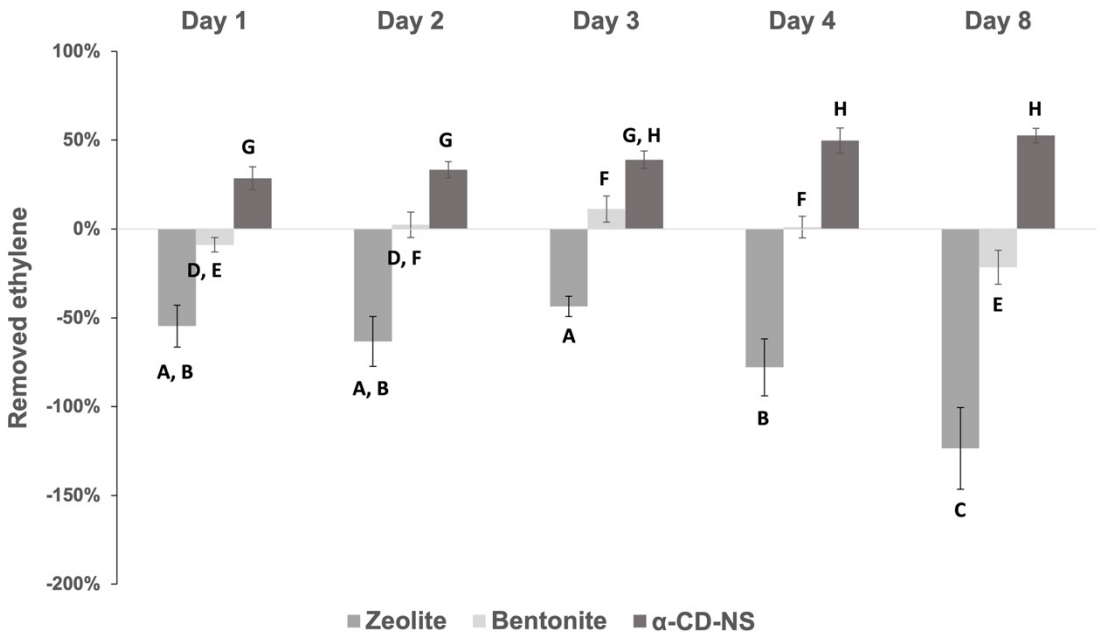

Figure 1.13. Ethylene removal percentage of α-CD-NS and commercial bentonite and zeolite across time. Mean ± SD of three replicates is shown. Different letters show significant differences ($p<0.05$) between samples.

5. Conclusions

Nowadays, the use of ethylene scavengers in the food packaging industry is often limited to different forms of potassium permanganate based products, creating the need for a non-toxic, robust, environmentally friendly ethylene removal solution. In this work, a solvent-free, green synthesis of α-CD-NS was successfully scaled-up 10 times using α-cyclodextrin and carbonyldiimidazole at a 1:4 (α-CD:CDI) molar ratio by mechanical alloying (3 h, 350 rpm rotation frequency) using a PM 100 planetary ball mill, as confirmed by FTIR, XRD and TG analyses. A washing step with water was optimized by monitoring the presence of contaminants (unreactive CDI and imidazole) with a validated liquid chromatography coupled to a diode array detector (HPLC-DAD) method targeting imidazole, allowing to achieve high yield (>95 %) contaminant-free CD-NS. Optimum washing conditions (99.39 ± 1.32 % imidazole extraction) were reached at 6 hours under constant stirring at 40 ºC, with no pH monitoring required. To our knowledge, this is the first time that α-CD-NS are successfully scaled-up with a mechanochemistry method and the first time their ethylene scavenging properties are reported. With a 93 μL h^{-1} $kg_{adsorbent}^{-1}$ ethylene

removal capacity, the synthesized α-CD-NS can be considered a green, biodegradable and safe ethylene scavenging alternative when compared to traditional potassium permanganate. Overall, this work demonstrates the potential of α-CD-NS to be a key player in the food packaging industry as ethylene scavenger, helping towards a better produce management and reducing fruit and vegetable losses throughout the food chain due to uncontrolled ripening.

Chapter 2:

Controlling beef microbial spoilage with diacetyl-based active packaging sachet

1. Introduction

As recently reported by the European Food Safety Authority (EFSA), the number of deaths related to foodborne outbreaks in the EU have been the highest of the last 10 years, with *L. monocytogenes* being the most common pathogen, and *Salmonella* spp. to a lesser degree (EFSA, 2023). This clearly justifies the great focus of the industry in demanding new active food packaging technologies targeting the control of pathogenic and spoilage microorganisms' growth in all packaged foods (Gracia-Vallés et al., 2022; Mukurumbira et al., 2022; Omerović et al., 2021).

In broad terms, active food packaging can be categorized into two types: non-migratory active packaging, involving scavengers that remove unwanted elements from the packaging environment; and active releasing packaging, where emitters enable migration of active, usually antimicrobial substances, into the packaging environment (Ahmed et al., 2022). Some examples of the main current antimicrobial agent trends used in active food packaging are inorganic nanoparticles (I. Kim et al., 2022), polysaccharides displaying natural properties such as chitosan (Bhowmik et al., 2022b; Flórez et al., 2022; Umaraw et al., 2020), and volatile organic compounds and essential oils (Becerril et al., 2007, 2020; Gutiérrez et al., 2011; López et al., 2007; Otero et al., 2014; F. Silva, Caldera, et al., 2019c). Another area of increasing interest is the exploitation of probiotics and bacterial antimicrobial metabolites as active components, which include compounds such as organic acids (e.g. propionic acid), acetoin, diacetyl, hydrogen peroxide and bacteriocins (Djebari et al., 2021; Espitia et al., 2016; Settier-Ramírez et al., 2021).

Diacetyl (2,3-Butanodione) is a volatile organic compound and one of the antibacterial molecules produced by lactic acid bacteria during fermentation (Novak et al., 2010). It is non-toxic, is considered a flavouring agent with no restrictions [FL-No 07.052] by EFSA and has been awarded the Generally Recognised As Safe (GRAS) status by the U.S. Food and Drug Administration (USFDA). Even though the antimicrobial properties of diacetyl have been known for many decades (Jay, 1982), its use in active food packaging has been limited due to its high volatility and strong buttery aroma (Teshome et al., 2022). Sodium stearate,

also a GRAS compound and food additive [E470a], is widely used in the food industry as emulsifier, stabilizer, thickener or gelling agent. Its ability to form hydrogels has recently been explored in active food packaging by using it as a carrier (Vanmathi Mugasundari & Anandakumar, 2022) often supported onto porous and adsorbent materials, such as diatomite, to increase its surface area and applicability (Mu et al., 2017). Such characteristics, together with its low market price, can make sodium stearate a good carrier for diacetyl in the development of an effective antimicrobial active packaging solution, adding an extra value to the food chain and market.

In a more than ever globalised food consumption, it is paramount to ensure not only quality, but also safety, while aligning to the customer trends for fresher, preservative-free foods. Over the last decades, the food industry has evolved towards this trend with the development of active food packaging, where the preservatives are incorporated within the packaging material rather than in the food product. Thus, this study aims to characterize and evaluate the effectiveness of an active antimicrobial sachet based on two GRAS components, diacetyl and sodium stearate, to inhibit *Salmonella enterica* growth, along with normal spoilage microbiota such as pseudomonads, total viable counts and lactic acid bacteria, in fresh beef filets.

2. Objectives

The objective of this chapter was to evaluate the antimicrobial susceptibility of *S. Enterica* and *L. Monocytogenes* to the VOC diacetyl. Then, active materials using diacetyl and sodium stearate, and sodium stearate embedded onto α-CD-NS, will be developed and their *in vitro* and *in vivo* antimicrobial capacity tested in *S. Enterica* inoculated fresh beef filets (Figure 2.1).

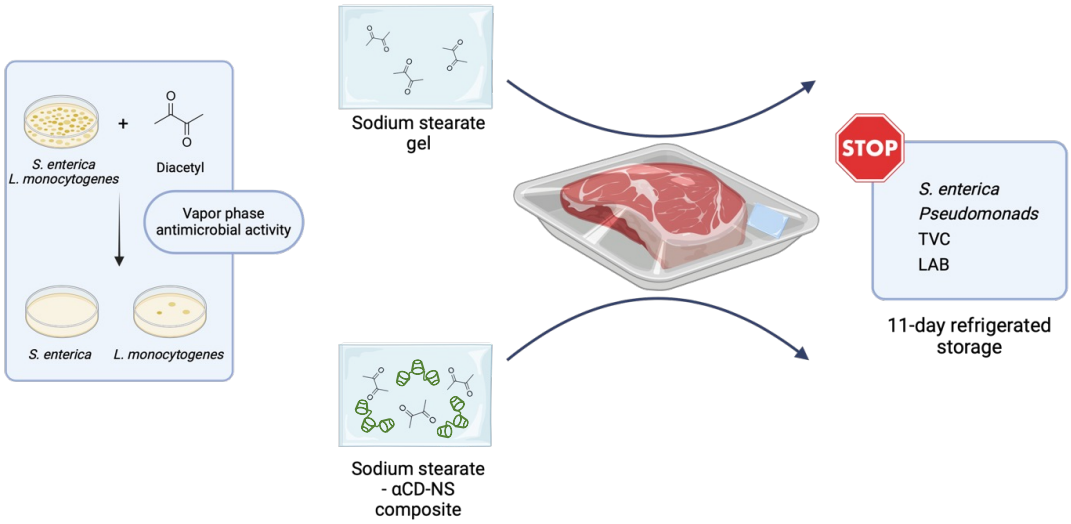

Figure 2.1. Process for the evaluation of the antimicrobial susceptibility of S. enterica and L. monocytogenes to diacetyl, and the evaluation of diacetyl-based active packaging materials in fresh beef meat.

3. Materials and methods

3.1. Materials

Diacetyl (2,3-Butanedione) was purchased from Sigma Aldrich (St. Louis, Missouri, U.S.). Sodium stearate (NaSt) was acquired from ThermoFisher (Kandel, Germany). Analytical grade ethanol was purchased from Honeywell (Charlotte, North Carolina, U.S.). Ultrapure water was generated using an Ultramatic Wasserlab purification system (Navarra, Spain).

3.2. Bacterial strains and growth conditions

Reference bacterial strains were obtained from the Spanish Type Culture Collection (CECT). Two strains were used in this study for its importance as pathogenic foodborne bacteria: one Gram-positive strain (*Listeria monocytogenes* CECT 911, serotype 1/2c) and one Gram-negative strain (*Salmonella enterica* subsp. *enterica* CECT 556). Bacterial strains were stored in the appropriate culture medium (Brain Heart Infusion broth for *L. monocytogenes* and Mueller–Hinton broth for *S. enterica*, both from Scharlab, Spain) supplemented with 20% (*v/v*) glycerol at − 80 ºC prior to use. *L. monocytogenes* CECT 911 was subcultured in Brain Heart Infusion agar (BHI agar, Scharlab, Spain) plates at 37 ºC in aerobic conditions, whereas *S. enterica* CECT 556 was subcultured on Mueller–Hinton agar (MHA, Scharlab, Spain) plates at the same temperature and atmospheric conditions.

3.3. Antimicrobial susceptibility of *L. monocytogenes* and *S. enterica* to diacetyl

3.3.1. Broth microdilution method

To evaluate the antimicrobial susceptibility of these two specific strains of *L. monocytogenes* and *S. enterica* to diacetyl, a broth microdilution method according to Clinical Laboratory Standards Institute guidelines (CLSI, 2012, 2015) was performed to determine the minimal inhibitory concentration (MIC). *L. monocytogenes* and *S. enterica* suspensions (approximately 1×10^8 CFU/mL) were prepared in 0.9% NaCl solution from overnight grown colonies at 37 ºC in BHI agar and MHA plates, respectively. An inoculum dilution (1×10^6 CFU/mL) was prepared from the previous suspension in the appropriate culture media and used as the final inoculum for the test. Diacetyl stock solution (25 mg/mL) was prepared in sterile physiological saline buffer. Serial two-fold dilutions ranging from 1024 to 8 µg/mL of diacetyl were prepared in MHB or Mueller Hinton Fastidious (MH-F) broth for *S. enterica* and *L. monocytogenes*, respectively Then, 50 µL of bacterial inoculum were added to each well containing 50 µL of diacetyl dilutions. Positive controls were carried out in diacetyl-free culture media. Negative controls were carried out with diacetyl dilutions and culture medium without bacterial inoculum. The minimal

inhibitory concentration (MIC) was assessed after 24h of aerobic growth at 37ºC and was defined as the lowest diacetyl concentration where no visible growth was observed. The absence of growth was further confirmed in a microplate reader at 620 nm.

3.3.2. Vapor diffusion assays

The surface of BHI agar and MHA plates were first inoculated by spreading 100 µL of *L. monocytogenes* and *S. enterica*, respectively, containing approximately 10^6 CFU/mL in physiological saline solution, prepared from overnight-grown colonies at 37 ºC in the respective culture media. Then, different volumes (0.5 µL, 1 µL, 2.5 µL and 5 µL) of diacetyl were added to a 9 mm sterile filter disc placed at the middle of the Petri dish lid. Control samples were prepared by adding the same volume of physiological saline solution to the sterile filter discs. Petri dishes were then sealed using Parafilm® and incubated overnight at 37 ºC. Antimicrobial activity was then evaluated in terms of the inhibition halo formed measured with a digital caliper.

3.4. Diacetyl active material formulations

3.4.1. Preparation and characterization of sodium stearate active gel formulations

Sodium stearate was dissolved in a 20 % (*v/v*) ethanol aqueous solution to achieve a 6 % w/v mixture which was heated at 60 ºC under constant stirring until a homogeneous gel was obtained. Then, different diacetyl volumes were added to the hot mixture to achieve 10 mL blends containing 0, 0.25, 0.5, 1, 2, 3, 4 or 5 % v/w of the active component. The blends were poured into 4.5 cm inner diameter Petri plates (Scharlab, Spain), left to cool down at room temperate until an opaque gel was obtained, sealed with Parafilm® and stored at 4 ºC until further use.

To evaluate the influence of diacetyl percentage in the mechanical characteristics of the active gel, the texture of diacetyl gel formulations was studied using a TA-XT2i Texture Analyzer (Stable Micro Systems, United Kingdom) fitted with a one-inch stainless steel cylindrical probe. The analysis was carried out on pieces (L x W x H)

of 3 x 3 x 3 cm coming from 3 independent replicates of gels containing diacetyl at concentrations of 0, 1, 2 and 5 % v/w. Data was processed using Exponent Stable Micro Systems version 6.1.10.0 (2016) software.

3.4.2. Preparation of sodium stearate – alpha cyclodextrin nanosponges composites

A 6 % w/v NaSt mixture in a 20 % (*v/v*) aqueous solution was prepared as described above. Food-grade alpha-cyclodextrin nanosponges (α-CD-NS) were prepared by mechanochemical synthesis as previously reported (Rupérez et al., 2022). Active materials were prepared by thoroughly mixing 1 gram of α-CD-NS per 1.5 mL of hot NaSt blend containing the necessary amount of diacetyl to achieve a 2 % v/w granular composite.

3.5. *In vitro* antibacterial activity of active materials

MHA surface was first inoculated by spreading 100 µL of *S. enterica* inoculum containing approximately 10^6 CFU/mL in physiological saline solution, prepared from overnight-grown colonies at 37 ºC in MHA. Each material was placed on the middle of the Petri dish lid. The plates were then sealed with Parafilm and incubated at 37 ºC overnight. In order to determine the optimum gel formulation, the antimicrobial testing of NaSt active materials containing different diacetyl concentrations (0, 0.25, 0.5, 1, 2, 3, 4 or 5 % v/w) was performed by cutting gel pieces of two sizes (L x W x H): 1.5 x 1.5 x 0.5 cm and 3 x 1.5 x 0.5 cm, weighing approximately 1.3 and 2.6 grams respectively. Optimal gel formulation as well as the equivalent amount of NaSt-α-CD-NS composite was also tested embedded in in-house made non-woven PP (40 g/m^2) (Dorsan, Spain) sealed active sachets.

Antimicrobial activity was evaluated in terms of the inhibition halo formed. All results were the product of at least three independent replicates.

3.6. Ethanol and diacetyl release quantification

To determine the amount of ethanol and diacetyl released at the *in vitro* antimicrobial testing, 1.3 grams of both NaSt gel and NaSt-α-CD-NS composite

active materials were placed in 20 mL vials, closed with N 24 PP screw caps fitted with a 3.2 mm Mackerey-Nagel Silicone/ PTFE septum (Allentown, PA, USA) and incubated at 37 ºC for 24 hours.

Ethanol and diacetyl were measured using an Agilent 8860 gas chromatography system (Santa Clara, CA, USA) coupled to a flame ionization detector (FID) and fitted with a Zebrom Z-624 column (0.32 mm internal diameter, 30 m length, and 1.80 µm film thickness) from Phenomenex (Torrance, CA, USA). Separation was performed maintaining an initial temperature of 35 ºC for 4 min and then raising it to 150 ºC at a 10 ºC/min rate. Inlet and detector temperatures were both 150 ºC, and the run time was 15 min, with ethanol and diacetyl reaching the detector at 4.13 and 7.31 min, respectively. Helium gas was used as a carrier at a flow of 1.6 mL/min. Quantification standards were prepared gravimetrically in methanol and sampled using the Full Evaporative Technique (FET) (C. Y. Zhang et al., 2015) by heating 10 µL of each standard in 20 mL vials sealed with N 24 PP screw caps fitted with a 3.2 mm Mackerey-Nagel Silicone/ PTFE septum (Allentown, PA, USA) at 80 ºC for 20 minutes. 0.5 mL gas samples were manually injected into the GC-FID using a 60 ºC pre-heated Trajan 1 mL air-tight syringe fitted with a 50 mm length 0.63 mm OD side hole Luer-lock needle (Ringwood, VIC, Australia) in Splitless mode. Five-point calibration curves were constructed over the concentration range of interest (10, 50, 200, 300 and 400 mg/mL for ethanol and 0.25, 0.5, 1, 2.5 and 5 mg/mL for diacetyl). Diacetyl and ethanol concentrations in the vial atmosphere were calculated by considering both the density of the solvent and the total volume of the vials. Limits of detection (LOD) and quantification (LOQ) were calculated using the equations $LOD = 3.3 * \sigma / S$ and $LOQ = 10 * \sigma / S$ respectively, where σ is the relative error of the calibration and S the slope.

3.7. *In vivo* anti-bacterial activity of active NaSt formulations sachets in fresh beef

Modified atmosphere packaged (MAP) fresh beef fillets were sourced from a nearby supermarket and cut into 100 g pieces in a safety cabinet. Beef samples were then inoculated by immersing the fillets for 30 s in a 100 mL *S. enterica* suspension (10^8

CFU/mL) and draining them for 10 seconds before placing them on top of a perforated cellulose/PP absorbent pads (Linpac Packaging, Spain) on a PET tray to dry for 20 min (Cancio et al., 2023). In-house made non-woven PP (40 g/m^2) (Dorsan Filtration, Spain) sealed sachets containing 10 g of active NaSt gel or active NaSt-α-CD-NS composites were attached to the inner side of the tray using double-sided tape. The package was then sealed using a multilayer PET-PE film and incubated at 4 ºC for up to 11 days. Sampling was performed at days 0, 3, 5, 7 and 11. Blanks containing diacetyl-free gels and composites were also analyzed on each sampling day. After incubation, 5 pieces of meat weighing approximately 10 grams were sampled across each beef tray and homogenized with buffered peptone water (1:10 dilution) in stomacher bags using a Stomacher 400 circulator (Seward, UK) at 300 rpm for 3 minutes. Serial dilutions of the stomached sample in peptone water were performed in sterile saline solution and an aliquot of 0.1 mL of each dilution was spread on the surface of different solid media. *S. enterica* was determined using Brilliant Green Agar (Scharlab, Spain) after incubation for 1 day at 35 ºC (Rambach, 1990). Total Viable Counts (TVC) were determined on Plate Count Agar (Scharlab, Spain) following incubation for 2 days at 30 ºC (F. Silva et al., 2018). Pseudomonads were determined on Cetrimide Agar (Scharlab, Spain) after incubation for 2 days at 20 ºC (F. Silva et al., 2018). Finally, total lactic acid bacteria were plate counted on Man Rogosa Sharpe agar (MRS, Scharlab, Spain) plates after incubation for 3 days at 30 ºC under microaerophilic conditions (F. Silva et al., 2018).

3.8. Statistical analysis

Data analysis was performed using Microsoft Excel software (Redmond, WA, USA), version 16.58. For variables with 3 or more categories, statistical analysis was performed using one-way ANOVA, where a p -value indicating the probability of significance of <0.05 was used to indicate statistically significant differences.

4. Results and discussion

4.1. Antimicrobial susceptibility of *L. monocytogenes* and *S. enterica* to diacetyl

The antimicrobial activity of diacetyl is deeply affected by the pH and additives of the growth substrate (Jay, 1982). So, in addition to its high volatility, it was not surprising that the broth microdilution assays did not yield any minimal inhibitory concentration values even at the highest concentration tested of 1024 mg/mL for any of the strains. However, the vapor diffusion assays showed complete inhibition of *S. enterica* for the smallest volume (0.5 µL) of diacetyl tested. *L. monocytogenes* was 10 fold less susceptible to diacetyl with complete inhibition obtained only with the highest volume (5 µL) of diacetyl tested. The results are in agreement with literature reports that indicate a higher efficacy of diacetyl in vapor phase than in liquid media (Lanciotti et al., 2003) and also a higher antimicrobial activity against Gram-negative than Gram-positive bacteria (Abouloifa et al., 2022; Dillon, 2014).

Given the increased susceptibility of S. enterica to diacetyl as well as its prevalence in fresh meat products (EFSA, 2022; EFSA, 2023) and with *Salmonella* producing 1103 illnesses during 2012 and 2019 in the US alone (Canning et al., 2023) for all further experiments *Salmonella enterica* subsp. *enterica* was selected as the model species.

4.2. Diacetyl-based active formulations

4.2.1. Sodium stearate active gel

A 6 % w/v sodium stearate load was considered adequate to ensure a valid network gel structure with sufficient intermolecular hydrogen bonds and Van der Waals forces (Mu et al., 2017; Vayachuta et al., 2021). The amount of ethanol, which is necessary to aid NaSt solubilization, was set at 20 % (*v/v*), as no detrimental effects on bacterial growth were obtained at this concentration (data not shown).

The chosen NaSt gel formulation was tested at different diacetyl percentages to assess its antimicrobial effect against *S. enterica* in solid medium (Table 2.1).

Correlative results showed complete *S. enterica* growth inhibition for a NaSt gel with 4 % diacetyl for size A, and with 2 % diacetyl for size B.

Table 2.1. Effect of Diacetyl percentage in NaSt gel on the growth of S. enterica in solid medium for two gel sizes (L x W x H); 1.5 x 1.5 x 0.5 cm (A) and 3 x 1.5 x 0.5 cm (B). Values are presented as mean ± standard deviation of at least three independent replicates. Means ± standard deviation followed by the same letter are not significantly different using one-way ANOVA ($p > 0.05$). C.I. stands for Complete Inhibition.

Diacetyl % *(v/v)*	**Inhibition halo (mm)**	
in gel	**A**	**B**
0.25	0	7.3 ± 4.0^{d}
0.5	0	48.3 ± 4.7^{b}
1	37.0 ± 2.6^{a}	82.3 ± 10.8^{c}
2	51.7 ± 1.5^{b}	C. I.
3	64.3 ± 3.1^{c}	C. I.
4	C. I.	C. I.
5	C. I.	C. I.

Mechanical properties on hydrogels are subject to an equilibrium of hydrogen bond and Van der Waals forces between the substrates, solvent and water. During gel preparation, a change on the physical characteristics of gel formulations as diacetyl percentages increased was observed, as can be seen by the texture profile analysis results of 6 % *w/v* NaSt gel samples with different diacetyl percentages (Table 2.2). The results showed that, while springiness and cohesiveness were not significantly affected, hardness and gumminess were influenced by the addition of diacetyl. At a percentage of 2 % (*v/v*), both parameters showed a significant increase and were in line with values previously reported for similar NaSt gels (Vayachuta et al., 2021), indicating a well-structured hydrogel network with good mechanical properties. However, as the percentage increased to 5 % (*v/v*), hardness and gumminess dramatically decreased. This phenomenon could be due to a disruption in the gel inner structure, leading to a loss in strength (Jakubczyk et al., 2022).

Table 2.2. Texture Profile Analysis (TPA) performed on 6 % w/v NaSt 20 % (*v/v*) Ethanol gels with varying diacetyl percentages. Values are presented as mean ± standard deviation of at least three independent replicates. Means ± standard

deviation followed by the same letter are not significantly different using one-way ANOVA ($p > 0.05$) between attributes in columns.

Diacetyl % *(v/v)* in gel	Hardness, N	Springiness	Cohesiveness	Gumminess, N
0	43.194 ± 1.472^{a}	0.148 ± 0.006^{a}	$0.069 \pm 0.003^{a,b}$	2.962 ± 0.190^{a}
1	41.939 ± 1.735^{a}	0.149 ± 0.003^{a}	0.064 ± 0.002^{a}	2.674 ± 0.213^{a}
2	47.626 ± 1.415^{b}	0.166 ± 0.018^{a}	$0.070 \pm 0.003^{a,b}$	3.334 ± 0.215^{b}
5	19.602 ± 1.639^{c}	0.139 ± 0.020^{a}	0.077 ± 0.006^{b}	1.495 ± 0.116^{c}

Based on both assays, a formulation with 2 % (*v/v*) of diacetyl was chosen for all further experiments. This selection was based on the ability to generate complete growth inhibition of *S. enterica* in solid medium and its mechanical properties that were considered like those of a soap bar in terms of hardness, and with the appropriate consistency for practical manipulation.

4.2.2. Sodium stearate – alpha cyclodextrin nanosponges active composites

Some porous and absorbent materials can increase both stability and release of volatile compounds on sodium stearate by increasing the surface area while providing a network where the gel can be embedded (Mu et al., 2017). Aiming to maximize the release of diacetyl, a sodium stearate – alpha-cyclodextrin nanosponges (NaSt-CDNS) composite containing 2 % diacetyl was prepared. The anti-*Salmonella* activity of a composite equivalent to that of a gel size (L x W x H) 3 x 1.5 x 0.5 cm showed complete inhibition of *S. enterica* in solid medium indicating that the composites have a similar antimicrobial effect as their gel counterparts.

4.3. Quantification of ethanol and diacetyl reléase

To assess the release differences between the NaSt gel and the NaSt-CDNS composite active materials, a GC-FID method allowing for simultaneous quantification of ethanol and diacetyl in vapor phase was developed. For both compounds, good linearity was obtained ($R^2 > 0.99$) over the desired working range (10-400 mg/mL for ethanol and 0.25-5 mg/mL for diacetyl) and the relative error between the measured and the spiked concentrations obtained was always under

5 %. While the LOD and LOQ for ethanol are slightly lower than what has been described by other authors (C. Y. Zhang et al., 2015), most methods measuring diacetyl use very different concentration ranges and are likely reported to the concentration in solution rather than the amount within the atmosphere of the vial (Salmerón et al., 2015), making it difficult to compare parameters. Nonetheless, quantification methods for similar-structure volatile organic compounds such as butanone, analyzed under similar concentration ranges, showed similar linearity values (Aguiar et al., 2023).

Table 2.3. Linearity data. All concentrations are in mg/mL. RE, relative error [(measured concentration−spiked concentration/spiked concentration) × 100].

Compound	Linearity	RE	LOD	LOQ	Slope	Intercept	R^2
Ethanol	10 - 400	0.19 – 2.36 %	2.83	8.57	4.08×10^{-4}	7.51	0.9999
Diacetyl	0.25 - 5	0.11 – 3.84 %	0.06	0.19	2.58×10^{-4}	5.23×10^{-2}	0.9999

The results of ethanol and diacetyl release after 24h at 37 ºC from the NaSt gel (and NaSt-CDNS composite can be observed in Figure 2.2. With a release of 319.63 ± 5.45 (A) and 298.00 ± 5.45 (C) milligrams of ethanol per gram of material, there were no significant differences ($p < 0.05$) between the release behavior of both control samples. In the same way, there were no significant differences between the ethanol release on active materials, with both active gel (269.47 ± 16.26) and active composite (253.81 ± 9.90) releasing similar milligrams of ethanol per gram of material. There is, however, a significant difference on ethanol release between control and active materials, likely due to the influence of diacetyl in the ethanol partitioning behavior between vapor and liquid media (Mackay, 1980). Figure 2.2 b) showcases a significant difference on diacetyl release from active NaSt gel and active NaSt-CDNS composite with 1.12 ± 0.09 and 2.97 ± 0.07 milligrams per gram of each material, respectively. This result attests to the advantages of embedding a material containing a volatile component within a porous network while increasing the surface area aimed to maximize release (Mu et al., 2017; Simionato et al., 2019; Utto, 2014).

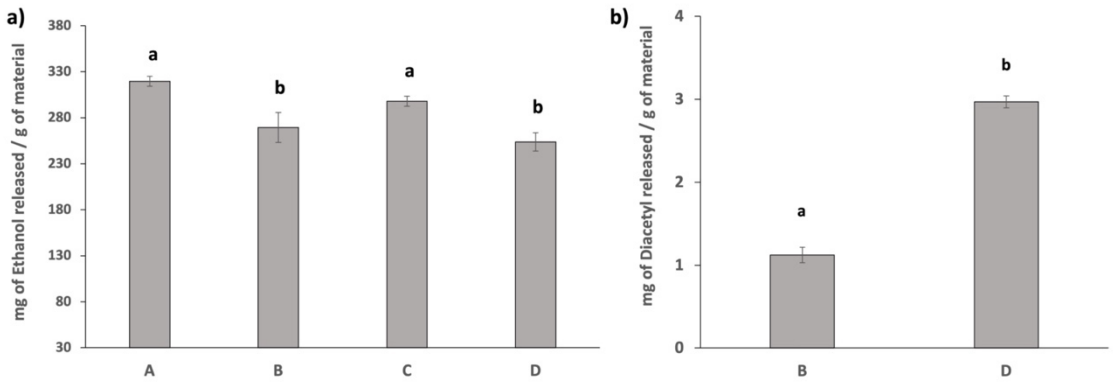

Figure 2.2. Milligrams of ethanol (a) and/or diacetyl (b) released in 24 h at 37 ºC per gram of material (A: control NaSt gel, B: active NaSt gel, C: control NaSt-CDNS composite, D: active NaSt-CDNS composite). Different letters show significant differences ($p < 0.05$) between samples.

4.4. *In vivo* antibacterial activity of active diacetyl-NaSt sachets in beef filets

Given the results obtained for the *in vitro* results for the active NaSt gel and the active NaSt-CDNS composite sachets, their anti-*Salmonella* activity and antimicrobial activity on beef microflora were evaluated over a refrigerated (4 ºC) storage period of 11 days. The effects of active sachets on growth inhibition and the percentage of bacterial growth reduction are presented on Figures 2.3 and 2.4, respectively.

Throughout the refrigerated storage period, control samples showed a higher microbial growth rate than the sample containing active sachets. For *S. enterica*, pseudomonads and total viable counts, the microbial growth kinetics were similar. During the first 3 days of storage, initial beef microbial loads remained almost unchanged, followed by an exponential growth on the fifth day after which a stationary phase was reached for both *S. enterica* and pseudomonads at day. In the case of lactic acid bacteria, a strong increase was shown at 11 days of storage, which may be due to the decrease of oxygen inside the package, that is known to favor the growth of this type of bacteria (EFSA, 2016). This late growth of lactic acid bacteria can also be explained by the great influence of temperature on the

development of lactic acid bacteria (A. P. R. da Silva et al., 2018), resulting in a higher lag phase when incubated at low temperatures (Feng et al., 2014).

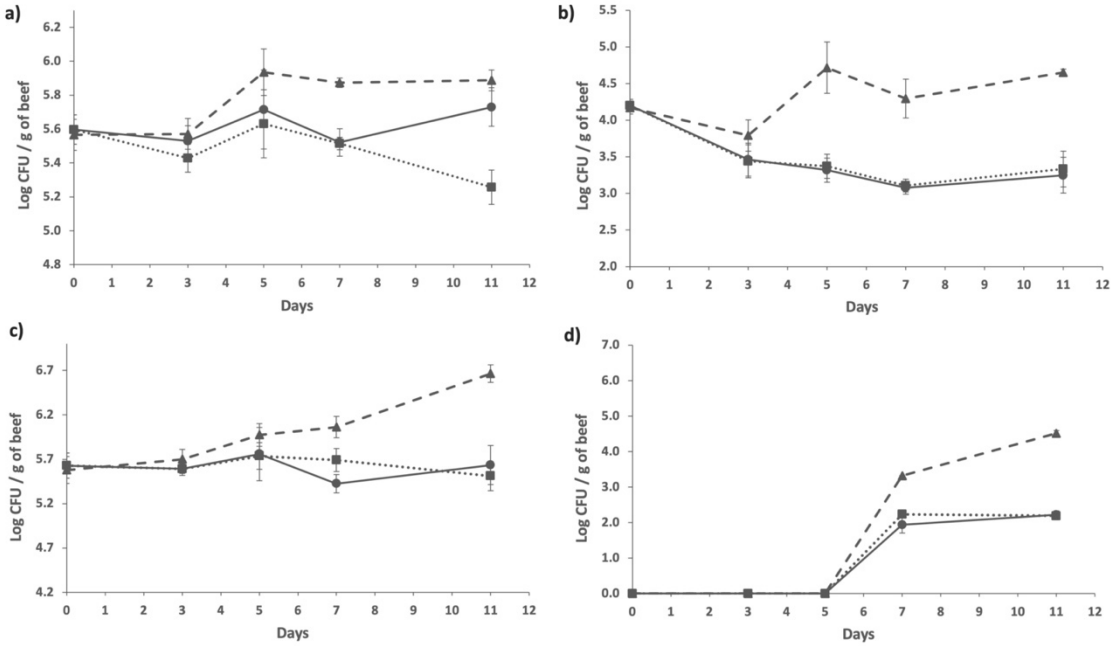

Figure 2.3. Effect of active diacetyl NaSt formulation sachets on growth kinetics of S. enterica (a) and beef microbiota: total viable counts (b), pseudomonads (c) and lactic acid bacteria (d) in S. enterica inoculated beef samples. Values for days 0, 3, 5, 7 and 11 are presented as mean values ± standard deviation of three independent replicates for the samples with three different sachets: control without diacetyl (dashed line, triangle), active NaSt gel (solid line, circle) and active NaSt-CDNS composite (dotted line, square).

S. enterica counts (Fig. 2.4, a) were decreased by both active NaSt gels and composites. At day 7, *Salmonella* counts for the active NaSt gel and the active NaSt-CDNS composite were 5.52 ± 0.08 and 5.51 ± 0.04 log CFU / g respectively, compared to 5.87 ± 0.03 log CFU / g of the control sample, resulting in a non-significantly different ($p > 0.05$) growth inhibition of 61 %. However, at day 11 with 5.73 ± 0.11 and 5.26 ± 0.10 log CFU / g compared to 5.89 ± 0.06 log CFU / g, the active NaSt gel showed a 33 % growth inhibition compared to a 77 % shown by the active NaSt-CDNS composite. This confirms the higher diacetyl release from NaSt-CDNS composites already observed by GC-FID and suggests a more controlled diacetyl liberation across time, because the antimicrobial activity of sachet is maintained for longer. Pseudomonads appeared to be more susceptible to the

active NaSt gel and the active NaSt-CDNS composite sachets, because both active sachets caused a growth inhibition of 60 % on day three and reaching a maximum of 94 % inhibition by day 5, which was able to be maintained over the 11-day period. In this case, the activity of the two active sachets did not differ at the end point of the assay. This trend was also repeated for total viable counts and lactic acid bacteria, where there were no significant differences ($p > 0.05$) between the antimicrobial action of the two sachets. The effectiveness of the active sachets against total viable counts increased progressively from 27 % inhibition on day 3 to 93 % inhibition on day 11. As for lactic acid bacteria, inhibition was maintained at 99 % as soon as they exited the lag phase on day 7.

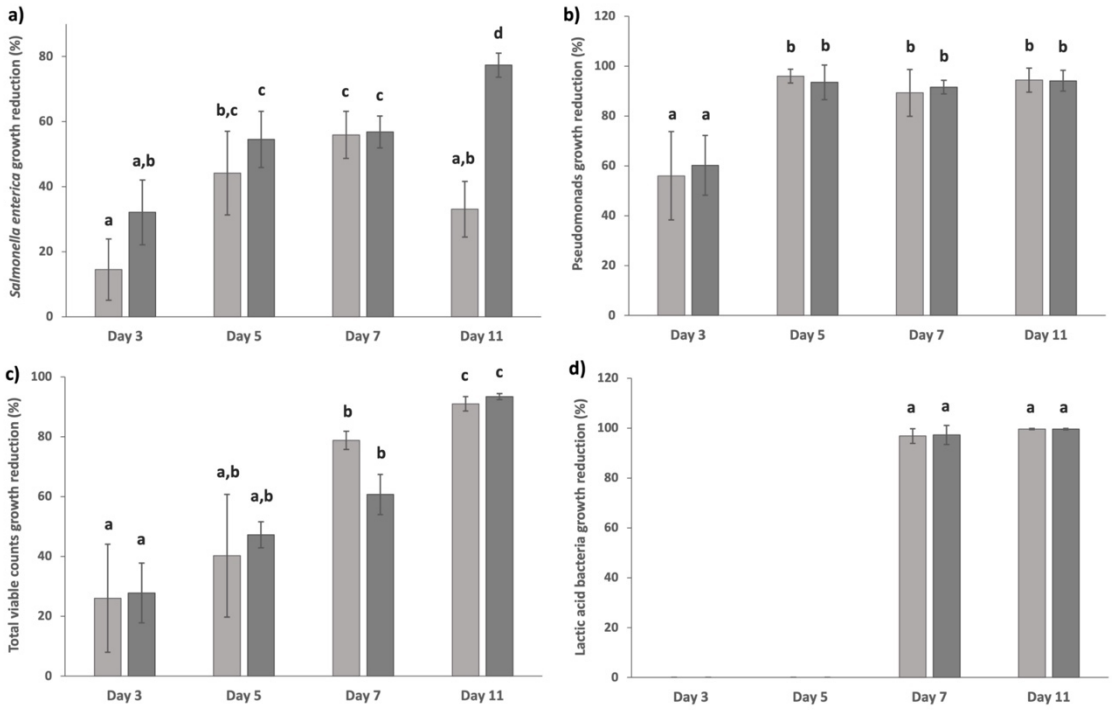

Figure 2.4. Effect of active diacetyl NaSt formulation sachets on S. enterica growth (a) and beef microbiota: total viable counts (b), pseudomonads (c) and lactic acid bacteria (d) in S. enterica inoculated beef samples. Values for days 3, 5, 7 and 11 are presented as mean values ± standard deviation of three independent replicates for the samples with the different sachets: active NaSt gel ( ) and active NaSt-CDNS composite ( ). Means ± SD followed by the same latter are not significantly different ($p > 0.05$) using one-way ANOVA.

Only a few studies have been performed on the antimicrobial action of diacetyl in beef alone, as they are normally performed together with other volatile organic

compounds and metabolites coming from fermentation extracts (Arrioja-Bretón et al., 2020; Özogul & Hamed, 2018). However, one study performed by directly adding diacetyl onto minced beef did not show any effect on the microbial growth (Williams-Campbell & Jay, 2002). Therefore, the results obtained in the present study which, as previously mentioned, take advantage of the higher efficacy of diacetyl in the vapor phase (Lanciotti et al., 2003), highlight the suitability of the active diacetyl-NaSt active sachets for their application in antimicrobial active food packaging.

5. Conclusions

In this study, the applicability of GRAS diacetyl and sodium stearate to make an active antimicrobial sachet that could be able to tackle microbial growth on fresh meat has been explored. Diacetyl showed a high *in vitro* antimicrobial activity, especially against Salmonella enterica, even when entrapped into sodium stearate gel either supported or not into porous food-grade cyclodextrin nanosponges (CD-NS). *In vivo* testing of both components in the form of diacetyl-releasing active sachet demonstrated a higher efficacy of the sodium stearate-CD-NS composite in inhibiting *Salmonella enterica* growth (77 %) in artificially-inoculated refrigerated beef filets when compared with the gel (33 %). This enhanced efficacy of the composite sachet is supported by the higher diacetyl release from the composite matrix when compared with the stearate gel alone. Additionally, both sachets proved very effective for common microbiota present in beef meat such as total viable counts, pseudomonads and lactic acid bacteria, with growth inhibitions ranging from 93 to 99 %. The efficacy showed by the inexpensive and easy to make antimicrobial GRAS sachets encourages their use as active food packaging towards shelf-life and safety increase of fresh meat products or other food products prone to pathogen contamination or spoilage.

Chapter 3:

Synthesis and quantification of oligoesters migrating from starch-based food packaging materials

1. Introduction

Regarding plastics, the prefix bio- can refer to polymers coming from renewable sources and/or having a biological origin, to their biodegradability or compostability, or to a combination of both (Rosenboom et al., 2022). This feature, together with acceptable physical and mechanical properties and a low carbon footprint, contributes to their increasing market growth rate (Mehmood et al., 2023). Whilst plastic uses comprise consumer goods, electronics, agriculture, etc., the packaging sector represents the major market (48%) for bioplastic materials (Romero García et al., 2022).

Starch-based biopolymers are one of the most popular (about 18% of market share) bio-based plastic choices (Romero García et al., 2022). The widely available starch has to be mixed with plasticizers and other chemical moieties to improve its physical properties. The incorporation of reinforcements, chemical modifications and the blending with other co-polymers is a common practice to minimize the limitations of starch-based materials such as poor mechanical properties or high hydrophilicity (Agarwal et al., 2023). When it comes to food packaging applications, research has focused on developing starch-based blends with poly(lactic acid) (PLA), polyvinyl alcohol (PVA) or poly(butylene adipate-co-terephtalate) (PBAT), among others, to improve both their physical and chemical properties (García-Guzmán et al., 2022). However, the presence of a large and diverse number of blends represents a challenge for the risk assessment of both intentionally added substances (IAS) and non-intentionally added substances (NIAS) in food contact materials.

IAS as well as NIAS can be transferred from a packaging material into the packaged food, making migration tests a widely applied tool for the proper chemical risk assessment of a plastic food contact material (EU10/2011). IAS are usually well under control with fulfilled risk assessments and defined specific migration limits (Groh et al., 2021). However, as diverse substances coming from impurities in the raw materials, incomplete polymerization, or polymer degradation, NIAS are still being discovered, especially in new food packaging materials (Aznar et al., 2019;

E.L. Bradley, 2010; Hayrapetyan et al., 2024; Nerin et al., 2013; Nerín et al., 2022b; Ubeda et al., 2021; Vázquez-Loureiro et al., 2023). Oligomers, low molecular weight polymers, constitute one of the primary forms of NIAS (Shi et al., 2023). Due to their low molecular weight (generally below 1,000 Da), they can migrate from the packaging material matrix into the food and are often overlooked by polymer scientists, who focus their attention on the 10^4 up to 10^6 Da range (Shi et al., 2023). As most biopolymers are formed by a polycondensation reaction of various monomers, structurally and chemically diverse oligoesters often represent the dominant form of NIAS (Ubeda et al., 2021).

Nonetheless, the lack of isolated oligoester standards results in an analytical challenge for the identification and quantification of NIAS (Nerin et al., 2013; Omer et al., 2018). Moreover, it limits the ability to perform toxicological risks assessments that would shed some light into the human and environmental exposure and absorption, distribution, metabolism, excretion and toxicity (ADMET) of these oligoesters. Hence, in recent years, efforts have been made to contribute towards the availability of migrant oligoesters (Cariou et al., 2022; Paseiro-Cerrato et al., 2016; Pietropaolo et al., 2018). Nevertheless, the need for oligoester reference standards is nothing but increasing (Alberto Lopes & Tsochatzis, 2023b).

In the present study, migration extracts of three starch-based biopolymer films for packaging fruits and vegetables were analysed by non-targeted LC/HRMS. From this analysis, a variety of eleven linear and cyclic oligoester combinations composed by 1,4-butanediol, propylene glycol, phthalic acid and adipic acid, were identified as possible NIAS. Based on a stepwise synthetic strategy, they were synthesized, and they were used to unequivocally confirm and quantify the NIAS oligoesters migrating from the three starch-based biopolymer samples.

2. Objectives

This chapter aims to assess the food safety of new starch-based packaging materials (Figure 3.1a) . First, the migration profile of the materials will be evaluated using different food simulants (Figure 3.1b). Then, a stepwise synthesis approach will be implemented to synthesise a series migrant oligoesters standards based on adipic acid, 1,4-butanediol, isophthalic acid, and propylene glycol (Figure 3.1c). Finally, the synthesized oligoester standards will be used to assess the food safety of the bio-based materials, by unequivocally identifying and quantifying them in the samples (Figure 3.1d).

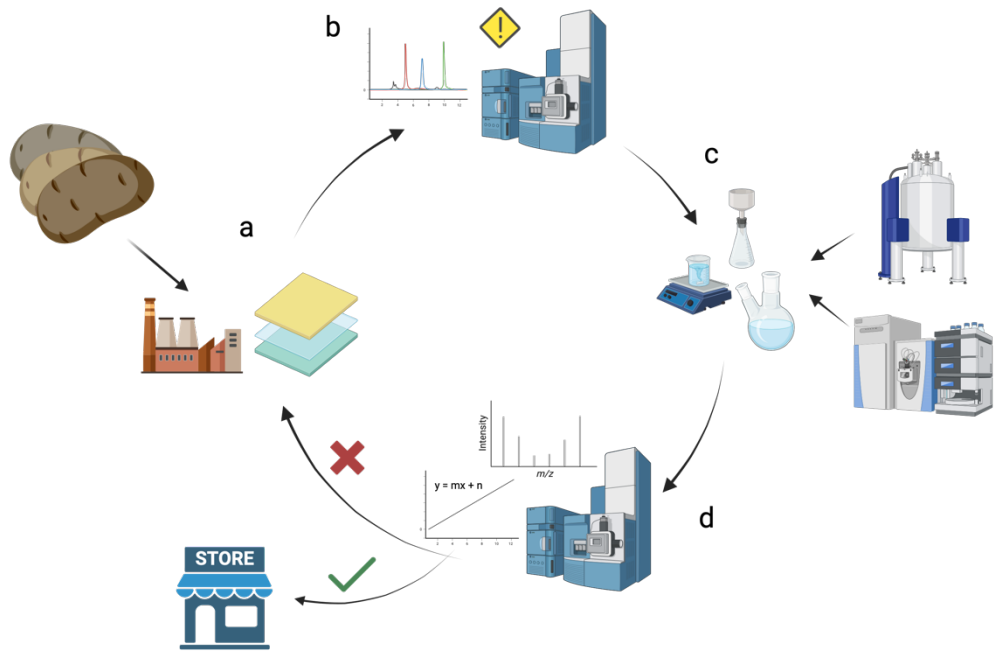

Figure 3.1. Process to achieve the objectives of chapter 3. a) Starch-based food contact materials, b) Analysis of migration extracts by UPLC-HRMS, c) Stepwise synthesis of migrant oligoesters standards, and their characterization by ^{1}H and ^{13}C NMR, and UPLC-HRMS, d) Identification and quantification of migrant oligoesters using the synthesized standards to assess their food safety.

3. Materials and methods

3.1. Reagents

For analytical and migration purposes, LC-MS grade methanol (MeOH), dichloromethane (DCM) and acetonitrile (ACN), as well as analytical grade ethanol (EtOH) were provided by Honeywell (Seelze, Germany). Ultrapure water was generated using an Ultramatic Wasserlab purification system (Navarra, Spain). Ammonium and sodium acetate salts were purchased from Merck (Emsure® grade, Darmstadt, Germany). MS grade formic acid was acquired from Waters (Milford, MA, USA). PTFE syringe filters (0.45 µm) were purchased from Sigma-Aldrich (St. Louis, MO, USA).

For synthetic purposes, isophthalic acid (iPA), benzyl bromide (BnBr), 1-ethyl-3-carbodiimide hydrochloride (EDC.HCl), 4-dimethylaminopyridine (DMAP), palladium hydroxide ($Pd(OH)_2$) and *tert*-butyldimethylsilyl chloride (TBDMSCl), were provided by Fluorochem (Hadfield, United Kingdom). 1,4-Butanediol (BD), propylene glycol (PG), hydrogen fluoride-pyridine (HF.Pyr), dioxane and dimethylformamide (DMF) were purchased from Sigma-Aldrich (St. Louis, MO, USA). Adipic acid (AA) was acquired from Acros (Antwerp, Belgium). Triethylamine (Et_3N) was provided by Merck (Darmstadt, Germany). Hydrogen chloride (HCl) and ammonium chloride were acquired from VWR (Radnor, PA, USA). Sodium sulphate was purchased from Thermo-Scientific (Waltham, MA, USA). Sodium chloride, sodium bicarbonate, ethyl acetate, cyclohexane, isopropyl alcohol, tetrahydrofuran (THF) and dichloromethane (DCM) were provided by Fisher (Waltham, MA, USA). All reagents were used without further purification. If necessary, THF and DCM were dried using a MBraun SPS-800 dry solvent system (Garching, Germany).

3.2. Samples

The food safety of three commercial starch-based films (S1, S2 and S3) for food packaging applications were investigated in this study. Samples were provided by a local manufacturer and their formulation was not disclosed. Their thicknesses were

measured using a digimatic micrometer from Mitutoyo (Kanagawa, Japan) as being 26.5±1.1, 25.5±1.8 and 29.8±2.4 m for films S1, S2 and S3, respectively.

3.3. Migration tests

All the migration experiments were performed in triplicate and according to the European Regulation for food contact materials EU/10/2011 (European Commission, 2011). Migration tests were performed using three different food simulants: ethanol 10% (*v/v*, simulant A), acetic acid 3% (*w/v*, simulant B) and Tenax® (simulant E). For simulants A and B, migration tests were performed by total immersion of 5×1 cm cut-offs in 20 mL vials which were filled according to the 6 dm^2 contact surface/kg of simulant rate, established by the Regulation EU/10/2011. For simulant E migration experiments, 4×2 cm cut-offs of were placed in direct contact with 0.32 grams of Tenax® inside aluminium foil pouches following the 4 $g.dm^{-2}$ ratio established by UNE-EN-14338 (AENOR, 2004) and placed inside glass Petri dishes. Migration experiments took place in an oven at 40 °C for 10 days. Migration extracts from simulants A and B were directly injected in the UPLC-MS(QTOF) system. Prior to injection, Tenax® samples from each migration experiment were extracted twice with ethanol following the methodology designed by Vera *et al.* (Vera et al., 2011). The recovered ethanol was then filtered with a PTFE syringe filter (0.45 µm) and concentrated to approximately 0.5 mL under a gentle stream of nitrogen. This concentration step was gravimetrically monitored.

3.4. UPLC-HRMS analysis of migration extracts

Chromatographic separation was carried out on a CORTECS UPLC BEH C18 column (1.6 µm, 2.1×100 mm) using an UPLC Acquity system, both from Waters (Milford, MA, USA). Chromatography was performed at 0.3 $mL.min^{-1}$ column flow using water (phase A) and methanol (phase B) both with 0.1% (*v/v*) formic acid as mobile phases. Column temperature was set at 35 ºC and the injection volume was 10 µL. Chromatography started at A:B gradient of 95:5 (*v/v*), changed to 5:95 (*v/v*) in 6 min and stayed at these conditions for an additional 4 min, going back to the initial 95:5 (*v/v*) gradient conditions to pre-condition the column for 3 min.

The UPLC system was connected through an ESI probe to a Xevo G2 QTOF mass spectrometer from Waters. Instrument configuration was as follows: capillary at 2.8 kV, sampling cone at 35 V, extraction cone at 3 V, source temperature at 150 ºC, desolvation temperature at 450 ºC, cone gas flow at 40 L h^{-1} and desolvation flow at 600 L h^{-1}. Acquisition was carried out in sensitivity MS^E mode, allowing the acquisition over a range of collision cell energies (CE) from 15 to 30 V during the same run. Data were recorded using Masslynx® v4.1 software.

The identification of compounds was performed by comparing migration extracts with a migration blank and following a previously described methodology (Aznar et al., 2016) to achieve level 2b of the scale proposed by Schymanski *et al*. (Schymanski et al., 2014). Level 5 (lowest) comprises an accurate measurement of the mass-to-charge ratio (*m/z*). Level 4 is achieved with an unambiguous molecular formula. Level 3 is obtained when multiple potential structures are feasible. Level 2 can be claimed by the proposal of a single structure supported by experimental diagnostic evidence such as MS^2 (2b) or matching library spectra (2a). Final confirmation of the structure (level 1) is only reached through comparison with a reference standard. Briefly, using the low energy spectrum, the precise mass of precursor ions was used to determine the lowest mass error and the highest isotopic fit of the elemental composition options proposed by Masslynx. Afterwards, the selected elemental compositions were linked to a chemical structure using different chemical databases (e.g. Chemspider, Scifinder) and freely available software (NIAS-db 1.0, Cariou et al., 2022) by paying attention to the chemical criteria and background experience about NIAS and IAS in bio-based polymers. Finally, a candidate molecule was selected using its high-energy mass spectrum. For being selected as a candidate, at least two main fragment ions of the high energy mass spectrum showed a score value below 3 using the MassFragment® tool from Masslynx. The score value was calculated by the software based on fragmentation probabilities.

3.5. Synthesis and characterization of oligoester standards

The selection of oligoester candidates to be synthesized was made with regards to obtain as many structurally diverse oligoesters as possible but firstly considering the hypothesised oligoesters in the migration extracts. An optimized stepwise oligoester synthesis strategy previously described (Cariou et al., 2022) was readapted for the preparation of the new identified substances arising from the above-mentioned migration protocols. The synthesis of these oligoester standards involves the use of new diol monomers and new diacid counterparts. Figure 3.2 briefly summarises all reactions in the stepwise synthesis sequentially implemented involving successive monosilylation, monobenzylation, debenzylation, desilylation, esterification and macrolactonization. Products were purified after each reaction by flash column chromatography using an automatic Reveleris Büchi apparatus (Flawil, Switzerland) fitted with pre-packed high purity 40 µm silica cartridges (4 to 220 grams, Büchi). An in-depth description of the synthesis protocol, monitoring, and characterisation equipment (^{1}H and ^{13}C NMR, ESI-TOF-HRMS) is provided in the Annexes.

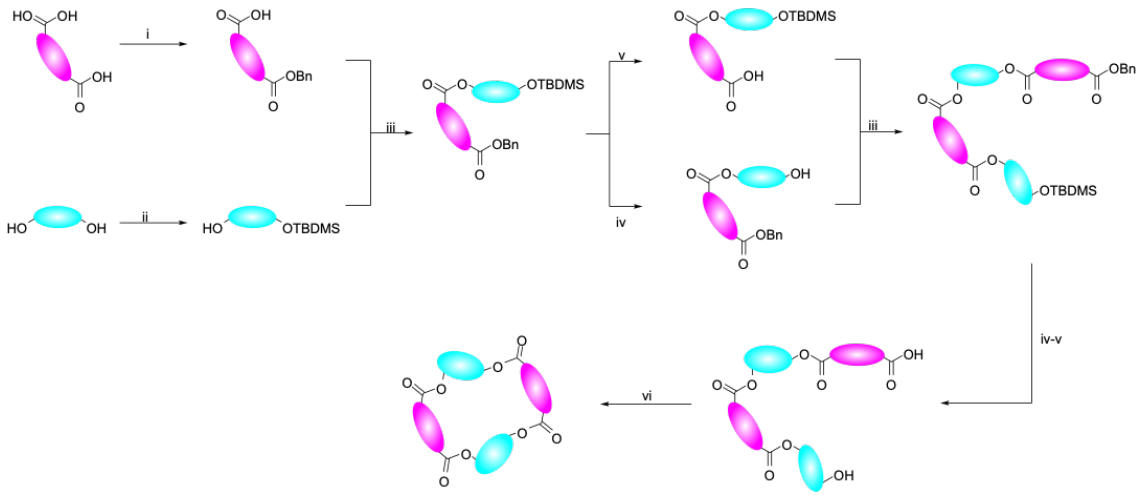

Figure 3.2. Reaction sequence involved in the stepwise synthesis of oligoester standards. Method A: (i) BnBr, $NaHCO_3$, Dioxane/DMF ; Method B: (ii) TBDMSCl, Et_3N, DMAP, DCM ; Method C: (iii) EDC.HCl, DMAP, DCM ; Method D: (iv) HF.Pyr, THF ; Method E: (v) H_2, $Pd(OH)_2$, iPrOH ; Method F: (vi) 2,4,6-Trichlorobenzoyl chloride, Et_3N, DMAP, 10^{-3}M in THF.

3.6. Purity assessment of oligoester standards

To perform a purity assessment of the synthesized oligoester compounds, each standard was first solubilised with DCM and further diluted gravimetrically with ACN to obtain a 10 µg.g^{1} solution. Each solution was characterised on a UHPLC UltiMate 3000 coupled to an Orbitrap Q Exactive instrument fitted with a heated electrospray ionisation source (UHPLC-ESI-MS-Orbitrap), both from Thermo Scientific (Waltham, MA, USA). Chromatographic separation was achieved at 40 ºC on a C_{18} Hypersil Gold column (1.9 µm, 2.1 × 100 mm) from Thermo Fisher Scientific (San José, CA, USA). The flow rate was set at 0.4 mL.min^{-1} and the mobile phase was composed of 10 mM ammonium acetate in both water (A) and acetonitrile (B). Separation began with a A:B gradient of 95:5 (*v/v*) (1 min) and ramped to a gradient of A:B 100:0 (*v/v*) over 16 min, to be maintained over 9 minutes before going back to the initial conditions (2 min). The ionization parameters were as follows: sheath gas flow, 50 arbitrary units (AU); auxiliary gas flow, 10 AU; capillary temperature, 350 °C; heater temperature, 300 °C; spray voltage, 3.5 kV; S-lens radio frequency, 70 AU. Data were acquired in full scan by using the positive/negative switching mode over the *m/z* range 100 – 1,064 at a nominal resolving power of 70,000. Automatic gain control (AGC Target) was set at high dynamic range (1 × 10^5) and maximum injection time (IT) at 250 ms. Purity percentage was determined by measuring the peak area of the $[M + H]^+$, $[M + Na]^+$, $[M + K]^+$, $[M + NH_4]^+$, $[M – H]^-$ and $[M + HAc – H]^-$ present adducts of the oligoester and the impurities.

3.7. Identification and quantification of oligoesters in migration extracts

In the present study, synthesized oligoester standards were used to achieve Schymanski's level 1 identification, putting together the information obtained from section 2.4. and the relative retention time, chromatographic peak shape and MS^2 fragmentation pattern. To this end, migration extracts, migration blanks and a 10 µg g^{-1} solution containing the synthesized oligoester were analysed by UPLC-MS(QTOF). Chromatographic parameters and instrument configuration were kept the same as in section 2.3. However, data acquisition was performed using the MS^2 function by selecting the most abundant adduct (as observed in full scan mode) as

parent ion to then apply a CE potential ramp (20 to 50 V) to favour both low and high mass fragments. To avoid co-eluting interferences, only one parent ion was fragmented at each time window.

Quantification was conducted using the external calibration method. To account for impurities between oligoester standards, different sets of 14 points calibration curves were gravimetrically prepared at the following concentrations: 10,000, 5,000, 2,500, 1,000, 750, 500, 300, 150, 100, 50, 20, 10, 5 and 1 $ng.g^{-1}$. The analysis method was the same as that employed for the analysis of migration samples in section 2.3. The limit of detection (LOD) and the limit of quantification (LOQ) were calculated as the smallest concentration of analyte that provided a signal to noise ratio three times and ten times the blank signal, respectively.

4. Results and discussion

4.1. NIAS migration in starch-based biopolymer films

Detected compounds in food simulants A, B and E after contact with the three starch-based biopolymer film samples are shown in Table 3.1. No IAS were detected in any of the samples through the non-targeted analysis. However, 22 oligoester combinations were identified as suggested by MassFragment, which accounted for 90% of the cumulative area of signals after blank subtraction (n = 23, 175 × 10^3 AU). Migrant oligoesters added up to 97%, 96% and 85% in simulant A (n = 11, 75 × 10^3 AU), B (n = 18, 54 × 10^3 AU) and E (n = 10, 46 × 10^3 AU), respectively.

In terms of monomeric units, even cyclic combinations were dominated by 4-unit combinations (n=4, 91 × 10^3 AU), followed by 6-units (n=2, 13 × 10^3 AU), 8-units (n=2, 9 × 10^3 AU) and 2-units (n=2, 8 × 10^3 AU) combinations. The only odd cyclic combinations hypothesised were composed of lactic acid monomers alone and were a 7-units (11 × 10^3 AU) and a 5-units (3 × 10^3 AU) combination. Linear oligoesters were less abundant, ranging from 2 to 7 units oligomers, the most intense being the 5-units (n=2, 13 × 10^3 AU), followed by 2-units (n=2, 10 × 10^3 AU) and 4-units (n=2, 8 × 10^3 AU). Only one combination for each of the 3-units (2 × 10^3

AU), 6-units (0.1×10^3 AU) and 7-units (0.2×10^3 AU) could be found. It could be highlighted that cyclic oligoesters are favoured compared to linear oligoesters, the latter being diols or hydroxy acids. No diacid linear combinations were found, maybe due to their properties and to their higher reactivity. Oligoester combinations involved 5 diols: butanediol (BD), ethylene glycol (EG), propylene glycol (PG), diethylene glycol (DEG) and trimethylolpropane (TMP); and 3 diacids: adipic acid (AA), sebacic acid (SA) and phthalic acid (PA, undefined isomer). Lactic acid (LA) did not combine with any other monomer as it was not found in combination with any diol or diacid monomers. BD and PG were the most abundant diols, being present in 42% and 21% of the oligomers, respectively. Likewise, AA was the most common diacid, being 64% of the oligoester combinations, followed by phthalic acid (8%) and sebacic acid (4%).

Linear and cyclic combinations of AA and BD were common across samples 1 and 3, which indicated a type of blend using poly(1,4-butylene adipate) (PBA), a biopolymer commonly blended with other polyesters to increase their biodegradability and mechanical properties (Debuissy et al., 2016). Various oligoester forms of AA and BD have been reported in other biodegradable food contact materials, with the most common being the cyclic form of the tetramer c[2BD+2AA] (Aznar et al., 2019; Canellas et al., 2015c; Cariou et al., 2022; Debuissy et al., 2016; E.L. Bradley, 2010). As blends of PLA and PBA with PBAT increase the barrier properties of the resulting material (Bheemaneni et al., 2018; H. Zhang et al., 2013), we hypothesized that oligomer combinations containing BD, AA, and PA indicate an attempt to improve the barrier properties of the resulting starch-based material.

When comparing the 3 starch-based materials, two lactic acid oligomers, lin[2LA+C_2H_5] and c[7LA], were the only combinations found across all three samples, suggesting a common PLA component. Ethoxylation (+C_2H_5) of LA oligomers occurs during the migration process in contact with ethanol, meaning no ethoxylated oligoesters would have migrated into the foodstuff (Aznar et al., 2019). Sample 2 showed forms of PG and EG with adipic acid, pointing in this case to the presence of poly(propylene glycol adipate) (PPA) and poly(ethylene glycol adipate)

(PEA) as plasticisers (Slobodinyuk et al., 2023; Tang et al., 2020). Only one combination of SA and DEG, commonly used as raw materials in polyester manufacturing (Úbeda et al., 2017; N. Zhang et al., 2020), was found forming a cyclic dimer in sample 3. TMP is a substance used in the production of hyperbranched polyesters, a type of polymer with good properties as coating agents (Zhang et al., 2017). Interestingly, another cyclic dimer containing AA and TMP, could also be hypothesised in sample 3.

Table 3.1. Compounds hypothesised in the migration of three biopolymers samples (S1, S2 & S3) in food simulants A, B and E. Molecular formula (MF); linear (lin) and cyclic (c) proposed candidates; remarks, main fragments, and their scores (S) obtained by MassFragment. LA: lactic acid, BD: 1,4-butanediol, AA: adipic acid, EG: ethylene glycol, PG: propylene glycol, DEG: diethylene glycol, SA: sebacic acid, PA: phthalic acid, TMP: trimethylolpropane, Rt: retention time, nd: not detected.

Rt	*m/z* [MNa]$^+$	MF	S1	S2	S3	Candidate	ID level	Remarks/Fragments(scores)
4.37	213.0738	$C_8H_{14}O_5$	E	E	E	lin[2LA+C_2H_5]	2a	PLA oligomer. 161.0450 (S0.5) 158.0256 (S1)
4.4	241.1047	$C_{10}H_{18}O_5$	A	nd	A	lin[BD+AA] (86923-79-7)	1	Polyester oligomer. 202.1232 (S0.5) 147.0637 (S.05)
4.9	367.1349	$C_{16}H_{24}O_8$	nd	A,B,E	nd	c[2EG+2AA]	2a	Polyester oligomer. 346.1604 (S0.5) 174.0846 (S0.5)
4.96	313.1623	$C_{14}H_{26}O_6$	A	nd	A	lin[2BD+AA] (20985-13-1)	1	Polyester oligomer. 155.0724 (S1.5) 111.0431 (S1)
5.00	281.1478	-	E	nd	E	-	-	259.1628, 143.0996
5.08	413.1784	$C_{18}H_{30}O_9$	nd	A	nd	lin[2PG+2AA]	1	Polyester oligomer. 331.1837 (S1) 245.1081 (S1)
5.14	301.2847	$C_{17}H_{37}N_2O_2$	nd	nd	A,E	-	-	301.2847, 149.0060
5.54	395.1679	$C_{18}H_{28}O_8$	nd	A,B,E	nd	c[2PG+2AA]	1	Polyester oligomer. 203.0996 (S2) 115.0793 (S2)
5.60	357.1162	$C_{14}H_{22}O_9$	nd	E	nd	lin[4LA+C_2H_5]	2a	PLA oligomer. 315.0782 (S3) 119.0626 (S3)
5.67	383.0966	$C_{15}H_{20}O_{10}$	E	nd	E	c[5LA]	2a	PLA oligomer. 158.0196 (S2) 89.0230 (S2)
5.71	369.1543	$C_{16}H_{26}O_8$	A	nd	A	-	-	329.1606, 201.1153
5.85	441.2094	$C_{20}H_{34}O_9$	A	nd	A	lin[2BD+2AA]	1	Polyester oligomer. 401.2176 (S0.5) 291.1791 (S0.5)
5.87	455.1153	$C_{18}H_{24}O_{12}$	A,B,E	nd	E	c[6LA]	2a	PLA oligomer. 307.1044 (S2) 273.0987 (S2)
5.90	295.1526	$C_{14}H_{24}O_5$	nd	nd	E	c[DEG+SA]	2a	Polyester oligomer. 227.1252 (S2) 203.1207 (S2)
5.92	513.2682	$C_{24}H_{42}O_{10}$	nd	nd	A	lin[3BD+2AA]	1	Polyester oligomer. 458.2516 (S1) 329.1677 (S1)
6.01	567.2431	$C_{28}H_{38}O_{12}$	nd	A,B	nd	lin[2BD+2AA+PA]	2a	Polyester oligomer. 228.1633 (S1) 129.0535 (S0.5)
6.15	527.1379	$C_{21}H_{28}O_{14}$	A,B	A,B	A	c[7LA]	2a	PLA oligomer. 158.0272 (S2) 175.1000 (S3)
6.23	423.1999	$C_{20}H_{32}O_8$	A,B,E	nd	A,B,E	c[2BD+2AA] (CAS 78837-87-3)	1	Polyester oligomer. 311.1474 (S2) 213.1034 (S3)
6.27	739.3167	$C_{34}H_{52}O_{16}$	nd	A,B	nd	c[2EG+2PG+4AA]	2a	Polyester oligomer. 373.1862 (S0.5) 315.1352 (S0.5)

6.30	641.3145	$C_{30}H_{50}O_{13}$	nd	nd	A	lin[3BD+3AA]	1	Polyester oligomer. 547.2840 (S0.5) 431.2293 (S1)
6.31	595.2734	$C_{28}H_{44}O_{12}$	nd	A,B	nd	c[2BD+3AA+EG]	2a	Polyester oligomer. 402.2205 (S2) 301.1345 (S2)
6.49	767.3488	$C_{36}H_{56}O_{16}$	nd	A,B	nd	c[4PG+4AA]	1	Polyester oligomer. 333.1578 (S2) 261.1282 (S2)
6.58	279.1573	$C_{14}H_{24}O_4$	nd	nd	E	c[AA+TMP]	2a	Polyester oligomer. 257.1755 (S0.5) 130.1387 (S0.5)
6.63	443.1689	$C_{22}H_{28}O_8$	A,B	nd	A,B,E	c[2BD+AA+PA]	1	Polyester oligomer. 307.1150 (S2) 221.0857 (S2)
6.67	623.3052	$C_{30}H_{48}O_{12}$	A,B	nd	A,B	c[3BD+3AA]	1	Polyester oligomer. 457.2471 (S3) 429.2100 (S3)
7.03	545.1516	$C_{21}H_{30}O_{15}$	A	nd	nd	lin[7LA]	2a	PLA oligomer. 319.1362 (S1.5)
7.74	256.2641	$C_{16}H_{34}NO$	nd	nd	B	-	-	125.9877, 158.0055
7.86	282.2764	$C_{16}H_{37}NO$	nd	nd	B	-	-	125.9877, 247.2442
8.36	284.2945	$C_{18}H_{38}NO$	nd	nd	B	-	-	125.9865, 158.0121
8.45	319.1955	-	nd	nd	B	-	-	125.9862, 365.2050
10.6	536.1666	-	E	nd	nd	-	-	125.9881, 369.2711

4.2. Synthesis of oligoester standards

4.2.1. Selection of combinations

Overall, the lack of NIAS reference compounds represents a major obstacle not only for their use as analytical standard to unequivocally identifying and quantifying them in samples, but also for the need to perform mechanistic and toxicological studies (Shi et al., 2023). When it comes to oligoesters, only a few syntheses have been attempted. Regarding oligoesters containing AA as diacid and BD as diol, only c[2BD+2AA] was available to purchase (LGC standards, Middlesex, UK). However, to the best of our knowledge, no attempt has been performed to synthesize a series of AA and BD oligoesters, so the stepwise synthesis (Figure 3) was seen as an opportunity to obtain not only c[2BD+2AA], but the rest of linear and cyclic oligoesters ranging from 2 to 6 units. As some oligoesters containing EG combined with terephthalic acid (Paseiro-Cerrato et al., 2016) and LA oligomers (Schliecker et al., 2003) have already been synthesized, the efforts were focused in attempting the synthesis of oligomers containing PG as diol (Figure 4). Most of the described oligomeric syntheses involve the use of PA (both isophthalic, iPA, and terephthalic, tPA) as diacid (Cariou et al., 2022; Eckardt et al., 2019; Paseiro-Cerrato et al., 2016; Pietropaolo et al., 2018). However, as none involved the production of c[2BD+iPA+AA], it was decided to attempt it specially because oligoesters containing an aromatic moiety have a higher toxicity potential (He et al., 2015). In this case, iPA was chosen as PA isomer due to its preferable use to improve barrier properties in biopolymer production (T.-H. Lee et al., 2022).

4.2.2. Synthesis

Similarly to the procedure described by Cariou et al., 2022, a stepwise synthetic approach was applied in this work to prepare new linear or cyclic oligomers based on new diacid monomer such as adipic acid, or new diols units such as butane-1,4-diol or propylene glycol. This robust and well-adaptable multistep synthesis allowed us to yield the expected oligomers with an excellent control of the size and with clean purity for further semi-quantitative analysis.

Our efforts were first dedicated to the preparation of oligoesters derived from butanediol (BD) and adipic acid (AA) (Figure 3.3). In comparison to the original synthesis described by Cariou et al., 2022, a slight modification was implemented for the monobenzylation reaction to furnish the monobenzylated ester **1** in view of facilitating the treatment of the reaction while also improving the yield (Škalamera et al., 2017). Likewise, the rest of the synthesis worked very effectively for the size elongation of the linear oligomer in a well-controlled fashion. Along with this sequential synthesis, the linear oligomers lin[BD+AA], lin[2BD+AA], lin[3BD+2AA], lin[2BD+2AA], lin[3BD+3AA] were successfully obtained as highly valuable intermediates which are also part of the identified NIAS detected as migrants from the biopolymer films. Our results showed that the final and tedious macrolactonization was well amenable for different size of cyclic oligomers to obtain either the 4-units c[2BD+2AA] or the 6-units c[3BD+3AA], with yields of 26% and 18%, respectively.

As represented by the following cyclic oligoester c[2BD+iPA+AA] (Scheme 3.4), the stepwise synthesis allowed the preparation of this expected cyclic 4-units-compound with a global yield of 38% over 11 synthetic steps. This result showed the great efficacy of the synthesis and that this synthetic strategy was well-adaptable to produce hybrid oligomers based on several diacid units (*i.e*. AA and iPA). Finally, our results showed that this stepwise synthesis was highly suitable for the preparation of non-symmetrical oligomers bearing a diol unit represented with two differential reactivity of the hydroxyl groups such as a primary and a secondary alcohol (Scheme 3.5). This type of dual reactivity of the diol partner was applied for the preparation of propylene glycol-based oligomers which are consistent with other NIAS arising from biofilms. Once again, the stepwise synthesis was very appropriate for the synthesis of linear and cyclic oligoesters derived from propylene glycol (PG) and adipic acid (AA). The linear oligomer lin[2PG+2AA] was cleanly obtained with a global yield of 52% over 9 steps. This compound was used as precursor of the macrolactonization for the most critical step as intramolecular reactions can be favoured over intermolecular ones. While good macrolactonization yields were generally observed (up to 80%), the macrolactonization of lin[2PG+2AA] afforded

the expected cyclic tetramer c[2PG+2AA] with a lower yield (73%), because of the concomitant formation of the octamer c[4PG+4AA] (15%) along with the dodecamer c[6PG+6AA] (5 %). The complex mixture components were separated by flash chromatography and only c[2PG+2AA] and c[4PG+4AA] reached adequate quantities for a complete characterisation and further use as reference standards.

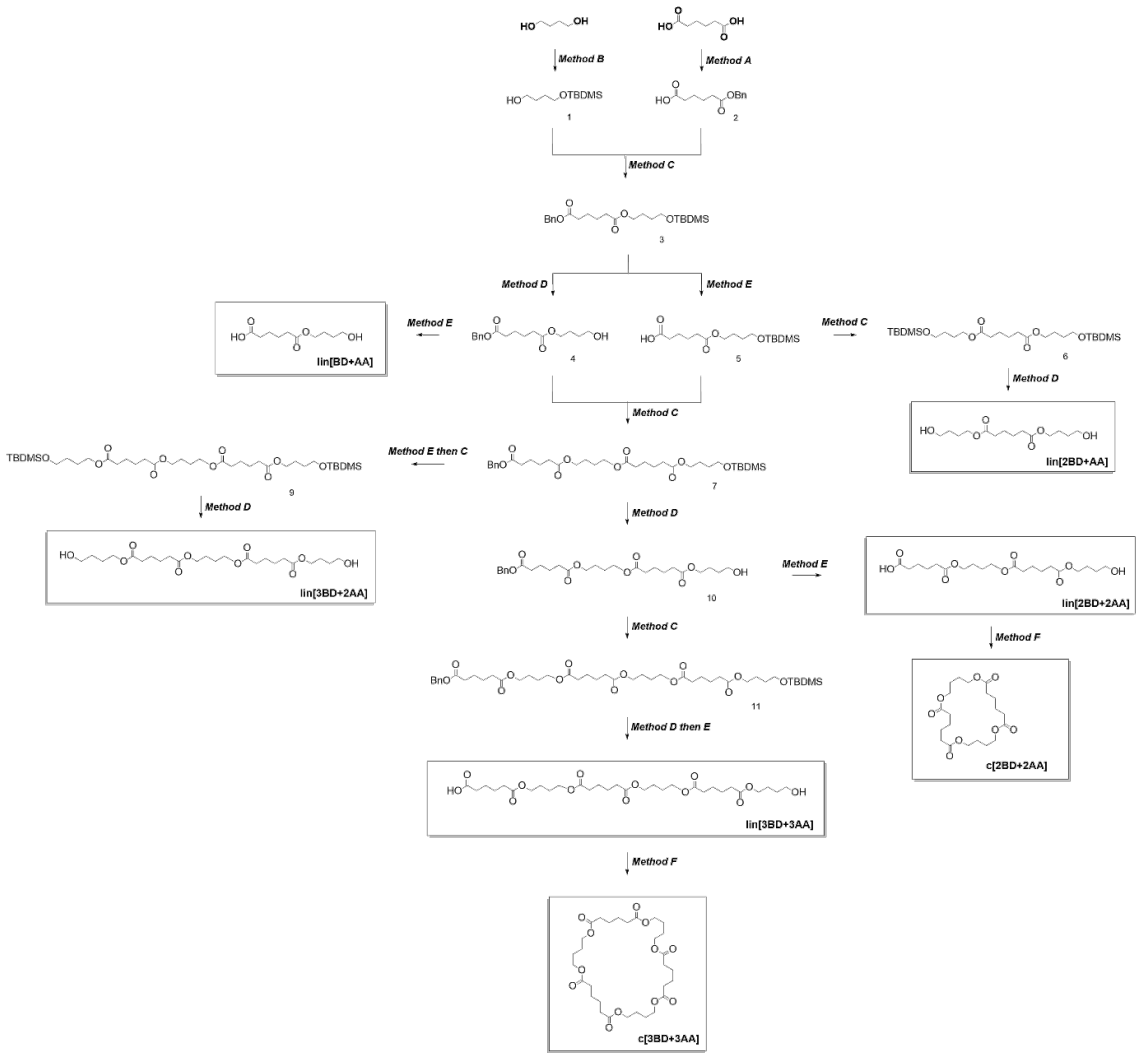

Figure 3.3. Stepwise synthesis of linear and cyclic oligoesters derived from butanediol (BD) and adipic acid (AA).

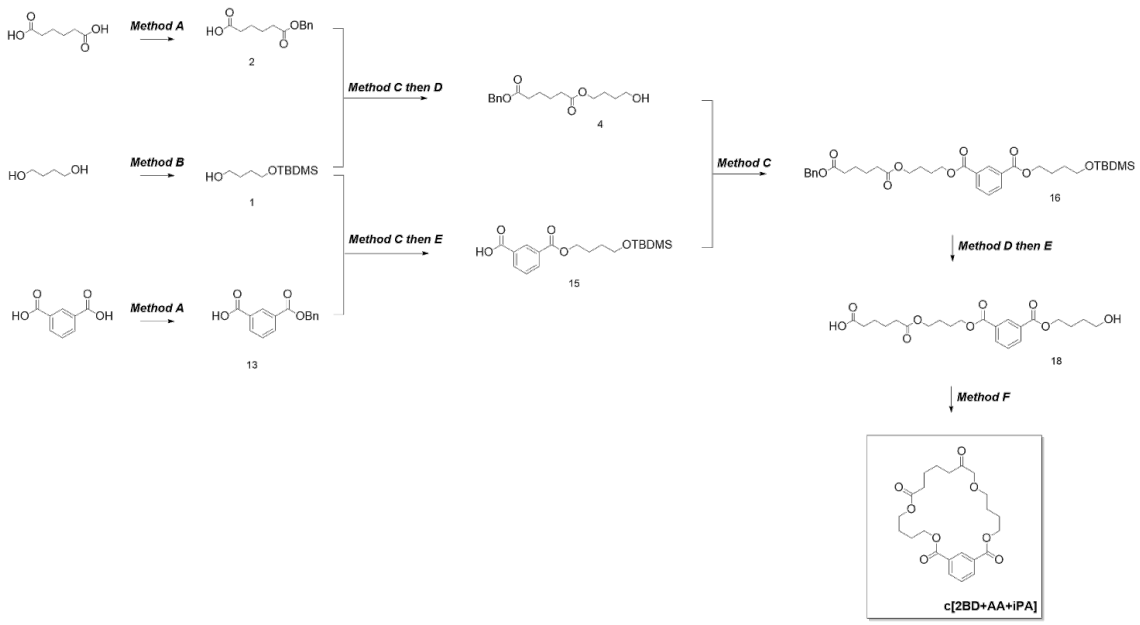

Figure 3.4. Stepwise synthesis of cyclic tetramer oligoester c[2BD+iPA+AA].

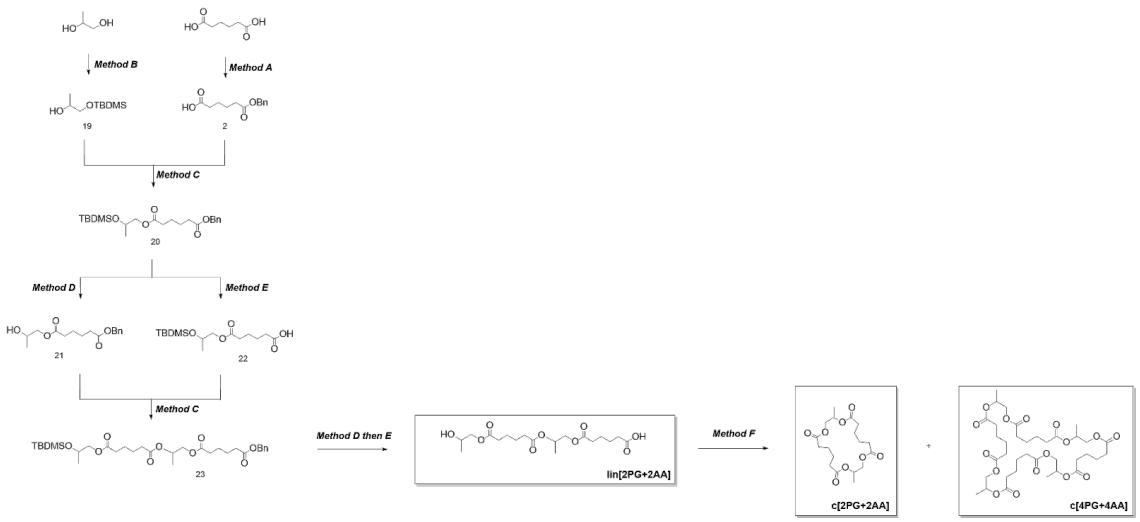

Figure 3.5. Stepwise synthesis of linear and cyclic oligoesters derived from propylene glycol (PG) and adipic acid (AA).

4.2.3. Characterisation

Characterisation data of the 11 synthesized oligoesters and their reaction intermediates (^{1}H and ^{13}C NMR, ESI-TOF-HRMS and melting point if applicable) can be found in the supplementary information. Table 2 showcases the chemical purities (*w/w*) of the final products. No impurities were identified for c[2BD+2AA], and most of the compounds showed a purity above 98% *w/w*. The three hydroxy

acids from AA and BD; lin[BD+AA], lin[2BD+2AA] and lin[3BD+3AA] were the products with the highest impurity percentages (29.7 to 98.8%). Most of the impurities involved side esterification reactions that resulted in larger chain oligoesters. This might be due to the fact that these impurities were formed during co-evaporation of the products under heat and vacuum, as continued removal of water can pull the equilibrium of the esterification reaction (Khan et al., 2021).

Table 3.2. LC-ESI-MS(Orbitrap) purity percentages of the synthesised oligoesters (w/w) and their impurities.

Compound	Purity	Impurities
lin[BD+AA]	29.7 %	lin[2BD+2AA] 54.3%, lin[3BD+3AA] 11.4%, lin[BD+AA+C_2H_5] 3.0%, lin[2BD+2AA+C_2H_5] 1.7%
lin[2BD+AA]	99.3 %	lin[3BD+2AA] 0.7%
lin[2BD+2AA]	81.6 %	lin[4BD+4AA] 13.6%, lin[3BD+3AA] 2.3%, lin[2BD+2AA+C_3H_8] 1.0%, c[2BD+2AA] 0.8%, lin[2BD+AA] 0.6%, lin[BD+AA] 0.1%
c[2BD+2AA]	100 %	-
lin[3BD+2AA]	97.3 %	$C_{18}H_{24}NO$ 2.3%, $C_{12}H_{28}NO_3$ 0.4%, lin[2BD+AA] 0.1%
lin[3BD+3AA]	98.8 %	$C_{34}H_{60}NO_{14}$ 1.0%, lin[3BD+2AA] 0.1%, lin[2BD+2AA] 0.1%
c[3BD+3AA]	98.6 %	$C_{16}H_{36}NO_2$ 1.1%, 650.3743 m/z [M+NH_4] 0.3%
c[2BD+AA+iPA]	98.7 %	c[2BD+2AA] 1.3%
lin[2PG+2AA]	98.7 %	lin[3PG+3AA] 0.9%, c[2PG+2AA] 0.4%
c[2PG+2AA]	98.0 %	$C_{48}H_{20}O_2$ 1.0%, $C_{49}H_{22}O_2$ 1.0%
c[4PG+4AA]	98.2 %	$C_{47}H_{56}NO_{23}$ 1.3%, $C_{49}H_{57}O_6$ 0.4%, c[2PG+2AA] 0.1%

4.3. Unequivocal identification and quantification

In order to verify the chemical structure of the oligomer candidates proposed during the identification of migration extracts, MS^2 spectra of precursor ions were compared with the spectra of a 10 $mg.kg^{-1}$ oligoesters solution. All synthesised oligoesters were identified with the retention time criteria and a minimum of 4 matching MS fragments. The application of the collision energy ramp proved to be a good tool to generate low and high mass fragments (see supplementary information). To the best of our knowledge, this is the first time that lin[BD+AA], lin[2BD+AA], lin[2BD+2AA] c[2BD+2AA], lin[3BD+2AA], lin[3BD+3AA], c[3BD+3AA],

c[2BD+AA+iPA], lin[2PG+2AA], c[2PG+2AA] and c[4PG+4AA] have been unequivocally identified as migrant oligoesters from biopolymer samples.

For quantification purposes, linearity and sensitivity were first determined on standard calibration curves. Gravimetrically prepared solutions of the oligoester standards were analysed by UPLC-MS(QTOF) and the area of the most abundant adduct for each compound ($[M + H]^+$ or $[M + Na]^+$) was obtained with a 10 ppm *m/z* tolerance. Linearity parameters for each analyte are presented in Table 3.3. Relative error or bias in the proposed linear range was within the acceptable order of ±20 %. Limits of detection (LOD) ranged from 0.03 to 2.54 $\mu g.kg^{-1}$, which is in range of what other authors found for similar compounds (Ubeda et al., 2020). Given that the slope represents the sensitivity of a method towards an analyte, we found differences between slopes of up to 30 times of c[2BD+AA+iPA] and lin[3BD+3AA]. Although the variation is less pronounced when comparing more chemically alike oligoesters, it is still relevant and will affect the final concentration values and, consequently, the safety compliance of the material. For example, between cyclic oligomers differences in response ranged from 1.1 to 6 times and for linear oligomers from 1.1 to 14 times. Even though differences in the ionization efficiency and transmission between analytes are known to be dependent on several factors (e.g. polarity, size, mobile phase composition), the understanding of the ESI process is still limited (Cech & Enke, 2001; Liigand et al., 2017). Moreover, the lack of oligomer standards makes semi-quantification the only alternative strategy to be applied for reporting purposes (Ubeda et al., 2021).

Table 3.3. Linearity data of the oligoester standards analysed by UPLC-MS(Q-TOF). Linear range, LOD and LOQ values are expressed in μg kg^{-1}. QS: quantifying standard.

QS no.	Compound	Quant *m/z*	Adduct	Slope	Interc ept	R^2	Linear range	LOD	LOQ
Q1	lin[BD+AA]	241.105	$[M + Na]^+$	10.18	21.87	0.999	6.2 - 1,000	1.87	6.22
Q2	lin[2BD+AA]	313.162	$[M + Na]^+$	18.02	206.84	0.998	1.5 - 1,000	0.44	1.47
Q3	lin[2BD+2AA]	441.210	$[M + Na]^+$	12.80	107.87	0.999	1 - 1,000	0.31	1.04
Q4	c[2BD+2AA]	401.217	$[M + H]^+$	8.73	35.35	0.999	1.7 - 1,000	0.52	1.74
Q5	lin[3BD+2AA]	513.267	$[M + Na]^+$	24.39	62.91	0.999	0.4 - 150	0.13	0.44
Q6	lin[3BD+3AA]	619.332	$[M + H]^+$	1.66	-29.39	0.998	8.5 - 1,000	2.54	8.46
Q7	c[3BD+3AA]	601.322	$[M + H]^+$	7.86	-56.86	0.999	1.1 - 1,000	0.33	1.11
Q8	c[2BD+AA+iPA]	443.168	$[M + Na]^+$	48.52	477.25	0.999	0.1 - 500	0.03	0.09
Q9	lin[2PG+2AA]	413.178	$[M + Na]^+$	14.19	29.18	0.998	3.5 - 1,000	1.04	3.46
Q10	c[2PG+2AA]	373.186	$[M + H]^+$	13.29	126.19	0.998	0.7 - 1,000	0.19	0.65
Q11	c[4PG+4AA]	745.364	$[M + H]^+$	8.166	-145.62	0.998	50-1,000	0.39	1.28

Migration values of migrant oligoesters (μg.kg^{-1} of food simulant) are summarised in Table 3.4. For oligoesters for which a standard was not synthesised, a quantifying standard from Table 3 was chosen according to their structure-type (linear or cyclic), size and free functional groups.

Comparing migration results from the 3 food simulants, simulant E showed the lowest migration values. In addition, due to Tenax different migration profile compared to simulants A and B, simulant E values were similar across all three samples. Despite being considerably higher than in Tenax, migration values in simulant B were lower than in simulant A, probably due to a lower solubility and the acid effect on the stability of oligoesters (Ubeda et al., 2020).

Considering samples, overall oligoester migration was higher in S2 than in S1 and S3, which were more similar. For example, c[2PG+2AA] was the dominant contributor to the migration from S2, while c[2BD+2AA] was the dominant for both S1 and S3. Concentrations of corresponding linear oligoesters were lower than their cyclic counterparts but, in both cases, still exceeded the value established by EU/10/2011 for non-listed substances (10 μg.kg^{-1}) except for c[2BD+AA+iPA] (S1, simulant B & S3, simulant E) and lin[4LA+C_2H_5] (S2, Simulant E). As recently stressed by the scientific community, there is hardly any toxicological data available on oligoesters (Cariou et al., 2022; Lestido-Cardama et al., 2022) which hinders a correct risk assessment. Recent studies showed androgen receptor (AR) activity of cyclic oligomers from food packaging adhesives (Ubeda et al., 2020) and the potential of PLA oligomers to bioaggregate in the liver, intestine, and brain (M. Wang et al., 2023). In these situations, a *read-cross* approach, such as the threshold of toxicological concern (TTC), could be used (More et al., 2019). TTC assigns a theoretical toxicity class to each compound depending on its chemical structure (Cramer et al., 1976). For this purpose, the software Toxtree v3.1.0 (Ideaconsult Ltd., Sofia, Bulgaria) was used. All compounds are divided into three classes according to their theoretical toxicities – low (I), intermediate (II), and high (III) – and are subject to a maximum daily intake above which further *in vitro* testing is required: 1.8, 0.54 and 0.09 mg per person per day, respectively. Moreover, compounds must not be potential mutagens, carcinogens, organophosphates, or carbamates. Assuming a food consumption of 1 kg/person/day, these intakes can be transformed to maximum recommended migration values. Most of the migrant compounds were listed as Class I, having a maximum recommended migration of 1,800 ng.g^{-1}, which was not exceeded for any of the oligomers. However, four oligoesters (c[2EG+2PG+4AA], lin[3BD+3AA], c[2BD+3AA+EG] and c[2BD+AA+PA]) were classified as class III, having a recommended migration limit of 90 ng.g^{-1}. From these four class III oligoesters, only c[2BD+AA+PA] did not exceed the limit, making S1 the only biopolymer sample to comply with the legislation under these premisses.

Although TTC values tend to be conservative, underestimation can occur for some compounds (Partosch et al., 2015; Reilly et al., 2019), evidencing the need of a

thorough toxicological assessment of oligoester migrants regardless of their Cramer class.

Table 3.4. Mean concentration values of oligomers (μg kg^{-1}) with standard deviation (n=3) in the three biopolymers (S1, S2 & S3) migration extracts in simulant A, B and E. In brackets in the first column: assigned quantification standard when different (see Table 3.3 for code). Concentration values in bold represent those surpassing their TTC value.

Compound	Cramer Class	Acetic Acid 3% (*v/v*)			Ethanol 10% (*v/v*)			Tenax®		
		S1	S2	S3	S1	S2	S3	S1	S2	S3
lin[2LA+C_2H_5] (Q1)	I	-	-	-	-	-	-	18.7 ± 2.2	28.7 ± 10.1	32.4 ± 13.8
lin[BD+AA]	I	86.9 ± 9.4	-	156.5 ± 4.9	-	-	-	-	-	-
c[2EG+2AA] (Q10)	I	-	801.6 ± 9.1	-	-	1,064.9 ± 5.9	-	-	34.0 ± 8.2	-
lin[2BD+AA]	I	23.6 ± 2.3	-	51.8 ± 2.7	-	-	-	-	-	-
lin[2PG+2AA]	I	-	301.1 ± 3.6	-	-	-	-	-	-	-
c[2PG+2AA]	I	-	692.2 ± 10.0	-	-	1,282.8 ± 5.7	-	-	15.1 ± 4.1	-
lin[4LA+C_2H_5] (Q9)	I	-	-	-	-	-	-	-	3.8 ± 1.7	-
c[5LA] (Q4)	I	-	-	-	-	-	-	19.6 ± 1.1	-	10.2 ± 2.3
lin[2BD+2AA]	I	124.2 ± 9.9	-	201.1 ± 6.9	-	-	-	-	-	-
c[6LA] (Q7)	I	84.6 ± 6.7	-	-	60.5 ± 3.5	-	-	15.8 ± 0.7	-	11.7 ± 2.8
c[DEG+SA] (Q4)	I	-	-	-	-	-	-	-	-	12.4 ± 3.2
lin[3BD+2AA]	I	-	-	165.8 ± 3.3	-	-	-	-	-	-
lin[2BD+2AA+PA] (Q6)	I	-	385.5 ± 9.7	-	-	840.3 ± 20.5	-	-	-	-
c[7LA] (Q7)	I	147.1 ± 12.9	501.8 ± 6.9	59.4 ± 4.2	133.7 ± 9.3	764.1 ± 39.7	-	-	-	-
c[2BD+2AA]	I	374.2 ± 17.5	-	472.1 ± 13.4	814.6 ± 46.8	-	971.3 ± 41.6	46.1 ± 3.9	-	90.4 ± 16.3
c[2EG+2PG+4AA] (Q11)	III	-	**251.5 ± 7.0**	-	-	**688.4 ± 10.5**	-	-	-	-

lin[3BD+3AA]	III	-	-	**143.5 ± 8.7**	-	-	-	-	-	-
c[2BD+3AA+EG] (Q7)	III	-	**205.1 ± 2.5**	-	-	**684.9 ± 17.8**	-	-	-	-
c[4PG+4AA]	I	-	65.2 ± 6.2	-	-	273.8 ± 4.8	-	-	-	-
c[AA+TMP] (Q10)	I	-	-	-	-	-	-	-	-	12.1 ± 2.1
c[2BD+AA+PA]	III	2.5 ± 0.8	-	11.6 ± 0.8	11.4 ± 0.7	-	19.5 ± 1.2	-	-	0.5 ± 0.1
c[3BD+3AA]	I	50.8 ± 2.1	-	99.6 ± 1.6	168.8 ± 8.3	-	255.6 ± 6.9	-	-	-
lin[7LA] (Q6)	I	31.4 ± 1.6	-	-	-	-	-	-	-	-
Total linear oligoesters		266.1 ± 20.2	683.6 ± 8.6	724.7 ± 21.0	-	840.3 ± 20.5	-	19.1 ± 2.4	32.5 ± 9.0	32.44 ± 13.8
Total cyclic oligoesters		659.2 ± 39.2	2,517.2 ± 20.8	543.0 ± 16.2	1,140.4 ± 103.0	4,758.8 ± 30.6	1,246.5 ± 45.0	82.0 ± 4.9	49.1 ± 12.2	137.3 ± 26.6
Total oligoesters		925.2 ± 59.3	3,200.9 ± 25.5	1,267.7 ± 35.1	1,140.4 ± 103.0	5,599.1 ± 40.5	1,246.5 ± 45.0	101.1 ± 6.9	81.54 ± 10.1	169.7 ± 14.5

5. Conclusions

In this work, the food safety of three starch-based biopolymer films has been assessed using three food simulants: ethanol 10%, acetic acid 3% and Tenax. A series of non-volatile migrant oligoesters arising mainly from adipic acid, 1,4-butanediol, propylene glycol, ethylene glycol and phthalic acid were detected in the migration extracts by UPLC-MS(QTOF). For identification and quantification purposes, 11 linear and cyclic oligoester combinations (lin[BD+AA], lin[2BD+AA], lin[2BD+2AA] c[2BD+2AA], lin[3BD+2AA], lin[3BD+3AA], c[3BD+3AA], c[2BD+AA+iPA], lin[2PG+2AA], c[2PG+2AA] and c[4PG+4AA]) were successfully synthesized by a multi-step approach and characterized by ^{1}H and ^{13}C NMR and LC-MS(Orbitrap). For the first time, these synthesised oligoester standards allowed to unequivocally identify and quantify the migrant oligoesters detected in biopolymer films. This allowed a more precise and concrete analysis of their theoretical toxicity, with only one of the three samples compliant according to the TTC approach. The protocol herein described aims to contribute towards the availability of oligoester standards, a prerequisite for the highly demanded toxicological studies of these packaging oligomers that will be able to shed some light into a grey area in the food packaging sector.

Section IV: Conclusions

Conclusions

Modern food systems still face important challenges regarding food losses and waste, foodborne outbreaks, as well as the growing unsustainable plastic food packaging management and production. Over this PhD thesis, different contributions towards food safety, either by **developing new active packaging systems** or by assessing the chemical risk of novel bio-based packaging materials, have been made. To this end, the **synthesis of α-CD-NS to be used as ethylene scavenger** has been performed, intended to decrease senescence of fruits and vegetables and increase their shelf-life. Moreover, **a diacetyl-based antimicrobial active packaging solution has been developed** and successfully tested in fresh meat. Finally, the safety of three starch-based food contact materials has been assessed by **synthesizing a new series of migrating oligoesters**.

To validate the potential of α-CD-NS production at an industrial level, the **scalability of the crosslinking reaction between α-CD and CDI through mechanochemical means** using a planetary ball mill, was validated using FTIR-ATR, demonstrating the capacity for this synthesis to be implemented at a bigger scale. Moreover, the **validated HPLC-DAD method** herein developed is sensitive, fast, and robust to monitor the washing step of the synthetized α-CD-NS, yielding safe, food-grade materials. The scaled-up α-CD-NS showed great potential to be a greener and effective alternative as ethylene scavengers when compared to other common absorbents such as bentonite and zeolite, paving the way for an active food packaging solution targeting fruits and vegetable spoilage. Even though the crosslinking of α-CD did not influence the specific surface area of α-CD-NS, it provided a polymer with higher physical and chemical stability, expanding their potential applications. Overall, the results obtained for α-CD-NS as ethylene scavenger show a new opportunity for active packaging solutions non-dependent in difficult to discard, toxic, metal-based alternatives such as potassium permanganate or palladium. As food-grade materials, the use of CD-NS opens a new field in the food sector, an area in which their use has not been sufficiently explored yet.

Regarding the **development of an antimicrobial active packaging solution**, antimicrobial *in vitro* testing of diacetyl showed no minimal inhibitory concentration in liquid phase, but high inhibition in vapor phase against *L. monocytogenes* and *S. enterica*. Furthermore, the vapor antimicrobial activity of diacetyl was higher for *S. enterica* than for *L. monocytogenes*, suggesting a higher antimicrobial susceptibility against Gram-negative than Gram-positive bacteria. However, the high volatility of diacetyl posed challenges for its incorporation in active packaging. To solve this issue, sodium stearate gels were found as a cheap and safe alternative to entrap diacetyl, although its concentration deeply affected the rheological properties of the resulting material. Moreover, embedding sodium stearate gels onto an absorbent material such as α-CD-NS proved to boost diacetyl release. Even though the sodium stearate gel and the α-CD-NS-NaSt composite active materials showed identical *in vitro* antimicrobial activity against *S. enterica*, *in vivo* experiments in inoculated packaged fresh beef filets demonstrated a two fold inhibition efficacy for the composite material. Moreover, both materials showed high *in vivo* antimicrobial activity towards common fresh meat microbiota such as total viable counts, pseudomonads, and lactic acid bacteria. These results, together with the fact that the diacetyl-based active packaging solutions are made of GRAS components, makes their usage in food packaging to control fresh meat spoilage and safety very promising. Moreover, they pave the way for other active packaging applications, as their effect towards other microorganisms and food products is yet to be studied.

Bio-based polymers aim to yield more sustainable alternatives to fossil-based plastic materials and are emerging materials in areas such as food packaging. However, new food contact materials may pose new risks and that is why its chemical safety should be thoroughly studied. In this work, for the safety assessment of three starch-based food contact materials, migration experiments were conducted according to EU regulation 10/2011. Non-targeted UPLC-HRMS migrant assessment revealed that oligoesters were the main form of NIAS, with cyclic oligoesters being the most prevalent across all samples when compared to their linear counterparts. Moreover, migrant oligoesters were mainly composed of adipic acid, isophthalic acid, lactic acid, 1,4-butanediol, and propylene glycol

monomers. Since the lack of oligoester standards continues to be a hurdle for the correct identification and quantification of these compounds in migration extracts, for the first time, a stepwise synthesis approach was performed to obtain oligoester standard combinations of: adipic acid and 1,4-butanediol, adipic acid and propylene glycol, and adipic acid, isophthalic acid and 1,4-butanediol. This stepwise **synthesis approach allowed to obtain the desired oligoester standards with good overall yields and purity**, indicating its suitability to be applied for the synthesis of other oligomer combinations. Using the synthesized oligoester combinations, the migrating oligoesters were unequivocally identified and quantified for the first time in bio-based food packaging materials. Interestingly, differences in the analytical responses of the synthesized oligoester standards used to quantify the migrant oligoesters, indicate the unsuitability of semi-quantification approaches, and stress the need for the availability of oligomer standards. In conclusion, **the synthesis, identification, and quantification of migrating oligoesters from starch-based samples has shed some light into the knowledge gaps about oligomers**. This stepwise synthesis approach will allow to further obtain more oligoester combinations and perform the necessary toxicological risk assessments for these substances, contributing towards safer plastic alternatives in the near future.

Conclusiones

La actual cadena alimentaria sigue enfrentando importantes desafíos en cuanto a pérdidas y desperdicio alimentario, brotes de enfermedades transmitidas por alimentos, así como la creciente e insostenible gestión y producción de envases alimentarios de plástico. A lo largo de esta tesis doctoral, se han realizado diferentes contribuciones enfocadas a la seguridad alimentaria, ya sea desarrollando **nuevos sistemas de envase activo** o evaluando el riesgo químico de nuevos biomateriales de envase. Con este fin, se llevó a cabo la **síntesis de α-CD-NS para ser utilizadas como captadores de etileno**, con la intención de disminuir el envejecimiento de frutas y verduras y aumentar su vida útil. Además, **se desarrolló y probó con éxito en carne fresca una solución de envase activo antimicrobiano basada en diacetilo**. Finalmente, se evaluó la seguridad de tres materiales de contacto alimentario con base de almidón mediante la **síntesis de una serie de oligoésteres migrantes**.

Para validar el potencial de producción de α-CD-NS a nivel industrial, **se comprobó la escalabilidad de la reacción de entrecruzamiento de α-CD con CDI por métodos mecanoquímicos** utilizando un molino de bolas planetario. La utilización de FTIR-ATR, demostró la posibilidad de implementar esta síntesis a una mayor escala. Además, **se desarrolló y validó un método de HPLC-DAD** suficientemente sensible, rápido y robusto como para monitorear y optimizar el proceso de lavado de las α-CD-NS sintetizadas, permitiendo el desarrollo de materiales entrecruzados con CDI seguros y aptos para alimentos. Las α-CD-NS escaladas mostraron un gran potencial como alternativa más ecológica y efectiva a los captadores de etileno convencionales, en comparación con otros adsorbentes comúnmente utilizados como la bentonita y la zeolita, abriendo el camino para una solución de envase activo dirigida al ralentizar el deterioro de frutas y verduras. Aunque el entrecruzamiento de α-CD no influyó en el área superficial de las α-CD-NS, proporcionó un polímero con mayor estabilidad física y química, lo que amplía sus potenciales aplicaciones. En general, los resultados obtenidos para las α-CD-NS como captadores de etileno proporcionan una nueva oportunidad para

soluciones de envase activo frente a las actuales alternativas con metales, difíciles de desechar y tóxicas, como el permanganato potásico o el paladio. Como materiales de grado alimenticio, el uso de CD-NS abre un nuevo campo en el sector alimentario, un área en la que su uso aún no se ha explorado suficientemente.

Respecto al **desarrollo de una solución de envase activo antimicrobiano**, las pruebas *in vitro* de susceptibilidad antimicrobiana del diacetilo no mostraron una concentración mínima inhibitoria en fase líquida. Sin embargo, se obtuvo una alta inhibición en fase vapor frente a *L. monocytogenes* y *S. entérica*, si bien la actividad antimicrobiana del diacetilo en fase vapor fue mayor para esta última, lo que sugiere una mayor susceptibilidad antimicrobiana frente a bacterias Gram-negativas que frente a Gram-positivas. Sin embargo, la alta volatilidad del diacetilo dificulta su incorporación en envasado activo. Para resolver este problema, se optó por geles de estearato de sodio como una alternativa económica y segura para retener el diacetilo, aunque se observó que su concentración en el gel tuvo un gran efecto sobre las propiedades reológicas del material resultante. Además, la incorporación de geles de estearato de sodio soportados sobre un material poroso como las α-CD-NS demostró aumentar la liberación de diacetilo. Aunque el gel activo de estearato de sodio y los materiales activos compuestos por α-CD-NS-NaSt mostraron una actividad antimicrobiana *in vitro* idéntica frente *S. enterica*, los experimentos *in vivo* con filetes inoculados de ternera fresca demostraron una eficacia de inhibición dos veces mayor para el material compuesto. Además, ambos materiales mostraron una alta actividad antimicrobiana *in vivo* frente a microbiota comúnmente presente en carne fresca, como los recuentos totales, *pseudomonas* y bacterias ácido-lácticas. Estos resultados, junto con el hecho de que las soluciones de envase activo desarrolladas se componen de elementos GRAS, hacen que su uso en envasado de alimentos para controlar el deterioro y la seguridad de carne fresca sea muy prometedor. Además, aplanan el camino para otras potenciales aplicaciones de envase activo, ya que su efecto hacia otros microorganismos y productos alimenticios aún debe ser estudiado.

Los biomateriales poliméricos tienen como objetivo proporcionar alternativas más sostenibles a los materiales plásticos basados en combustibles fósiles, siendo

materiales emergentes en áreas como el envasado de alimentos. Sin embargo, los nuevos materiales de contacto con alimentos pueden plantear nuevos riesgos, por lo que su seguridad química debe ser estudiada minuciosamente. Este trabajo, ha evaluado la seguridad de tres materiales de contacto alimentario con base de almidón, realizándose experimentos de migración de acuerdo con la regulación UE 10/2011. La evaluación de compuestos migrantes por UPLC-HRMS reveló que los oligoésteres fueron la forma principal de NIAS, siendo los cíclicos los más abundantes en todas las muestras en comparación con sus contrapartes lineales. Además, se determinó que los oligoésteres migrantes estaban formados principalmente por ácido adípico, ácido isoftálico, ácido láctico, 1,4-butanodiol y monómeros de propilenglicol. Dado que la ausencia de estándares de oligoésteres continúa siendo un obstáculo para la correcta identificación y cuantificación de estos compuestos en extractos de migración, por primera vez, se utilizó un enfoque de síntesis por etapas para obtener combinaciones de estándares de oligoésteres de: ácido adípico y 1,4-butanodiol, ácido adípico y propilen glicol, y ácido adípico, ácido isoftálico y 1,4-butanodiol. **Este método de síntesis por etapas permitió obtener los estándares de oligoésteres deseados con alta pureza y rendimientos generales**, indicando su idoneidad para ser aplicado en la síntesis de otras combinaciones de oligómeros. Además, utilizando las combinaciones de oligoésteres sintetizados, los oligoésteres migrantes fueron identificados y cuantificados inequívocamente por primera vez en materiales de envase alimentario con base de almidón. Curiosamente, las diferencias en las respuestas analíticas de los estándares sintetizados utilizados para cuantificar los oligoésteres migrantes indicaron la inadecuación de enfoques de semi-cuantificación, y resaltaron, una vez más, la necesidad de disponibilidad de estándares de oligómeros. En conclusión, **la síntesis, identificación y cuantificación de oligoésteres migrantes a partir de muestras con base de almidón ha arrojado luz sobre las lagunas de conocimiento sobre oligómeros**. Además, este enfoque sintético por etapas permitirá obtener más combinaciones de oligoésteres y realizar las necesarias evaluaciones de riesgo toxicológico para estas sustancias, contribuyendo hacia alternativas de plástico más seguras en un futuro cercano.

Section V: References

References

Abeles, F. B., Morgan, P. W., & Saltveit, M. E. (Mikal E. (1992). *Ethylene in plant biology* (2nd ed.). Academic Press.

Abouloifa, H., Hasnaoui, I., Rokni, Y., Bellaouchi, R., Ghabbour, N., Karboune, S., Brasca, M., Abousalham, A., Jaouadi, B., Saalaoui, E., & Asehraou, A. (2022). *Antifungal activity of lactic acid bacteria and their application in food biopreservation* (pp. 33–77). https://doi.org/10.1016/bs.aambs.2022.07.001

AENOR. (2004). Paper and board intended to come into contact with foodstuffs - conditions for determination of migration from paper and board using modified polyphenylene oxide (MPPO) as a simulant. *UNE-EN 14338*.

Agarwal, S., Singhal, S., Godiya, C. B., & Kumar, S. (2023). Prospects and Applications of Starch based Biopolymers. *International Journal of Environmental Analytical Chemistry*, *103*(18), 6907–6926. https://doi.org/10.1080/03067319.2021.1963717

Aguiar, M. S., Coelho, A. F. S. M. R., Almeida, P. J., & Santos, J. R. (2023). Fan Assisted Extraction of Volatile Carbonyl Compounds from Coffee Brews Based on the Full Evaporation Technique. *Foods*, *12*(18), 3389. https://doi.org/10.3390/foods12183389

Ahmed, M. W., Haque, M. A., Mohibbullah, M., Khan, M. S. I., Islam, M. A., Mondal, M. H. T., & Ahmmed, R. (2022). A review on active packaging for quality and safety of foods: Current trends, applications, prospects and challenges. *Food Packaging and Shelf Life*, *33*, 100913. https://doi.org/10.1016/J.FPSL.2022.100913

Alamri, M. S., Qasem, A. A. A., Mohamed, A. A., Hussain, S., Ibraheem, M. A., Shamlan, G., Alqah, H. A., & Qasha, A. S. (2021). Food packaging's materials: A food safety perspective. In *Saudi Journal of Biological Sciences* (Vol. 28, Issue 8, pp. 4490–4499). Elsevier B.V. https://doi.org/10.1016/j.sjbs.2021.04.047

Alberto Lopes, J., & Tsochatzis, E. D. (2023a). Poly(ethylene terephthalate), Poly(butylene terephthalate), and Polystyrene Oligomers: Occurrence and Analysis in Food Contact Materials and Food. *Journal of Agricultural and Food Chemistry*, *71*(5), 2244–2258. https://doi.org/10.1021/acs.jafc.2c08558

Alberto Lopes, J., & Tsochatzis, E. D. (2023b). Poly(ethylene terephthalate), Poly(butylene terephthalate), and Polystyrene Oligomers: Occurrence and Analysis in Food Contact Materials and Food. *Journal of Agricultural and Food Chemistry*, *71*(5), 2244–2258. https://doi.org/10.1021/acs.jafc.2c08558

Alegbeleye, O., Odeyemi, O. A., Strateva, M., & Stratev, D. (2022). Microbial spoilage of vegetables, fruits and cereals. *Applied Food Research*, *2*(1), 100122. https://doi.org/10.1016/j.afres.2022.100122

Alizadeh-Sani, M., Moghaddas Kia, E., Ghasempour, Z., & Ehsani, A. (2021). Preparation of Active Nanocomposite Film Consisting of Sodium Caseinate,

ZnO Nanoparticles and Rosemary Essential Oil for Food Packaging Applications. *Journal of Polymers and the Environment*, *29*(2), 588–598. https://doi.org/10.1007/s10924-020-01906-5

Alkan Tas, B., Sehit, E., Erdinc Tas, C., Unal, S., Cebeci, F. C., Menceloglu, Y. Z., & Unal, H. (2019). Carvacrol loaded halloysite coatings for antimicrobial food packaging applications. *Food Packaging and Shelf Life*, *20*, 100300. https://doi.org/10.1016/j.fpsl.2019.01.004

Almenar, E., Catala, R., Hernandez-Muñoz, P., & Gavara, R. (2009). Optimization of an active package for wild strawberries based on the release of 2-nonanone. *LWT - Food Science and Technology*, *42*(2), 587–593. https://doi.org/10.1016/j.lwt.2008.09.009

Alp, A. C., & Yerlikaya, P. (2020). Phthalate ester migration into food: effect of packaging material and time. *European Food Research and Technology*, *246*(3), 425–435. https://doi.org/10.1007/s00217-019-03412-y

Álvarez-Hernández, M. H., Martínez-Hernández, G. B., Castillejo, N., Martínez, J. A., & Artés-Hernández, F. (2021). Development of an antifungal active packaging containing thymol and an ethylene scavenger. Validation during storage of cherry tomatoes. *Food Packaging and Shelf Life*, *29*, 100734. https://doi.org/10.1016/j.fpsl.2021.100734

Amiri, A., Sourestani, M. M., Mortazavi, S. M. H., Kiasat, A. R., & Ramezani, Z. (2022). Fabrication of the antimicrobial sachet by encapsulation of peppermint essential oil in active packaging of strawberry fruit. *Journal of Food Processing and Preservation*, *46*(12). https://doi.org/10.1111/jfpp.17181

Anastas, P. T., & Warner, J. C. (1998). *Green Chemistry: Theory and Practice*. Oxford University Press.

Andrade, R., Skurtys, O., & Osorio, F. (2015). Drop impact of gelatin coating formulated with cellulose nanofibers on banana and eggplant epicarps. *LWT - Food Science and Technology*, *61*(2), 422–429. https://doi.org/10.1016/j.lwt.2014.12.035

Ansari, K. A., Vavia, P. R., Trotta, F., & Cavalli, R. (2011). Cyclodextrin-based nanosponges for delivery of resveratrol: In vitro characterisation, stability, cytotoxicity and permeation study. *AAPS PharmSciTech*, *12*(1), 279–286. https://doi.org/10.1208/S12249-011-9584-3/FIGURES/13

Arrioja-Bretón, D., Mani-López, E., Palou, E., & López-Malo, A. (2020). Antimicrobial activity and storage stability of cell-free supernatants from lactic acid bacteria and their applications with fresh beef. *Food Control*, *115*, 107286. https://doi.org/10.1016/j.foodcont.2020.107286

Artiga-Artigas, M., Acevedo-Fani, A., & Martín-Belloso, O. (2017). Improving the shelf life of low-fat cut cheese using nanoemulsion-based edible coatings containing oregano essential oil and mandarin fiber. *Food Control*, *76*, 1–12. https://doi.org/10.1016/j.foodcont.2017.01.001

Arvanitoyannis, I. S., & Kotsanopoulos, K. V. (2014). Migration Phenomenon in Food Packaging. Food-Package Interactions, Mechanisms, Types of Migrants,

Testing and Relative Legislation-A Review. In *Food and Bioprocess Technology* (Vol. 7, Issue 1, pp. 21–36). https://doi.org/10.1007/s11947-013-1106-8

Ashter, S. A. (2016). Types of Biodegradable Polymers. In *Introduction to Bioplastics Engineering* (pp. 81–151). Elsevier. https://doi.org/10.1016/B978-0-323-39396-6.00005-1

Aytac, Z., Ipek, S., Durgun, E., Tekinay, T., & Uyar, T. (2017). Antibacterial electrospun zein nanofibrous web encapsulating thymol/cyclodextrin-inclusion complex for food packaging. *Food Chemistry*, *233*, 117–124. https://doi.org/10.1016/j.foodchem.2017.04.095

Azevedo, V. M., Silva, E. K., Gonçalves Pereira, C. F., da Costa, J. M. G., & Borges, S. V. (2015). Whey protein isolate biodegradable films: Influence of the citric acid and montmorillonite clay nanoparticles on the physical properties. *Food Hydrocolloids*, *43*, 252–258. https://doi.org/10.1016/j.foodhyd.2014.05.027

Aznar, M., Alfaro, P., Nerín, C., Jones, E., & Riches, E. (2016). Progress in mass spectrometry for the analysis of set-off phenomena in plastic food packaging materials. *Journal of Chromatography A*, *1453*, 124–133. https://doi.org/10.1016/j.chroma.2016.05.032

Aznar, M., Domeño, C., & Nerin, C. (2023). Determination of volatile migrants from breast milk storage bags. *Food Packaging and Shelf Life*, *40*. https://doi.org/10.1016/j.fpsl.2023.101196

Aznar, M., Ubeda, S., Dreolin, N., & Nerín, C. (2019). Determination of non-volatile components of a biodegradable food packaging material based on polyester and polylactic acid (PLA) and its migration to food simulants. *Journal of Chromatography A*, *1583*, 1–8. https://doi.org/10.1016/j.chroma.2018.10.055

Aznar, M., Vera, P., Canellas, E., Nerín, C., Mercea, P., & Störmer, A. (2011). Composition of the adhesives used in food packaging multilayer materials and migration studies from packaging to food. *Journal of Materials Chemistry*, *21*(12), 4358. https://doi.org/10.1039/c0jm04136j

Barbiroli, A., Musatti, A., Capretti, G., Iametti, S., & Rollini, M. (2017). Sakacin-A antimicrobial packaging for decreasing *Listeria* contamination in thin-cut meat: preliminary assessment. *Journal of the Science of Food and Agriculture*, *97*(3), 1042–1047. https://doi.org/10.1002/jsfa.8120

Barnard, E., Rubio Arias, J. J., & Thielemans, W. (2021). Chemolytic depolymerisation of PET: a review. *Green Chemistry*, *23*(11), 3765–3789. https://doi.org/10.1039/D1GC00887K

Becerril, R., Gómez-Lus, R., Goñi, P., López, P., & Nerín, C. (2007). Combination of analytical and microbiological techniques to study the antimicrobial activity of a new active food packaging containing cinnamon or oregano against E. coli and S. aureus. *Analytical and Bioanalytical Chemistry*, *388*(5–6), 1003–1011. https://doi.org/10.1007/s00216-007-1332-x

Becerril, R., Manso, S., Nerin, C., & Gómez-Lus, R. (2013). Antimicrobial activity of Lauroyl Arginate Ethyl (LAE), against selected food-borne bacteria. *Food Control*, *32*(2), 404–408. https://doi.org/10.1016/j.foodcont.2013.01.003

Becerril, R., Nerín, C., & Silva, F. (2020). Encapsulation Systems for Antimicrobial Food Packaging Components: An Update. *Molecules*, *25*(5), 1134. https://doi.org/10.3390/molecules25051134

Becerril, R., Precone, M., & Nerin, C. (2023). Antibiofilm activity of LAE (ethyl lauroyl arginate) against food-borne fungi and its application in polystyrene surface coating. *Food Microbiology*, *113*, 104284. https://doi.org/10.1016/j.fm.2023.104284

Bennett, J. W., & Klich, M. (2003). Mycotoxins. *Clinical Microbiology Reviews*, *16*(3), 497–516. https://doi.org/10.1128/CMR.16.3.497-516.2003

Bheemaneni, G., Saravana, S., & Kandaswamy, R. (2018). Processing and Characterization of Poly (butylene adipate-co-terephthalate) / Wollastonite Biocomposites for Medical Applications. *Materials Today: Proceedings*, *5*(1), 1807–1816. https://doi.org/10.1016/j.matpr.2017.11.279

Bhowmik, S., Agyei, D., & Ali, A. (2022a). Bioactive chitosan and essential oils in sustainable active food packaging: Recent trends, mechanisms, and applications. *Food Packaging and Shelf Life*, *34*, 100962. https://doi.org/10.1016/J.FPSL.2022.100962

Bhowmik, S., Agyei, D., & Ali, A. (2022b). Bioactive chitosan and essential oils in sustainable active food packaging: Recent trends, mechanisms, and applications. *Food Packaging and Shelf Life*, *34*, 100962. https://doi.org/10.1016/J.FPSL.2022.100962

Biedermann-Brem, S., Kasprick, N., Simat, T., & Grob, K. (2011). Migration of polyolefin oligomeric saturated hydrocarbons (POSH) into food. *Food Additives & Contaminants: Part A*, 1–12. https://doi.org/10.1080/19440049.2011.641164

Birck, C., Degoutin, S., Maton, M., Neut, C., Bria, M., Moreau, M., Fricoteaux, F., Miri, V., & Bacquet, M. (2016). Antimicrobial citric acid/poly(vinyl alcohol) crosslinked films: Effect of cyclodextrin and sodium benzoate on the antimicrobial activity. *LWT - Food Science and Technology*, *68*, 27–35. https://doi.org/10.1016/j.lwt.2015.12.009

Blanke, M. (2015). Challenges of Reducing Fresh Produce Waste in Europe—From Farm to Fork. *Agriculture 2015, Vol. 5, Pages 389-399*, *5*(3), 389–399. https://doi.org/10.3390/AGRICULTURE5030389

Bugatti, V., Vertuccio, L., Viscusi, G., & Gorrasi, G. (2018). Antimicrobial Membranes of Bio-Based PA 11 and HNTs Filled with Lysozyme Obtained by an Electrospinning Process. *Nanomaterials*, *8*(3), 139. https://doi.org/10.3390/nano8030139

Burgos, N., Tolaguera, D., Fiori, S., & Jiménez, A. (2014). Synthesis and Characterization of Lactic Acid Oligomers: Evaluation of Performance as Poly(Lactic Acid) Plasticizers. *Journal of Polymers and the Environment*, *22*(2), 227–235. https://doi.org/10.1007/s10924-013-0628-5

Busetti, S., & Pace, N. (2022). *Food Loss and Waste Policy*. Routledge. https://doi.org/10.4324/9781003226932

Caldera, F., Tannous, M., Cavalli, R., Zanetti, M., & Trotta, F. (2017). Evolution of Cyclodextrin Nanosponges. *International Journal of Pharmaceutics*, *531*(2), 470–479. https://doi.org/10.1016/J.IJPHARM.2017.06.072

Calvo, J., Lavandera, J. L., Agüeros, M., & Irache, J. M. (2011). Cyclodextrin/poly(anhydride) nanoparticles as drug carriers for the oral delivery of atovaquone. *Biomedical Microdevices*, *13*(6), 1015–1025. https://doi.org/10.1007/S10544-011-9571-1/FIGURES/5

Camele, I., Sadeek, S. A., Racioppi, R., & Elshafie, H. S. (2023). Antimicrobial Activity of Diffusible and Volatile Metabolites Emitted by Beauveria bassiana: Chemical Profile of Volatile Organic Compounds (VOCs) Using SPME-GC/MS Analysis. *Plants*, *12*(15), 2854. https://doi.org/10.3390/plants12152854

Cameron, G. (2020). *Future of Packaging: Long-Term Strategic Forecasts to 2030*. http://www.smitherspira.com/

Cancio, L. P. M., Danao, M. C., Sullivan, G. A., & Chaves, B. D. (2023). Evaluation of peroxyacetic acid, liquid buffered vinegar, and cultured dextrose fermentate as potential antimicrobial interventions for raw chicken livers. *Journal of Food Safety*, *43*(4). https://doi.org/10.1111/jfs.13054

Canellas, E., Vera, P., & Nerín, C. (2015a). Risk assessment derived from migrants identified in several adhesives commonly used in food contact materials. *Food and Chemical Toxicology*, *75*, 79–87. https://doi.org/10.1016/j.fct.2014.10.029

Canellas, E., Vera, P., & Nerín, C. (2015b). Risk assessment derived from migrants identified in several adhesives commonly used in food contact materials. *Food and Chemical Toxicology*, *75*, 79–87. https://doi.org/10.1016/j.fct.2014.10.029

Canellas, E., Vera, P., & Nerín, C. (2015c). UPLC-ESI-Q-TOF-MS E and GC-MS identification and quantification of non-intentionally added substances coming from biodegradable food packaging. *Anal Bioanal Chem*, *407*, 6781–6790. https://doi.org/10.1007/s00216-015-8848-2

Canellas, E., Vera, P., & Nerín, C. (2015d). UPLC–ESI-Q-TOF-MSE and GC–MS identification and quantification of non-intentionally added substances coming from biodegradable food packaging. *Analytical and Bioanalytical Chemistry*, *407*(22), 6781–6790. https://doi.org/10.1007/s00216-015-8848-2

Canellas, E., Vera, P., & Nerín, C. (2017). Migration assessment and the 'threshold of toxicological concern' applied to the safe design of an acrylic adhesive for food-contact laminates. *Food Additives & Contaminants: Part A*, *34*(10), 1721–1729. https://doi.org/10.1080/19440049.2017.1308017

Canellas, E., Vera, P., & Nerín, C. (2019). Ion mobility quadrupole time-of-flight mass spectrometry for the identification of non-intentionally added substances in UV varnishes applied on food contact materials. A safety by design study. *Talanta*, *205*, 120103. https://doi.org/10.1016/j.talanta.2019.06.103

Canellas, E., Vera, P., Nerín, C., Dreolin, N., & Goshawk, J. (2020). Ion mobility quadrupole time-of-flight high resolution mass spectrometry coupled to ultra-high pressure liquid chromatography for identification of non-intentionally added substances migrating from food cans. *Journal of Chromatography A*, *1616*, 460778. https://doi.org/10.1016/j.chroma.2019.460778

Canellas, E., Vera, P., Nerin, C., Goshawk, J., & Dreolin, N. (2021). The application of ion mobility time of flight mass spectrometry to elucidate neo-formed compounds derived from polyurethane adhesives used in champagne cork stoppers. *Talanta*, *234*, 122632. https://doi.org/10.1016/j.talanta.2021.122632

Canning, M., Birhane, M. G., Dewey-Mattia, D., Lawinger, H., Cote, A., Gieraltowski, L., Schwensohn, C., Tagg, K. A., Francois Watkins, L. K., Park Robyn, M., & Marshall, K. E. (2023). Salmonella Outbreaks Linked to Beef, United States, 2012–2019. *Journal of Food Protection*, *86*(5), 100071. https://doi.org/10.1016/j.jfp.2023.100071

Cariou, R., Rivière, M., Hutinet, S., Tebbaa, A., Dubreuil, D., Mathé-Allainmat, M., Lebreton, J., Le Bizec, B., Tessier, A., & Dervilly, G. (2022). Thorough investigation of non-volatile substances extractible from inner coatings of metallic cans and their occurrence in the canned vegetables. *Journal of Hazardous Materials*, *435*. https://doi.org/10.1016/j.jhazmat.2022.129026

CDC. (2009, May). *Multistate Outbreak of Salmonella Typhimurium Infections Linked to Peanut Butter, 2008-2009*. Https://Www.Cdc.Gov/Salmonella/2009/Peanut-Butter-2008-2009.Html#print.

CDC, FDA, USDA-FSIS, & IFSAC. (2018, July). *Foodborne Illness Source Attribution Estimates in 2013 for Salmonella, Escherichia coli O157, Listeria monocytogenes, and Campylobacter Using Multi-year Outbreak Surveillance Data, United States*.

Cech, N. B., & Enke, C. G. (2001). Practical implications of some recent studies in electrospray ionization fundamentals. *Mass Spectrometry Reviews*, *20*(6), 362–387. https://doi.org/10.1002/mas.10008

Cho, M., Yang, J., Noh, S., Joe, H., & Han, M. (2016). Production of PBT(polybutylene terephthalate) Oligomer from Recycled PET(polyethylene terephthalate). *Korean Chemical Engineering Research*, *54*(4), 437–442. https://doi.org/10.9713/kcer.2016.54.4.437

Choi, J. O., Jitsunari, F., Asakawa, F., & sun Lee, D. (2005). Migration of styrene monomer, dimers and trimers from polystyrene to food simulants. *Food Additives and Contaminants*, *22*(7), 693–699. https://doi.org/10.1080/02652030500160050

Choosung, P., Utto, W., Boonyaritthongchai, P., Wasusri, T., & Wongs-Aree, C. (2019). Ethanol vapor releasing sachet reduces decay and improves aroma attributes in mulberry fruit. *Food Packaging and Shelf Life*, *22*, 100398. https://doi.org/10.1016/j.fpsl.2019.100398

Clemente, I., Aznar, M., Nerín, C., & Bosetti, O. (2016). Migration from printing inks in multilayer food packaging materials by GC-MS analysis and pattern recognition with chemometrics. *Food Additives & Contaminants: Part A*, 1–12. https://doi.org/10.1080/19440049.2016.1155757

Clemente, I., Aznar, M., Silva, F., & Nerín, C. (2016). Antimicrobial properties and mode of action of mustard and cinnamon essential oils and their combination against foodborne bacteria. *Innovative Food Science & Emerging Technologies*, *36*, 26–33. https://doi.org/10.1016/j.ifset.2016.05.013

Clinical and Laboratory Standards Institute (CLSI). (2012). M07-A9: Methods for dilution antimicrobial susceptibility tests for bacteria that grow aerobically; approved standard—ninth edition. CLSI document M07-A9. . *Www.Clsi.Org*.

Clinical and Laboratory Standards Institute (CLSI). (2015). M45: Methods for antimicrobial dilution and disk susceptibility testing of infrequently isolated or Fastidious bacteria. Guidelines CLSI, 35. *Www.Clsi.Org*.

Colacino, E., Isoni, V., Crawford, D., & García, F. (2021). Upscaling Mechanochemistry: Challenges and Opportunities for Sustainable Industry. *Trends in Chemistry*, *3*(5), 335–339. https://doi.org/10.1016/J.TRECHM.2021.02.008

Coltro, L., Pitta, J. B., da Costa, P. A., Fávaro Perez, M. Â., de Araújo, V. A., & Rodrigues, R. (2014). Migration of conventional and new plasticizers from PVC films into food simulants: A comparative study. *Food Control*, *44*, 118–129. https://doi.org/10.1016/j.foodcont.2014.03.058

Commision Regulation (EU) No 10/2011 of 14 January 2011 on Plastic Materials and Articles Intended to Come into Contact with Food (2011).

Corkovi´ccorkovi´c, I., Pichler, A., Ivi´c, I. I., Šimunovi´c, J. Š., Kopjar, M., Wagemans, A. M., & Keppler, J. (2021). *Microencapsulation of Chokeberry Polyphenols and Volatiles: Application of Alginate and Pectin as Wall Materials*. https://doi.org/10.3390/gels7040231

Coulier, L., Orbons, H. G. M., & Rijk, R. (2007). Analytical protocol to study the food safety of (multiple-)recycled high-density polyethylene (HDPE) and polypropylene (PP) crates: Influence of recycling on the migration and formation of degradation products. *Polymer Degradation and Stability*, *92*(11), 2016–2025. https://doi.org/10.1016/j.polymdegradstab.2007.07.022

Cramer, G. M., Ford, R. A., & Hall, R. L. (1976). Estimation of toxic hazard—A decision tree approach. *Food and Cosmetics Toxicology*, *16*(3), 255–276. https://doi.org/10.1016/S0015-6264(76)80522-6

Cui, H. Y., Wu, J., Li, C. Z., & Lin, L. (2016). Anti-listeria effects of chitosan-coated nisin-silica liposome on Cheddar cheese. *Journal of Dairy Science*, *99*(11), 8598–8606. https://doi.org/10.3168/jds.2016-11658

Dainelli, D. (2008). Recycling of food packaging materials: an overview. In *Environmentally Compatible Food Packaging* (pp. 294–325). Elsevier. https://doi.org/10.1533/9781845694784.2.294

Debuissy, T., Pollet, E., & Avérous, L. (2016). Synthesis of potentially biobased copolyesters based on adipic acid and butanediols: Kinetic study between 1,4- and 2,3-butanediol and their influence on crystallization and thermal properties. *Polymer*, *99*, 204–213. https://doi.org/10.1016/j.polymer.2016.07.022

Del Valle, E. M. M. (2004). Cyclodextrins and their uses: a review. *Process Biochemistry*, *39*(9), 1033–1046. https://doi.org/10.1016/S0032-9592(03)00258-9

Dillon, V. M. (2014). NATURAL ANTI-MICROBIAL SYSTEMS | Preservative Effects During Storage. In *Encyclopedia of Food Microbiology* (pp. 941–947). Elsevier. https://doi.org/10.1016/B978-0-12-384730-0.00238-X

Djebari, S., Wrona, M., Boudria, A., Salafranca, J., Nerin, C., Bedjaoui, K., & Madani, K. (2021). Study of bioactive volatile compounds from different parts of Pistacia lentiscus L. extracts and their antioxidant and antibacterial activities for new active packaging application. *Food Control*, *120*, 107514. https://doi.org/10.1016/J.FOODCONT.2020.107514

Domeño, C., Aznar, M., Nerín, C., Isella, F., Fedeli, M., & Bosetti, O. (2017). Safety by design of printed multilayer materials intended for food packaging. *Food Additives & Contaminants: Part A*, *34*(7), 1239–1250. https://doi.org/10.1080/19440049.2017.1322221

Dreolin, N., Aznar, M., Moret, S., & Nerin, C. (2019). Development and validation of a LC–MS/MS method for the analysis of bisphenol a in polyethylene terephthalate. *Food Chemistry*, *274*, 246–253. https://doi.org/10.1016/j.foodchem.2018.08.109

Duarte, A., Alves, A. C., Ferreira, S., Silva, F., & Domingues, F. C. (2015). Resveratrol inclusion complexes: Antibacterial and anti-biofilm activity against Campylobacter spp. and Arcobacter butzleri. *Food Research International*, *77*, 244–250. https://doi.org/10.1016/J.FOODRES.2015.05.047

EC. (2004). Regulation (EC) No 1935/2004 of the European Parliament and of the Council of 27 October 2004 on materials and articles intended to come into contact with food and repealing Directives 80/590/EEC and 89/109/EEC. In *European Commission*. http://data.europa.eu/eli/reg/2004/1935/2021-03-27

EC. (2005). *Commission Regulation (EC) No 1895/2005 of 18 November 2005 on the restriction of use of certain epoxy derivatives in materials and articles intended to come into contact with food*. http://data.europa.eu/eli/reg/2005/1895/oj

EC. (2006). *Commission Regulation (EC) No 2023/2006 of 22 December 2006 on good manufacturing practice for materials and articles intended to come into contact with food*. http://data.europa.eu/eli/reg/2006/2023/2008-04-17

EC. (2007). *Commission Directive 2007/42/EC of 29 June 2007 relating to materials and articles made of regenerated cellulose film intended to come into contact with foodstuffs*. http://data.europa.eu/eli/dir/2007/42/oj

EC. (2009). *Commission Regulation (EC) No 450/2009 of 29 May 2009 on active and intelligent materials and articles intended to come into contact with food*. http://data.europa.eu/eli/reg/2009/450/oj

EC. (2011). *Commission Regulation (EU) No 284/2011 of 22 March 2011 laying down specific conditions and detailed procedures for the import of polyamide and melamine plastic kitchenware originating in or consigned from the People's Republic of China and Hong Kong Special Administrative Region, China*.

ECHA. (2012). *Harmonised Classification and Labelling report for Imidazole*.

Eckardt, M., Schneider, J., & Simat, T. J. (2019). *In vitro* intestinal digestibility of cyclic aromatic polyester oligomers from polyethylene terephthalate (PET) and polybutylene terephthalate (PBT). *Food Additives & Contaminants: Part A*, *36*(12), 1882–1894. https://doi.org/10.1080/19440049.2019.1658903

EEC. (1984). *Council Directive 84/500/EEC of 15 October 1984 on the approximation of the laws of the Member States relating to ceramic articles intended to come into contact with foodstuffs*. http://data.europa.eu/eli/dir/1984/500/oj

EEC. (1993). *Commission Directive 93/11/EEC of 15 March 1993 concerning the release of the N-nitrosamines and N- nitrosatable substances from elastomer or rubber teats and soothers*. http://data.europa.eu/eli/dir/1993/11/oj

EFSA. (2016). Growth of spoilage bacteria during storage and transport of meat. *EFSA Journal - Panel on Biological Hazards (BIOHAZ)*, *14*(6). https://doi.org/10.2903/j.efsa.2016.4523

EFSA. (2023). The European Union One Health 2022 Zoonoses Report. *EFSA Journal*, *21*(12). https://doi.org/10.2903/j.efsa.2023.8442

Eicher, A., Biedermann, M., Zurfluh, M., & Grob, K. (2015). Migration by 'direct' or 'indirect' food contact? 'Dry' and 'wetting' foods? Experimental data for 'touching' contact of dry foods with paper and board. *Food Additives & Contaminants: Part A*, *32*(1), 110–119. https://doi.org/10.1080/19440049.2014.975753

E.L. Bradley. (2010). *Biobased Materials Used in Food Contact Applications: An Assessment of the Migration Potential*.

Enderle, A. G., Franco-Castillo, I., Atrián-Blasco, E., Martín-Rapu, R., Lizarraga, L., Culzoni, M. J., Bollini, M., de la Fuente, M., Silva, F., Streb, C., & Mitchell, S. G. (2022). Hybrid Antimicrobial Films Containing a Polyoxometalate-Ionic Liquid. *Cite This: ACS Appl. Polym. Mater*, *2022*, 4144–4153. https://doi.org/10.1021/acsapm.2c00110

Espitia, P. J. P., Batista, R. A., Azeredo, H. M. C., & Otoni, C. G. (2016). Probiotics and their potential applications in active edible films and coatings. *Food Research International*, *90*, 42–52. https://doi.org/10.1016/J.FOODRES.2016.10.026

Eto, K. (2000). Minamata disease. *Neuropathology*, *20*(s1), 14–19. https://doi.org/10.1046/j.1440-1789.2000.00295.x

EU. (2011). *Commission Regulation (EU) No 10/2011 of 14 January 2011 on plastic materials and articles intended to come into contact with food*. http://data.europa.eu/eli/reg/2011/10/2023-08-31

EU. (2018). *Commission Regulation (EU) 2018/213 of 12 February 2018 on the use of bisphenol A in varnishes and coatings intended to come into contact with food and amending Regulation (EU) No 10/2011 as regards the use of that substance in plastic food contact materials*. http://data.europa.eu/eli/reg/2018/213/oj

EU. (2022). *Commission Regulation (EU) 2022/1616 of 15 September 2022 on recycled plastic materials and articles intended to come into contact with foods, and repealing Regulation (EC) No 282/2008*. http://data.europa.eu/eli/reg/2022/1616/oj

FAO. (2021). *FAO. Food Authority Organisation. United Nations Environment Programme, Food Waste Index Report. Nairobi*.

FAO. (2023a). *General principles of food hygiene (CXC 1-1969)*. https://doi.org/10.4060/cc6125en

FAO. (2023b). The State of Food Security and Nutrition in the World 2023. In *The State of Food Security and Nutrition in the World 2023*. FAO; IFAD; UNICEF; WFP; WHO; https://doi.org/10.4060/cc3017en

FAO. United Nations Environment Programme (2021). Food Waste Index Report 2021. Nairobi. (n.d.).

FDA. (2020, July 23). *All about BSE (Mad cow disease)*. Https://Www.Fda.Gov/Animal-Veterinary/Animal-Health-Literacy/All-about-Bse-Mad-Cow-Disease.

Félix, J. S., Isella, F., Bosetti, O., & Nerín, C. (2012). Analytical tools for identification of non-intentionally added substances (NIAS) coming from polyurethane adhesives in multilayer packaging materials and their migration into food simulants. *Analytical and Bioanalytical Chemistry*, *403*(10), 2869–2882. https://doi.org/10.1007/s00216-012-5965-z

Feng, C.-H., Drummond, L., & Sun, D.-W. (2014). *Modelling the growth parameters of lactic acid bacteria and total viable count in vacuum-packaged Irish cooked sausages cooled by different methods*. https://doi.org/10.1111/ijfs.12603

Flórez, M., Guerra-Rodríguez, E., Cazón, P., & Vázquez, M. (2022). Chitosan for food packaging: Recent advances in active and intelligent films. *Food Hydrocolloids*, *124*, 107328. https://doi.org/10.1016/J.FOODHYD.2021.107328

Forsyth, F. R., Eaves, C. A., & Lockhart, C. L. (2011). Controlling ethylene levels in the atmosphere of small containers of apples. *Canadian Journal of Plant Science*, *47*(6), 717–718. https://doi.org/10.4141/CJPS67-126

Fung, F., Wang, H.-S., & Menon, S. (2018). Food safety in the 21st century. *Biomedical Journal*, *41*(2), 88–95. https://doi.org/10.1016/j.bj.2018.03.003

García-Guzmán, L., Cabrera-Barjas, G., Soria-Hernández, C. G., Castaño, J., Guadarrama-Lezama, A. Y., & Llamazares, S. R. (2022). *Progress in Starch-Based Materials for Food Packaging Applications*. https://doi.org/10.3390/polysaccharides3010007

Garlotta, D. (2001). A Literature Review of Poly(Lactic Acid). *Journal of Polymers and the Environment*, *9*(2).

Garzoli, S., Turchetti, G., Giacomello, P., Tiezzi, A., Masci, V. L., & Ovidi, E. (2019). Liquid and vapour phase of lavandin (Lavandula × intermedia) Essential Oil: Chemical composition and antimicrobial activity. *Molecules*, *24*(15). https://doi.org/10.3390/MOLECULES24152701

Georg, H. C., Coutinho, K., & Canuto, S. (2005). A look inside the cavity of hydrated α-cyclodextrin: A computer simulation study. *Chemical Physics Letters*, *413*(1–3), 16–21. https://doi.org/10.1016/J.CPLETT.2005.07.036

Georgiopoulou, I., Pappa, G. D., Vouyiouka, S. N., & Magoulas, K. (2021). Recycling of post-consumer multilayer Tetra Pak® packaging with the Selective Dissolution-Precipitation process. *Resources, Conservation and Recycling*, *165*. https://doi.org/10.1016/j.resconrec.2020.105268

Giannakourou, M. C., & Tsironi, T. N. (2021). Application of Processing and Packaging Hurdles for Fresh-Cut Fruits and Vegetables Preservation. *Foods*, *10*(4), 830. https://doi.org/10.3390/foods10040830

Gold, K., Slay, B., Knackstedt, M., & Gaharwar, A. K. (2018). Antimicrobial Activity of Metal and Metal-Oxide Based Nanoparticles. *Advanced Therapeutics*, *1*(3). https://doi.org/10.1002/adtp.201700033

Golden, K. D., Williams, O. J., & Dunkley, H. M. (2014). Ethylene in Postharvest Technology: A Review. In *Asian Journal of Biological Sciences* (Vol. 7, Issue 4, pp. 135–143). https://doi.org/10.3923/ajbs.2014.135.143

Gómez-Estaca, J., López-de-Dicastillo, C., Hernández-Muñoz, P., Catalá, R., & Gavara, R. (2014). Advances in antioxidant active food packaging. *Trends in Food Science & Technology*, *35*(1), 42–51. https://doi.org/10.1016/j.tifs.2013.10.008

Gossner, C. M.-E., Schlundt, J., Ben Embarek, P., Hird, S., Lo-Fo-Wong, D., Beltran, J. J. O., Teoh, K. N., & Tritscher, A. (2009). The Melamine Incident: Implications for International Food and Feed Safety. *Environmental Health Perspectives*, *117*(12), 1803–1808. https://doi.org/10.1289/ehp.0900949

Gracia-Vallés, N., Ruiz-Torrubia, F., Mitchell, S. G., Nerín, C., & Silva, F. (2022). Developing ethyl lauroyl arginate antimicrobial films to combat Listeria monocytogenes in cured ham. *Food Control*, *141*. https://doi.org/10.1016/j.foodcont.2022.109164

Granero-García, R., Lahoz, F. J., Paulmann, C., Saouane, S., & Fabbiani, F. P. A. (2012). A novel hydrate of α-cyclodextrin crystallised under high-pressure

conditions. *CrystEngComm*, *14*(24), 8664–8670. https://doi.org/10.1039/C2CE26362A

Groh, K. J., Geueke, B., Martin, O., Maffini, M., & Muncke, J. (2021). Overview of intentionally used food contact chemicals and their hazards. *Environment International*, *150*, 106225. https://doi.org/10.1016/j.envint.2020.106225

Grujić, R., Vujadinović, D., & Savanović, D. (2017). Biopolymers as food packaging materials. In *Advances in Applications of Industrial Biomaterials* (pp. 139–160). Springer International Publishing. https://doi.org/10.1007/978-3-319-62767-0_8

Guan, M.-Y., Hu, C.-Y., Peng, Q.-S., Zeng, Y., A., W.-W., Wu, Z.-C., Wang, Z.-W., & Zhong, H.-N. (2023). Formation and migration of 5-hydroxymethylfurfural and furfural from food contact bamboo sticks during heating and their safety evaluation. *Journal of Food Composition and Analysis*, *117*, 105146. https://doi.org/10.1016/j.jfca.2023.105146

Guerreiro, A. C., Gago, C. M. L., Faleiro, M. L., Miguel, M. G. C., & Antunes, M. D. C. (2017). The effect of edible coatings on the nutritional quality of 'Bravo de Esmolfe' fresh-cut apple through shelf-life. *LWT - Food Science and Technology*, *75*, 210–219. https://doi.org/10.1016/j.lwt.2016.08.052

Gutiérrez, L., Batlle, R., Andújar, S., Sánchez, C., & Nerín, C. (2011). Evaluation of Antimicrobial Active Packaging to Increase Shelf Life of Gluten-Free Sliced Bread. *Packaging Technology and Science*, *24*(8), 485–494. https://doi.org/10.1002/pts.956

Hammond, S. T., Brown, J. H., Burger, J. R., Flanagan, T. P., Fristoe, T. S., Mercado-Silva, N., Nekola, J. C., & Okie, J. G. (2015). *Food Spoilage, Storage, and Transport: Implications for a Sustainable Future*. *65*(8). https://doi.org/10.1093/biosci/biv081

Hayrapetyan, R., Cariou, R., Platel, A., Santos, J., Huot, L., Monneraye, V., Chagnon, M.-C., & Séverin, I. (2024). Identification of non-volatile non-intentionally added substances from polyester food contact coatings and genotoxicity assessment of polyester coating's migrates. *Food and Chemical Toxicology*, *185*, 114484. https://doi.org/10.1016/j.fct.2024.114484

He, J., Li, J. J., Wen, Y., Tai, H. W., Yu, Y., Qin, W. C., Su, L. M., & Zhao, Y. H. (2015). Investigation on modes of toxic action to rats based on aliphatic and aromatic compounds and comparison with fish toxicity based on exposure routes. *Chemosphere*, *128*, 111–117. https://doi.org/10.1016/j.chemosphere.2015.01.028

Hoppe, M., de Voogt, P., & Franz, R. (2018). Oligomers in polyethylene naphthalate and polybutylene terephthalate – Identification and exploring migration. *Food Packaging and Shelf Life*, *17*, 171–178. https://doi.org/10.1016/j.fpsl.2018.07.001

Hossain, F., Follett, P., Salmieri, S., Vu, K. D., Fraschini, C., & Lacroix, M. (2019). Antifungal activities of combined treatments of irradiation and essential oils (EOs) encapsulated chitosan nanocomposite films in in vitro and in situ

conditions. *International Journal of Food Microbiology*, *295*, 33–40. https://doi.org/10.1016/j.ijfoodmicro.2019.02.009

Hossain, M., Karim, M., & Juthee, S. (2020). Postharvest physiological and biochemical alterations in fruits: a review. *Fundamental and Applied Agriculture*, *0*, 1. https://doi.org/10.5455/faa.22077

Inthamat, P., Lee, Y. S., Boonsiriwit, A., & Siripatrawan, U. (2022). Improving moisture barrier and functional properties of active film from genipin-crosslinked chitosan/astaxanthin film by heat curing. *International Journal of Food Science & Technology*, *57*(1), 137–144. https://doi.org/10.1111/IJFS.15396

Isella, F., Canellas, E., Bosetti, O., & Nerin, C. (2013). Migration of non intentionally added substances from adhesives by UPLC–Q-TOF/MS and the role of EVOH to avoid migration in multilayer packaging materials. *Journal of Mass Spectrometry*, *48*(4), 430–437. https://doi.org/10.1002/jms.3165

Jaén, J., Domeño, C., Vera, P., & Nerín, C. (2022). Migration of mineral oil aromatic hydrocarbon (MOAH) from hot melt adhesives used in food packaging materials. *Food Packaging and Shelf Life*, *33*, 100885. https://doi.org/10.1016/j.fpsl.2022.100885

Jakubczyk, E., Kamińska-Dwórznicka, A., & Kot, A. (2022). The Rheological Properties and Texture of Agar Gels with Canola Oil—Effect of Mixing Rate and Addition of Lecithin. *Gels*, *8*(11). https://doi.org/10.3390/gels8110738

James, A., & Zikankuba, V. (2017). Postharvest management of fruits and vegetable: A potential for reducing poverty, hidden hunger and malnutrition in sub-Sahara Africa. *Cogent Food & Agriculture*, *3*(1), 1312052. https://doi.org/10.1080/23311932.2017.1312052

Jay, J. M. (1982). Antimicrobial properties of diacetyl. *Applied and Environmental Microbiology*, *44*(3), 525–532. https://doi.org/10.1128/aem.44.3.525-532.1982

Jicsinszky, L., Caporaso, M., Gaudino, E. C., Giovannoli, C., Cravotto, G., & Martel, B. (2017). Synthesis of Randomly Substituted Anionic Cyclodextrins in Ball Milling. *Molecules 2017, Vol. 22, Page 485*, *22*(3), 485. https://doi.org/10.3390/MOLECULES22030485

Kader, A. A. (2013). Postharvest Technology of Horticultural Crops-An Overview from Farm to Fork. *J. Appl. Sci. Technol. (Special Issue*, *1*, 1–8.

Kader, A. A., Cavalieri, R., & Ferguson, I. (2003). A Perspective on Postharvest Horticulture (1978-2003). *HortScience*, *38*(5), 1004–1008. https://doi.org/10.21273/HORTSCI.38.5.1004

Kaewklin, P., Siripatrawan, U., Suwanagul, A., & Lee, Y. S. (2018). Active packaging from chitosan-titanium dioxide nanocomposite film for prolonging storage life of tomato fruit. *International Journal of Biological Macromolecules*, *112*, 523–529. https://doi.org/10.1016/j.ijbiomac.2018.01.124

Kasmi, N., Papageorgiou, G., Achilias, D., & Bikiaris, D. (2018). Solid-State Polymerization of Poly(Ethylene Furanoate) Biobased Polyester, II: An Efficient

and Facile Method to Synthesize High Molecular Weight Polyester Appropriate for Food Packaging Applications. *Polymers*, *10*(5), 471. https://doi.org/10.3390/polym10050471

Kato, L. S., & Conte-Junior, C. A. (2021). *polymers Safety of Plastic Food Packaging: The Challenges about Non-Intentionally Added Substances (NIAS) Discovery, Identification and Risk Assessment*. https://doi.org/10.3390/polym13132077

Keller, N., Ducamp, M. N., Robert, D., & Keller, V. (2013). Ethylene removal and fresh product storage: A challenge at the frontiers of chemistry. Toward an approach by photocatalytic oxidation. *Chemical Reviews*, *113*(7), 5029–5070. https://doi.org/10.1021/cr900398v

Khan, Z., Javed, F., Shamair, Z., Hafeez, A., Fazal, T., Aslam, A., Zimmerman, W. B., & Rehman, F. (2021). Current developments in esterification reaction: A review on process and parameters. *Journal of Industrial and Engineering Chemistry*, *103*, 80–101. https://doi.org/10.1016/j.jiec.2021.07.018

Kildeeva, N., Chalykh, A., Belokon, M., Petrova, T., Matveev, V., Svidchenko, E., Surin, N., & Sazhnev, N. (2020). Influence of Genipin Crosslinking on the Properties of Chitosan-Based Films. *Polymers 2020, Vol. 12, Page 1086*, *12*(5), 1086. https://doi.org/10.3390/POLYM12051086

Kim, I., Viswanathan, K., Kasi, G., Thanakkasaranee, S., Sadeghi, K., & Seo, J. (2022). ZnO Nanostructures in Active Antibacterial Food Packaging: Preparation Methods, Antimicrobial Mechanisms, Safety Issues, Future Prospects, and Challenges. *Food Reviews International*, *38*(4), 537–565. https://doi.org/10.1080/87559129.2020.1737709

Kim, S. I., Aida, T., & Niiyama, H. (2005). Binary adsorption of very low concentration ethylene and water vapor on mordenites and desorption by microwave heating. *Separation and Purification Technology*, *45*(3), 174–182. https://doi.org/10.1016/J.SEPPUR.2005.03.006

Kirsch, J. F., & Jencks, W. P. (2002). Nonlinear Structure-Reactivity Correlations. The Imidazole-Catalyzed Hydrolysis of Esters. *Journal of the American Chemical Society*, *86*(5), 837–846. https://doi.org/10.1021/JA01059A019

Kirwan, M. J., Plant, S., & Strawbridge, J. W. (2011). Plastics in Food Packaging. In *Food and Beverage Packaging Technology* (pp. 157–212). Wiley. https://doi.org/10.1002/9781444392180.ch7

Köckerling, E., Karrasch, L., Schweitzer, A., Razum, O., & Krause, G. (2017). Public Health Research Resulting from One of the World's Largest Outbreaks Caused by Entero-Hemorrhagic Escherichia coli in Germany 2011: A Review. *Frontiers in Public Health*, *5*. https://doi.org/10.3389/fpubh.2017.00332

Kreuzenbeck, N. B., Dhiman, S., Roman, D., Burkhardt, I., Conlon, B. H., Fricke, J., Guo, H., Blume, J., Görls, H., Poulsen, M., Dickschat, J. S., Köllner, T. G., Arndt, H.-D., & Beemelmanns, C. (2023). Isolation, (bio)synthetic studies and evaluation of antimicrobial properties of drimenol-type sesquiterpenes of Termitomyces fungi. *Communications Chemistry*, *6*(1), 79. https://doi.org/10.1038/s42004-023-00871-z

Kumar, L., Deshmukh, R. K., Hakim, L., & Gaikwad, K. K. (2024). Halloysite Nanotube as a Functional Material for Active Food Packaging Application: A Review. *Food and Bioprocess Technology*, *17*(1), 33–46. https://doi.org/10.1007/s11947-023-03092-3

Lanciotti, R., Patrignani, F., Bagnolini, F., Guerzoni, M. E., & Gardini, F. (2003). Evaluation of diacetyl antimicrobial activity against Escherichia coli, Listeria monocytogenes and Staphylococcus aureus. *Food Microbiology*, *20*(5), 537–543. https://doi.org/10.1016/S0740-0020(02)00159-4

Lawton, A. R. (1991). *Measurement of Ethylene Gas Prior to and During Transport*.

Laycock, B., Nikolić, M., Colwell, J. M., Gauthier, E., Halley, P., Bottle, S., & George, G. (2017). Lifetime prediction of biodegradable polymers. *Progress in Polymer Science*, *71*, 144–189. https://doi.org/10.1016/j.progpolymsci.2017.02.004

Lee, J., Chang, Y., Lee, E., Song, H., Chang, P., & Han, J. (2018). Ascorbic Acid-Based Oxygen Scavenger in Active Food Packaging System for Raw Meatloaf. *Journal of Food Science*, *83*(3), 682–688. https://doi.org/10.1111/1750-3841.14061

Lee, T.-H., Yu, H., Forrester, M., Wang, T., Shen, L., Liu, H., Li, J., Li, W., Kraus, G., & Cochran, E. (2022). Next-Generation High-Performance Bio-Based Naphthalate Polymers Derived from Malic Acid for Sustainable Food Packaging. *ACS Sustainable Chemistry & Engineering*, *10*(8), 2624–2633. https://doi.org/10.1021/acssuschemeng.1c06726

Lei, K., Wang, X., Li, X., & Wang, L. (2019). The innovative fabrication and applications of carvacrol nanoemulsions, carboxymethyl chitosan microgels and their composite films. *Colloids and Surfaces B: Biointerfaces*, *175*, 688–696. https://doi.org/10.1016/j.colsurfb.2018.12.054

Lestido-Cardama, A., Vázquez-Loureiro, P., Sendón, R., Bustos, J., Santillana, M. I., Losada, P. P., Rodríguez, A., & De Quirós, B. (2022). *Characterization of Polyester Coatings Intended for Food Contact by Different Analytical Techniques and Migration Testing by LC-MS n*. https://doi.org/10.3390/polym14030487

Li, G., Shankar, S., Rhim, J.-W., & Oh, B.-Y. (2015). Effects of preparation method on properties of poly(butylene adipate-co-terephthalate) films. *Food Science and Biotechnology*, *24*(5), 1679–1685. https://doi.org/10.1007/s10068-015-0218-5

Li, W., Liu, H., Li, L., Liu, K., Liu, J., Tang, T., & Jiang, W. (2019). Green synthesis of citric acid-crosslinked β-cyclodextrin for highly efficient removal of uranium(VI) from aqueous solution. *Journal of Radioanalytical and Nuclear Chemistry*, *322*(3), 2033–2042. https://doi.org/10.1007/S10967-019-06901-2/FIGURES/16

Liang, X., Feng, S., Ahmed, S., Qin, W., & Liu, Y. (2019). Effect of Potassium Sorbate and Ultrasonic Treatment on the Properties of Fish Scale Collagen/Polyvinyl Alcohol Composite Film. *Molecules*, *24*(13), 2363. https://doi.org/10.3390/molecules24132363

Liigand, P., Kaupmees, K., Haav, K., Liigand, J., Leito, I., Girod, M., Antoine, R., & Kruve, A. (2017). Think Negative: Finding the Best Electrospray Ionization/MS Mode for Your Analyte. *Anal. Chem*, *89*, 31. https://doi.org/10.1021/acs.analchem.7b00096

Limbo, S., & Khaneghah, A. M. (2015). Active packaging of foods and its combination with electron beam processing. In *Electron Beam Pasteurization and Complementary Food Processing Technologies* (pp. 195–217). Elsevier. https://doi.org/10.1533/9781782421085.2.195

Liu, Z.-X., Park, J.-N., Abdi, S. H. R., Park, S.-K., Park, Y.-K., & Lee, C. W. (2006). Nano-sized carbon hollow spheres for abatement of ethylene. *Topics in Catalysis 2006 39:3*, *39*(3), 221–226. https://doi.org/10.1007/S11244-006-0060-3

López, P., Sánchez, C., Batlle, R., & Nerín, C. (2007). Development of Flexible Antimicrobial Films Using Essential Oils as Active Agents. *Journal of Agricultural and Food Chemistry*, *55*(21), 8814–8824. https://doi.org/10.1021/jf071737b

López-Cervantes, J., & Paseiro-Losada, P. (2003). Determination of bisphenol A in, and its migration from, PVC stretch film used for food packaging. *Food Additives and Contaminants*, *20*(6), 596–606. https://doi.org/10.1080/0265203031000109495

Luo, R., Lin, Q., Zhu, L., Yan, J., & Li, Z. (2022). Detection of primary aromatic amines content in food packaging ink and migration from printed plastic bags. *Food Packaging and Shelf Life*, *32*, 100820. https://doi.org/10.1016/j.fpsl.2022.100820

Mackay, D. (1980). Solubility, Partition Coefficients, Volatility, and Evaporation Rates. In *Reactions and processes: Vol. 2 / 2A* (pp. 31–45). https://doi.org/10.1007/978-3-540-38519-6_3

Manso, S., Becerril, R., Nerín, C., & Gómez-Lus, R. (2015). Influence of pH and temperature variations on vapor phase action of an antifungal food packaging against five mold strains. *Food Control*, *47*, 20–26. https://doi.org/10.1016/j.foodcont.2014.06.014

Manso, S., Cacho-Nerin, F., Becerril, R., & Nerín, C. (2013). Combined analytical and microbiological tools to study the effect on Aspergillus flavus of cinnamon essential oil contained in food packaging. *Food Control*, *30*(2), 370–378. https://doi.org/10.1016/j.foodcont.2012.07.018

Manso, S., Nerín, C., & Gómez-Lus, R. (2011). Antifungal Activity Of The Essential Oil Of Cinnamon (Cinnamomum Zeylanicum), Oregano (Origanum Vulgare) And Lauramide Argine Ethyl Ester (Lae) Against The Mold Aspergillus Flavus Cect 2949. *Italian Journal of Food Science and Technology*, 151–157.

Manso, S., Wrona, M., Salafranca, J., Nerín, C., Alfonso, M. J., & Caballero, M. Á. (2021). Evaluation of New Antimicrobial Materials Incorporating Ethyl Lauroyl Arginate or Silver into Different Matrices, and Their Safety in Use as Potential Packaging. *Polymers*, *13*(3), 355. https://doi.org/10.3390/polym13030355

Marra, A., Silvestre, C., Duraccio, D., & Cimmino, S. (2016). Polylactic acid/zinc oxide biocomposite films for food packaging application. *International Journal of Biological Macromolecules*, *88*, 254–262. https://doi.org/10.1016/j.ijbiomac.2016.03.039

Mehmood, A., Raina, N., Phakeenuya, V., Wonganu, B., & Cheenkachorn, K. (2023). The current status and market trend of polylactic acid as biopolymer: Awareness and needs for sustainable development. *Materials Today: Proceedings*, *72*, 3049–3055. https://doi.org/10.1016/j.matpr.2022.08.387

Meira, S. M. M., Zehetmeyer, G., Werner, J. O., & Brandelli, A. (2017). A novel active packaging material based on starch-halloysite nanocomposites incorporating antimicrobial peptides. *Food Hydrocolloids*, *63*, 561–570. https://doi.org/10.1016/j.foodhyd.2016.10.013

Meitha, K., Pramesti, Y., & Suhandono, S. (2020). Reactive Oxygen Species and Antioxidants in Postharvest Vegetables and Fruits. *International Journal of Food Science*, *2020*, 1–11. https://doi.org/10.1155/2020/8817778

Monteiro, M., Nerín, C., & Reyes, F. G. R. (1999). *Migration of Tinuvin P, a UV Stabilizer, from PET Bottles into Fatty-food Simulants*. https://doi.org/10.1002/(SICI)1099-1522(199909/10)12:5<241::AID-PTS478>3.0.CO;2-V

More, S. J., Bampidis, V., Benford, D., Bragard, C., Halldorsson, T. I., Hernández-Jerez, A. F., Hougaard Bennekou, S., Koutsoumanis, K. P., Machera, K., Naegeli, H., Nielsen, S. S., Schlatter, J. R., Schrenk, D., Silano, V., Turck, D., Younes, M., Gundert-Remy, U., Kass, G. E. N., Kleiner, J., … Wallace, H. M. (2019). Guidance on the use of the Threshold of Toxicological Concern approach in food safety assessment. *EFSA Journal*, *17*(6). https://doi.org/10.2903/j.efsa.2019.5708

Mousavi Khaneghah, A., Hashemi, S. M. B., & Limbo, S. (2018). Antimicrobial agents and packaging systems in antimicrobial active food packaging: An overview of approaches and interactions. *Food and Bioproducts Processing*, *111*, 1–19. https://doi.org/10.1016/j.fbp.2018.05.001

Mu, H., Gao, H., Chen, H., Fang, X., & Han, Q. (2017). A novel controlled release ethanol emitter: preparation and effect on some postharvest quality parameters of Chinese bayberry during storage. *Journal of the Science of Food and Agriculture*, *97*(14), 4929–4936. https://doi.org/10.1002/JSFA.8369

Mukurumbira, A. R., Shellie, R. A., Keast, R., Palombo, E. A., & Jadhav, S. R. (2022). Encapsulation of essential oils and their application in antimicrobial active packaging. *Food Control*, *136*, 108883. https://doi.org/10.1016/J.FOODCONT.2022.108883

Nerín, C. (2010). Antioxidant active food packaging and antioxidant edible films. In *Oxidation in Foods and Beverages and Antioxidant Applications* (pp. 496–515). Elsevier. https://doi.org/10.1533/9780857090331.3.496

Nerin, C., Alfaro, P., Aznar, M., & Domeño, C. (2013). The challenge of identifying non-intentionally added substances from food packaging materials: A review.

Analytica Chimica Acta, *775*, 14–24. https://doi.org/10.1016/j.aca.2013.02.028

Nerin, C., Becerril, R., Manso, S., & Silva, F. (2016). Ethyl Lauroyl Arginate (LAE). In *Antimicrobial Food Packaging* (pp. 305–312). Elsevier. https://doi.org/10.1016/B978-0-12-800723-5.00023-1

Nerín, C., Bourdoux, S., Faust, B., Gude, T., Lesueur, C., Simat, T., Stoermer, A., Van Hoek, E., & Oldring, P. (2022a). Guidance in selecting analytical techniques for identification and quantification of non-intentionally added substances (NIAS) in food contact materials (FCMS). *Food Additives & Contaminants: Part A*, *39*(3), 620–643. https://doi.org/10.1080/19440049.2021.2012599

Nerín, C., Bourdoux, S., Faust, B., Gude, T., Lesueur, C., Simat, T., Stoermer, A., Van Hoek, E., & Oldring, P. (2022b). Guidance in selecting analytical techniques for identification and quantification of non-intentionally added substances (NIAS) in food contact materials (FCMS). *Food Additives & Contaminants: Part A*, *39*(3), 620–643. https://doi.org/10.1080/19440049.2021.2012599

Nerín, C., Contín, E., & Asensio, E. (2007). Kinetic migration studies using Porapak as solid-food simulant to assess the safety of paper and board as food-packaging materials. *Analytical and Bioanalytical Chemistry*, *387*(6), 2283–2288. https://doi.org/10.1007/s00216-006-1080-3

Norouzbeigi, S., Vahid-Dastjerdi, L., Yekta, R., Farhoodi, M., & Mortazavian, A. M. (2021). Effects of using different O2 scavengers on the qualitative attributes of bifidus yogurt during refrigerated storage. *Food Research International*, *140*, 109953. https://doi.org/10.1016/j.foodres.2020.109953

Novak, J., Leboš Pavunc, A., Habjanič, K., ukovi, J., Kos, B., Beganovi, J., Lebo Pavunc, A., Habjani, K., & Matoi, S. (2010). Antimicrobial activity-The most important property of probiotic and starter lactic acid bacteria. *Food Technology and Biotechnology*. https://www.researchgate.net/publication/281367114

Ohyama, K. I., Nagai, F., & Tsuchiya, Y. (2001). Certain styrene oligomers have proliferative activity on MCF-7 human breast tumor cells and binding affinity for human estrogen receptor. *Environmental Health Perspectives*, *109*(7), 699–703. https://doi.org/10.1289/ehp.01109699

Oldring, P. , F. B. , G. T. , L. C. , S. T. , S. A. , V. H. E. , & N. C. (2023). An Overview of Approaches for Analysing NIAS from different FCMs. *Zenodo*. https://doi.org/https://doi.org/10.5281/zenodo.7828612

Omer, E., Cariou, R., Remaud, G., Guitton, Y., Germon, H., Hill, P., Dervilly-Pinel, G., & Le Bizec, B. (2018). Elucidation of non-intentionally added substances migrating from polyester-polyurethane lacquers using automated LC-HRMS data processing. *Analytical and Bioanalytical Chemistry*, *410*(22), 5391–5403. https://doi.org/10.1007/s00216-018-0968-z

Omerović, N., Djisalov, M., Živojević, K., Mladenović, M., Vunduk, J., Milenković, I., Knežević, N. Ž., Gadjanski, I., & Vidić, J. (2021). Antimicrobial nanoparticles and biodegradable polymer composites for active food packaging

applications. *Comprehensive Reviews in Food Science and Food Safety*, *20*(3), 2428–2454. https://doi.org/10.1111/1541-4337.12727

Ooka, C., Yoshida, H., Suzuki, K., & Hattori, T. (2004). Effect of surface hydrophobicity of TiO2-pillared clay on adsorption and photocatalysis of gaseous molecules in air. *Applied Catalysis A: General*, *260*(1), 47–53. https://doi.org/10.1016/J.APCATA.2003.10.001

Otero, V., Becerril, R., Santos, J. A., Rodríguez-Calleja, J. M., Nerín, C., & García-López, M.-L. (2014). Evaluation of two antimicrobial packaging films against Escherichia coli O157:H7 strains in vitro and during storage of a Spanish ripened sheep cheese (Zamorano). *Food Control*, *42*, 296–302. https://doi.org/10.1016/j.foodcont.2014.02.022

Ousji, O., & Sleno, L. (2020). Identification of In Vitro Metabolites of Synthetic Phenolic Antioxidants BHT, BHA, and TBHQ by LC-HRMS/MS. *International Journal of Molecular Sciences*, *21*(24), 9525. https://doi.org/10.3390/ijms21249525

Özogul, F., & Hamed, I. (2018). The importance of lactic acid bacteria for the prevention of bacterial growth and their biogenic amines formation: A review. *Critical Reviews in Food Science and Nutrition*, *58*(10), 1660–1670. https://doi.org/10.1080/10408398.2016.1277972

Partosch, F., Mielke, H., Stahlmann, R., Kleuser, B., Barlow, S., & Gundert-Remy, U. (2015). Internal threshold of toxicological concern values: enabling route-to-route extrapolation. *Archives of Toxicology*, *89*(6), 941–948. https://doi.org/10.1007/s00204-014-1287-6

Paseiro-Cerrato, R., De Jager, L., & Begley, T. H. (2021). Migration of phenolic brominated flame retardants from contaminated food contact articles into food simulants and foods. *Food Additives & Contaminants: Part A*, *38*(3), 464–475. https://doi.org/10.1080/19440049.2020.1871082

Paseiro-Cerrato, R., MacMahon, S., Ridge, C. D., Noonan, G. O., & Begley, T. H. (2016). Identification of unknown compounds from polyester cans coatings that may potentially migrate into food or food simulants. *Journal of Chromatography A*, *1444*, 106–113. https://doi.org/10.1016/j.chroma.2016.03.038

Passarinho, A. T. P., Dias, N. F., Camilloto, G. P., Cruz, R. S., Otoni, C. G., Moraes, A. R. F., & Soares, N. de F. F. (2014). Sliced Bread Preservation through Oregano Essential Oil-Containing Sachet. *Journal of Food Process Engineering*, *37*(1), 53–62. https://doi.org/10.1111/jfpe.12059

Pech, J., Purgatto, E., Bouzayen, M., & Latché, A. (2018). Ethylene and Fruit Ripening. In *Annual Plant Reviews online* (pp. 275–304). Wiley. https://doi.org/10.1002/9781119312994.apr0483

Pedrazzo, A. R., Caldera, F., Zanetti, M., Appleton, S. L., Dhakar, N. K., & Trotta, F. (2020). Mechanochemical green synthesis of hyper-crosslinked cyclodextrin polymers. *Beilstein Journal of Organic Chemistry*, *16*(Cdi), 1554–1563. https://doi.org/10.3762/BJOC.16.127

Petersen, K., Væggemose Nielsen, P., Bertelsen, G., Lawther, M., Olsen, M. B., Nilsson, N. H., & Mortensen, G. (1999). Potential of biobased materials for food packaging. *Trends in Food Science & Technology*, *10*(2), 52–68. https://doi.org/10.1016/S0924-2244(99)00019-9

Pietropaolo, E., Albenga, R., Gosetti, F., Toson, V., Koster, S., Marin-Kuan, M., Veyrand, J., Patin, A., Schilter, B., Pistone, A., & Tei, L. (2018). Synthesis, identification and quantification of oligomers from polyester coatings for metal packaging. *Journal of Chromatography A*, *1578*, 15–27. https://doi.org/10.1016/j.chroma.2018.10.002

Prince, J. D. (1904). The Code of Hammurabi, King of Babylon about 2250 B. C. . *The American Journal of Theology*, *8*(3), 601–609. https://doi.org/10.1086/478479

Rafiqah, S. A., Khalina, A., Harmaen, A. S., Amin Tawakkal, I., Zaman, K., Asim, M., Nurrazi, M. N., & Lee, C. H. (2021). *A Review on Properties and Application of Bio-Based Poly(Butylene Succinate)*. https://doi.org/10.3390/polym13091436

Rambach, A. (1990). New plate medium for facilitated differentiation of Salmonella spp. from Proteus spp. and other enteric bacteria. *Applied and Environmental Microbiology*, *56*(1), 301–303. https://doi.org/10.1128/aem.56.1.301-303.1990

Ramírez Carnero, A., Lestido-Cardama, A., Vazquez Loureiro, P., Barbosa-Pereira, L., Rodríguez Bernaldo de Quirós, A., & Sendón, R. (2021). Presence of Perfluoroalkyl and Polyfluoroalkyl Substances (PFAS) in Food Contact Materials (FCM) and Its Migration to Food. *Foods*, *10*(7), 1443. https://doi.org/10.3390/foods10071443

Reilly, L., Serafimova, R., Partosch, F., Gundert-Remy, U., Cortiñas Abrahantes, J., Dorne, J.-L. M. C., & Kass, G. E. N. (2019). Testing the thresholds of toxicological concern values using a new database for food-related substances. *Toxicology Letters*, *314*, 117–123. https://doi.org/10.1016/j.toxlet.2019.07.019

Reinas, I., Oliveira, J., Pereira, J., Machado, F., & Poças, M. F. (2012). Migration of two antioxidants from packaging into a solid food and into Tenax®. *Food Control*, *28*(2), 333–337. https://doi.org/10.1016/j.foodcont.2012.05.023

Risch, S. J. (2009). Food Packaging History and Innovations. *J. Agric. Food Chem*, *57*, 8089–8092. https://doi.org/10.1021/jf900040r

Robertson, G. L. (2016). *Food Packaging*. CRC Press. https://doi.org/10.1201/b21347

Romero García, A., Jayarathna, S., Andersson, M., & Andersson, R. (2022). *Recent Advances in Starch-Based Blends and Composites for Bioplastics Applications*. https://doi.org/10.3390/polym14214557

Rosenboom, J.-G., Langer, R., & Traverso, G. (2022). Bioplastics for a circular economy. *Nature Reviews Materials*, *7*(2), 117–137. https://doi.org/10.1038/s41578-021-00407-8

Rupérez, D., Gracia-Vallés, N., Clavero, E., Silva, F., & Nerín, C. (2022). Mechanochemically Scaled-Up Alpha Cyclodextrin Nanosponges: Their Safety and Effectiveness as Ethylene Scavenger. *Nanomaterials (Basel, Switzerland)*, *12*(17). https://doi.org/10.3390/NANO12172900

Sadeghi, K., Lee, Y., & Seo, J. (2021). Ethylene Scavenging Systems in Packaging of Fresh Produce: A Review. *Food Reviews International*, *37*(2), 155–176. https://doi.org/10.1080/87559129.2019.1695836

Salafranca, J., Clemente, I., Isella, F., Nerín, C., & Bosetti, O. (2015). Influence of oxygen and long term storage on the profile of volatile compounds released from polymeric multilayer food contact materials sterilized by gamma irradiation. *Analytica Chimica Acta*, *878*, 118–130. https://doi.org/10.1016/j.aca.2015.03.055

Salmerón, I., Loeza-Serrano, S., Pérez-Vega, S., & Pandiella, S. S. (2015). Headspace gas chromatography (HS-GC) analysis of imperative flavor compounds in Lactobacilli-fermented barley and malt substrates. *Food Science and Biotechnology*, *24*(4), 1363–1371. https://doi.org/10.1007/s10068-015-0175-z

Saltveit, M. E. (1999). Effect of ethylene on quality of fresh fruits and vegetables. *Postharvest Biology and Technology*, *15*(3), 279–292. https://doi.org/10.1016/S0925-5214(98)00091-X

Sarker, A. I., Aroonwilas, A., & Veawab, A. (2017). Equilibrium and Kinetic Behaviour of CO2 Adsorption onto Zeolites, Carbon Molecular Sieve and Activated Carbons. *Energy Procedia*, *114*, 2450–2459. https://doi.org/10.1016/J.EGYPRO.2017.03.1394

Schliecker, G., Schmidt, C., Fuchs, S., & Kissel, T. (2003). Characterization of a homologous series of d , l -lactic acid oligomers; a mechanistic study on the degradation kinetics in vitro. *Biomaterials*, *24*(21), 3835–3844. https://doi.org/10.1016/S0142-9612(03)00243-6

Schymanski, E. L., Jeon, J., Gulde, R., Fenner, K., Ruff, M., Singer, H. P., & Hollender, J. (2014). Identifying Small Molecules via High Resolution Mass Spectrometry: Communicating Confidence. *Environmental Science & Technology*, *48*(4), 2097–2098. https://doi.org/10.1021/es5002105

Şen, F., & Kahraman, M. V. (2018). Preparation and characterization of hybrid cationic hydroxyethyl cellulose/sodium alginate polyelectrolyte antimicrobial films. *Polymers for Advanced Technologies*, *29*(7), 1895–1901. https://doi.org/10.1002/pat.4298

Settier-Ramírez, L., López-Carballo, G., Gavara, R., & Hernández-Muñoz, P. (2021). Broadening the antimicrobial spectrum of nisin-producing Lactococcus lactis subsp. Lactis to Gram-negative bacteria by means of active packaging. *International Journal of Food Microbiology*, *339*, 109007. https://doi.org/10.1016/J.IJFOODMICRO.2020.109007

Sharma, S., Barkauskaite, S., Duffy, B., Jaiswal, A. K., & Jaiswal, S. (2020). Characterization and Antimicrobial Activity of Biodegradable Active Packaging

Enriched with Clove and Thyme Essential Oil for Food Packaging Application. *Foods*, *9*(8), 1117. https://doi.org/10.3390/foods9081117

Shi, C., Wang, M., Wang, Z., Qu, G., Jiang, W., Pan, X., & Fang, M. (2023). Oligomers from the Synthetic Polymers: Another Potential Iceberg of New Pollutants. *Environment & Health*, *1*(4), 228–235. https://doi.org/10.1021/envhealth.3c00086

Shimohata, T., Hirota, K., Takahashi, H., & Nishizawa, M. (2015). Clinical aspects of the Niigata Minamata disease. *Brain and Nerve = Shinkei Kenkyu No Shinpo*, *67*(1), 31–38. https://doi.org/10.11477/mf.1416200084

Silva, A. P. R. da, Longhi, D. A., Dalcanton, F., & Aragão, G. M. F. de. (2018). Modelling the growth of lactic acid bacteria at different temperatures. *Brazilian Archives of Biology and Technology*, *61*(0). https://doi.org/10.1590/1678-4324-2018160159

Silva, F., Becerril, R., & Nerín, C. (2019). *Safety Assessment of Active Food Packaging: Role of Known and Unknown Substances* (pp. 1–41). https://doi.org/10.2174/9789811421587119010004

Silva, F., Caldera, F., Trotta, F., Nerín, C., & Domingues, F. C. (2019a). Encapsulation of coriander essential oil in cyclodextrin nanosponges: A new strategy to promote its use in controlled-release active packaging. *Innovative Food Science & Emerging Technologies*, *56*, 102177. https://doi.org/10.1016/J.IFSET.2019.102177

Silva, F., Caldera, F., Trotta, F., Nerín, C., & Domingues, F. C. (2019b). Encapsulation of coriander essential oil in cyclodextrin nanosponges: A new strategy to promote its use in controlled-release active packaging. *Innovative Food Science & Emerging Technologies*, *56*, 102177. https://doi.org/10.1016/J.IFSET.2019.102177

Silva, F., Caldera, F., Trotta, F., Nerín, C., & Domingues, F. C. (2019c). Encapsulation of coriander essential oil in cyclodextrin nanosponges: A new strategy to promote its use in controlled-release active packaging. *Innovative Food Science & Emerging Technologies*, *56*, 102177. https://doi.org/10.1016/J.IFSET.2019.102177

Silva, F., Domingues, F. C., & Nerín, C. (2018). Control microbial growth on fresh chicken meat using pinosylvin inclusion complexes based packaging absorbent pads. *LWT*, *89*, 148–154. https://doi.org/10.1016/J.LWT.2017.10.043

Silva, F., Figueiras, A., Gallardo, E., Nerín, C., & Domingues, F. C. (2014). Strategies to improve the solubility and stability of stilbene antioxidants: A comparative study between cyclodextrins and bile acids. *Food Chemistry*, *145*, 115–125. https://doi.org/10.1016/J.FOODCHEM.2013.08.034

Silva Nascimento, L. E., Wrona, M., da Silva Oliveira, W., Nerín, C., & Teixeira Godoy, H. (2023). A study on the migration of primary aromatic amines in packaged açaí-based (Euterpe oleracea Mart.) products. *Food Packaging and Shelf Life*, *38*, 101118. https://doi.org/10.1016/j.fpsl.2023.101118

Simionato, I., Domingues, F. C., Nerín, C., & Silva, F. (2019). Encapsulation of cinnamon oil in cyclodextrin nanosponges and their potential use for antimicrobial food packaging. *Food and Chemical Toxicology*, *132*, 110647. https://doi.org/10.1016/j.fct.2019.110647

Sisler, E. C. (2006). The discovery and development of compounds counteracting ethylene at the receptor level. *Biotechnology Advances*, *24*(4), 357–367. https://doi.org/10.1016/J.BIOTECHADV.2006.01.002

Škalamera, Đ., Blažek Bregović, V., Antol, I., Bohne, C., & Basarić, N. (2017). Hydroxymethylaniline Photocages for Carboxylic Acids and Alcohols. *The Journal of Organic Chemistry*, *82*(23), 12554–12568. https://doi.org/10.1021/acs.joc.7b02314

Slobodinyuk, A. I., Senichev, V. Y., Perepada, M. V., Strelnikov, V. N., Belov, A. A., Kozlov, S. S., Savchuk, A. V., & Slobodinyuk, D. G. (2023). Structure and Properties of Urethane-Containing Elastomers Based on Adipic Acid Polyester and Ethylene Glycol, Isophorone Disocyanate, and Aromatic Diamine. *Polymer Science - Series D*, *16*(3), 576–581. https://doi.org/10.1134/S1995421223030413

Smulders, F. J. M., Paulsen, P., Vali, S., & Wanda, S. (2013). Effectiveness of a polyamide film releasing lactic acid on the growth of E. coli O157:H7, Enterobacteriaceae and Total Aerobic Count on vacuum-packed beef. *Meat Science*, *95*(2), 160–165. https://doi.org/10.1016/j.meatsci.2013.04.058

Soladoye, O. P., Juárez, M. L., Aalhus, J. L., Shand, P., & Estévez, M. (2015). Protein Oxidation in Processed Meat: Mechanisms and Potential Implications on Human Health. *Comprehensive Reviews in Food Science and Food Safety*, *14*(2), 106–122. https://doi.org/10.1111/1541-4337.12127

Stolle, A., Szuppa, T., Leonhardt, S. E. S., & Ondruschka, B. (2011). Ball milling in organic synthesis: solutions and challenges. *Chemical Society Reviews*, *40*(5), 2317–2329. https://doi.org/10.1039/C0CS00195C

Su, Q.-Z., Vera, P., Nerín, C., Lin, Q.-B., & Zhong, H.-N. (2021). Safety concerns of recycling postconsumer polyolefins for food contact uses: Regarding (semi-)volatile migrants untargetedly screened. *Resources, Conservation and Recycling*, *167*, 105365. https://doi.org/10.1016/j.resconrec.2020.105365

Su, Q.-Z., Vera, P., Salafranca, J., & Nerín, C. (2021). Decontamination efficiencies of post-consumer high-density polyethylene milk bottles and prioritization of high concern volatile migrants. *Resources, Conservation and Recycling*, *171*, 105640. https://doi.org/10.1016/j.resconrec.2021.105640

Sullivan, D. J., Azlin-Hasim, S., Cruz-Romero, M., Cummins, E., Kerry, J. P., & Morris, M. A. (2020). Antimicrobial effect of benzoic and sorbic acid salts and nano-solubilisates against Staphylococcus aureus, Pseudomonas fluorescens and chicken microbiota biofilms. *Food Control*, *107*, 106786. https://doi.org/10.1016/j.foodcont.2019.106786

Tang, M., Jia, R., Kan, H., Liu, Z., Yang, S., Sun, L., & Yang, Y. (2020). Kinetic, isotherm, and thermodynamic studies of the adsorption of dye from aqueous

solution by propylene glycol adipate-modified cellulose aerogel. *Colloids and Surfaces A: Physicochemical and Engineering Aspects*, *602*, 125009. https://doi.org/10.1016/j.colsurfa.2020.125009

Teshome, E., Forsido, S. F., Rupasinghe, H. P. V., & Olika Keyata, E. (2022). Potentials of Natural Preservatives to Enhance Food Safety and Shelf Life: A Review. *The Scientific World Journal*, *2022*, 1–11. https://doi.org/10.1155/2022/9901018

The European Union One Health 2021 Zoonoses Report. (2022). *EFSA Journal*, *20*(12). https://doi.org/10.2903/j.efsa.2022.7666

The European Union One Health 2022 Zoonoses Report. (2023). *EFSA Journal*, *21*(12). https://doi.org/10.2903/j.efsa.2023.8442

Tian, S., Qin, G., & Li, B. (2013). Reactive oxygen species involved in regulating fruit senescence and fungal pathogenicity. *Plant Molecular Biology*, *82*(6), 593–602. https://doi.org/10.1007/s11103-013-0035-2

Tian, Z., Kim, S.-K., & Hyun, J.-H. (2020). Environmental Distribution of Styrene Oligomers (SOs) Coupled with Their Source Characteristics: Tracing the Origin of SOs in the Environment. *Journal of Hazardous Materials*, *398*, 122968. https://doi.org/10.1016/j.jhazmat.2020.122968

Torres-Giner, S., Figueroa-Lopez, K. J., Melendez-Rodriguez, B., Prieto, C., Pardo-Figuerez, M., & Lagaron, J. M. (2021). Emerging Trends in Biopolymers for Food Packaging. In *Sustainable Food Packaging Technology* (pp. 1–33). Wiley. https://doi.org/10.1002/9783527820078.ch1

Triantafyllou, V., Akrida-Demertzi, K., & Demertzis, P. (2007). A study on the migration of organic pollutants from recycled paperboard packaging materials to solid food matrices. *Food Chemistry*, *101*(4), 1759–1768. https://doi.org/10.1016/j.foodchem.2006.02.023

Tropea, A. (2022). Microbial Contamination and Public Health: An Overview. *International Journal of Environmental Research and Public Health*, *19*(12), 7441. https://doi.org/10.3390/ijerph19127441

Trotta, F., Cavalli, R., Martina, K., Biasizzo, M., Vitillo, J., Bordiga, S., Vavia, P., & Ansari, K. (2011). Cyclodextrin nanosponges as effective gas carriers. *Journal of Inclusion Phenomena and Macrocyclic Chemistry*, *71*(1–2), 189–194. https://doi.org/10.1007/S10847-011-9926-5/FIGURES/7

Trotta, F., Shende, P., & Biasizzo, M. (2012). *Method for Preparing Dextrin Nanosponges.PCT Pat. Appl. WO2012/147069 A1*.

Ubeda, S., Aznar, M., & Nerín, C. (2018). Determination of oligomers in virgin and recycled polyethylene terephthalate (PET) samples by UPLC-MS-QTOF. *Analytical and Bioanalytical Chemistry*, *410*(9), 2377–2384. https://doi.org/10.1007/s00216-018-0902-4

Ubeda, S., Aznar, M., Nerín, C., & Kabir, A. (2021). Fabric phase sorptive extraction for specific migration analysis of oligomers from biopolymers. *Talanta*, *233*, 122603. https://doi.org/10.1016/j.talanta.2021.122603

Ubeda, S., Aznar, M., Rosenmai, A. K., Vinggaard, A. M., & Nerín, C. (2020). Migration studies and toxicity evaluation of cyclic polyesters oligomers from food packaging adhesives. *Food Chemistry*, *311*. https://doi.org/10.1016/j.foodchem.2019.125918

Úbeda, S., Aznar, M., Vera, P., Nerín, C., Henríquez, L., Taborda, L., & Restrepo, C. (2017). Overall and specific migration from multilayer high barrier food contact materials – kinetic study of cyclic polyester oligomers migration. *Food Additives & Contaminants: Part A*, *34*(10), 1784–1794. https://doi.org/10.1080/19440049.2017.1346390

Umaraw, P., Munekata, P. E. S., Verma, A. K., Barba, F. J., Singh, V. P., Kumar, P., & Lorenzo, J. M. (2020). Edible films/coating with tailored properties for active packaging of meat, fish and derived products. *Trends in Food Science & Technology*, *98*, 10–24. https://doi.org/10.1016/j.tifs.2020.01.032

UN General Assembly. (2015). Transforming our world : the 2030 Agenda for Sustainable Development. *A/RES/70/1*.

Urbelis, J. H., & Cooper, J. R. (2021). Migration of food contact substances into dry foods: A review. *Food Additives & Contaminants: Part A*, *38*(6), 1044–1073. https://doi.org/10.1080/19440049.2021.1905188

U.S. Department of Health and Human Services - Food and Drug Administration. (2001). *Guidance for Industry: Bioanalytical Method Validation*.

Utto, W. (2014). Factors affecting release of ethanol vapour in active modified atmosphere packaging systems for horticultural products. *Maejo International Journal of Science & Technology*, *8*(01), 75–85.

Utto, W., Preutikul, R., Malila, P., Noomhorm, A., & Bronlund, J. E. (2018). Delaying microbial proliferation in freshly peeled shallots by active packaging incorporating ethanol vapour-controlled release sachets and low storage temperature. *Food Science and Technology International*, *24*(2), 132–144. https://doi.org/10.1177/1082013217735951

Validation of Analytical Procedures: Methodology ICH Q2B. (2005).

Vanmathi Mugasundari, A., & Anandakumar, S. (2022). Shelf life extension of bread using ethanol emitters with different packaging materials. *Journal of Food Processing and Preservation*, e17143. https://doi.org/10.1111/JFPP.17143

Vayachuta, L., Thiramanas, R., Prompinit, P., Du-A-Man, S., Viboonratanasri, D., & Chotsuwan, C. (2021). Nanohybrid Ethanol Emitters for Disinfection of Bacteria and Viruses on Contaminated Surfaces. *Cite This: ACS Appl. Polym. Mater*, *2021*, 5105–5114. https://doi.org/10.1021/acsapm.1c00863

Vázquez-Loureiro, P., Lestido-Cardama, A., Sendón, R., Bustos, J., Cariou, R., Paseiro-Losada, P., & Rodríguez-Bernaldo de Quirós, A. (2023). Investigation of migrants from can coatings: Occurrence in canned foodstuffs and exposure assessment. *Food Packaging and Shelf Life*, *40*, 101183. https://doi.org/10.1016/j.fpsl.2023.101183

Vera, P., Aznar, M., Mercea, P., & Nerín, C. (2011). Study of hotmelt adhesives used in food packaging multilayer laminates. Evaluation of the main factors affecting migration to food. *J. Mater. Chem.*, *21*(2), 420–431. https://doi.org/10.1039/C0JM02183K

Vera, P., Canellas, E., Barknowitz, G., Goshawk, J., & Nerín, C. (2019). Ion-Mobility Quadrupole Time-of-Flight Mass Spectrometry: A Novel Technique Applied to Migration of Nonintentionally Added Substances from Polyethylene Films Intended for Use as Food Packaging. *Analytical Chemistry*, *91*(20), 12741–12751. https://doi.org/10.1021/acs.analchem.9b02238

Vera, P., Canellas, E., & Nerín, C. (2013). Identification of non-volatile compounds and their migration from hot melt adhesives used in food packaging materials characterized by ultra-performance liquid chromatography coupled to quadrupole time-of-flight mass spectrometry. *Analytical and Bioanalytical Chemistry*, *405*(14), 4747–4754. https://doi.org/10.1007/s00216-013-6881-6

Vera, P., Canellas, E., & Nerín, C. (2018). Identification of non volatile migrant compounds and NIAS in polypropylene films used as food packaging characterized by UPLC-MS/QTOF. *Talanta*, *188*, 750–762. https://doi.org/10.1016/j.talanta.2018.06.022

Vera, P., Uliaque, B., Canellas, E., Escudero, A., & Nerín, C. (2012). Identification and quantification of odorous compounds from adhesives used in food packaging materials by headspace solid phase extraction and headspace solid phase microextraction coupled to gas chromatography–olfactometry–mass spectrometry. *Analytica Chimica Acta*, *745*, 53–63. https://doi.org/10.1016/j.aca.2012.07.045

Wang, G. W. (2013). Mechanochemical organic synthesis. *Chemical Society Reviews*, *42*(18), 7668–7700. https://doi.org/10.1039/C3CS35526H

Wang, M., Li, Q., Shi, C., Lv, J., Xu, Y., Yang, J., Chua, S. L., Jia, L., Chen, H., Liu, Q., Huang, C., Huang, Y., Chen, J., & Fang, M. (2023). Oligomer nanoparticle release from polylactic acid plastics catalysed by gut enzymes triggers acute inflammation. *Nature Nanotechnology*, *18*(4), 403–411. https://doi.org/10.1038/s41565-023-01329-y

Wen, P., Zhu, D.-H., Feng, K., Liu, F.-J., Lou, W.-Y., Li, N., Zong, M.-H., & Wu, H. (2016). Fabrication of electrospun polylactic acid nanofilm incorporating cinnamon essential oil/ β -cyclodextrin inclusion complex for antimicrobial packaging. *Food Chemistry*, *196*, 996–1004. https://doi.org/10.1016/j.foodchem.2015.10.043

WHO. (2002). *WHO global strategy for food safety: safer food for better health*.

WHO. (2013). *Advancing food safety initiatives, strategic plan for food safety, including foodborne zoonoses 2013–2022*.

WHO. (2015). *WHO estimates of the global burden of foodborne diseases*. Foodborne disease burden epidemiology reference group 2007-2015.

WHO. (2022). *WHO Global strategy for food safety 2022-2030: Towards stronger food safety systems and global cooperation*.

Williams-Campbell, A. M., & Jay, J. M. (2002). Effects of Diacetyl and Carbon Dioxide on Spoilage Microflora in Ground Beef. *Journal of Food Protection*, *65*(3), 523–527. https://doi.org/10.4315/0362-028X-65.3.523

Wrona, M., Manso, S., Silva, F., Cardoso, L., Salafranca, J., Nerín, C., Alfonso, M. J., & Caballero, M. Á. (2023). New active packaging based on encapsulated carvacrol, with emphasis on its odour masking strategies. *Food Packaging and Shelf Life*, *40*, 101177. https://doi.org/10.1016/j.fpsl.2023.101177

Wrona, M., & Nerín, C. (2020). Analytical Approaches for Analysis of Safety of Modern Food Packaging: A Review. *Molecules*, *25*(3), 752. https://doi.org/10.3390/molecules25030752

Wrona, M., Silva, F., Salafranca, J., Nerín, C., Alfonso, M. J., & Caballero, M. Á. (2021). Design of new natural antioxidant active packaging: Screening flowsheet from pure essential oils and vegetable oils to ex vivo testing in meat samples. *Food Control*, *120*, 107536. https://doi.org/10.1016/j.foodcont.2020.107536

Wyrwa, J., & Barska, A. (2017). Innovations in the food packaging market: active packaging. *European Food Research and Technology*, *243*, 1681–1692. https://doi.org/10.1007/s00217-017-2878-2

Yeni, F., Yavaş, S., Alpas, H., & Soyer, Y. (2016). Most Common Foodborne Pathogens and Mycotoxins on Fresh Produce: A Review of Recent Outbreaks. *Critical Reviews in Food Science and Nutrition*, *56*(9), 1532–1544. https://doi.org/10.1080/10408398.2013.777021

Yeo, J. C. C., Muiruri, J. K., Thitsartarn, W., Li, Z., & He, C. (2018). Recent advances in the development of biodegradable PHB-based toughening materials: Approaches, advantages and applications. In *Materials Science and Engineering C* (Vol. 92, pp. 1092–1116). Elsevier Ltd. https://doi.org/10.1016/j.msec.2017.11.006

Yildirim, S., & Röcker, B. (2018). Active Packaging. In *Nanomaterials for Food Packaging* (pp. 173–202). Elsevier. https://doi.org/10.1016/B978-0-323-51271-8.00007-3

Younes, M., Aquilina, G., Castle, L., Engel, K., Fowler, P. J., Frutos Fernandez, M. J., Fürst, P., Gundert-Remy, U., Gürtler, R., Husøy, T., Manco, M., Moldeus, P., Passamonti, S., Shah, R., Waalkens-Berendsen, I., Wölfle, D., Wright, M., Benigni, R., Bolognesi, C., … Mennes, W. (2022). Scientific Opinion on Flavouring Group Evaluation 63, Revision 4 (FGE.63Rev4): consideration of aliphatic secondary saturated and unsaturated alcohols, ketones and related esters evaluated by JECFA (59th and 69th meetings) structurally related to flavouring substances evaluated by EFSA in FGE.07Rev6. *EFSA Journal*, *20*(2). https://doi.org/10.2903/j.efsa.2021.7102

Yousuf, B., Qadri, O. S., & Srivastava, A. K. (2018). Recent developments in shelf-life extension of fresh-cut fruits and vegetables by application of different edible coatings: A review. *LWT*, *89*, 198–209. https://doi.org/10.1016/j.lwt.2017.10.051

Zagory, D. (1995). *Ethylene removing packaging, in Active Food Packaging, Rooney, M.L. (ed)*. Blackie Academic and Professional.

Zhang, C., Feng, F., & Zhang, H. (2018). Emulsion electrospinning: Fundamentals, food applications and prospects. *Trends in Food Science & Technology*, *80*, 175–186. https://doi.org/10.1016/j.tifs.2018.08.005

Zhang, C. Y., Lin, N. B., Chai, X. S., Zhong-Li, & Barnes, D. G. (2015). A rapid method for simultaneously determining ethanol and methanol content in wines by full evaporation headspace gas chromatography. *Food Chemistry*, *183*, 169–172. https://doi.org/10.1016/J.FOODCHEM.2015.03.048

Zhang, H., Fang, J., Ge, H., Han, L., Wang, X., Hao, Y., Han, C., & Dong, L. (2013). Thermal, mechanical, and rheological properties of polylactide/poly(1,2-propylene glycol adipate). *Polymer Engineering & Science*, *53*(1), 112–118. https://doi.org/10.1002/pen.23238

Zhang, N., Kenion, G., Bankmann, D., Mezouari, S., & Hartman, T. G. (2018). Migration studies and chemical characterization of low molecular weight cyclic polyester oligomers from food packaging lamination adhesives. *Packaging Technology and Science*, *31*(4), 197–211. https://doi.org/10.1002/pts.2367

Zhang, N., Scarsella, J. B., & Hartman, T. G. (2020). Identification and Quantitation Studies of Migrants from BPA Alternative Food-Contact Metal Can Coatings. *Polymers*, *12*(12), 2846. https://doi.org/10.3390/polym12122846

Zhang, T., Howell, B. A., & Smith, P. B. (2017). Rational Synthesis of Hyperbranched Poly(ester)s. *Industrial & Engineering Chemistry Research*, *56*(6), 1661–1670. https://doi.org/10.1021/acs.iecr.6b04435

Zhao, X., Zhou, J., Tian, R., & Liu, Y. (2022). Microbial volatile organic compounds: Antifungal mechanisms, applications, and challenges. *Frontiers in Microbiology*, *13*. https://doi.org/10.3389/fmicb.2022.922450

Zhou, K., Li, Y., Li, Q., Du, Q., Wang, D., Sui, K., Wang, C., Li, H., & Xia, Y. (2018). Kinetic, Isotherm and Thermodynamic Studies for Removal of Methylene Blue Using β-Cyclodextrin/Activated Carbon Aerogels. *Journal of Polymers and the Environment*, *26*(8), 3362–3370. https://doi.org/10.1007/S10924-018-1219-2

Zhou, Y., Miao, X., Lan, X., Luo, J., Luo, T., Zhong, Z., Gao, X., Mafang, Z., Ji, J., Wang, H., & Tang, Y. (2020). Angelica Essential Oil Loaded Electrospun Gelatin Nanofibers for Active Food Packaging Application. *Polymers*, *12*(2), 299. https://doi.org/10.3390/polym12020299

Zhu, F. (2015). Composition, structure, physicochemical properties, and modifications of cassava starch. *Carbohydrate Polymers*, *122*, 456–480. https://doi.org/10.1016/j.carbpol.2014.10.063

Zhu, W., Jin, P., Yang, H., Li, F., Wang, C., Li, T., & Fan, J. (2023). A green extraction strategy for the detection of antioxidants in food simulants and beverages migrated from plastic packaging materials. *Food Chemistry*, *406*, 135060. https://doi.org/10.1016/j.foodchem.2022.135060

Zhu, Y., Ren, H., Wei, Y., Bie, Z., & Ji, L. (2015). Determination of Imidazole, 4-Methylimidazole, and 2-Methylimidazole in Cigarette Additives by Ultra-High Performance Liquid Chromatography. *Analytical Letters*, *48*(17), 2708–2714. https://doi.org/10.1080/00032719.2015.1045593

Zimet, P., Mombrú, Á. W., Mombrú, D., Castro, A., Villanueva, J. P., Pardo, H., & Rufo, C. (2019). Physico-chemical and antilisterial properties of nisin-incorporated chitosan/carboxymethyl chitosan films. *Carbohydrate Polymers*, *219*, 334–343. https://doi.org/10.1016/j.carbpol.2019.05.013

Section VI: Annexes

The following Annexes are related to Chapter 3 of this Thesis.

Synthesis, monitoring and characterisation

Synthesis

Method A : Diacid monobenzylation

To the corresponding diacid (1.00 eq) dissolved in a mixture of dioxane and DMF (1:1, 0.12 M) benzyl bromide (1.00 eq) was added, followed by the addition $NaHCO_3$ (1.03 eq). The suspension was stirred at 90 °C overnight. Solvents were evaporated and the residue was suspended in ethyl acetate. After filtration, the organic phase was washed with water and brine. Then, the organic phase was dried with Na_2SO_4, filtered and evaporated under reduced pressure. The crude was purified by flash chromatrography on silica gel.

Method B : Diol monosilylation

To a solution of the corresponding diol (3.00 eq) in dry DCM (0.40 M) were added TBDMSCl (1.00 eq) and a catalytic amount of DMAP (0.20 eq). Et_3N (1.20 eq) was slowly added to the reaction mixture at 0 °C. The reaction mixture was stirred at room temperature overnight. The mixture was then successively washed with a saturated aqueous solution of NH_4CI and H_2O. The aqueous layer was extracted with DCM. Combined organic layers were washed with brine, dried over Na_2SO_4, filtered and concentrated under reduced pressure. The crude was purified by flash chromatography on silica gel.

Method C : Coupling

To a solution of the corresponding acid (1.10 eq) and the corresponding alcohol (1.00 eq) in dry DCM (0.20 M) was added DMAP (2.00 eq). EDC.HCI (2.00 eq) was then added portionwise in 3 times, 2 times at 0 °C with 15 min interval. The reaction mixture was stirred for 4h at reflux and the 3rd part of the EDC.HCI was added. The reaction is stirred at reflux overnight. The mixture was quenched with an aqueous solution of HCI 1 M. The aqueous layer was extracted with DCM. Combined organic layers were washed with brine, dried over Na_2SO_4, filtered and concentrated under reduced pressure. The crude was purified by flash chromatography on silica gel.

Method D : Desilylation

To a solution of the corresponding fully protected compound (1.00 eq) in dry THF (0.10 M), Olah's reagent (10.00 eq) was added at 0°C. The reaction mixture was stirred 4h at 35°C. The mixture was cooled down to 0°C and quenched with a saturated aqueous solution of $NaHCO_3$. The aqueous layer was extracted three times with DCM. Combined organic layers were washed with brine, dried over Na_2SO_4, filtered and concentrated under reduced pressure. The crude was purified by flash chromatography on silica.

Method E : Debenzylation

To a solution of the corresponding benzylated compound (1.00 eq) in degassed isopropanol (0.10 M) was added Pearlman's catalyst (0.10 eq). Reaction mixture was stirred at room temperature under H_2 atmosphere until completion, monitoring the reaction by TLC. Palladium was filtered over celite pad, washed with isopropanol. The filtrate was concentrated under reduced pressure. The crude is directly used for the next step without further purification.

Method F : Lactonization

To a solution of triethylamine (2.00 eq.) in dry DCM (0.10 M) was added a solution of the corresponding unprotected compound (1.00 eq.) in dry DCM (0.10 M). A solution of 2,4,6-trichlorobenzoyl chloride (2.0 eq.) in dry DCM (0.10 M) was then added. The mixture was stirred overnight at room temperature. The mixture was then slowly added into a solution of DMAP (10.00 eq) in dry DCM (0.001 M) and stirred 3h at room temperature. The reaction mixture was concentrated under reduced pressure. The crude was then purified by flash chromatography on silica gel.

Monitoring and characterization

All reactions were monitored by TLC on commercially available precoated plates (Kieselgel 60 F254), and the compounds were visualized with $KMnO_4$ solution [$KMnO_4$ (3 g), K_2CO_3 (20 g), NaOH (5% aq.; 5 mL), H_2O (300 mL)] and heating or by UV (254 nm) when possible.

Intermediate and final products were characterised by ^1H and ^{13}C NMR as well as ESI-TOF-HRMS.

NMR. Intermediate and final products were characterised by ^1H and ^{13}C NMR. Spectra were recorded on a Bruker Avance 300 spectrometer fitted with a 5 mm i.d. BBO probe carefully tuned to the recording frequency of 300.13 MHz (for ^1H) and 75.47 MHz (for ^{13}C), the temperature of the probe was set at room temperature (around 293-294 K), on a Bruker Avance 400 spectrometer fitted with a 5 mm i.d. BBFO+ probe carefully tuned to the recording frequency of 400.13 MHz (for ^1H) and 100.61 MHz (for ^{13}C). The spectra are referenced to the solvent in which they were run (7.26 ppm for ^1H $CDCl_3$ and 77.16 ppm for ^{13}C $CDCl_3$). Chemical shifts (δ) are given in ppm and coupling constants (J) are given in Hz with the following splitting abbreviations: s = singlet, d = doublet, t = triplet, q = quartet, m = multiplet and br = broad. All assignments were confirmed with the aid of two-dimensional ^1H, ^1H (COSY), or ^1H, ^{13}C (HSQC) experiments using standard pulse programs.

ESI/ASAP-TOF-HRMS. Intermediate and final products were characterised by time of flight (TOF) high resolution mass spectrometry (HRMS) measurements using a Xevo G2-XS QTOF spectrometer (Waters, USA) fitted with an ESI or ASAP probe in both positive or negative mode by direct infusion of a 10 ppm solution (ESI) or by direct introduction of a glass capillary (ASAP).

Adipic acid & 1,4-Butanediol series

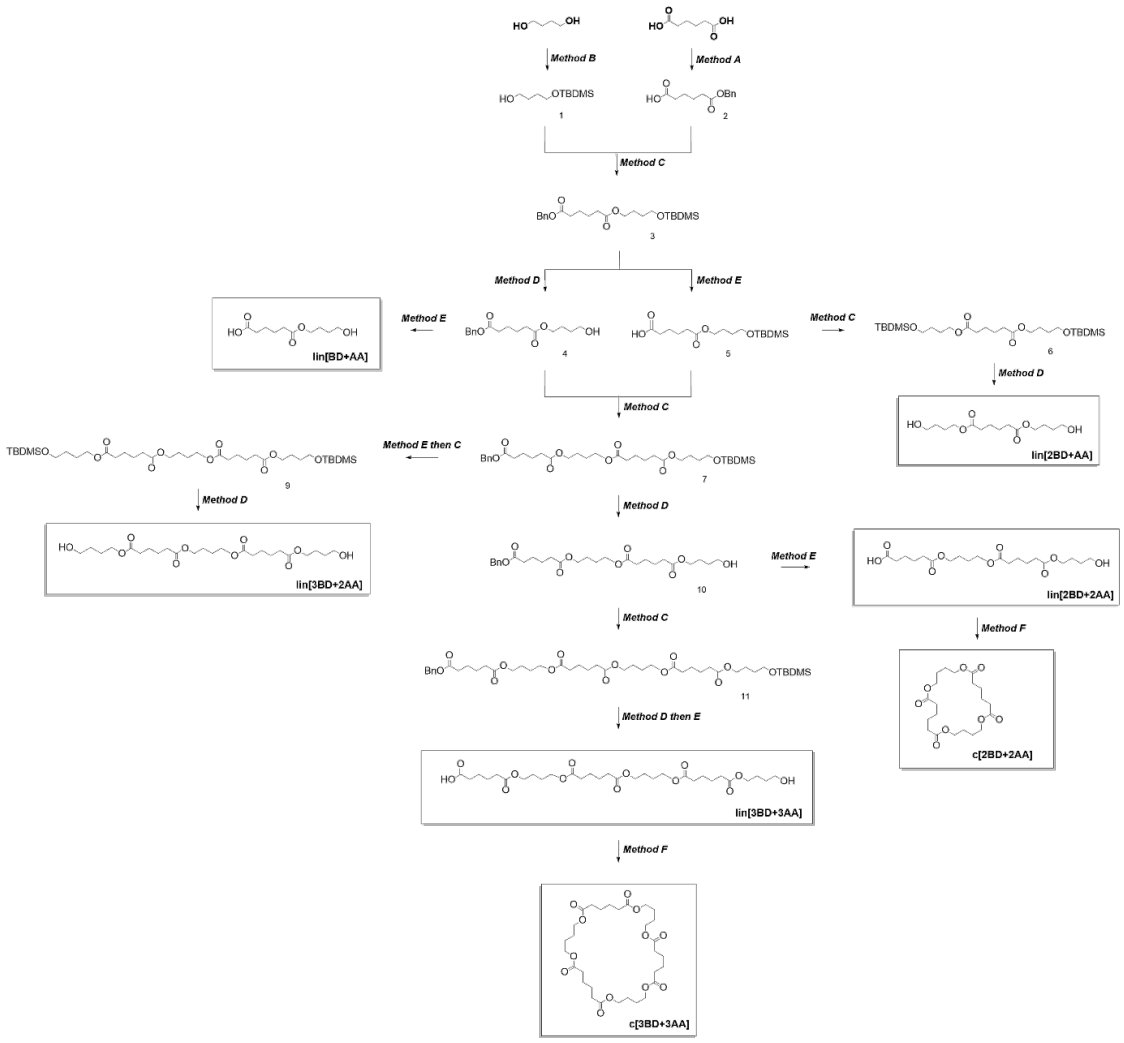

Figure A1 – Synthesis of linear and cyclic oligomer derived from Adipic acid (AA) and 1,4-Butanediol (BD).

4-((tert-butyldimethylsilyl)oxy)butan-1-ol (1) : Following **Method B,** the crude was then purified by flash chromatography (cyclohexane/ethyl acetate 90/10 to 80/20, v/v) to afford **1** with 71% yield as a colourless oil. ^{1}H NMR ($CDCl_3$, 400 MHz): 3.56 (m, 4H), 2.74-2.96 (br s, 1H), 1.54-1.67 (m, 4H), 0.87 (s, 9H), 0.04 (s, 6H) ; ^{13}C NMR ($CDCl_3$, 100 MHz): 63.4, 62.7, 30.2, 29.9, 26.0, 26.0, 26.0, 18.4, -5.3, -5.3 ; ESI(+)-TOF-HRMS m/z for $C_{10}H_{24}O_2Si$ $[M+Na]^+$: theoretical 227.1443, found 227.1436.

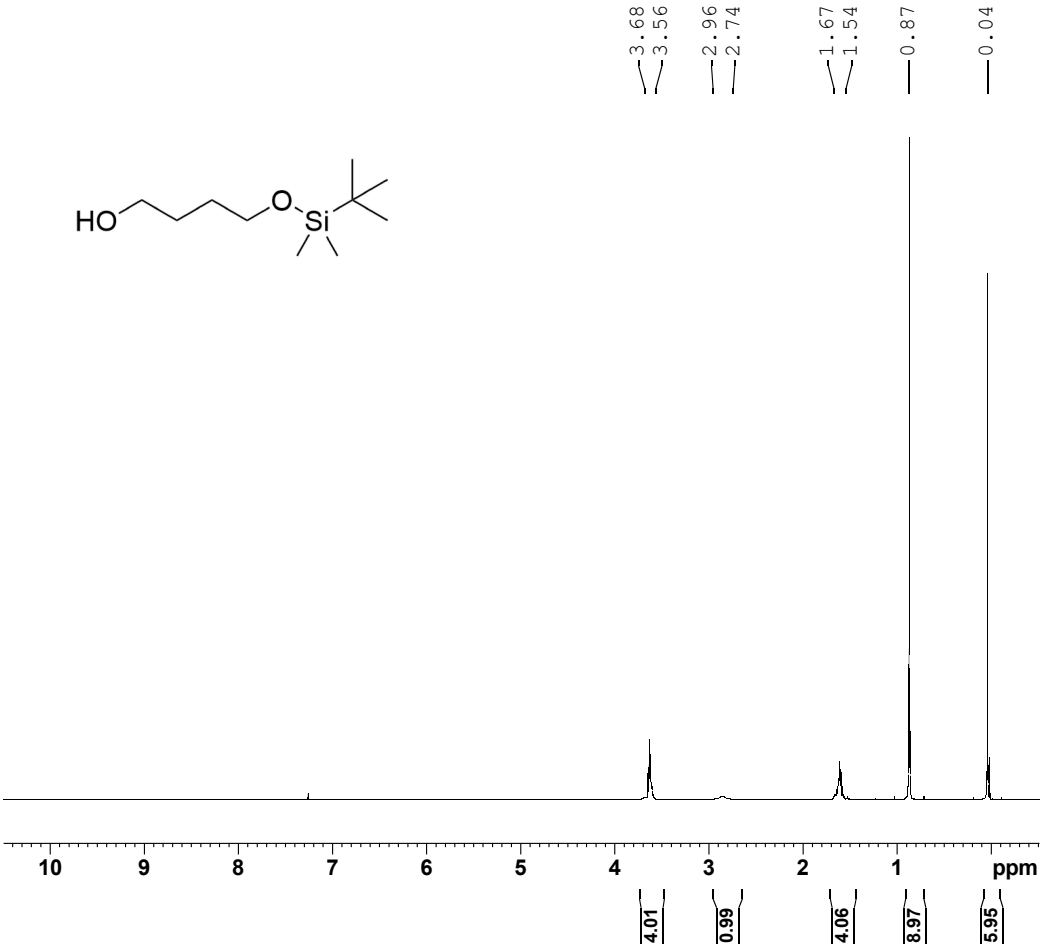

Figure A2- ^{1}H NMR (400 MHz, $CDCl_3$) spectrum obtained for compound **1**.

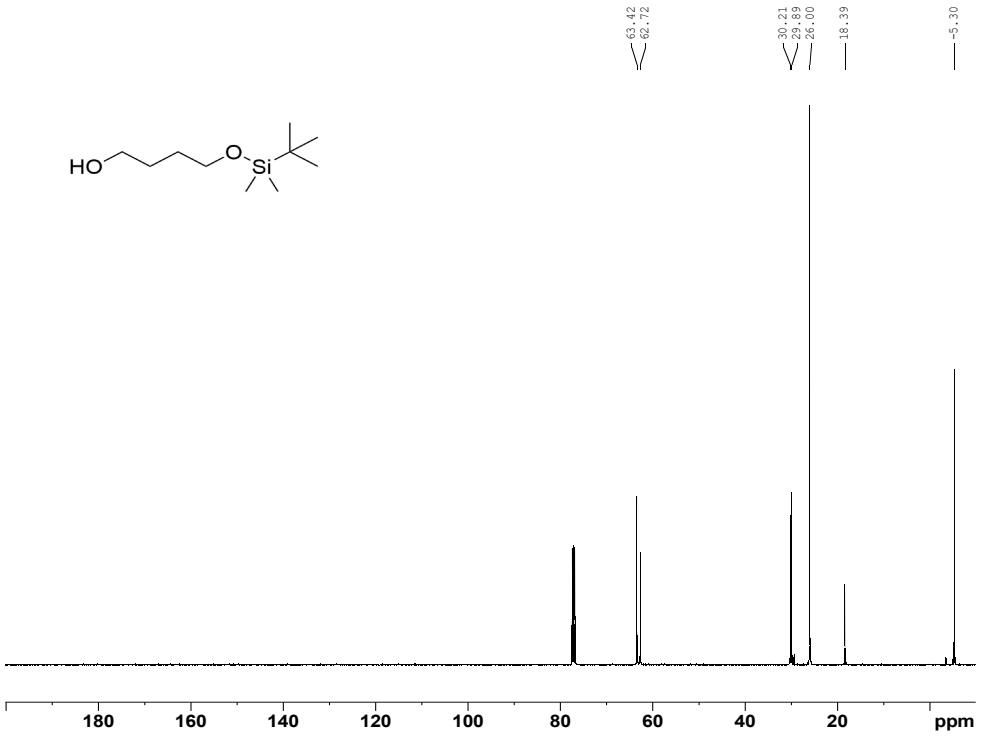

Figure A3- ^{13}C NMR (100 MHz, $CDCl_3$) spectrum obtained for compound **1**.

Elemental Composition Report **Page 1**

Single Mass Analysis
Tolerance = 5.0 PPM / DBE: min = -10.0, max = 1000.0
Element prediction: Off
Number of isotope peaks used for i-FIT = 4

Monoisotopic Mass, Even Electron Ions
243 formula(e) evaluated with 1 results within limits (all results (up to 1000) for each mass)
Elements Used:
C: 0-100 H: 0-200 N: 0-10 O: 0-10 Na: 1-1 Si: 1-1

DRC28 (DCM) - MeOH/H2O (95/5%) XEVO G2-XS QTOF 06-Oct-2023
20231006_KK_DRC28_01 76 (0.783) Cm (74:92) 1: TOF MS ES+
2.46e+006

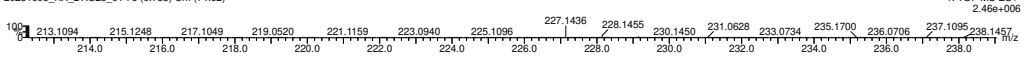

Minimum:				-10.0				
Maximum:		30.0	5.0	1000.0				
Mass	Calc. Mass	mDa	PPM	DBE	i-FIT	Norm	Conf(%)	Formula
227.1436	227.1443	-0.7	-3.1	-0.5	1870.6	n/a	n/a	C10 H24 O2 Na Si

Figure A4- ESI(+)-TOF-HRMS elemental composition report obtained for compound **1**.

6-(benzyloxy)-6-oxohexanoic acid (2) - Following **Method A,** the crude was then purified by flash chromatography (DCM/ethyl acetate 10/90 to 70/30, v/v) to afford **2** with 36% yield as a yellowish oil. ^{1}H NMR ($CDCl_3$, 400 MHz): 7.29-7.40 (m, 5H), 5.12 (s, 2H), 2.34-2.43 (m, 4H), 1.62-1.77 (m, 4H). ^{13}C NMR ($CDCl_3$, 100 MHz): 179.4, 173.2, 136.1, 128.7, 128.7, 128.4, 128.4, 128.4, 66.4, 34.0, 33.7, 24.4, 24.2. ESI(+)-TOF-HRMS m/z for $C_{13}H_{16}O_4$ $[M+Na]^+$: theoretical 259.0946, found 259.0953.

Figure A5- ^{1}H NMR (400 MHz, CDCl3) spectrum obtained for compound **2**.

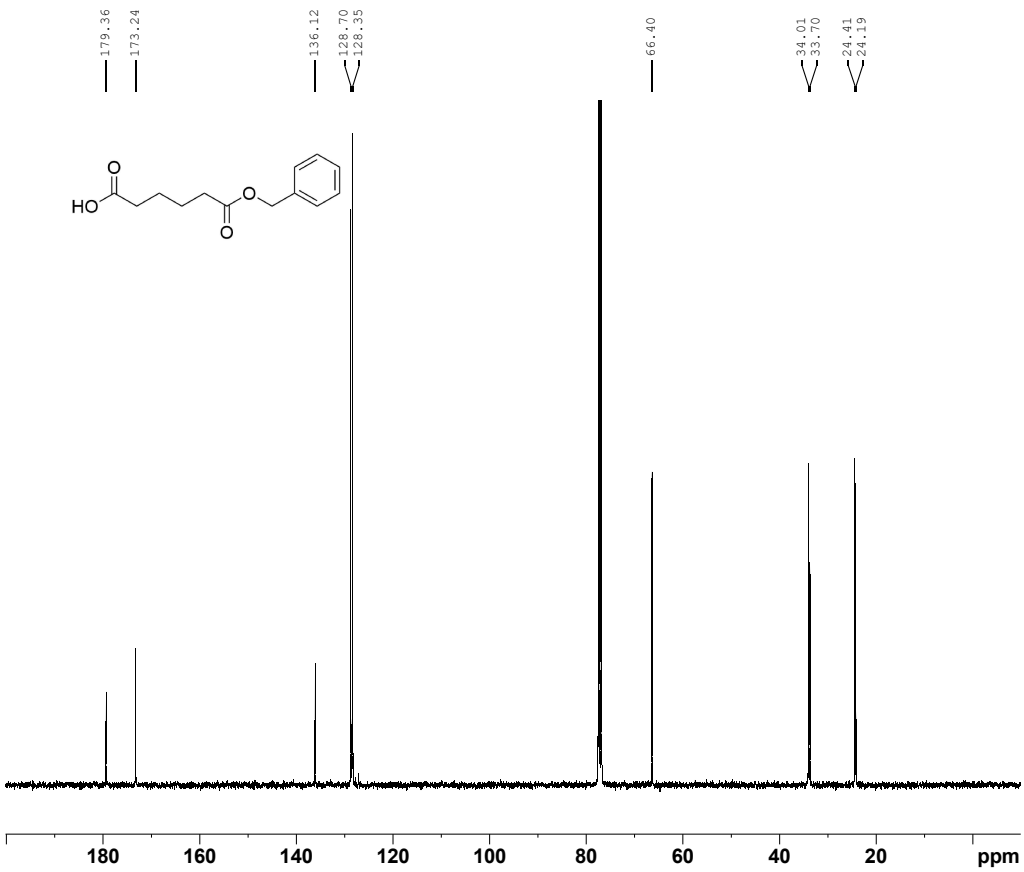

Figure A6- ^{13}C NMR (100 MHz, $CDCl_3$) spectrum obtained for compound **2**.

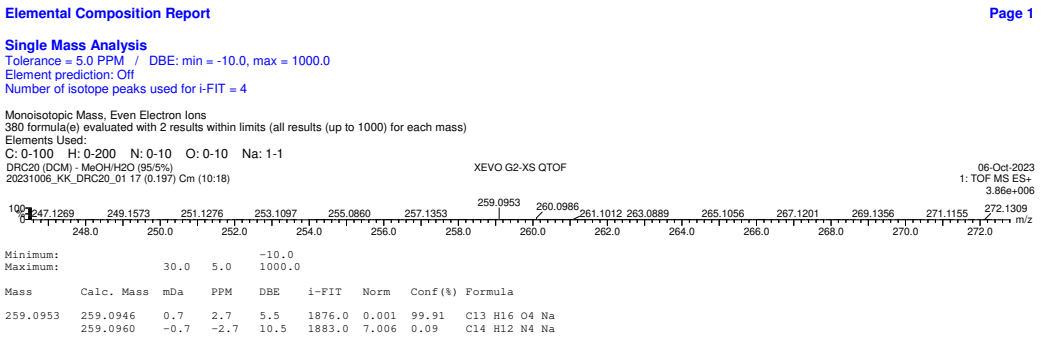

Elemental Composition Report Page 1

Single Mass Analysis
Tolerance = 5.0 PPM / DBE: min = -10.0, max = 1000.0
Element prediction: Off
Number of isotope peaks used for i-FIT = 4

Monoisotopic Mass, Even Electron Ions
380 formula(e) evaluated with 2 results within limits (all results (up to 1000) for each mass)
Elements Used:
C: 0-100 H: 0-200 N: 0-10 O: 0-10 Na: 1-1

DRC20 (DCM) - MeOH/H2O (95/5%)
20231006_KK_DRC20_01 17 (0.197) Cm (10:18)
XEVO G2-XS QTOF
06-Oct-2023
1: TOF MS ES+
3.86e+006

Minimum:			-10.0					
Maximum:		30.0	5.0	1000.0				
Mass	Calc. Mass	mDa	PPM	DBE	i-FIT	Norm	Conf(%)	Formula
259.0953	259.0946	0.7	2.7	5.5	1876.0	0.001	99.91	C13 H16 O4 Na
	259.0960	-0.7	-2.7	10.5	1883.0	7.006	0.09	C14 H12 N4 Na

Figure A7- ESI(+)-TOF-HRMS elemental composition report obtained for compound **2**.

benzyl (4-((tert-butyldimethylsilyl)oxy)butyl) adipate (3) - Following **Method C,** the crude was then purified by flash chromatography (cyclohexane/ethyl acetate 95/15 to 75/25, v/v) to afford **3** with 92% yield as a colourless oil. ^{1}H NMR ($CDCl_3$, 300 MHz): 7.25-7.35 (m, 5H), 5.07 (s, 2H), 4.04 (t, 2H, ^{3}J = 6.39 Hz), 3.58 (t, 2H, ^{3}J = 6.22 Hz), 2.33 (t, 2H, ^{3}J = 7.03 Hz), 2.27 (t, 2H, ^{3}J = 7.22 Hz), 1.57-1.69 (m, 6H), 1.45-1.56 (m, 2H), 0.85 (s, 9H), 0.00 (s, 6H). ^{13}C NMR ($CDCl_3$, 75 MHz): 173.5, 173.3, 136.2, 136.2, 128.7, 128.7, 128.3, 128.3, 66.3, 64.5, 62.7, 34.1, 34.1, 29.4, 26.1, 26.1, 26.1, 25.4, 25.4, 24.5, 18.5, -5.17, -5.17. ESI(+)-TOF-HRMS m/z for $C_{23}H_{38}O_5Si$ $[M+Na]^+$: theoretical 445.2386, found 445.2386.

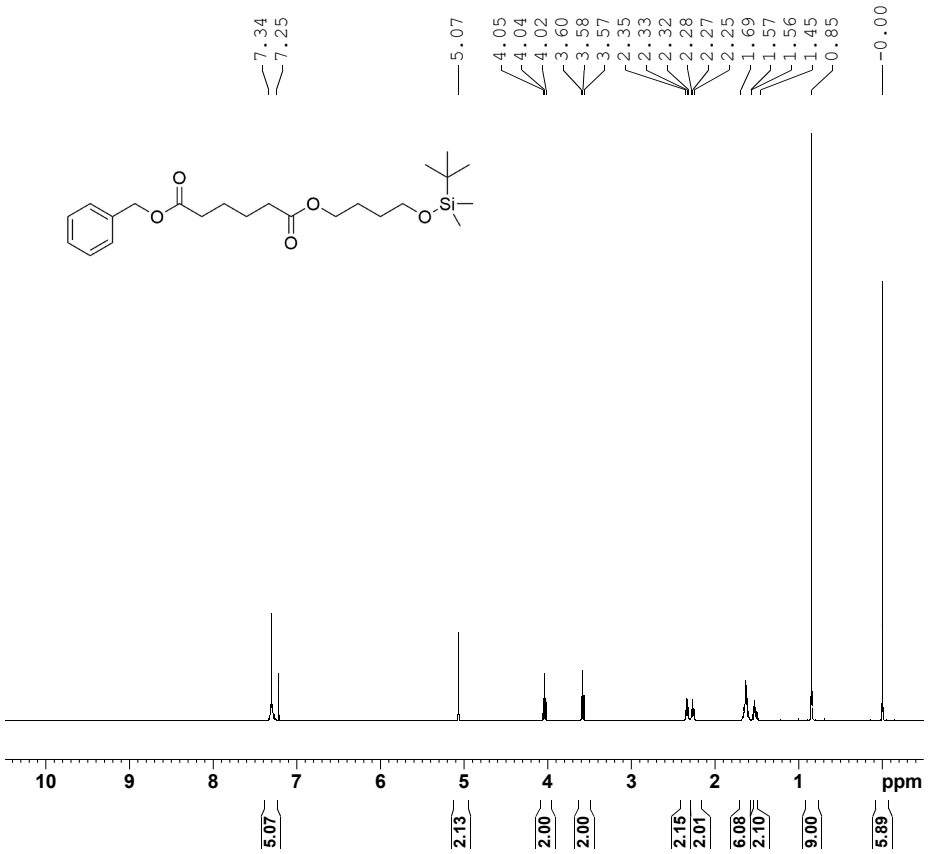

Figure A8- ^{1}H NMR (300 MHz, CDCl3) spectrum obtained for compound **3**.

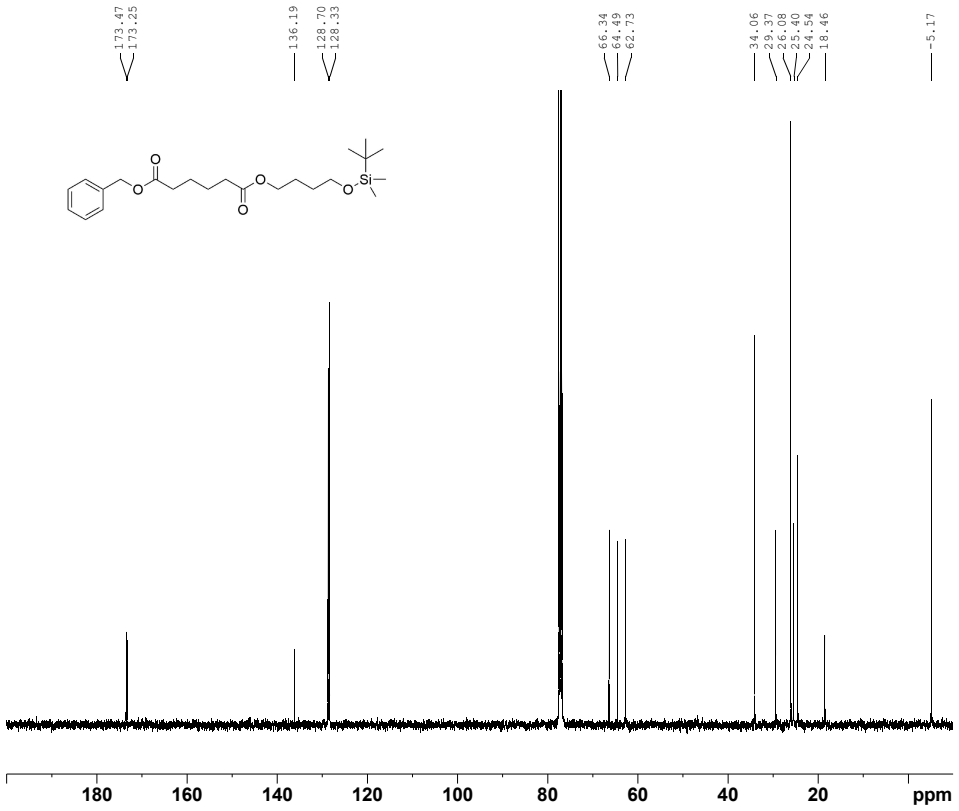

Figure A9- ^{13}C NMR (75 MHz, CDCl3) spectrum obtained for compound **3**.

Elemental Composition Report **Page 1**

Single Mass Analysis
Tolerance = 5.0 PPM / DBE: min = -10.0, max = 1000.0
Element prediction: Off
Number of isotope peaks used for i-FIT = 4

Monoisotopic Mass, Even Electron Ions
56 formula(e) evaluated with 1 results within limits (all results (up to 1000) for each mass)
Elements Used:
C: 0-100 H: 0-200 O: 0-8 Na: 1-1 Si: 1-1

DRC18 (DCM) - MeOH/H2O (95/5%)
20231009_XX_DRC18_01 23 (0.248) Cm (9:23)

XEVO G2-XS QTOF

09-Oct-2023
1: TOF MS ES+
7.60e+006

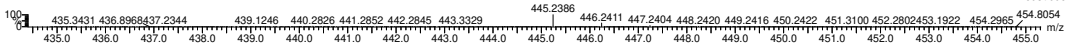

Minimum:				-10.0			
Maximum:		30.0	5.0	1000.0			
Mass	Calc. Mass	mDa	PPM	DBE	i-FIT	Norm	Conf(%) Formula
445.2386	445.2386	0.0	0.0	5.5	2098.3	n/a	n/a C23 H38 O5 Na Si

Figure A10- ESI(+)-TOF-HRMS elemental composition report obtained for compound **3**.

benzyl (4-hydroxybutyl) adipate (4) - Following **Method D,** the crude was then purified by flash chromatography (cyclohexane/ethyl acetate 90/10 to 60/40, v/v) to afford **4** with 93% yield as a colourless oil. ^{1}H NMR ($CDCl_3$, 400 MHz): 7.27-7.36 (m, 5H), 5.09 (s, 2H), 4.08 (t, 2H, ^{3}J = 6.59 Hz), 3.62 (t, 2H, ^{3}J = 6.40 Hz), 2.35 (t, 2H, ^{3}J = 7.09 Hz), 2.29 (t, 2H, ^{3}J = 6.95 Hz), 2.16-2.22 (br s, 1H), 1.54-1.74 (m, 8H). ^{13}C NMR ($CDCl_3$, 100 MHz): 173.4, 173.2, 136.0, 128.6, 128.2, 128.2, 128.2, 128.2, 66.2, 64.2, 62.1, 33.9, 33.9, 29.1, 25.1, 24.4, 24.4. ESI(+)-TOF-HRMS m/z for $C_{17}H_{24}O_5$ $[M+Na]^+$: theoretical 331.1521, found 331.1521.

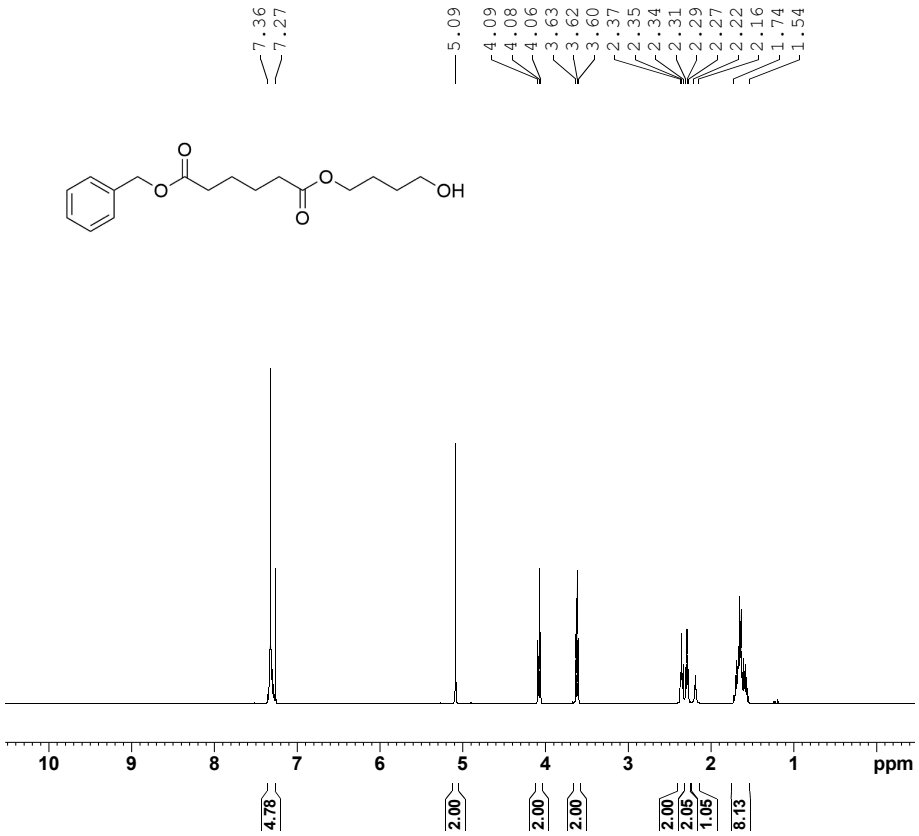

Figure A14- ^{1}H NMR (400 MHz, CDCl3) spectrum obtained for compound **4**.

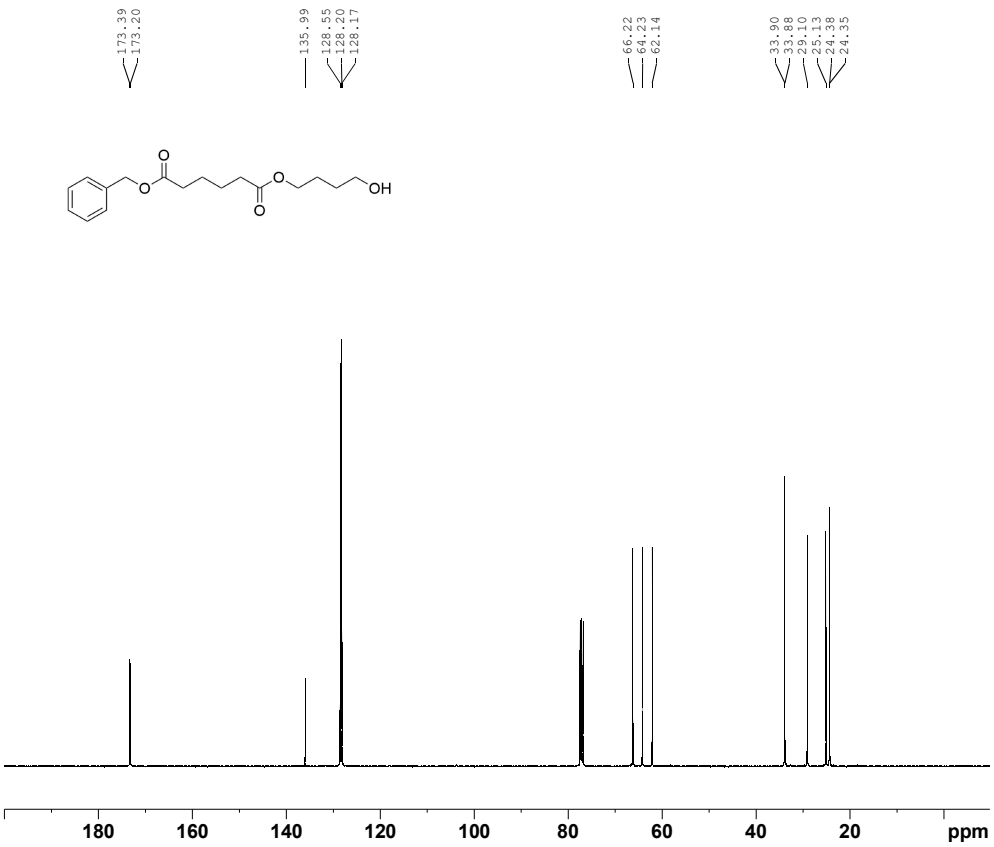

Figure A15- ^{13}C NMR (100 MHz, $CDCl_3$) spectrum obtained for compound **4**.

Elemental Composition Report **Page 1**

Single Mass Analysis
Tolerance = 5.0 PPM / DBE: min = -10.0, max = 1000.0
Element prediction: Off
Number of isotope peaks used for i-FIT = 4

Monoisotopic Mass, Even Electron Ions
47 formula(e) evaluated with 1 results within limits (all results (up to 1000) for each mass)
Elements Used:
C: 0-100 H: 0-200 O: 0-8 Na: 1-1

DRC22 (DCM) - MeOH/H2O (95/5%)
20231009_XX_DRC22_01 57 (0.597) Cm (57:70)

XEVO G2-XS QTOF

09-Oct-2023
1: TOF MS ES+
5.85e+006

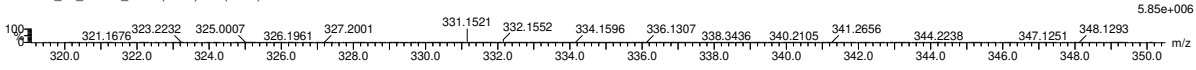

Minimum:				-10.0				
Maximum:		30.0	5.0	1000.0				
Mass	Calc. Mass	mDa	PPM	DBE	i-FIT	Norm	Conf(%)	Formula
331.1521	331.1521	0.0	0.0	5.5	2011.6	n/a	n/a	C17 H24 O5 Na

Figure A16- ESI(+)-TOF-HRMS elemental composition report obtained for compound **4**.

6-(4-((tert-butyldimethylsilyl)oxy)butoxy)-6-oxohexanoic acid (5) - Following **Method E, 5** was obtained with quantitative yield as a colourless oil. ^{1}H NMR ($CDCl_3$, 400 MHz): 4.09 (t, 2H, ^{3}J = 6.41 Hz), 3.63 (t, 2H, ^{3}J = 6.25 Hz), 2.28-2.42 (m, 4H), 1.51-1.75 (m, 8H), 0.89 (s, 9H), 0.04 (s, 6H). ^{13}C NMR ($CDCl_3$, 100 MHz): 179.1, 173.5, 64.5, 62.7, 34.0, 33.7, 29.3, 26.1, 26.1, 26.1, 25.3, 24.4, 24.2, 18.4, -5.2, -5.2. ESI(+)-TOF-HRMS m/z for $C_{16}H_{32}O_5Si$ $[M+Na]^+$: theoretical 355.1917, found 355.1913.

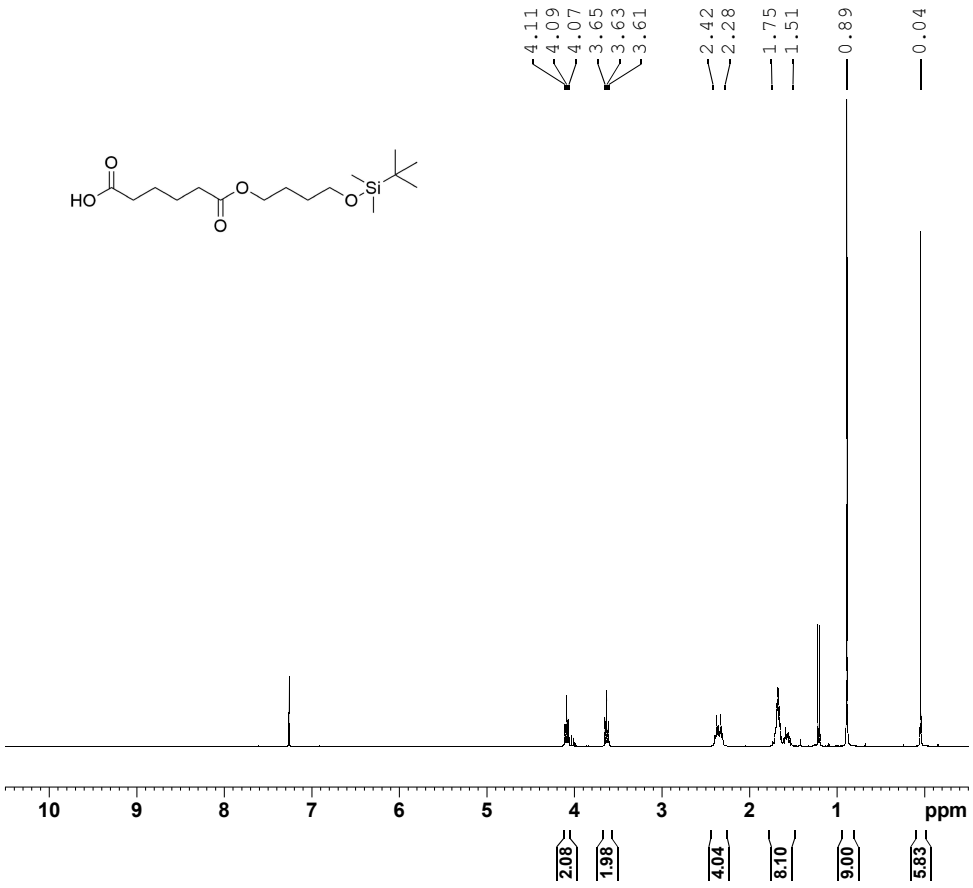

Figure A11- ^{1}H NMR (400 MHz, CDCl3) spectrum obtained for compound **5**.

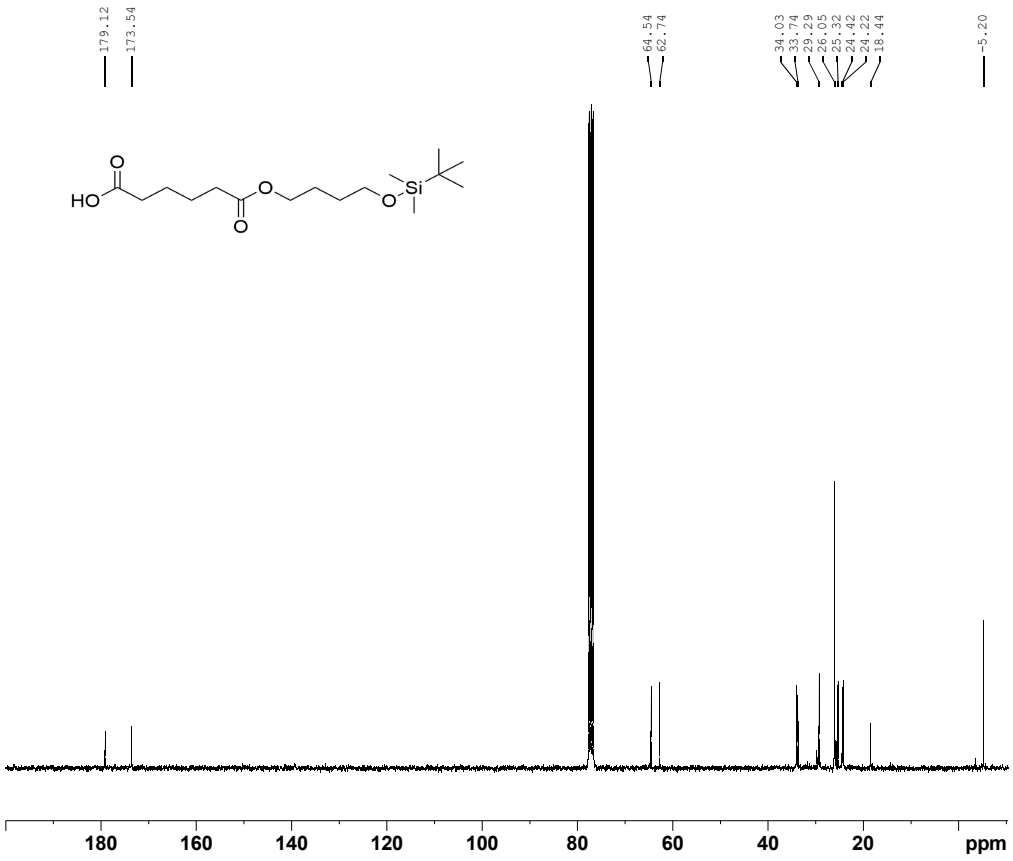

Figure A12- ^{13}C NMR (100 MHz, $CDCl_3$) spectrum obtained for compound **5**.

Elemental Composition Report **Page 1**

Single Mass Analysis
Tolerance = 5.0 PPM / DBE: min = -10.0, max = 1000.0
Element prediction: Off
Number of isotope peaks used for i-FIT = 4

Monoisotopic Mass, Even Electron Ions
47 formula(e) evaluated with 1 results within limits (all results (up to 1000) for each mass)
Elements Used:
C: 0-100 H: 0-200 O: 0-8 Na: 1-1 Si: 1-1

DRC24 (DCM) - MeOH/H2O (95/5%) XEVO G2-XS QTOF 09-Oct-2023
20231009_XX_DRC24_01 9 (0.117) Cm (6:14) 1: TOF MS ES+
2.72e+006

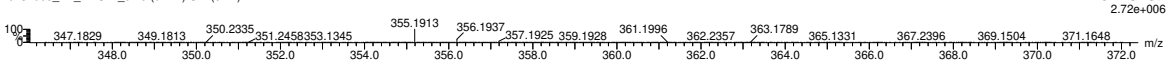

Minimum:				-10.0				
Maximum:		30.0	5.0	1000.0				
Mass	Calc. Mass	mDa	PPM	DBE	i-FIT	Norm	Conf(%)	Formula
355.1913	355.1917	-0.4	-1.1	1.5	1649.3	n/a	n/a	C16 H32 O5 Na Si

Figure A13- ESI(+)-TOF-HRMS elemental composition report obtained for compound **5**.

6-(4-hydroxybutoxy)-6-oxohexanoic acid (lin[BD+AA]) - Following **Method E, lin[BD+AA]** was obtained with quantitative yield as a yellowish oil. ^{1}H NMR ($CDCl_3$, 400 MHz): 5.88-6.62 (br s, 2H), 4.10 (t, 2H, ^{3}J = 6.30 Hz), 3.66 (t, 2H, ^{3}J = 6.46 Hz), 2.26-2.40 (m, 4H), 1.56-1.76 (m, 8H). ^{13}C NMR ($CDCl_3$, 100 MHz): 178.5, 173.6, 64.4, 62.4, 34.1, 33.7, 29.1, 25.2, 24.5, 24.2. ASAP(-)-TOF-HRMS m/z for $C_{10}H_{18}O_5$ $[M-H]^-$: theoretical 217.1076, found 217.1080

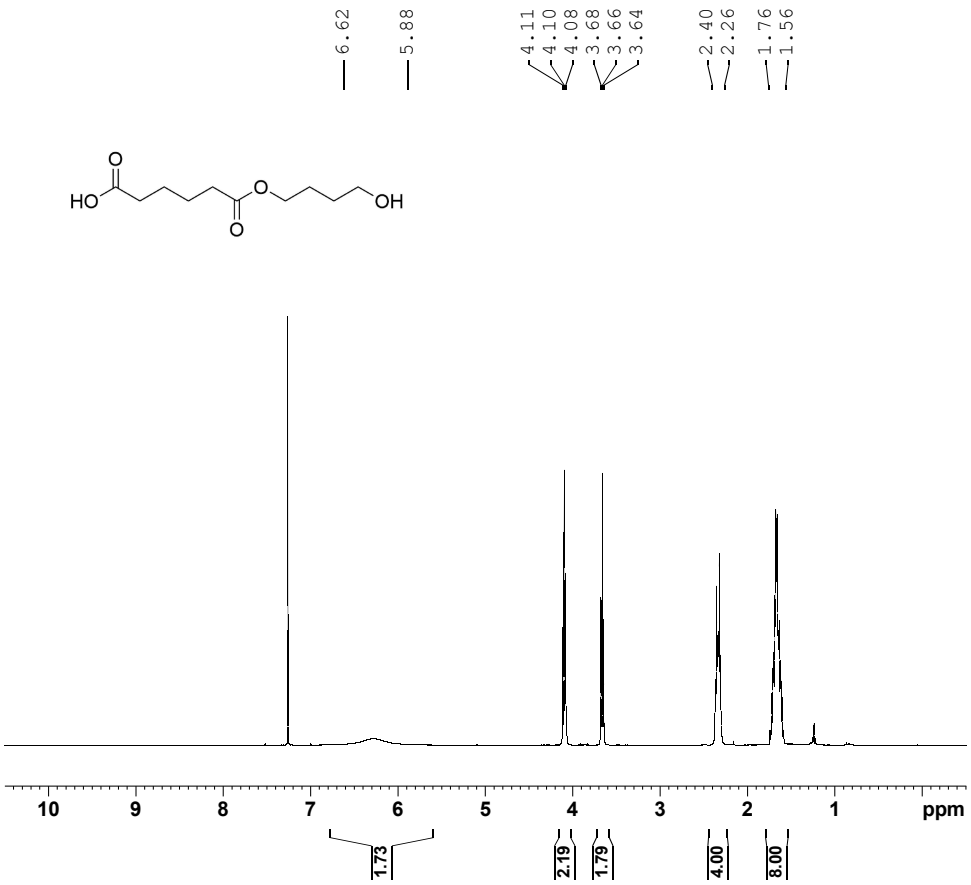

Figure A17- ^{1}H NMR (400 MHz, CDCl3) spectrum obtained for compound **lin[BD+AA]**.

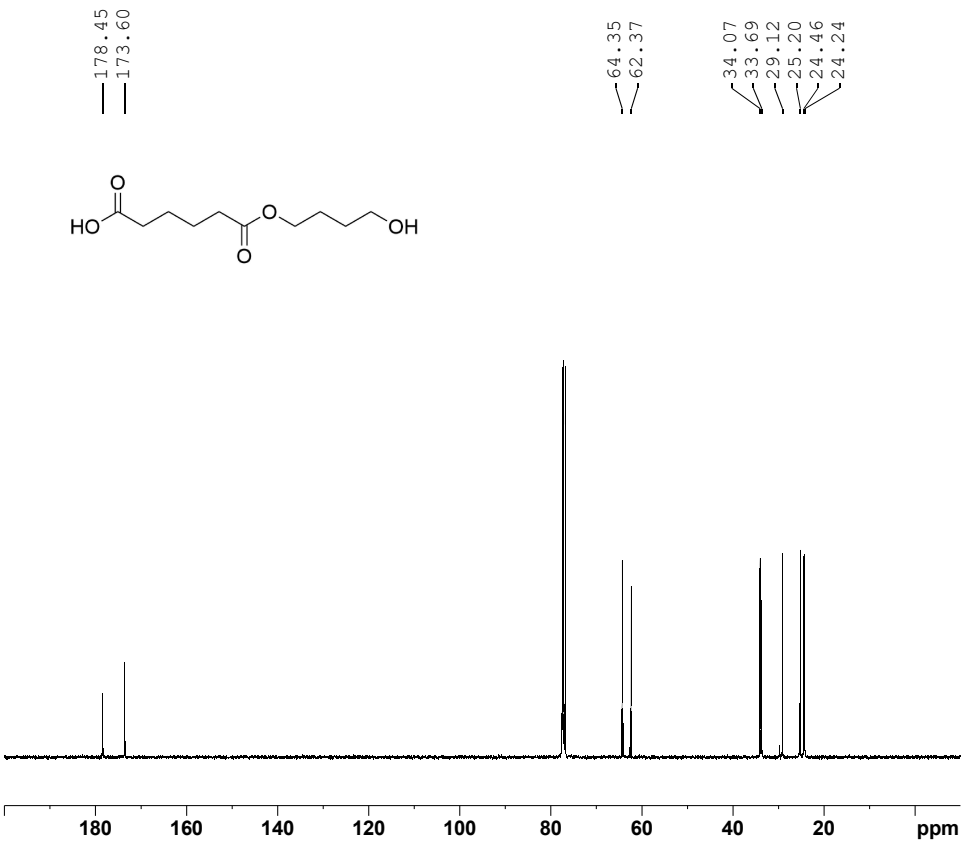

Figure A18- ^{13}C NMR (100 MHz, $CDCl_3$) spectrum obtained for compound **lin[BD+AA]**.

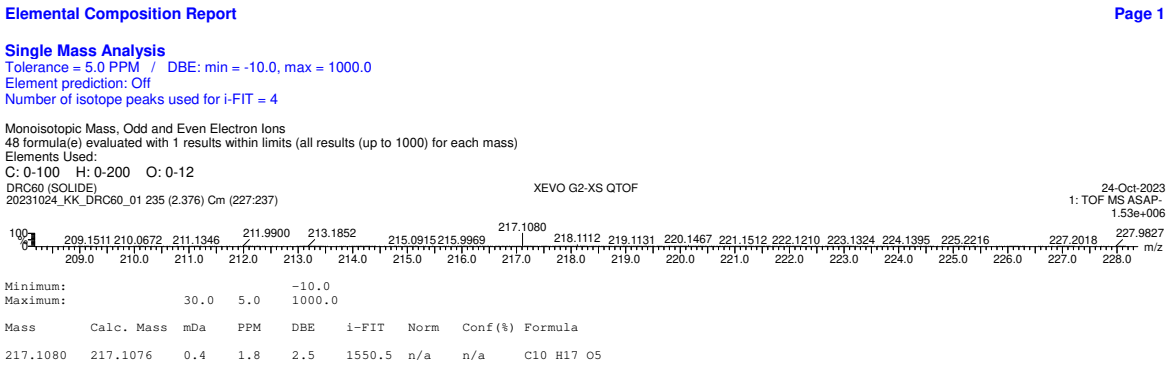

Elemental Composition Report Page 1

Single Mass Analysis
Tolerance = 5.0 PPM / DBE: min = -10.0, max = 1000.0
Element prediction: Off
Number of isotope peaks used for i-FIT = 4

Monoisotopic Mass, Odd and Even Electron Ions
48 formula(e) evaluated with 1 results within limits (all results (up to 1000) for each mass)
Elements Used:
C: 0-100 H: 0-200 O: 0-12

DRC60 (SOLIDE) XEVO G2-XS QTOF 24-Oct-2023
20231024_KK_DRC60_01 235 (2.376) Cm (227:237) 1: TOF MS ASAP- 1.53e+006

217.1080
209.1511 210.0672 211.1346 211.9900 213.1852 215.0915 215.9969 218.1112 219.1131 220.1467 221.1512 222.1210 223.1324 224.1395 225.2216 227.2018 227.9827
m/z

	Mass	Calc. Mass	mDa	PPM	DBE	i-FIT	Norm	Conf(%)	Formula
Minimum:					-10.0				
Maximum:			30.0	5.0	1000.0				
	217.1080	217.1076	0.4	1.8	2.5	1550.5	n/a	n/a	C10 H17 O5

Figure A19- ASAP(-)-TOF-HRMS elemental composition report obtained for compound **lin[BD+AA]**.

bis(4-((tert-butyldimethylsilyl)oxy)butyl) adipate (6) - Following **Method C,** the crude was then purified by flash chromatography (cyclohexane/ethyl acetate 90/10 to 70/30, v/v) to afford **6** with 95% yield as a colourless oil. ^{1}H NMR ($CDCl_3$, 300 MHz): 4.08 (t, 4H, ^{3}J = 6.46 Hz), 3.62 (t, 4H, ^{3}J = 6.25 Hz), 2.25-2.37 (m, 4H), 1.51-1.74 (m, 12H), 0.88 (s, 18H), 0.04 (s, 12H). ^{13}C NMR ($CDCl_3$, 75 MHz): 173.6, 173.6, 64.5, 64.5, 62.7, 62.7, 34.1, 34.1, 29.3, 29.3, 26.1, 26.1, 26.1, 26.1, 26.1, 26.1, 25.4, 25.4, 24.6, 24.6, 18.5, 18.5, -5.19, -5.19, -5.19, -5.19. ESI(+)-TOF-HRMS m/z for $C_{26}H_{54}O_6Si_2$ $[M+Na]^+$: theoretical 541.3357, found 541.3356.

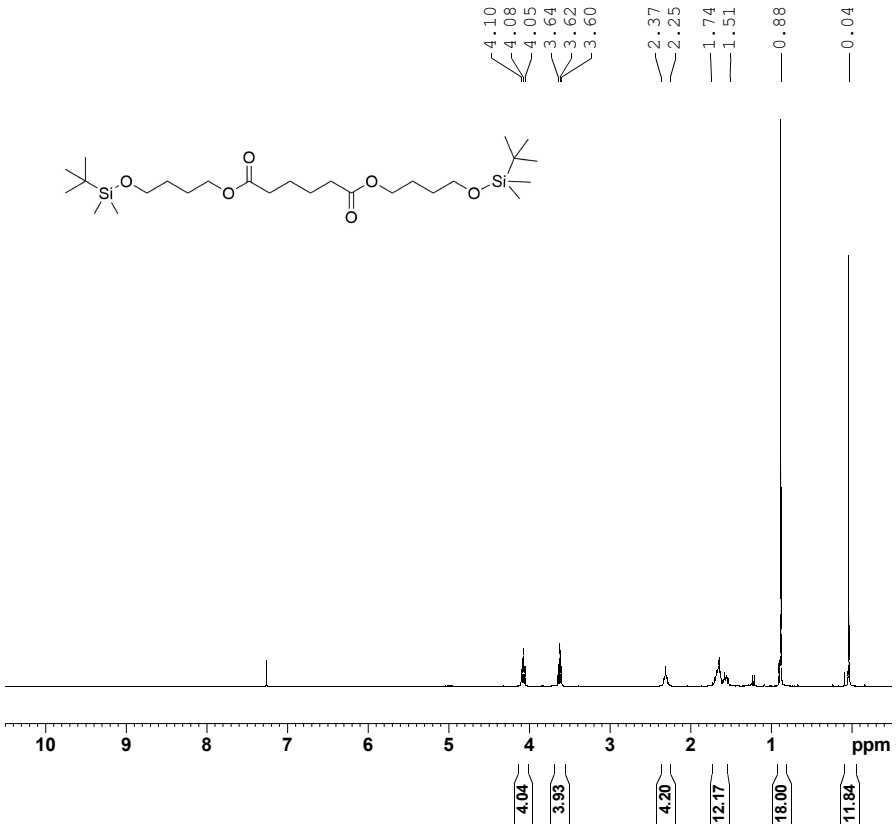

Figure A20- ^{1}H NMR (300 MHz, CDCl3) spectrum obtained for compound **6**.

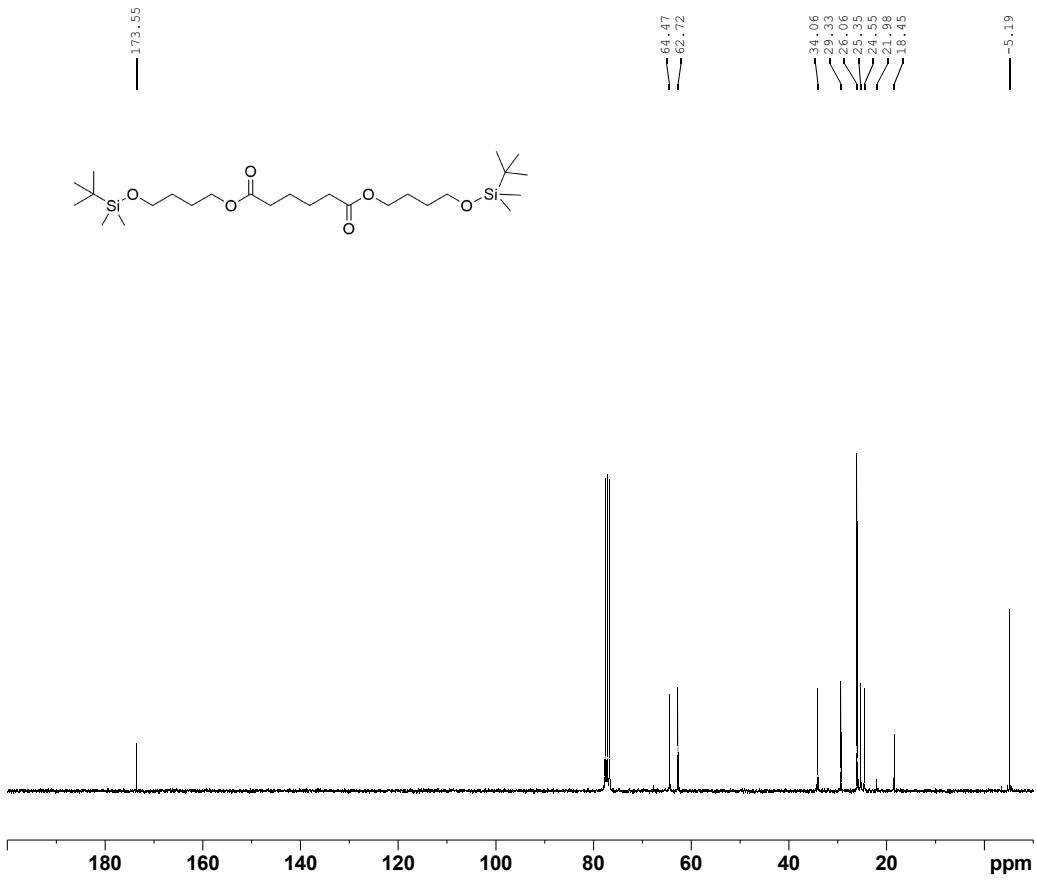

Figure A21- ^{13}C NMR (75 MHz, $CDCl_3$) spectrum obtained for compound **6**.

Elemental Composition Report **Page 1**

Single Mass Analysis
Tolerance = 10.0 PPM / DBE: min = -10.0, max = 1000.0
Element prediction: Off
Number of isotope peaks used for i-FIT = 4

Monoisotopic Mass, Even Electron Ions
125 formula(e) evaluated with 1 results within limits (all results (up to 1000) for each mass)
Elements Used:
C: 0-100 H: 0-200 O: 0-20 Na: 1-1 Si: 2-2

Minimum:				-10.0				
Maximum:		30.0	10.0	1000.0				
Mass	Calc. Mass	mDa	PPM	DBE	i-FIT	Norm	Conf(%)	Formula
541.3356	541.3357	-0.1	-0.2	1.5	1768.4	n/a	n/a	C26 H54 O6 Na Si2

Figure A22- ESI(+)-TOF-HRMS elemental composition report obtained for compound **6**.

bis(4-hydroxybutyl) adipate (lin[2BD+AA]) - Following **Method D,** the crude was then purified by flash chromatography (cyclohexane/ethyl acetate 60/40 to 0/100, v/v) to afford **lin[2BD+AA]** with 86% yield as a yellowish oil. ^{1}H NMR ($CDCl_3$, 400 MHz): 4.08 (t, 4H, ^{3}J = 6.37 Hz), 3.62 (t, 4H, ^{3}J = 6.43 Hz), 2.27-2.34 (m, 4H), 2.22-2.27 (br s, 2H), 1.54-1.74 (m, 12H). ^{13}C NMR ($CDCl_3$, 100 MHz): 173.6, 173.6, 64.4, 64.4, 62.2, 62.2, 34.0, 34.0, 29.2, 29.2, 25.2, 25.2, 24.5, 24.5. ESI(+)-TOF-HRMS m/z for $C_{14}H_{26}O_6$ $[M+Na]^+$: theoretical 313.1627, found 313.1627.

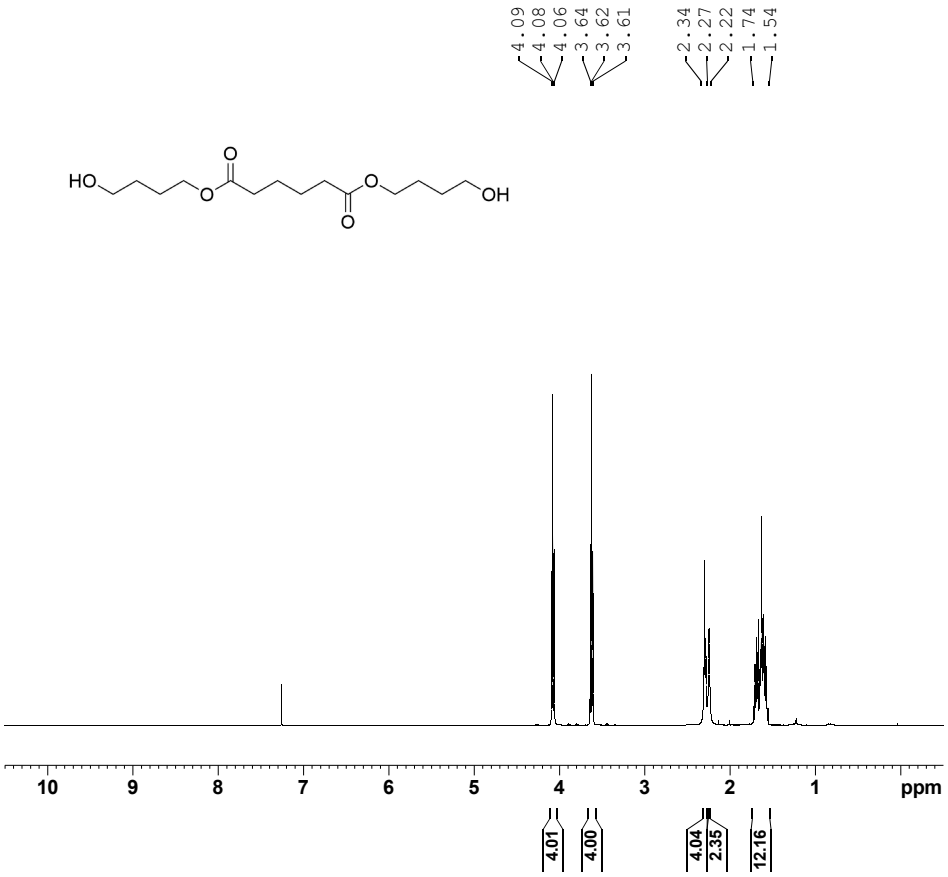

Figure A23- ^{1}H NMR (400 MHz, CDCl3) spectrum obtained for compound **lin[2BD+AA]**.

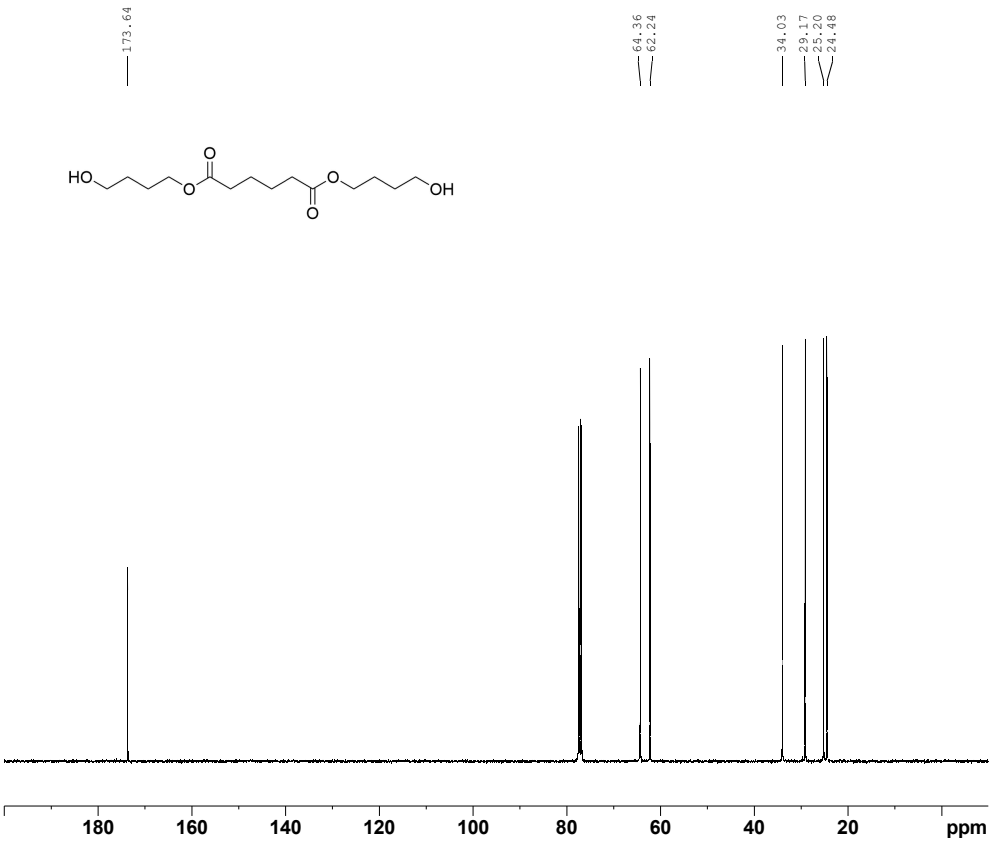

Figure A24- ^{13}C NMR (100 MHz, $CDCl_3$) spectrum obtained for compound **lin[2BD+AA]**.

Elemental Composition Report **Page 1**

Single Mass Analysis
Tolerance = 5.0 PPM / DBE: min = -10.0, max = 1000.0
Element prediction: Off
Number of isotope peaks used for i-FIT = 4

Monoisotopic Mass, Even Electron Ions
43 formula(e) evaluated with 1 results within limits (all results (up to 1000) for each mass)
Elements Used:
C: 0-100 H: 0-200 O: 0-8 Na: 1-1

DRC37 (DCM) - MeOH/H2O (95/5%)
20231009_XX_DRC37_01 49 (0.517) Cm (36:51)

XEVO G2-XS QTOF

09-Oct-2023
1: TOF MS ES+
1.44e+007

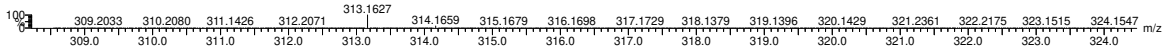

Minimum:				-10.0				
Maximum:		30.0	5.0	1000.0				
Mass	Calc. Mass	mDa	PPM	DBE	i-FIT	Norm	Conf(%)	Formula
313.1627	313.1627	0.0	0.0	1.5	2399.5	n/a	n/a	C14 H26 O6 Na

Figure A25- ESI(+)-TOF-HRMS elemental composition report obtained for compound **lin[2BD+AA]**.

benzyl (2,2,3,3-tetramethyl-10,15-dioxo-4,9,16-trioxa-3-silaicosan-20-yl) adipate (7) - Following **Method C,** the crude was then purified by flash chromatography (cyclohexane/ethyl acetate 90/10 to 50/50, v/v) to afford **7** with 89% yield as a colourless oil. ^{1}H NMR ($CDCl_3$, 400 MHz): 7.29-7.38 (m, 5H), 5.11 (s, 2H), 4.05-4.12 (m, 6H), 3.63 (t, 2H, ^{3}J = 6.26 Hz), 2.25-2.43 (m, 8H), 1.55-1.77 (m, 16H), 0.89 (s, 9H), 0.04 (s, 6H). ^{13}C NMR ($CDCl_3$, 100 MHz): 173.5, 173.4, 173.4, 173.2, 136.2, 128.7, 128.7, 128.4, 128.3, 128.3, 66.4, 64.5, 64.0, 64.0, 62.7, 34.1, 34.1, 34.0, 34.0, 29.4, 26.1, 26.1, 26.1, 25.8, 25.5, 25.5, 25.4, 24.6, 24.5, 24.5, 18.5, -5.2, -5.2. ASAP(+)-TOF-HRMS m/z for $C_{33}H_{54}O_9Si$ $[M+H]^+$: theoretical 623.3615, found 623.3633.

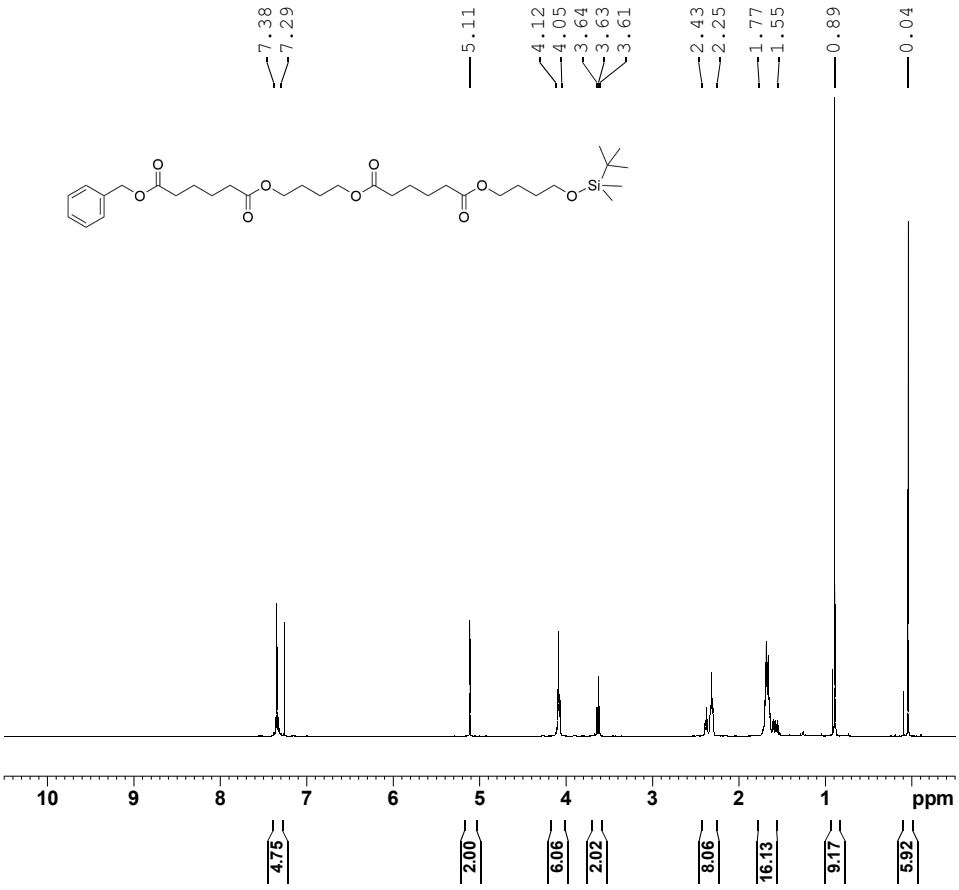

Figure A26- ^{1}H NMR (400 MHz, CDCl3) spectrum obtained for compound **7**.

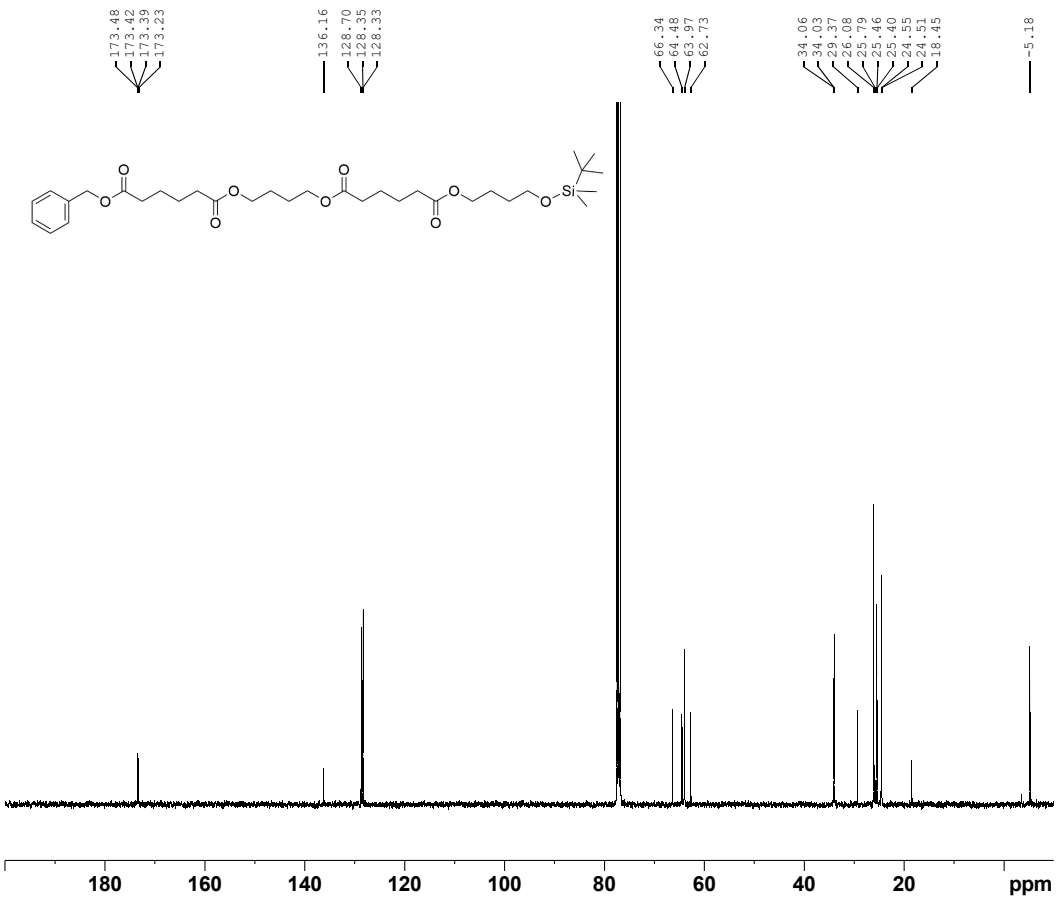

Figure A27- ^{13}C NMR (100 MHz, $CDCl_3$) spectrum obtained for compound **7**.

Elemental Composition Report **Page 1**

Single Mass Analysis
Tolerance = 5.0 PPM / DBE: min = -10.0, max = 1000.0
Element prediction: Off
Number of isotope peaks used for i-FIT = 4

Monoisotopic Mass, Even Electron Ions
130 formula(e) evaluated with 1 results within limits (all results (up to 1000) for each mass)
Elements Used:
C: 0-100 H: 0-200 O: 0-15 Si: 1-1

Minimum:				-10.0				
Maximum:		30.0	5.0	1000.0				
Mass	Calc. Mass	mDa	PPM	DBE	i-FIT	Norm	Conf(%)	Formula
623.3633	623.3615	1.8	2.9	7.5	593.2	n/a	n/a	C33 H55 O9 Si

Figure A28- ASAP(+)-TOF-HRMS elemental composition report obtained for compound **7**.

O,O'-(butane-1,4-diyl) bis(4-((tert-butyldimethylsilyl)oxy)butyl) diadipate (9) - Following **Method C,** the crude was then purified by flash chromatography (cyclohexane/ethyl acetate 95/5 to 85/15, v/v) to afford **9** with 83% yield as a colourless oil. ^{1}H NMR ($CDCl_3$, 400 MHz): 4.05-4.13 (m, 8H), 3.62 (t, 4H, ^{3}J = 6.35 Hz), 2.27-2.37 (m, 8H), 1.53-1.76 (m, 20H), 0.88 (s, 18H), 0.04 (s, 12H). ^{13}C NMR ($CDCl_3$, 100 MHz): 173.5, 173.5, 173.4, 173.4, 64.5, 64.5, 64.0, 64.0, 62.7, 62.7, 34.1, 34.1, 34.0, 34.0, 29.4, 29.4, 26.1, 26.1, 26.1, 26.1, 26.1, 26.1, 25.5, 25.5, 25.4, 25.4, 24.6, 24.6, 24.6, 24.6, 18.4, 18.4, -5.19, -5.19, -5.19, -5.19. ASAP(+)-TOF-HRMS m/z for $C_{36}H_{70}O_{10}Si_2$ $[M+H]^+$: theoretical 719.4586, found 719.4587.

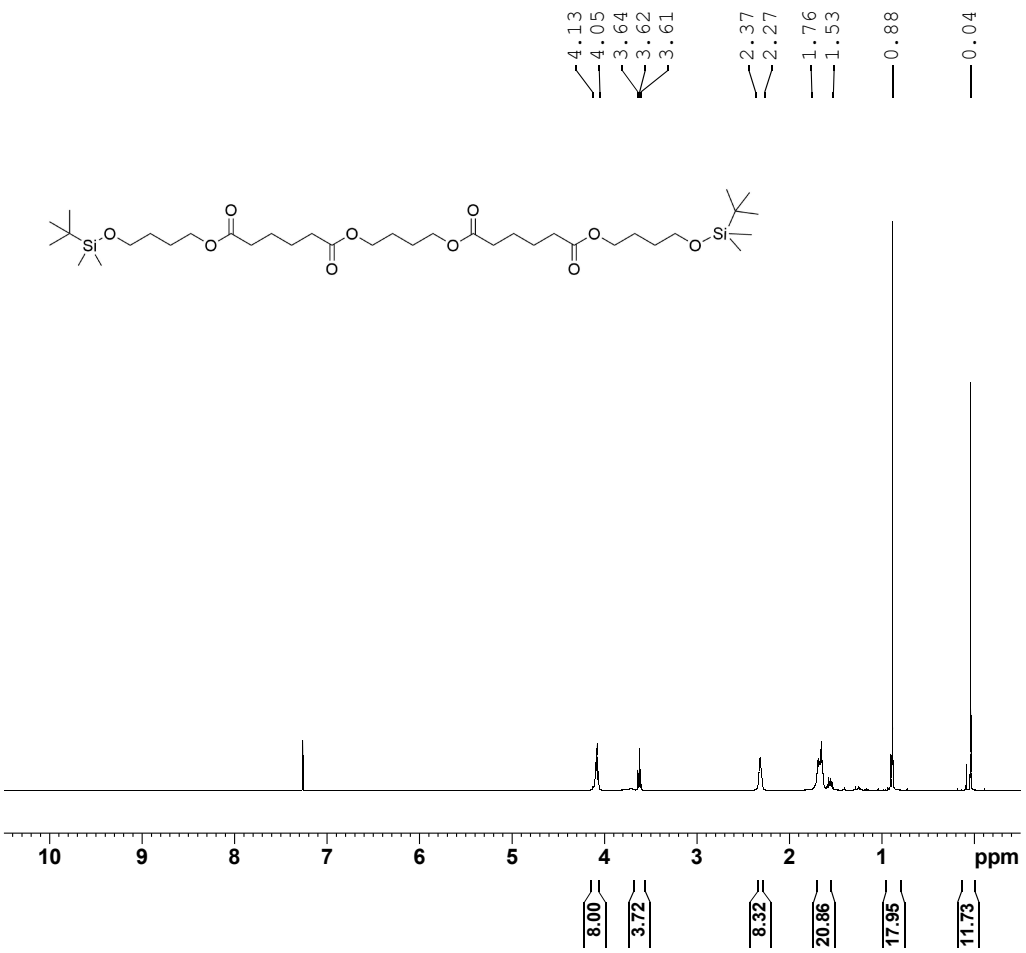

Figure A29- ^{1}H NMR (400 MHz, CDCl3) spectrum obtained for compound **9**.

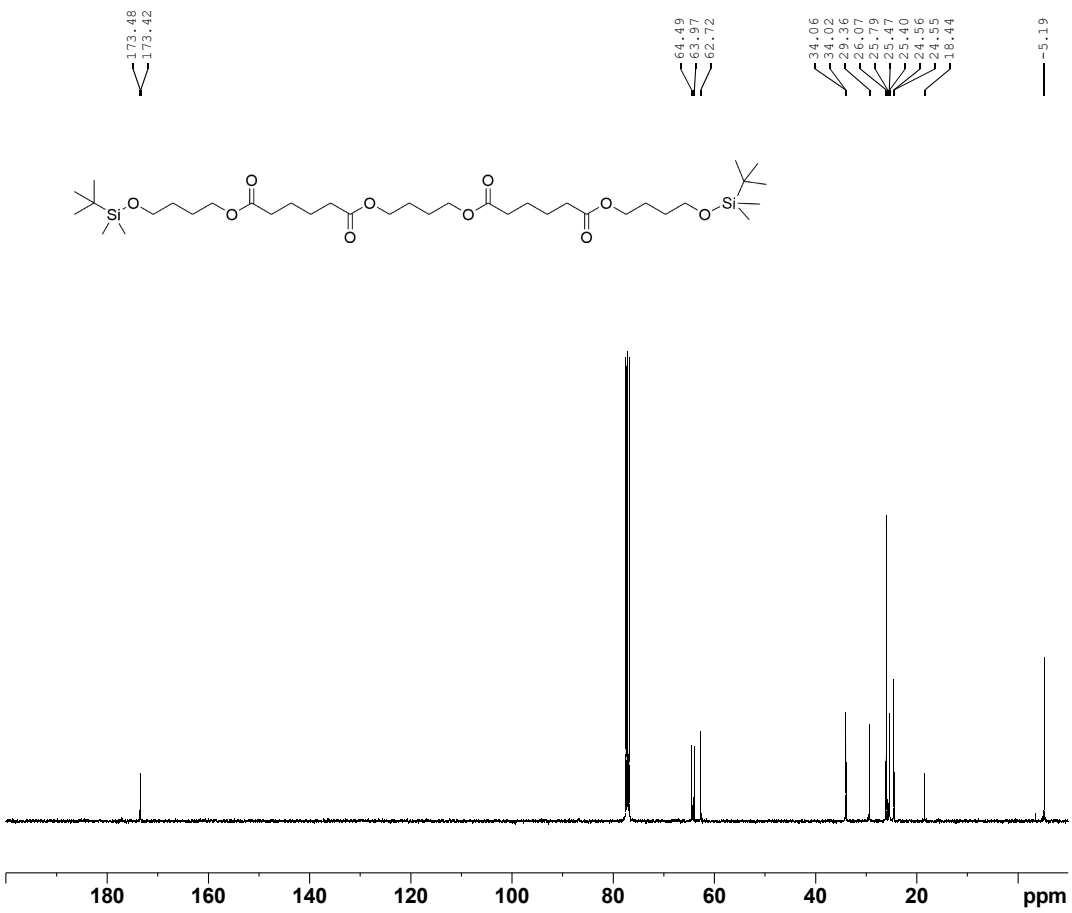

Figure A30- ^{13}C NMR (100 MHz, $CDCl_3$) spectrum obtained for compound **9**.

Elemental Composition Report **Page 1**

Single Mass Analysis
Tolerance = 5.0 PPM / DBE: min = -10.0, max = 1000.0
Element prediction: Off
Number of isotope peaks used for i-FIT = 4

Monoisotopic Mass, Even Electron Ions
448 formula(e) evaluated with 5 results within limits (all results (up to 1000) for each mass)
Elements Used:
C: 0-100 H: 0-200 O: 0-15 Si: 0-2

Minimum:				-10.0				
Maximum:		30.0	5.0	1000.0				
Mass	Calc. Mass	mDa	PPM	DBE	i-FIT	Norm	Conf(%)	Formula
719.4587	719.4586	0.1	0.1	3.5	2045.1	0.000	99.98	C36 H71 O10 Si2
	719.4554	3.3	4.6	8.5	2053.6	8.477	0.02	C40 H67 O9 Si
	719.4613	-2.6	-3.6	-0.5	2056.8	11.709	0.00	C33 H71 O14 Si
	719.4582	0.5	0.7	4.5	2062.6	17.513	0.00	C37 H67 O13
	719.4617	-3.0	-4.2	26.5	2062.7	17.557	0.00	C55 H59

Figure A31- ASAP(+)-TOF-HRMS elemental composition report obtained for compound **9**.

O,O'-(butane-1,4-diyl) bis(4-hydroxybutyl) diadipate (lin[3BD+2AA]) - Following **Method D,** the crude was then purified by flash chromatography (cyclohexane/ethyl acetate 70/30 to 10/90, v/v) to afford **lin[3BD+2AA]** with 82% yield as a white solid. ^{1}H NMR ($CDCl_3$, 400 MHz): 4.07-4.13 (m, 8H), 3.67 (t, 4H, ^{3}J = 6.40 Hz), 2.29-2.36 (m, 8H), 1.59-1.76 (m, 22H). ^{13}C NMR ($CDCl_3$, 100 MHz): 173.5, 173.5, 173.5, 173.5, 64.3, 64.3, 64.0, 64.0, 62.5, 62.5, 34.1, 34.1, 34.0, 34.0, 29.3, 29.3, 25.5, 25.5, 25.3, 25.3, 24.6, 24.6, 24.5, 24.5. ESI(+)-TOF-HRMS m/z for $C_{24}H_{42}O_{10}$ $[M+Na]^+$: theoretical 513.2676, found 513.2679. Aspect: white solid. Melting point: 46 ºC.

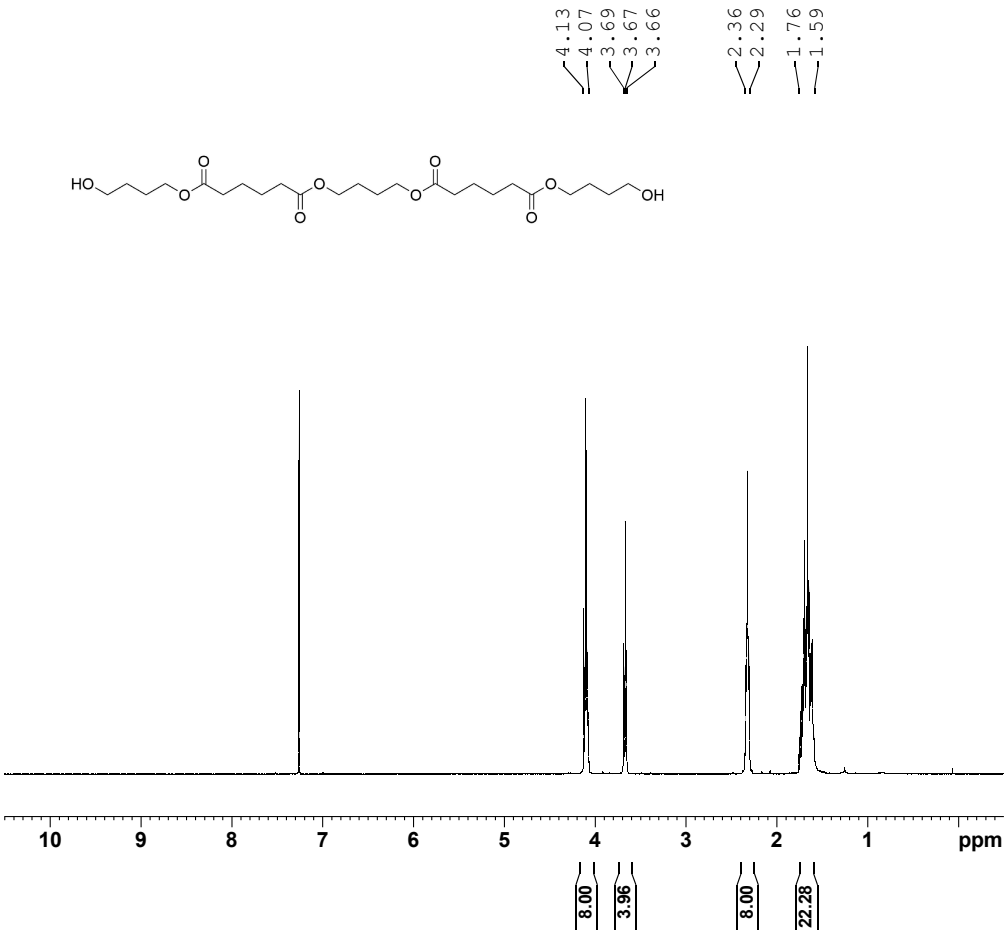

Figure A32- ^{1}H NMR (400 MHz, CDCl3) spectrum obtained for compound **lin[3BD+2AA]**.

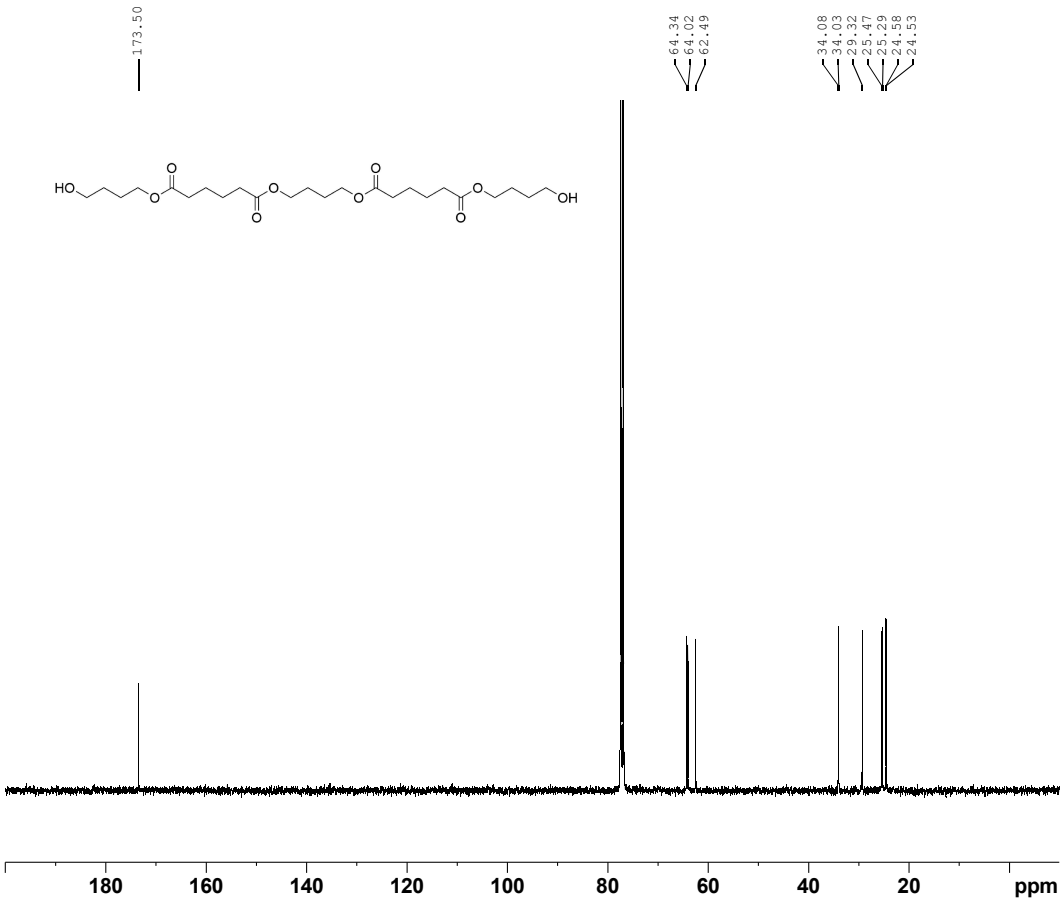

Figure A33- ^{13}C NMR (100 MHz, $CDCl_3$) spectrum obtained for compound **lin[3BD+2AA]**.

Elemental Composition Report **Page 1**

Single Mass Analysis
Tolerance = 5.0 PPM / DBE: min = -10.0, max = 1000.0
Element prediction: Off
Number of isotope peaks used for i-FIT = 4

Monoisotopic Mass, Even Electron Ions
126 formula(e) evaluated with 1 results within limits (all results (up to 1000) for each mass)
Elements Used:
C: 0-100 H: 0-200 O: 0-20 Na: 1-1

Minimum:				-10.0				
Maximum:		30.0	5.0	1000.0				
Mass	Calc. Mass	mDa	PPM	DBE	i-FIT	Norm	Conf(%)	Formula
513.2679	513.2676	0.3	0.6	3.5	2075.6	n/a	n/a	C24 H42 O10 Na

Figure A34- ESI(+)-TOF-HRMS elemental composition report obtained for compound **lin[3BD+2AA]**.

benzyl (4-((6-(4-hydroxybutoxy)-6-oxohexanoyl)oxy)butyl) adipate (10) - Following **Method D,** the crude was then purified by flash chromatography (cyclohexane/ethyl acetate 90/10 to 60/40, v/v) to afford **10** with 98% yield as a colourless oil. ^{1}H NMR ($CDCl_3$, 400 MHz): 7.29-7.38 (m, 5H), 5.10 (s, 2H), 4.05-4.13 (m, 6H), 3.66 (t, 2H, ^{3}J = 6.36 Hz), 2.26-2.40 (m, 8H), 1.58-1.75 (m, 16H). ^{13}C NMR ($CDCl_3$, 100 MHz): 173.5, 173.5, 173.4, 173.2, 136.12, 128.7, 128.7, 128.3, 128.3, 128.3, 66.3, 64.3, 64.0, 64.0, 62.4, 34.1, 34.1, 34.0, 34.0, 29.3, 25.4, 25.4, 25.3, 24.5, 24.5, 24.5, 24.5. ASAP(+)-TOF-HRMS m/z for $C_{27}H_{40}O_9$ $[M+H]^+$: theoretical 509.2751, found 509.2751.

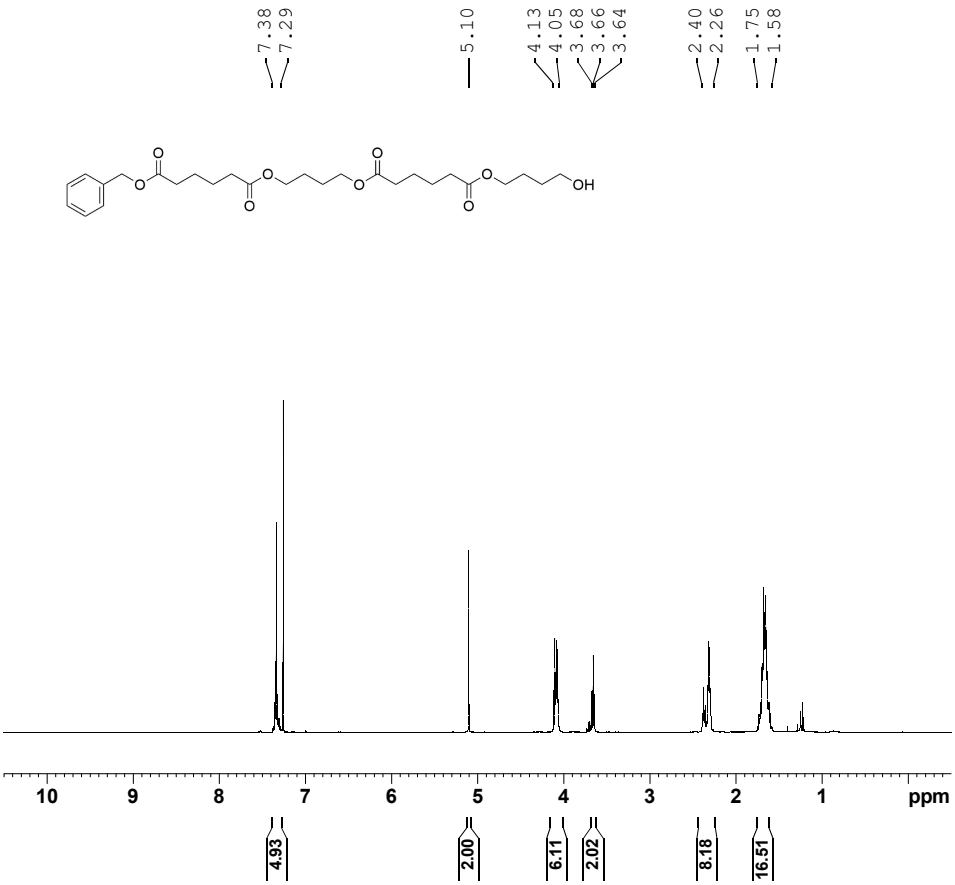

Figure A35- ^{1}H NMR (400 MHz, CDCl3) spectrum obtained for compound **10**.

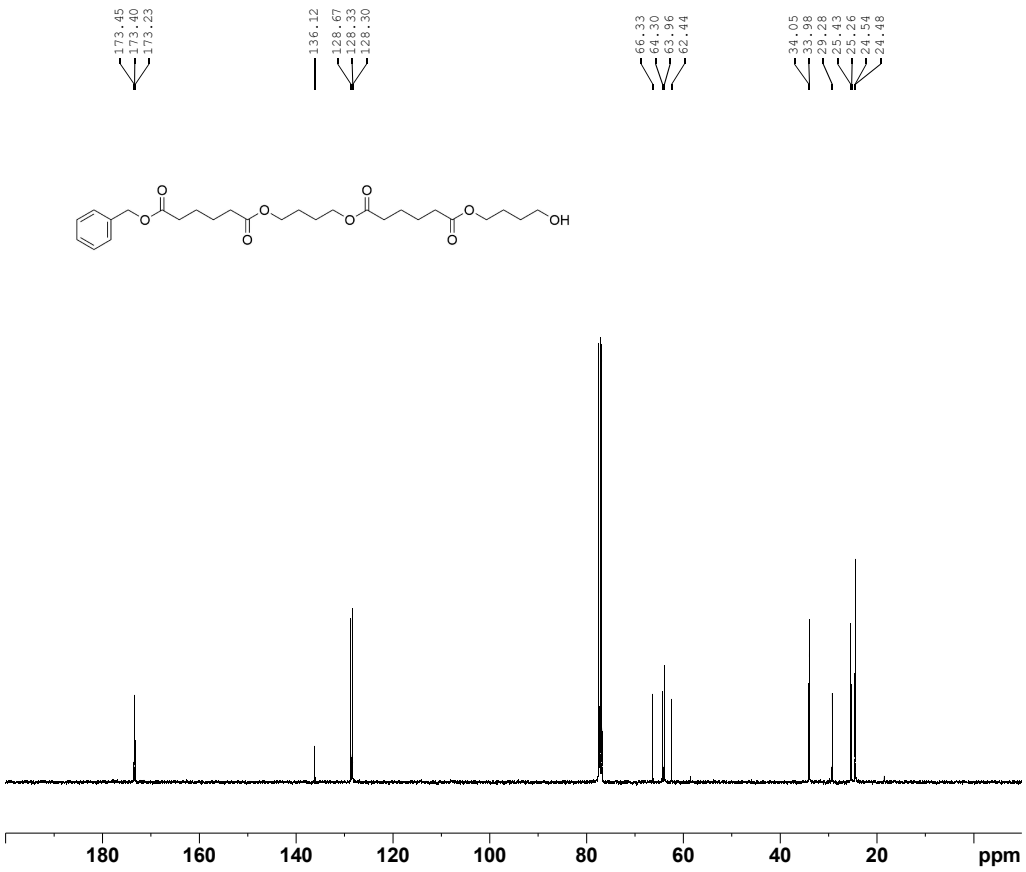

Figure A36- ^{13}C NMR (100 MHz, $CDCl_3$) spectrum obtained for compound **10**.

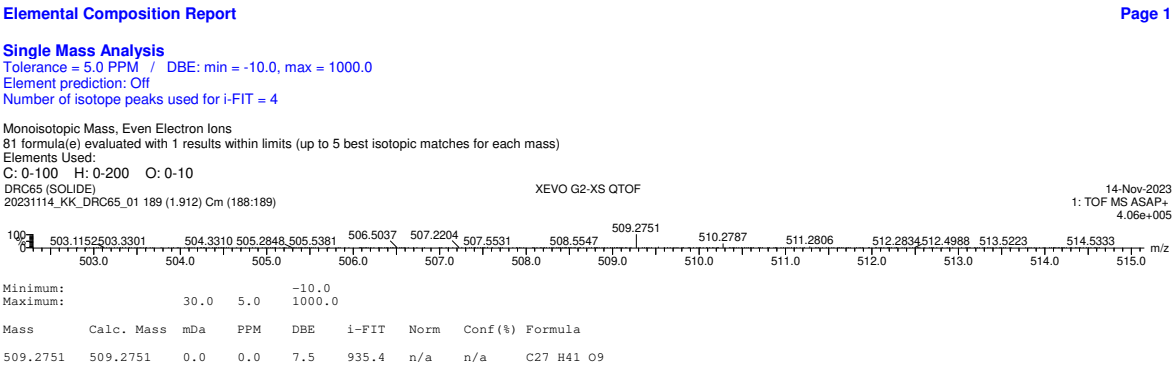

Figure A37- ASAP(+)-TOF-HRMS elemental composition report obtained for compound **10**.

benzyl (2,2,3,3-tetramethyl-10,15,22,27-tetraoxo-4,9,16,21,28-pentaoxa-3-siladotriacontan-32-yl) adipate (11) - Following **Method C,** the crude was then purified by flash chromatography (cyclohexane/ethyl acetate 90/10 to 50/50, v/v) to afford **11** with 84% yield as a colourless oil. ^{1}H NMR ($CDCl_3$, 400 MHz): 7.31-7.38 (m, 5H), 5.11 (s, 2H), 4.05-4.11 (m, 10H), 3.63 (t, 2H, ^{3}J = 6.27 Hz), 2.25-2.42 (m, 12H), 1.59-1.75 (m, 24H), 0.89 (s, 9H), 0.04 (s, 6H). ^{13}C NMR ($CDCl_3$, 100 MHz): 173.5, 173.5, 173.4, 173.4, 173.2, 173.2, 136.2, 128.7, 128.7, 128.3, 128.3, 128.3, 66.4, 64.5, 64.0, 64.0, 64.0, 64.0, 62.7, 34.0, 34.0, 34.0, 34.0, 34.0, 34.0, 26.1, 26.1, 26.1, 25.5, 25.5, 25.5, 25.5, 25.5, 25.5, 25.4, 24.5, 25.4, 24.5, 24.5, 24.5, 18.5, -5.2, -5.2. ASAP(+)-TOF-HRMS m/z for $C_{43}H_{70}O_{13}Si$ $[M+H]^+$: theoretical 823.4664, found 823.4633.

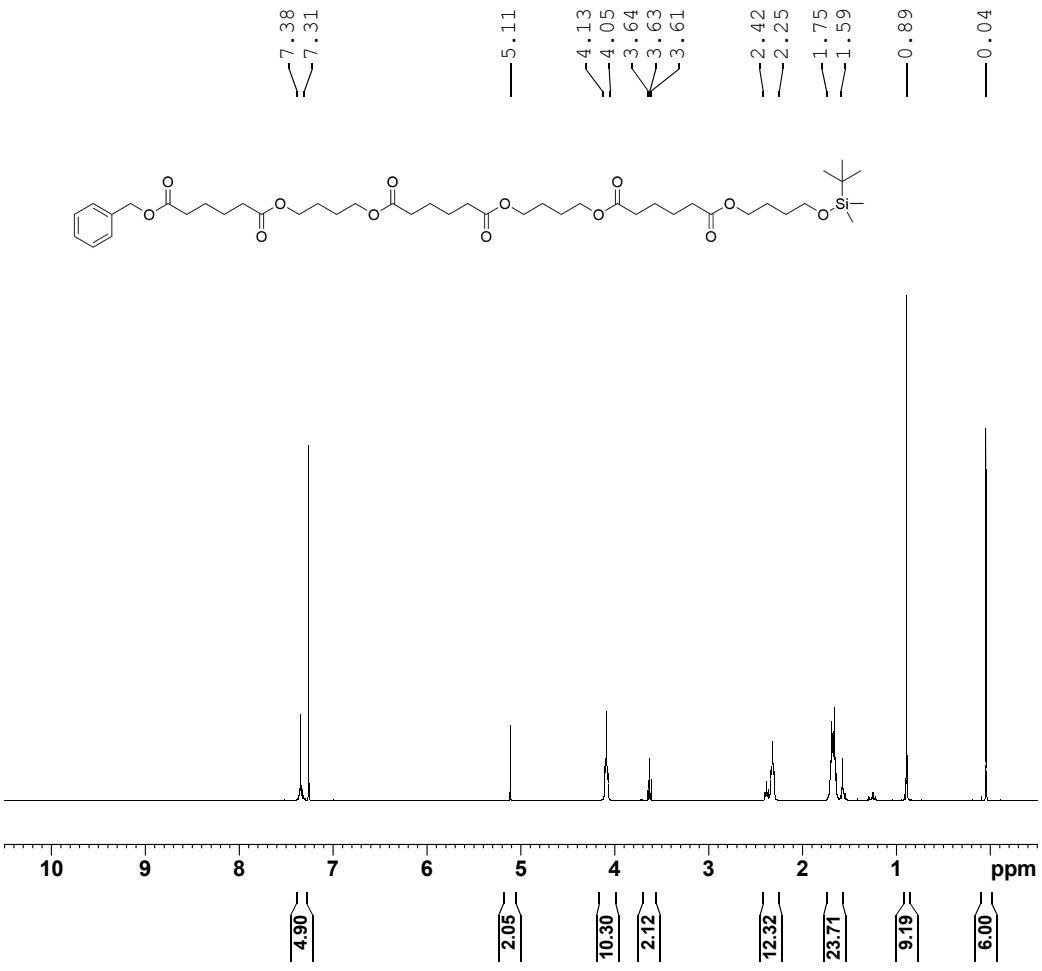

Figure A38- ^{1}H NMR (400 MHz, CDCl3) spectrum obtained for compound **11**.

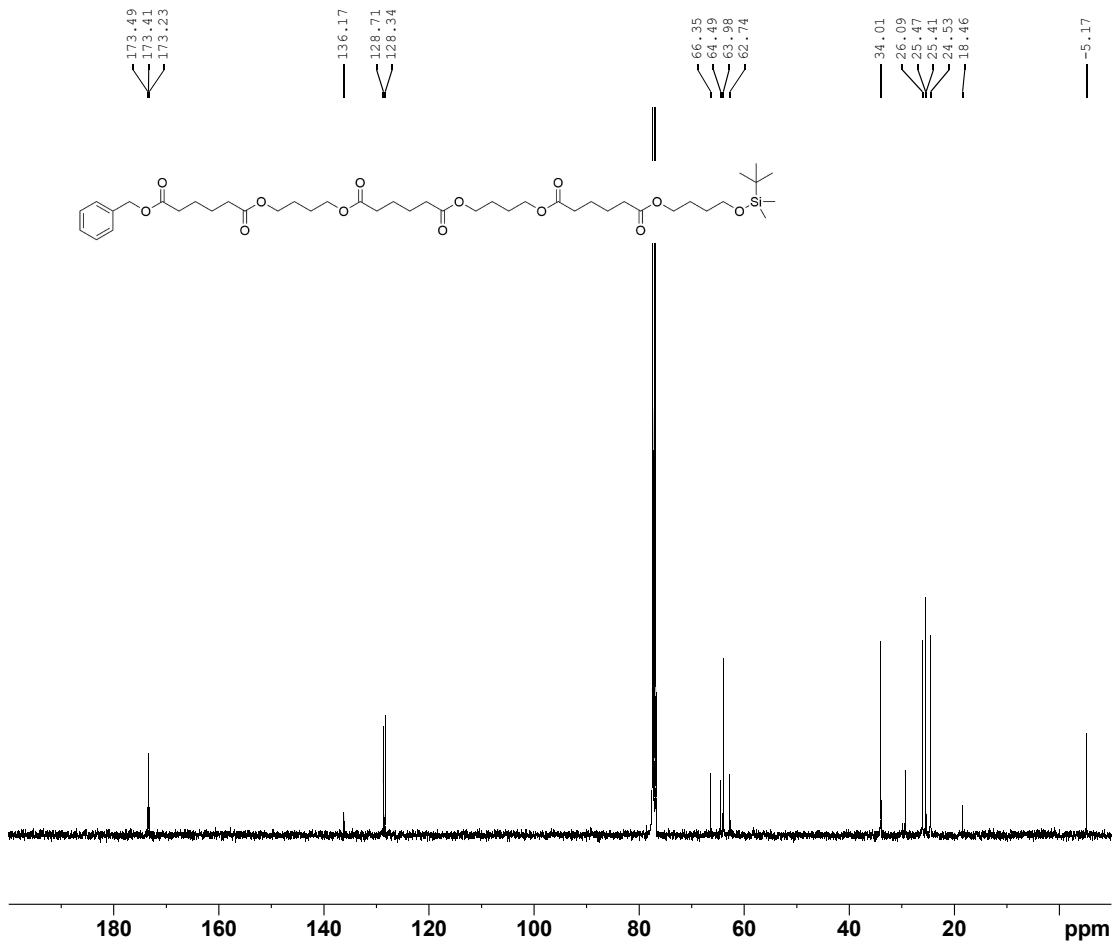

Figure A39- ^{13}C NMR (100 MHz, $CDCl_3$) spectrum obtained for compound **11**.

Elemental Composition Report **Page 1**

Single Mass Analysis
Tolerance = 5.0 PPM / DBE: min = -10.0, max = 1000.0
Element prediction: Off
Number of isotope peaks used for i-FIT = 4

Monoisotopic Mass, Even Electron Ions
341 formula(e) evaluated with 2 results within limits (all results (up to 1000) for each mass)
Elements Used:
C: 0-100 H: 0-200 O: 0-15 Si: 0-1

Minimum:				-10.0				
Maximum:		30.0	5.0	1000.0				
Mass	Calc. Mass	mDa	PPM	DBE	i-FIT	Norm	Conf(%)	Formula
823.4655	823.4664	-0.9	-1.1	9.5	818.9	0.082	92.12	C43 H71 O13 Si
	823.4633	2.2	2.7	14.5	821.4	2.541	7.88	C47 H67 O12

Figure A40- ASAP(+)-TOF-HRMS elemental composition report obtained for compound **11**.

benzyl (28-hydroxy-6,11,18,23-tetraoxo-5,12,17,24-tetraoxaoctacosyl) adipate (12) - Following **Method D,** the crude was then purified by flash chromatography (cyclohexane/ethyl acetate 50/50 to 0/100, v/v) to afford **12** with 87% yield as a white solid. ^{1}H NMR ($CDCl_3$, 400 MHz): 7.29-7.39 (m, 5H), 5.11 (s, 2H), 4.04-4.15 (m, 10H), 3.67 (t, 2H, ^{3}J= 6.38 Hz), 2.28-2.41 (m, 12H), 1.57-1.76 (m, 25H). ^{13}C NMR ($CDCl_3$, 100 MHz): 173.5, 173.5, 173.4, 173.4, 173.4, 173.3, 136.2, 128.7, 128.7, 128.4, 128.3, 128.3, 66.4, 64.3, 64.0, 64.0, 64.0, 64.0, 62.5, 34.1, 34.0, 34.0, 34.0, 34.0, 29.3, 25.5, 25.5, 25.5, 25.5, 25.5, 25.3, 24.6, 24.5, 24.5, 24.5, 24.5, 24.5. ASAP(+)-TOF-HRMS m/z for $C_{37}H_{56}O_{13}$ $[M+H]^+$: theoretical 709.3799, found 709.3790. Melting point: 35 ºC.

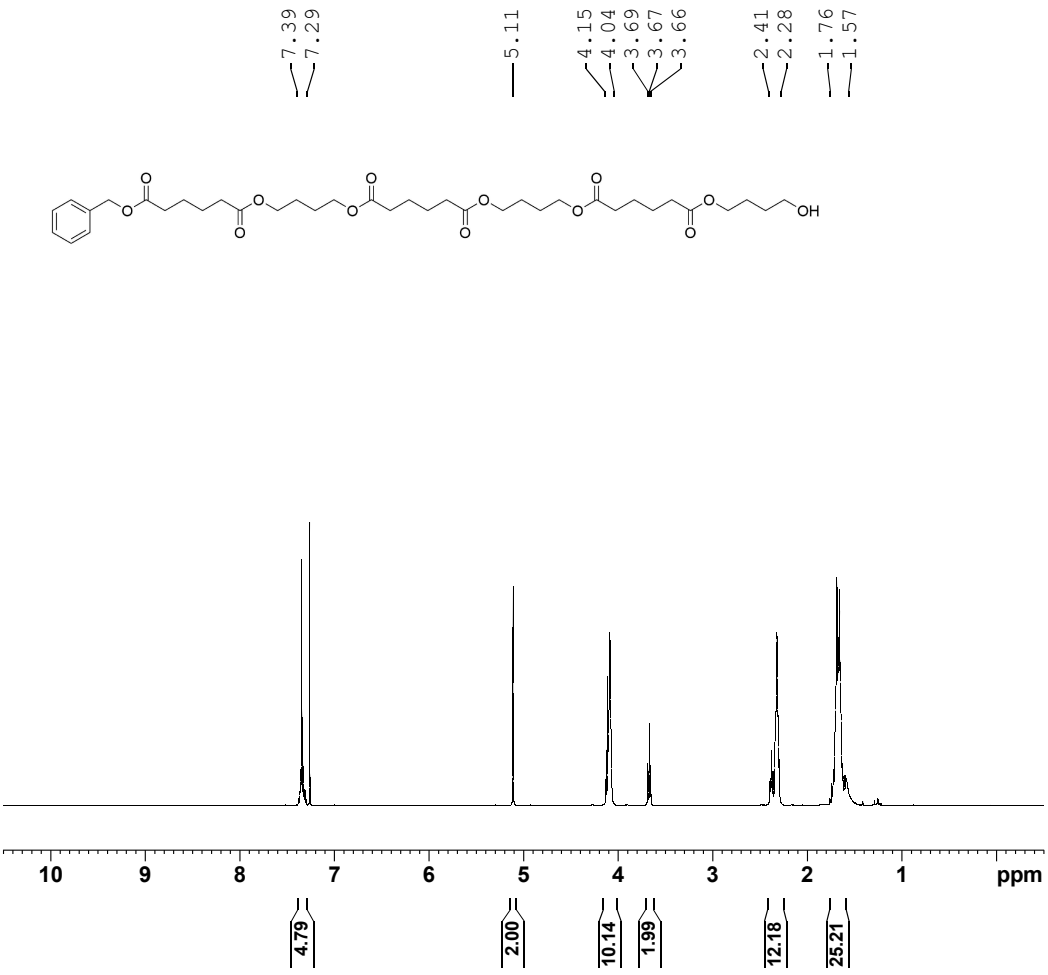

Figure A41- ^{1}H NMR (400 MHz, CDCl3) spectrum obtained for compound **12**.

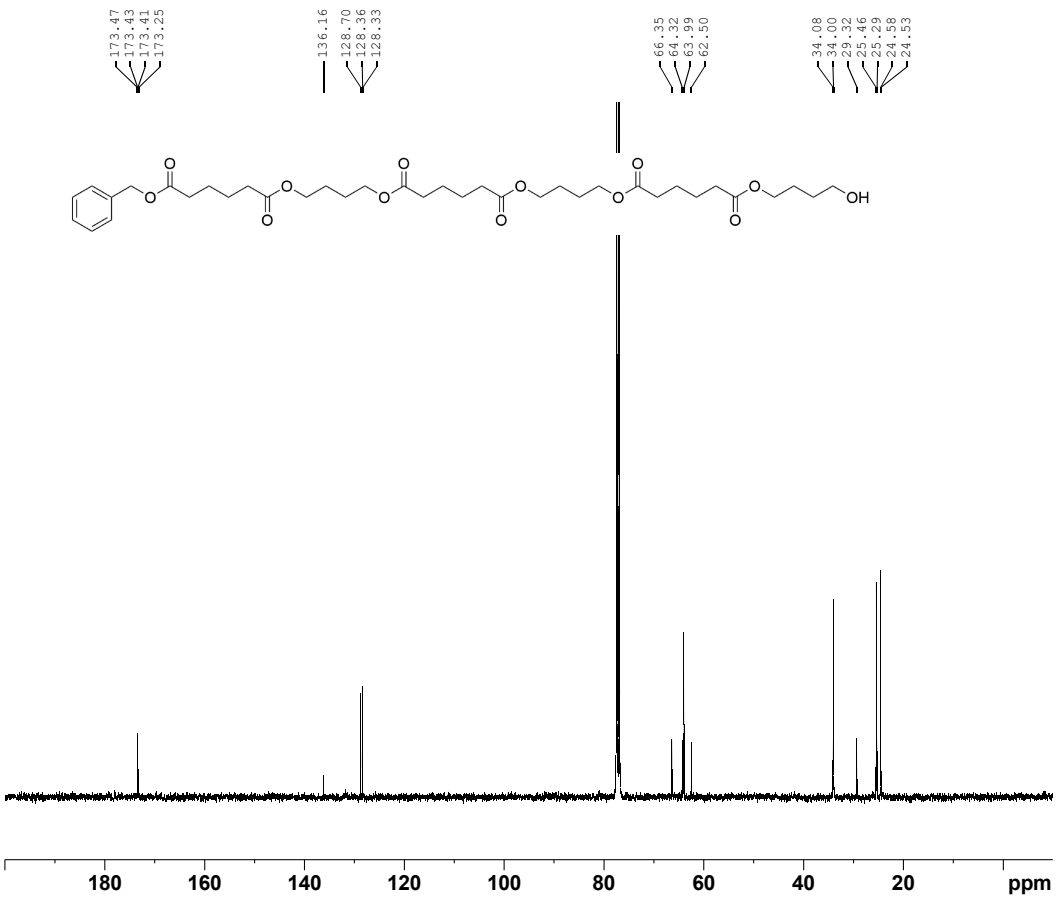

Figure A42- ^{13}C NMR (100 MHz, $CDCl_3$) spectrum obtained for compound **12**.

Elemental Composition Report **Page 1**

Single Mass Analysis
Tolerance = 5.0 PPM / DBE: min = -10.0, max = 1000.0
Element prediction: Off
Number of isotope peaks used for i-FIT = 4

Monoisotopic Mass, Even Electron Ions
148 formula(e) evaluated with 1 results within limits (all results (up to 1000) for each mass)
Elements Used:
C: 0-100 H: 0-200 O: 0-15

Minimum:				-10.0				
Maximum:		30.0	5.0	1000.0				
Mass	Calc. Mass	mDa	PPM	DBE	i-FIT	Norm	Conf(%)	Formula
709.3790	709.3799	-0.9	-1.3	9.5	684.4	n/a	n/a	C37 H57 O13

Figure A43- ASAP(+)-TOF-HRMS elemental composition report obtained for compound **12**.

1-hydroxy-6,11,18,23,30-pentaoxo-5,12,17,24,29-pentaoxapentatriacontan-35-oic acid (lin[3BD+3AA]) - Following **Method E, lin[3BD+3AA]** was obtained with 52% yield as a white solid. ^{1}H NMR ($CDCl_3$, 400 MHz): 4.06-4.15 (m, 10H), 3.68 (t, 2H, ^{3}J = 6.42 Hz), 2.29-2.41 (m, 12H), 1.60-1.76 (m, 24H). ^{13}C NMR ($CDCl_3$, 100 MHz): 173.6, 173.6, 173.6, 173.5, 173.4, 173.4, 64.4, 64.1, 64.1, 64.1, 64.1, 62.5, 34.1, 34.0, 34.0, 34.0, 34.0, 34.0, 29.3, 25.5, 25.5, 25.5, 25.5, 25.3, 24.6, 24.5, 24.5, 24.5, 24.5, 24.4. ASAP(+)-TOF-HRMS m/z for $C_{30}H_{50}O_{13}$ $[M-H]^-$: theoretical 617.3173, found 617.3170. Melting point: 50 ºC.

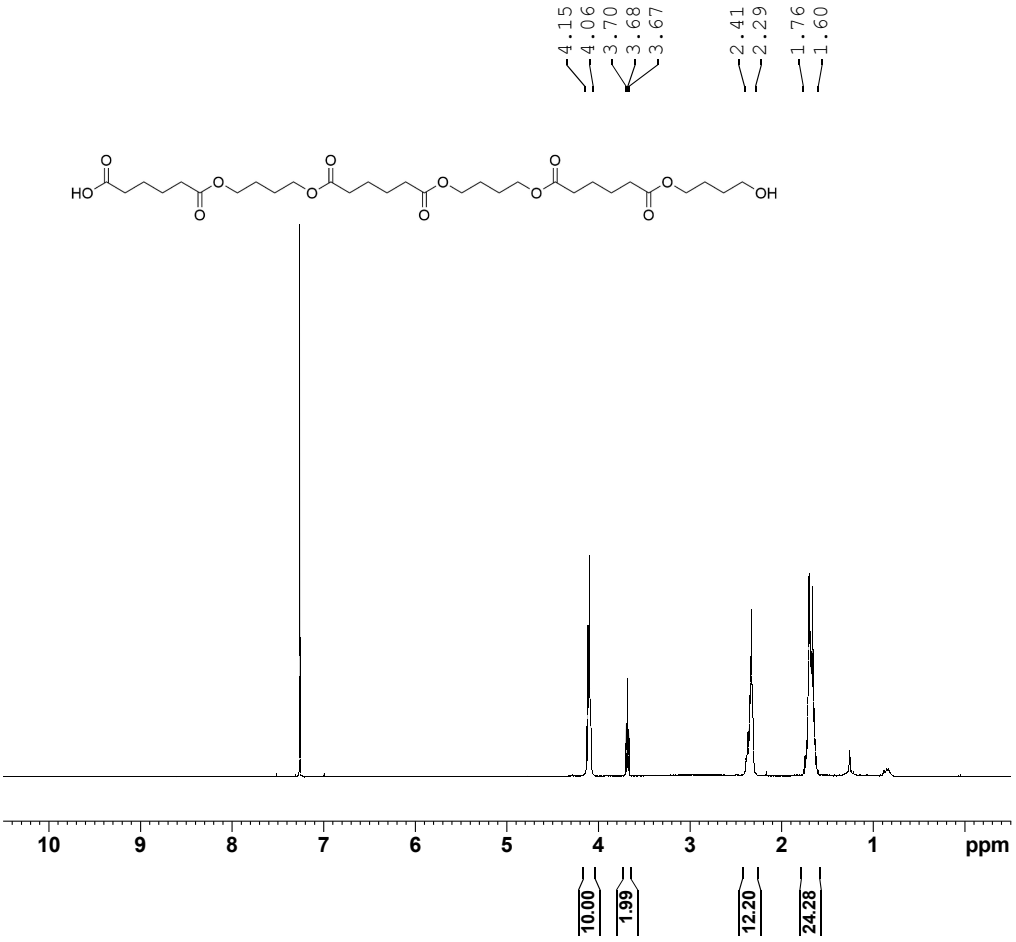

Figure A44- ^{1}H NMR (400 MHz, CDCl3) spectrum obtained for compound **lin[3BD+3AA]**.

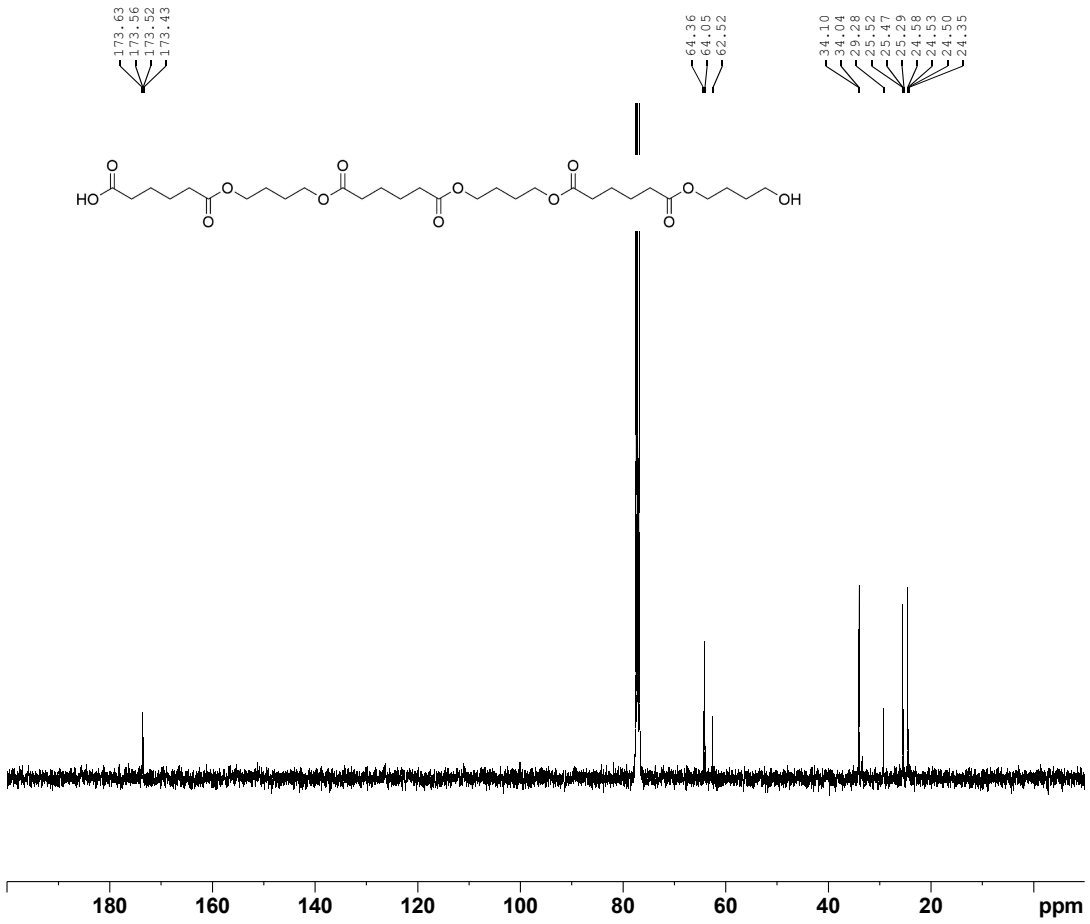

Figure A45- ^{13}C NMR (100 MHz, $CDCl_3$) spectrum obtained for compound **lin[3BD+3AA]**.

Elemental Composition Report **Page 1**

Single Mass Analysis
Tolerance = 5.0 PPM / DBE: min = -10.0, max = 1000.0
Element prediction: Off
Number of isotope peaks used for i-FIT = 4

Monoisotopic Mass, Odd and Even Electron Ions
131 formula(e) evaluated with 1 results within limits (all results (up to 1000) for each mass)
Elements Used:
C: 0-100 H: 0-200 O: 0-15

Minimum:				-10.0				
Maximum:		30.0	5.0	1000.0				
Mass	Calc. Mass	mDa	PPM	DBE	i-FIT	Norm	Conf(%)	Formula
617.3170	617.3173	-0.3	-0.5	6.5	669.9	n/a	n/a	C30 H49 O13

Figure A46- ASAP(-)-TOF-HRMS elemental composition report obtained for compound **lin[3BD+3AA]**.

1,6,13,18,25,30-hexaoxacyclohexatriacontane-7,12,19,24,31,36-hexaone (c[3BD+3AA]) - Following **Method F,** the crude was then purified by flash chromatography (cyclohexane/ethyl acetate 90/10 to 30/70, v/v) to afford **c[3BD+3AA]** with 92% yield as a yellowish oil. ^{1}H NMR ($CDCl_3$, 400 MHz): 4.04-4.17 (m, 12H), 2.26-2.38 (m, 12H), 1.60-1.75 (m, 24H). ^{13}C NMR ($CDCl_3$, 100 MHz): 173.3, 173.3, 173.3, 173.3, 173.3, 173.3, 64.0, 64.0, 64.0, 64.0, 64.0, 64.0, 34.0, 34.0, 34.0, 34.0, 34.0, 34.0, 25.5, 25.5, 25.5, 25.5, 25.5, 25.5, 24.5, 24.5, 24.5, 24.5, 24.5, 24.5. ASAP(+)-TOF-HRMS m/z for $C_{30}H_{48}O_{12}$ $[M+H]^+$: theoretical 601.3224, found 601.3226.

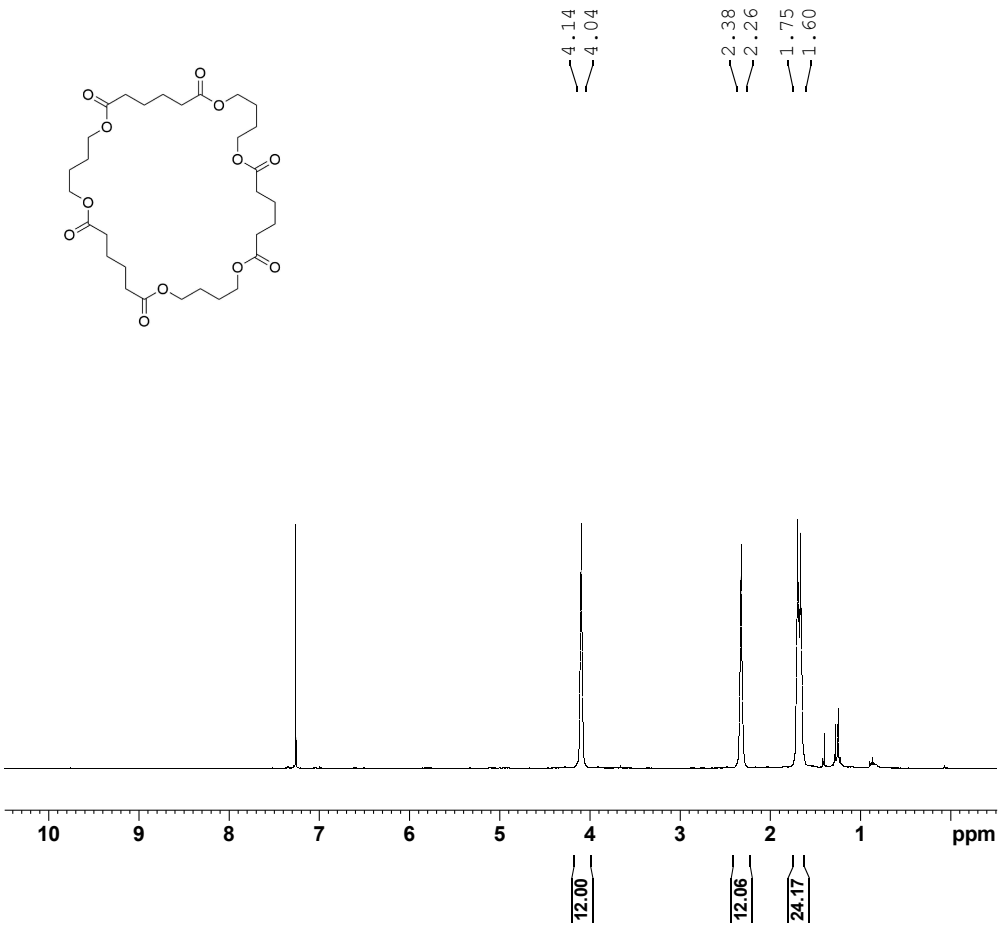

Figure A47- ^{1}H NMR (400 MHz, CDCl3) spectrum obtained for compound **c[3BD+3AA]**.

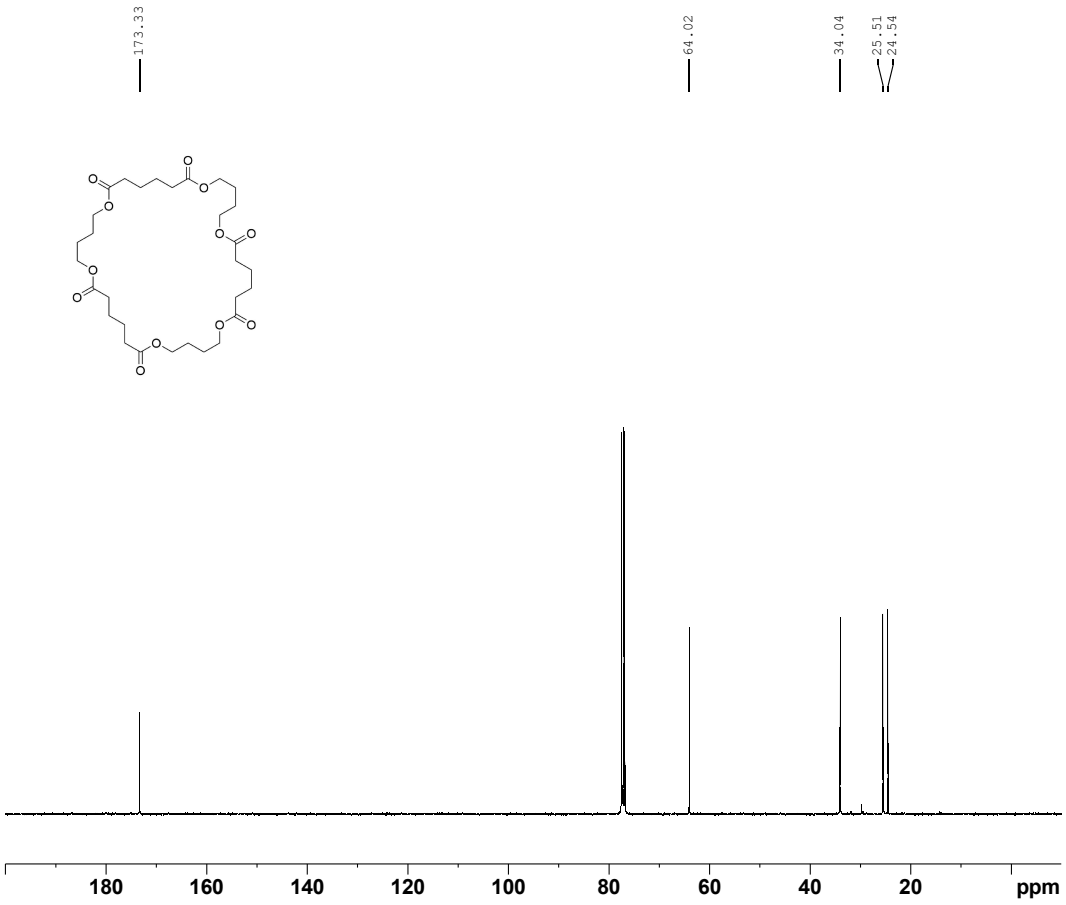

Figure A48- ^{13}C NMR (100 MHz, $CDCl_3$) spectrum obtained for compound **c[3BD+3AA]**.

Elemental Composition Report **Page 1**

Single Mass Analysis
Tolerance = 5.0 PPM / DBE: min = -10.0, max = 1000.0
Element prediction: Off
Number of isotope peaks used for i-FIT = 4

Monoisotopic Mass, Even Electron Ions
44 formula(e) evaluated with 1 results within limits (up to 5 best isotopic matches for each mass)
Elements Used:
C: 0-100 H: 0-200 O: 8-13

DRC80 (SOLIDE) XEVO G2-XS QTOF 23-Nov-2023
20231123_KK_DRC80_02 95 (0.969) Cm (93:103) 1: TOF MS ASAP+
3.78e+007

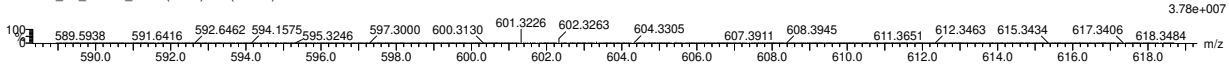

Minimum:				-10.0				
Maximum:		30.0	5.0	1000.0				
Mass	Calc. Mass	mDa	PPM	DBE	i-FIT	Norm	Conf(%)	Formula
601.3226	601.3224	0.2	0.3	6.5	2366.6	n/a	n/a	C30 H49 O12

Figure A49- ASAP(+)-TOF-HRMS elemental composition report obtained for compound **c[3BD+3AA]**.

6-(4-((6-(4-hydroxybutoxy)-6-oxohexanoyl)oxy)butoxy)-6-oxohexanoic acid (lin[2BD+2AA]) - Following **Method E,** the crude was then purified by flash chromatography (cyclohexane/ethyl acetate70/30 to 30/70, v/v) to afford **lin[2BD+2AA]** with 61% yield as a yellowish oil. ^{1}H NMR ($CDCl_3$, 400 MHz): 4.05-4.14 (m, 6H), 3.68 (t, 2H, ^{3}J = 6.30 Hz), 2.26-2.41 (m, 8H), 1.56-1.76 (m, 16H). ^{13}C NMR ($CDCl_3$, 100 MHz): 177.7, 173.6, 173.6, 173.5, 64.4, 64.0, 64.0, 62.5, 34.1, 34.0, 34.0, 33.6, 29.2, 25.5, 25.5, 25.3, 24.6, 24.5, 24.5, 24.3. ASAP(-)-TOF-HRMS m/z for $C_{20}H_{34}O_9$ $[M-H]^-$: theoretical 417.2125, found 417.2139.

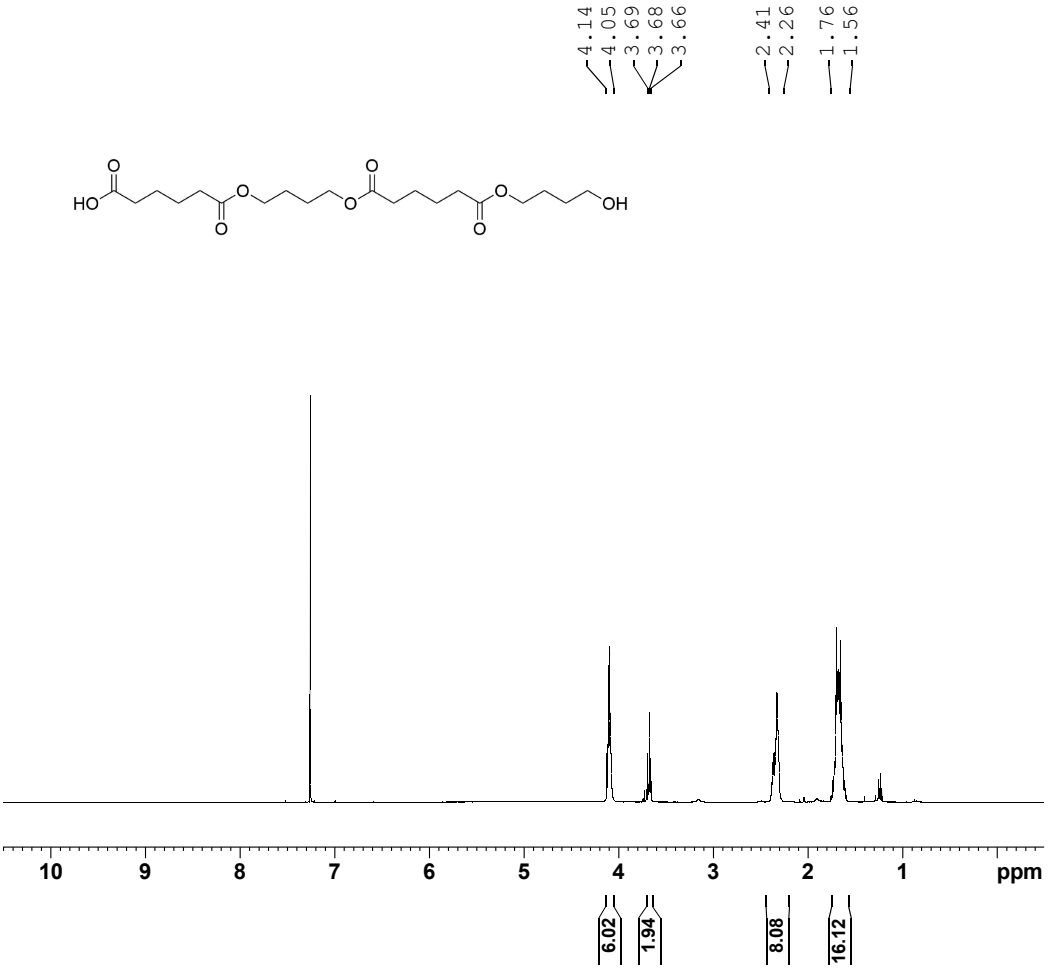

Figure A50- ^{1}H NMR (400 MHz, CDCl3) spectrum obtained for compound **lin[2BD+2AA]**.

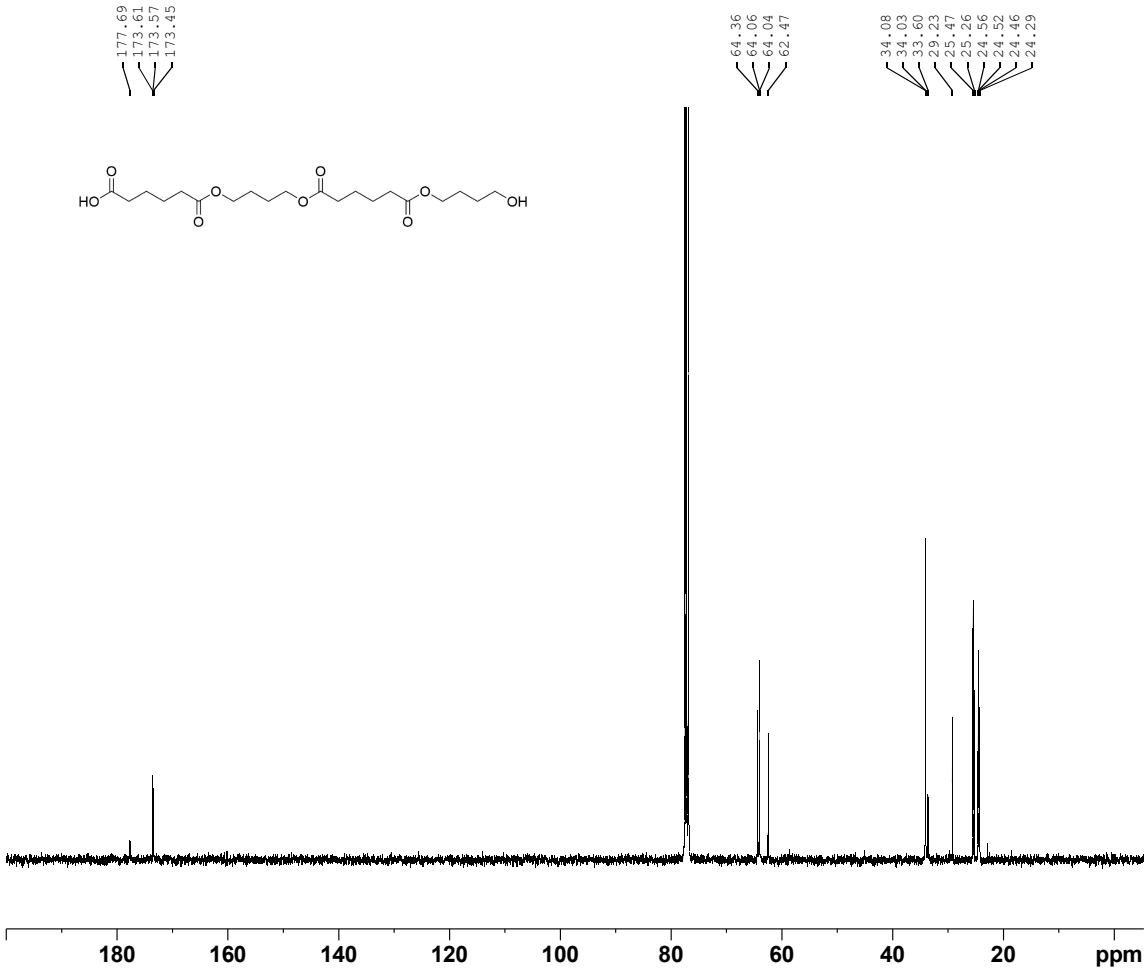

Figure A51- ^{13}C NMR (100 MHz, $CDCl_3$) spectrum obtained for compound **lin[2BD+2AA]**.

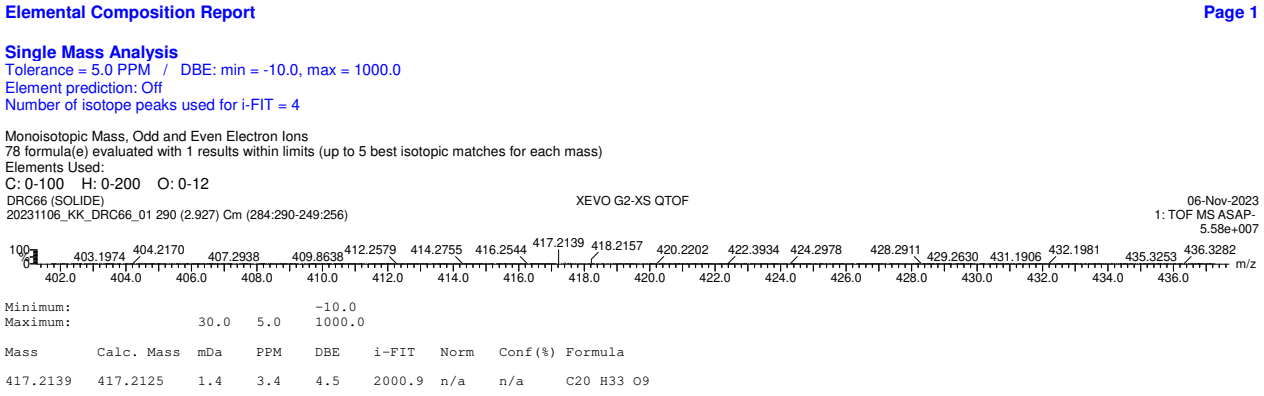

Elemental Composition Report Page 1

Single Mass Analysis
Tolerance = 5.0 PPM / DBE: min = -10.0, max = 1000.0
Element prediction: Off
Number of isotope peaks used for i-FIT = 4

Monoisotopic Mass, Odd and Even Electron Ions
78 formula(e) evaluated with 1 results within limits (up to 5 best isotopic matches for each mass)
Elements Used:
C: 0-100 H: 0-200 O: 0-12

DRC66 (SOLIDE) XEVO G2-XS QTOF 06-Nov-2023
20231106_KK_DRC66_01 290 (2.927) Cm (284:290-249:256) 1: TOF MS ASAP- 5.58e+007

Minimum:				-10.0				
Maximum:		30.0	5.0	1000.0				
Mass	Calc. Mass	mDa	PPM	DBE	i-FIT	Norm	Conf(%)	Formula
417.2139	417.2125	1.4	3.4	4.5	2000.9	n/a	n/a	C20 H33 O9

Figure A52- ASAP(-)-TOF-HRMS elemental composition report obtained for compound **lin[2BD+2AA]**.

1,6,13,18-tetraoxacyclotetracosane-7,12,19,24-tetraone (c[2BD+2AA]) - Following **Method F,** the crude was then purified by flash chromatography (cyclohexane/ethyl acetate 90/10 to 30/70, v/v) to afford **c[2BD+2AA]** with 71% yield as a yellowish solid. ^{1}H NMR ($CDCl_3$, 400 MHz): 4.08-4.14 (m, 8H), 2.29-2.37 (m, 8H), 1.62-1.76 (m, 16H). ^{13}C NMR ($CDCl_3$, 100 MHz): 173.3, 173.3, 173.3, 173.3, 64.1, 64.1, 64.1, 64.1, 34.1, 34.1, 34.1, 34.1, 25.6, 25.6, 25.6, 25.6, 24.5, 24.5, 24.5, 24.5. ASAP(+)-TOF-HRMS m/z for $C_{20}H_{32}O_8$ $[M+H]^+$: theoretical 401.2175, found 401.2195. Melting point: 60 ºC.

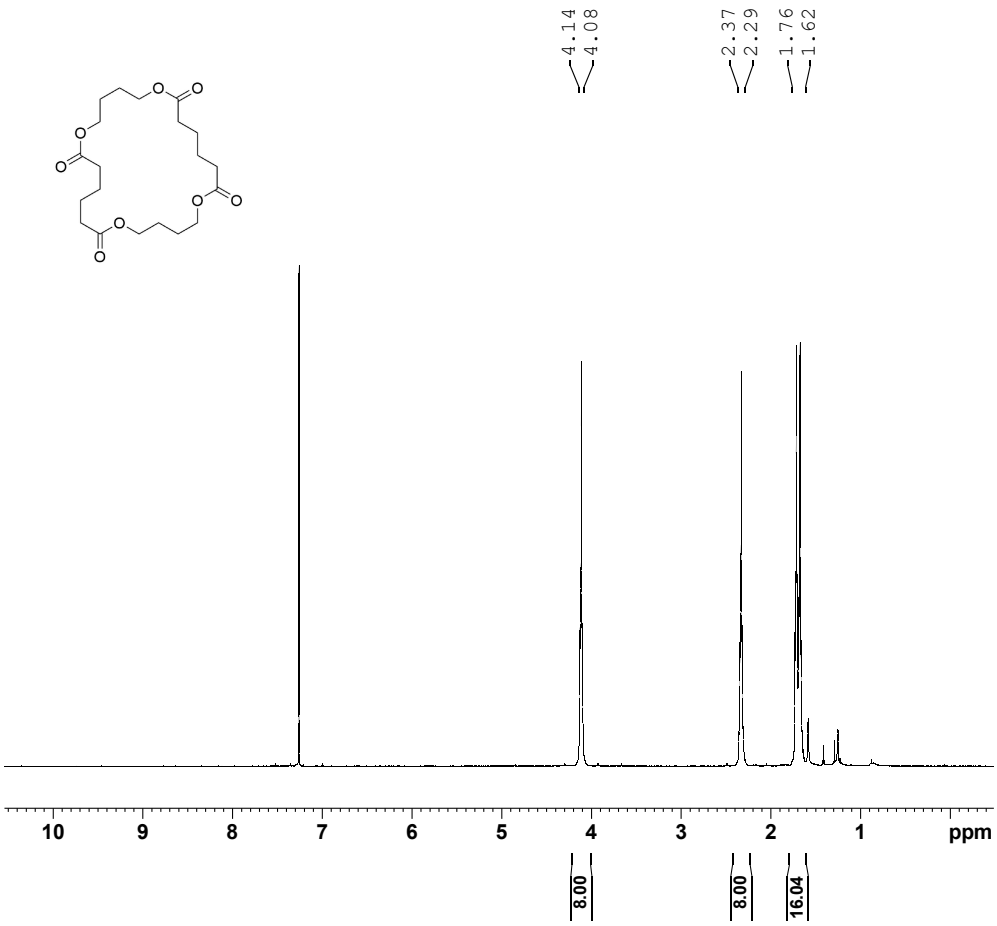

Figure A53- ^{1}H NMR (400 MHz, CDCl3) spectrum obtained for compound **c[2BD+2AA]**.

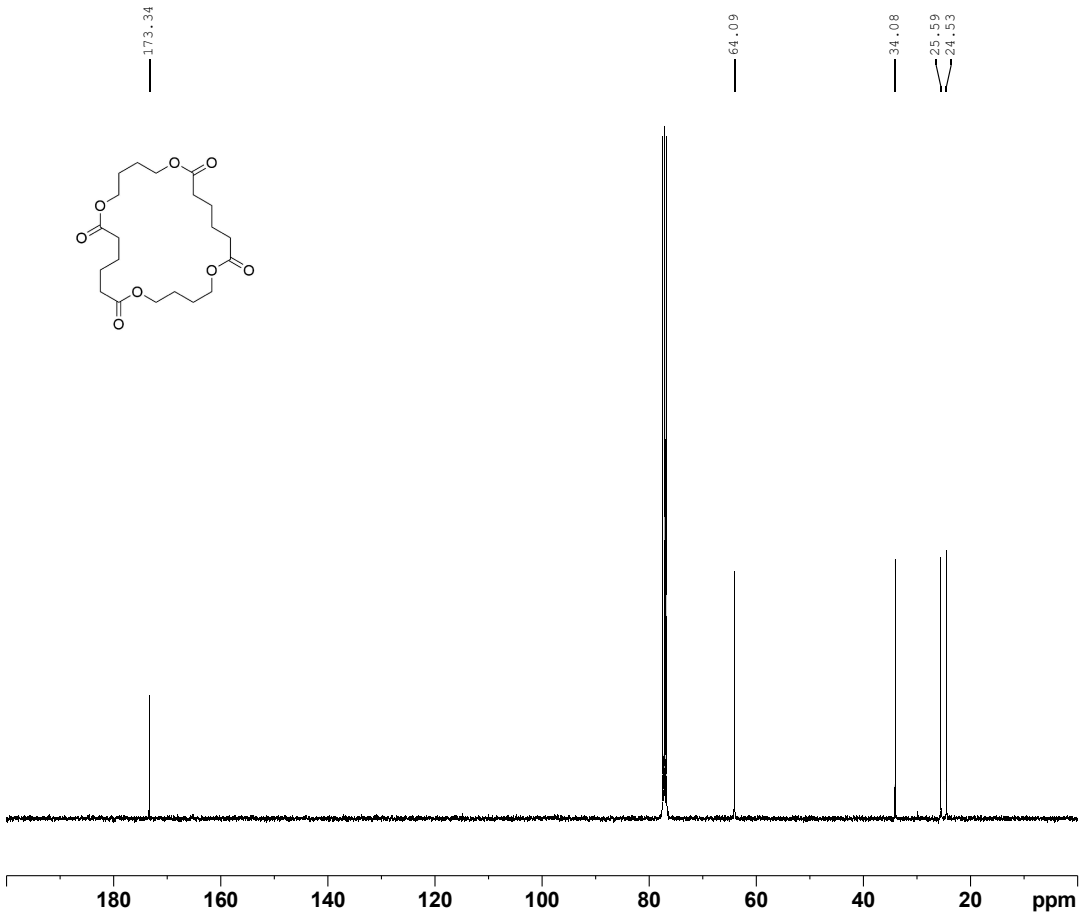

Figure A54- ^{13}C NMR (100 MHz, $CDCl_3$) spectrum obtained for compound **c[2BD+2AA]**.

Elemental Composition Report **Page 1**

Single Mass Analysis
Tolerance = 5.0 PPM / DBE: min = -10.0, max = 1000.0
Element prediction: Off
Number of isotope peaks used for i-FIT = 4

Monoisotopic Mass, Even Electron Ions
66 formula(e) evaluated with 1 results within limits (up to 5 best isotopic matches for each mass)
Elements Used:
C: 0-100 H: 0-200 O: 0-10

DRC75 (SOLIDE)
20231113_KK_DRC75_01 141 (1.432) Cm (141:142)

XEVO G2-XS QTOF

13-Nov-2023
1: TOF MS ASAP+
2.88e+007

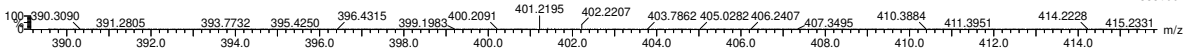

Minimum:				-10.0				
Maximum:		30.0	5.0	1000.0				
Mass	Calc. Mass	mDa	PPM	DBE	i-FIT	Norm	Conf(%)	Formula
401.2195	401.2175	2.0	5.0	4.5	1852.8	n/a	n/a	C20 H33 O8

Figure A55- ASAP(+)-TOF-HRMS elemental composition report obtained for compound **c[2BD+2AA]**.

Adipic acid, Isophthalic acid & 1,4-Butanediol series

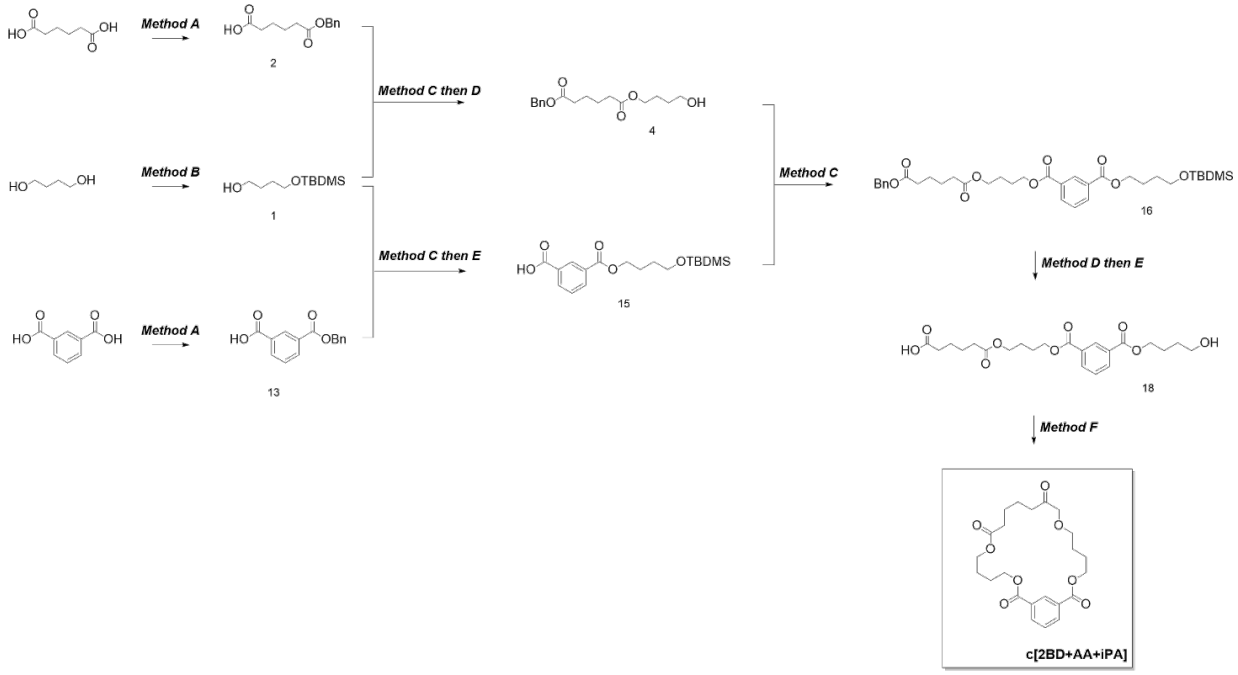

Figure A56 – Synthesis of cyclic oligomer derived from Adipic acid (AA) , isophthalic acid (PA) & 1,4-Butanediol (BD).

3-((benzyloxy)carbonyl)benzoic acid (13) - Following **Method A,** the crude was then purified by flash chromatography (cyclohexane/ethyl acetate 90/10 to 70/30, v/v) to afford **13** with 38% yield as a white solid. ^{1}H NMR ($CDCl_3$, 300 MHz): 8.81 (t, 1H, ^{4}J = 1.69 Hz), 8.28-8.36 (m, 2H), 7.58 (t, 1H, ^{3}J = 7.78 Hz), 7.33-7.50 (m, 5H), 5.41 (s, 2H). ^{13}C NMR ($CDCl_3$, 75 MHz): 171.3, 165.6, 135.8, 135.0, 134.6, 131.6, 130.9, 129.9, 139.0, 128.9, 128.9, 128.6, 128.5, 128.5, 67.3. ASAP(-)-TOF-HRMS m/z for $C_{15}H_{12}O_4$ $[M-H]^-$: theoretical 255.0660, found 255.0657. Melting point: 116 ºC.

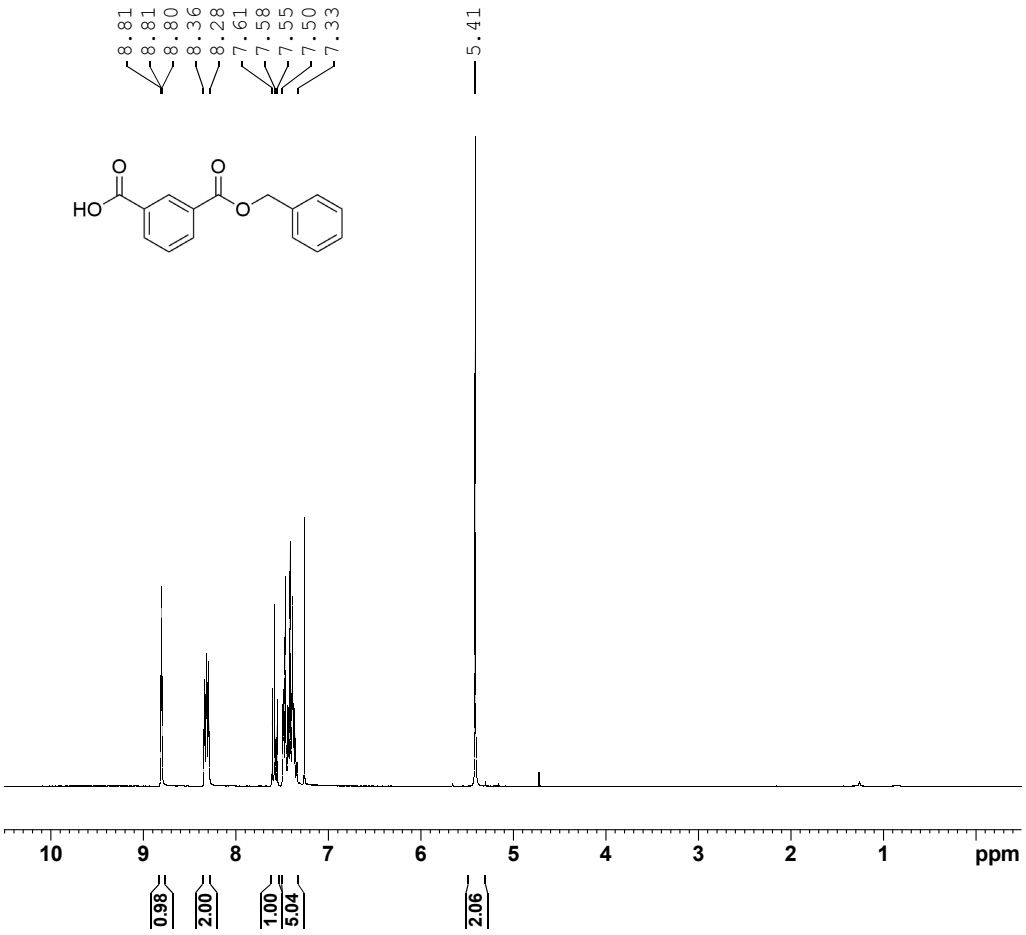

Figure A57- ^{1}H NMR (300 MHz, CDCl3) spectrum obtained for compound **13**.

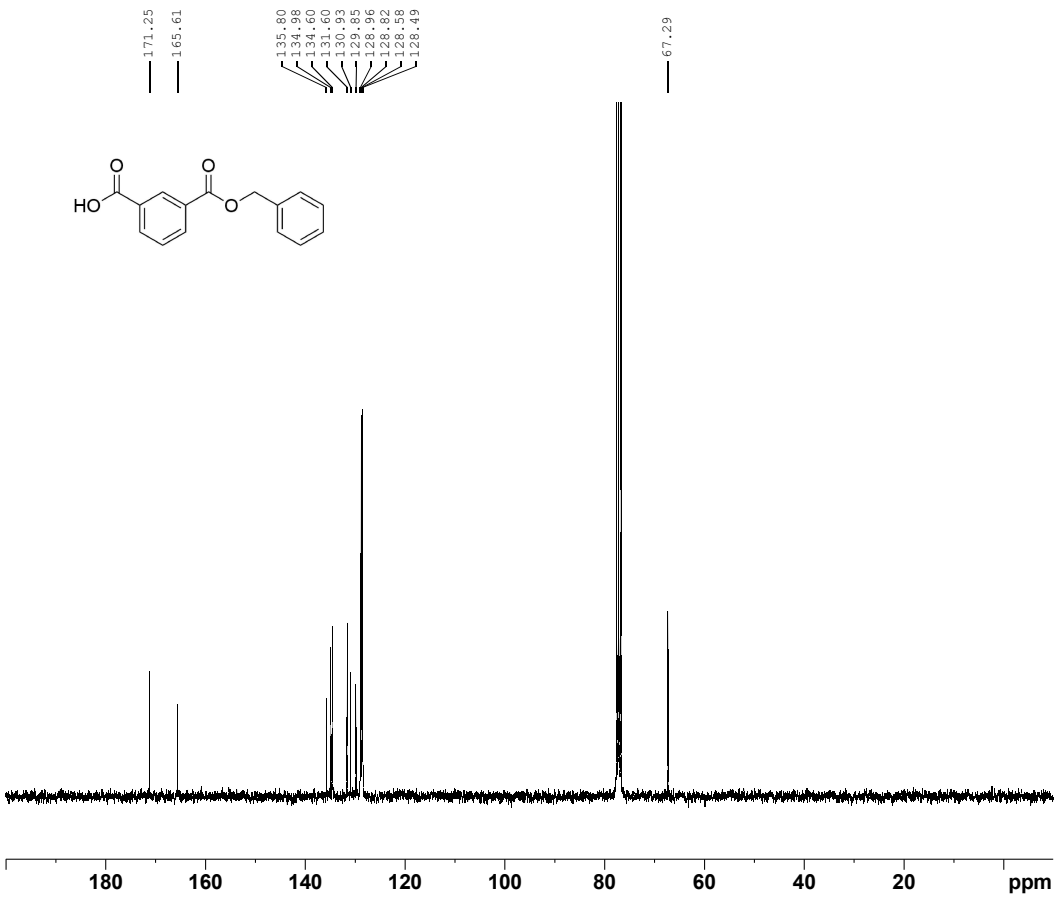

Figure A58- ^{13}C NMR (75 MHz, $CDCl_3$) spectrum obtained for compound **13**.

Elemental Composition Report **Page 1**

Single Mass Analysis
Tolerance = 5.0 PPM / DBE: min = -10.0, max = 1000.0
Element prediction: Off
Number of isotope peaks used for i-FIT = 4

Monoisotopic Mass, Even Electron Ions
56 formula(e) evaluated with 1 results within limits (all results (up to 1000) for each mass)
Elements Used:
C: 0-100 H: 0-200 O: 0-12

DRC51 (DCM) - MeOH/H2O (95/5%)
20231006_KK_DRC51_01 69 (0.711) Cm (63:71)

XEVO G2-XS QTOF

06-Oct-2023
1: TOF MS ES-
9.48e+006

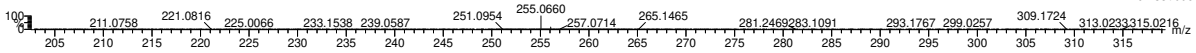

Minimum:				-10.0				
Maximum:		30.0	5.0	1000.0				
Mass	Calc. Mass	mDa	PPM	DBE	i-FIT	Norm	Conf(%)	Formula
255.0660	255.0657	0.3	1.2	10.5	2253.0	n/a	n/a	C15 H11 O4

Figure A59- ASAP(-)-TOF-HRMS elemental composition report obtained for compound **13**.

benzyl (4-((tert-butyldimethylsilyl)oxy)butyl) isophthalate (14) - Following **Method A,** the crude was then purified by flash chromatography (cyclohexane/ethyl acetate 90/10 to 80/20, v/v) to afford **14** with 97% yield as a colorless oil. ^{1}H NMR ($CDCl_3$, 400 MHz): 8.72 (td, 1H, ^{4}J = 1.73 Hz, ^{5}J = 0.53 Hz), 8.22-8.27 (m, 2H), 7.52 (td, 1H, ^{3}J = 7.78 Hz, ^{5}J = 0.53 Hz), 7.32-7.48 (m, 5H), 5.40 (s, 2H), 4.38 (t, 2H, ^{3}J = 6.61 Hz), 3.68 (t, 2H, ^{3}J = 6.24 Hz), 1.81-1.90 (m, 2H), 1.63-1.72 (m, 2H), 0.90 (s, 9H), 0.06 (s, 6H). ^{13}C NMR ($CDCl_3$, 100 MHz): 165.9, 165.8, 136.0, 134.0, 133.9, 131.1, 130.9, 130.8, 128.8, 128.8, 128.7, 128.5, 128.4, 128.4, 67.1, 65.5, 62.7, 29.4, 26.1, 26.1, 26.1, 25.5, 18.5, -5.2, -5.2. ASAP(+)-TOF-HRMS m/z for $C_{25}H_{34}O_5Si$ $[M+H]^+$: theoretical 443.2254, found 443.2249. Aspect: colourless oil.

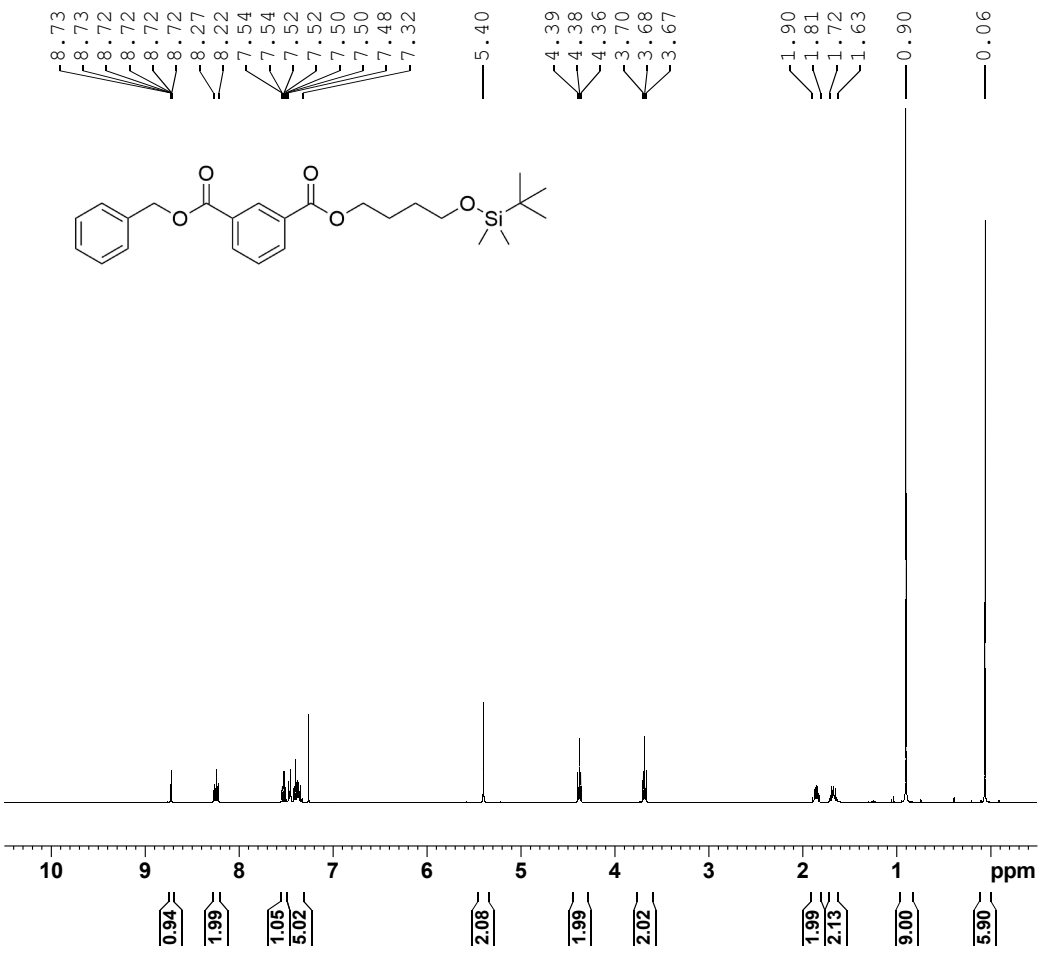

Figure A60- ^{1}H NMR (400 MHz, CDCl3) spectrum obtained for compound **14**.

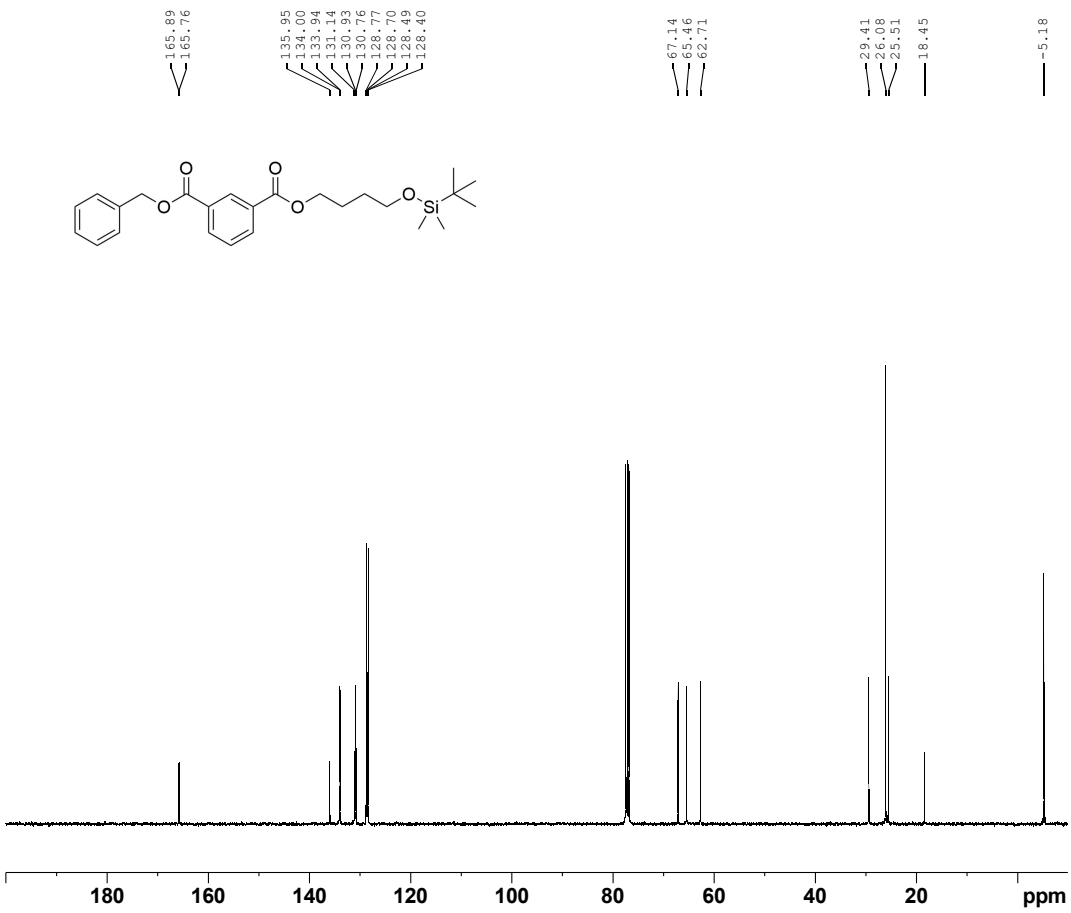

Figure A61- ^{13}C NMR (100 MHz, $CDCl_3$) spectrum obtained for compound **14**.

Elemental Composition Report **Page 1**

Single Mass Analysis
Tolerance = 5.0 PPM / DBE: min = -10.0, max = 1000.0
Element prediction: Off
Number of isotope peaks used for i-FIT = 4

Monoisotopic Mass, Even Electron Ions
71 formula(e) evaluated with 1 results within limits (up to 5 best isotopic matches for each mass)
Elements Used:
C: 0-100 H: 0-200 O: 0-10 Si: 1-1

DRC54 (SOLIDE)
20231113_KK_DRC54_01 103 (1.049) Cm (102:105)

XEVO G2-XS QTOF

13-Nov-2023
1: TOF MS ASAP+
5.83e+005

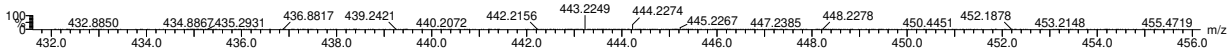

Minimum:				-10.0				
Maximum:		30.0	5.0	1000.0				
Mass	Calc. Mass	mDa	PPM	DBE	i-FIT	Norm	Conf(%)	Formula
443.2249	443.2254	-0.5	-1.1	9.5	1158.3	n/a	n/a	C25 H35 O5 Si

Figure A62- ASAP(+)-TOF-HRMS elemental composition report obtained for compound **14**.

3-((4-((tert-butyldimethylsilyl)oxy)butoxy)carbonyl)benzoic acid (15) - Following **Method E, 15** was obtained with 96% yield as a white solid. ^{1}H NMR ($CDCl_3$, 400 MHz): 8.76 (t, 1H, ^{4}J = 1.46 Hz), 8.27-8.32 (m, 2H), 7.58 (t, 1H, ^{3}J = 7.88 Hz), 4.40 (t, 2H, ^{3}J = 6.65 Hz), 3.70 (t, 2H, ^{3}J = 6.24 Hz), 1.81-1.95 (m, 2H), 1.63-1.76 (m, 2H), 0.90 (s, 9H), 0.07 (s, 6H). ^{13}C NMR ($CDCl_3$, 100 MHz): 170.7, 165.8, 134.8, 134.4, 131.5, 131.3, 129.9, 128.9, 65.6, 62.8, 29.5, 26.1, 26.1, 26.1, 25.5, 18.5, -5.2, -5.2. ASAP(+)-TOF-HRMS m/z for $C_{18}H_{28}O_5Si$ $[M+H]^+$: theoretical 535.1784, found 535.1783. Melting point: 70 ºC.

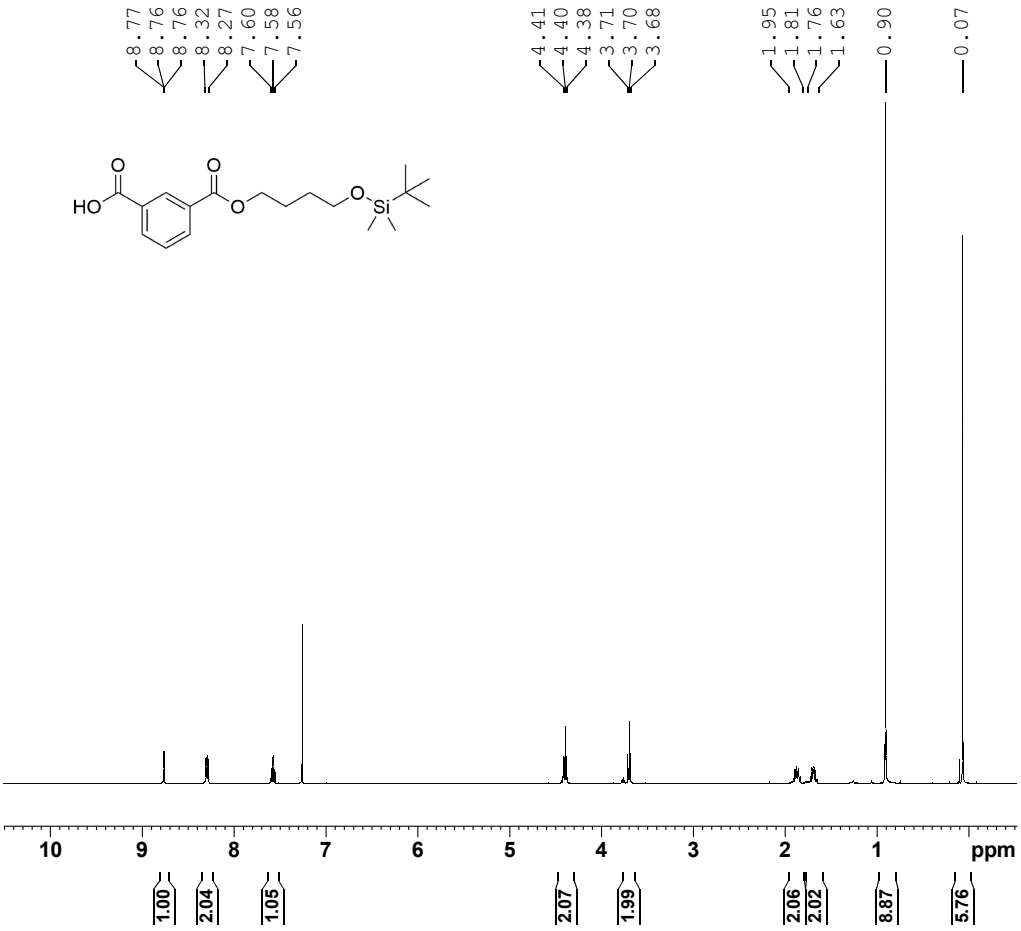

Figure A63- ^{1}H NMR (400 MHz, CDCl3) spectrum obtained for compound **15**.

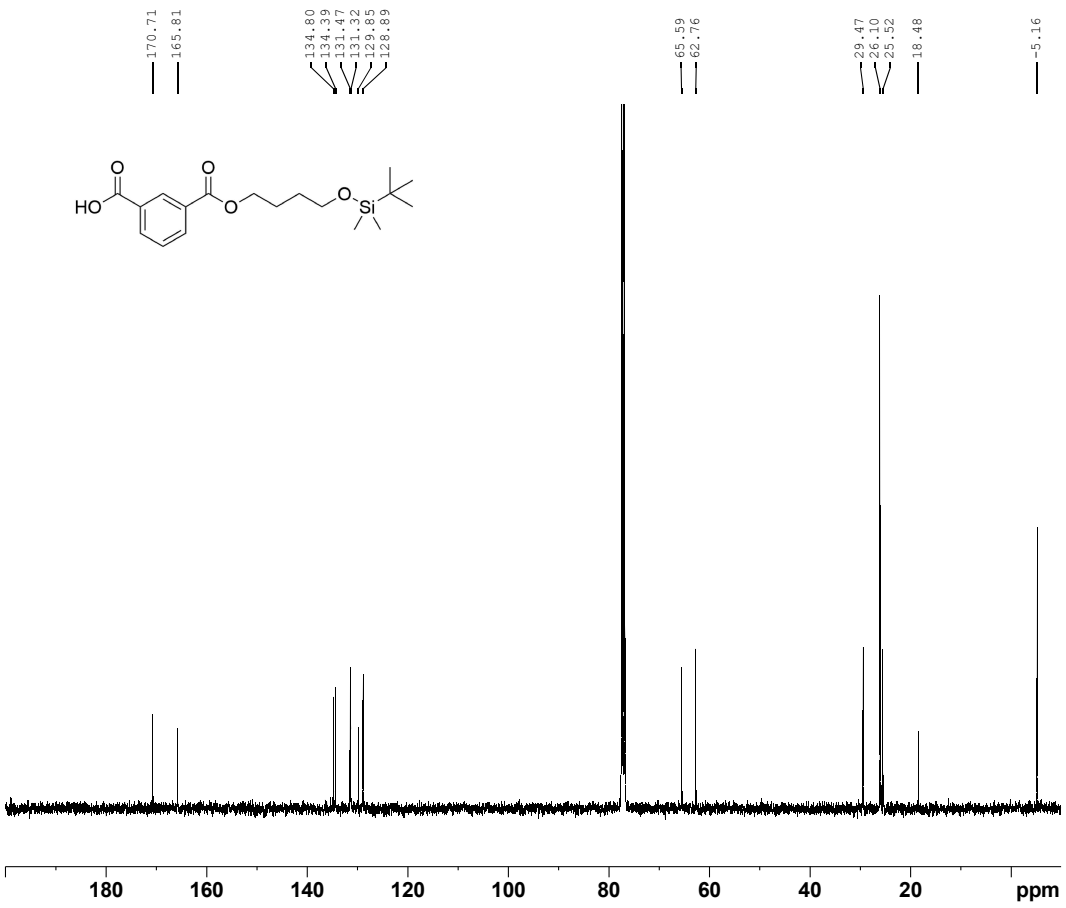

Figure A64- ^{13}C NMR (100 MHz, $CDCl_3$) spectrum obtained for compound **15**.

Elemental Composition Report **Page 1**

Single Mass Analysis
Tolerance = 50.0 PPM / DBE: min = -10.0, max = 1000.0
Element prediction: Off
Number of isotope peaks used for i-FIT = 4

Monoisotopic Mass, Even Electron Ions
59 formula(e) evaluated with 5 results within limits (up to 5 best isotopic matches for each mass)
Elements Used:
C: 0-100 H: 0-200 O: 0-10 Si: 1-1

Minimum:				-10.0				
Maximum:		30.0	50.0	1000.0				
Mass	Calc. Mass	mDa	PPM	DBE	i-FIT	Norm	Conf(%)	Formula
353.1783	353.1784	-0.1	-0.3	5.5	1275.1	0.005	99.50	C18 H29 O5 Si
	353.1632	15.1	42.8	1.5	1280.8	5.615	0.36	C14 H29 O8 Si
	353.1937	-15.4	-43.6	9.5	1282.0	6.827	0.11	C22 H29 O2 Si
	353.1726	5.7	16.1	14.5	1284.1	8.959	0.01	C25 H25 Si
	353.1843	-6.0	-17.0	-3.5	1284.3	9.115	0.01	C11 H33 O10 Si

Figure A65- ASAP(+)-TOF-HRMS elemental composition report obtained for compound **15**.

4-((6-(benzyloxy)-6-oxohexanoyl)oxy)butyl (4-((tert-butyldimethylsilyl)oxy)butyl) isophthalate (16) - Following **Method C,** the crude was then purified by flash chromatography (cyclohexane/ethyl acetate 90/10 to 80/20, v/v) to afford **16** with 82% yield as a colorless oil. ^{1}H NMR ($CDCl_3$, 400 MHz): 8.66 (br s, 1H), 8.21 (d, 2H, ^{3}J = 7.76 Hz), 7.51 (t, 1H, ^{3}J = 7.76 Hz), 7.28-7.37 (m, 5H), 5.09 (s, 2H), 4.36 (t, 4H, ^{3}J = 6.39 Hz), 4.13 (t, 2H, ^{3}J = 6.26 Hz), 3.67 (t, 2H, ^{3}J = 6.19 Hz), 2.29-2.39 (m, 4H), 1.76-1.89 (m, 6H), 1.61-1.72 (m, 6H), 0.88 (s, 9H), 0.04 (s, 6H). ^{13}C NMR ($CDCl_3$, 100 MHz): 173.4, 173.2, 165.9, 165.9, 136.2, 133.9, 133.8, 131.1, 130.9, 130.8, 128.7, 128.7, 128.7, 128.3, 128.3, 128.3, 66.4, 65.5, 65.3, 64.9, 63.9, 62.7, 62.5, 34.0, 34.0, 29.4, 26.1, 26.1, 26.1, 25.6, 25.5, 24.5, 18.5, -5.2, -5.2. ASAP(+)-TOF-HRMS m/z for $C_{35}H_{50}O_9Si$ $[M+H]^+$: theoretical 643.3302, found 643.3297.

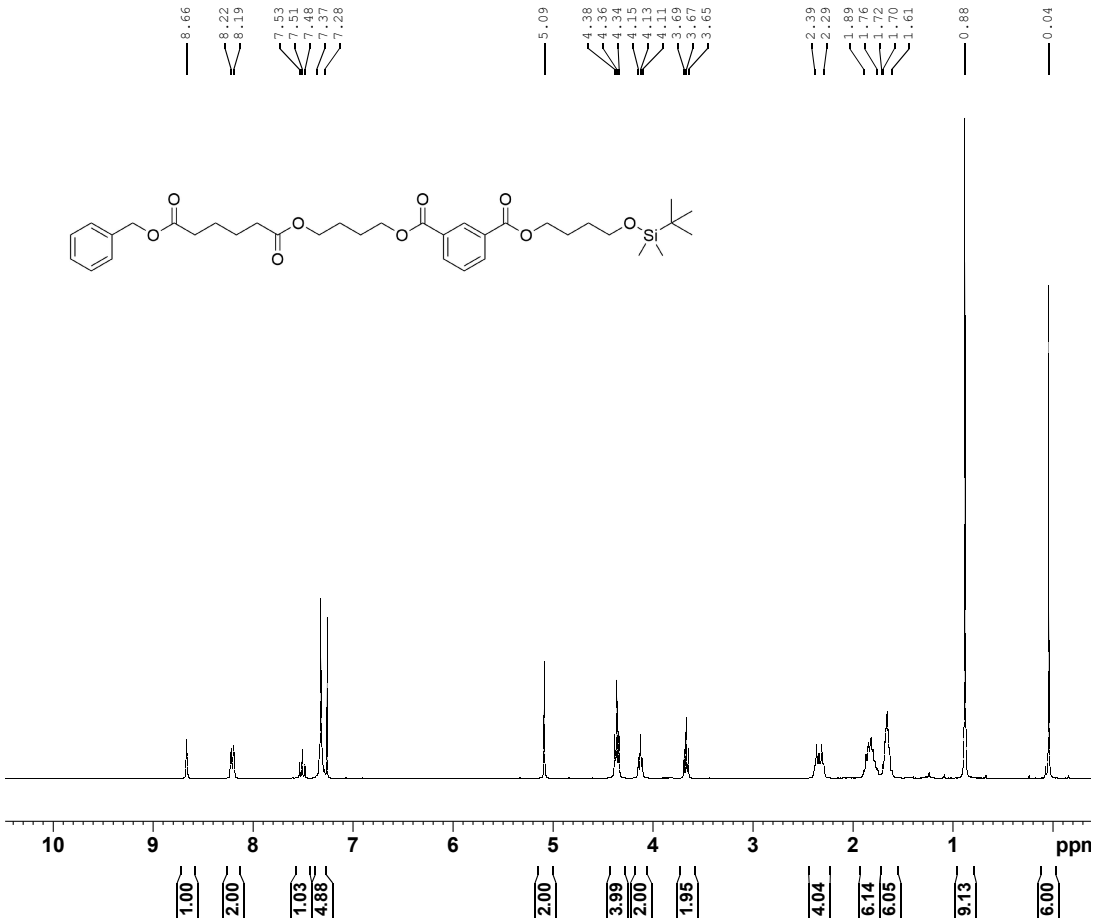

Figure A66- ^{1}H NMR (400 MHz, CDCl3) spectrum obtained for compound **16**.

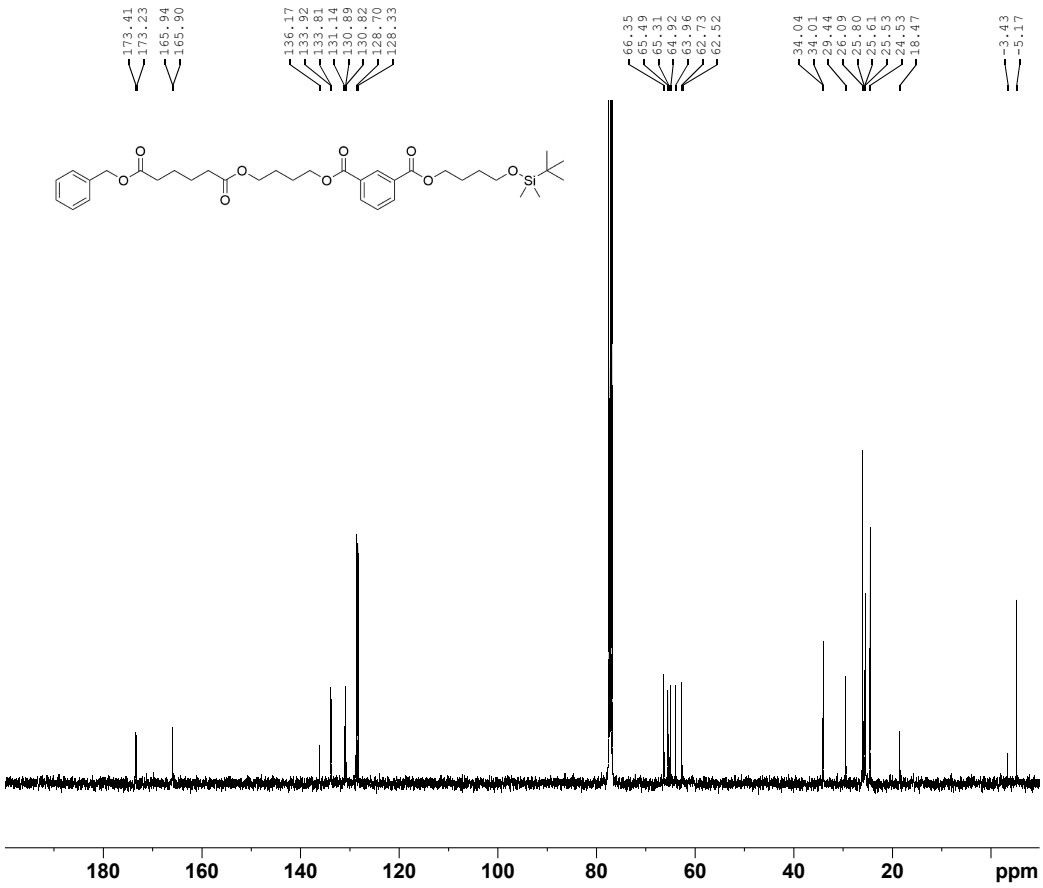

Figure A67- ^{13}C NMR (100 MHz, $CDCl_3$) spectrum obtained for compound **16**.

Elemental Composition Report **Page 1**

Single Mass Analysis
Tolerance = 5.0 PPM / DBE: min = -10.0, max = 1000.0
Element prediction: Off
Number of isotope peaks used for i-FIT = 4

Monoisotopic Mass, Even Electron Ions
135 formula(e) evaluated with 1 results within limits (up to 5 best isotopic matches for each mass)
Elements Used:
C: 0-100 H: 0-200 O: 0-15 Si: 1-1

Minimum:				-10.0				
Maximum:		30.0	5.0	1000.0				
Mass	Calc. Mass	mDa	PPM	DBE	i-FIT	Norm	Conf(%)	Formula
643.3297	643.3302	-0.5	-0.8	11.5	1420.0	n/a	n/a	C35 H51 O9 Si

Figure A68- ASAP(+)-TOF-HRMS elemental composition report obtained for compound **16**.

4-((6-(benzyloxy)-6-oxohexanoyl)oxy)butyl (4-hydroxybutyl) isophthalate (17)- Following **Method D,** the crude was then purified by flash chromatography (cyclohexane/ethyl acetate 90/10 to 60/40, v/v) to afford AA-BD-PA9 with 74% yield as a colorless oil. ^{1}H NMR ($CDCl_3$, 400 MHz): 8.67 (br s, 1H), 8.22 (d, 2H, ^{3}J = 7.79 Hz), 7.51 (t, 1H, ^{3}J = 7.79 Hz), 7.30-7.37 (m, 5H), 5.10 (s, 2H), 4.38 (q, 4H, ^{3}J = 6.49 Hz), 4.14 (t, 2H, ^{3}J = 6.16 Hz), 3.73 (t, 2H, ^{3}J = 6.49 Hz), 2.29-2.42 (m, 4H), 1.52-1.95 (m, 12H). ^{13}C NMR ($CDCl_3$, 100 MHz): 173.5, 173.3, 165.9, 168.9, 136.2, 133.9, 133.9, 131.0, 130.9, 130.8, 128.8, 128.7, 128.7, 128.4, 128.4, 128.3, 66.4, 65.3, 65.0, 64.0, 62.5, 34.0, 34.0, 29.4, 25.6, 25.6, 25.4, 25.4, 24.5. ASAP(+)-TOF-HRMS m/z for $C_{29}H_{36}O_9$ $[M+H]^+$: theoretical 529.2488, found 529.2446.

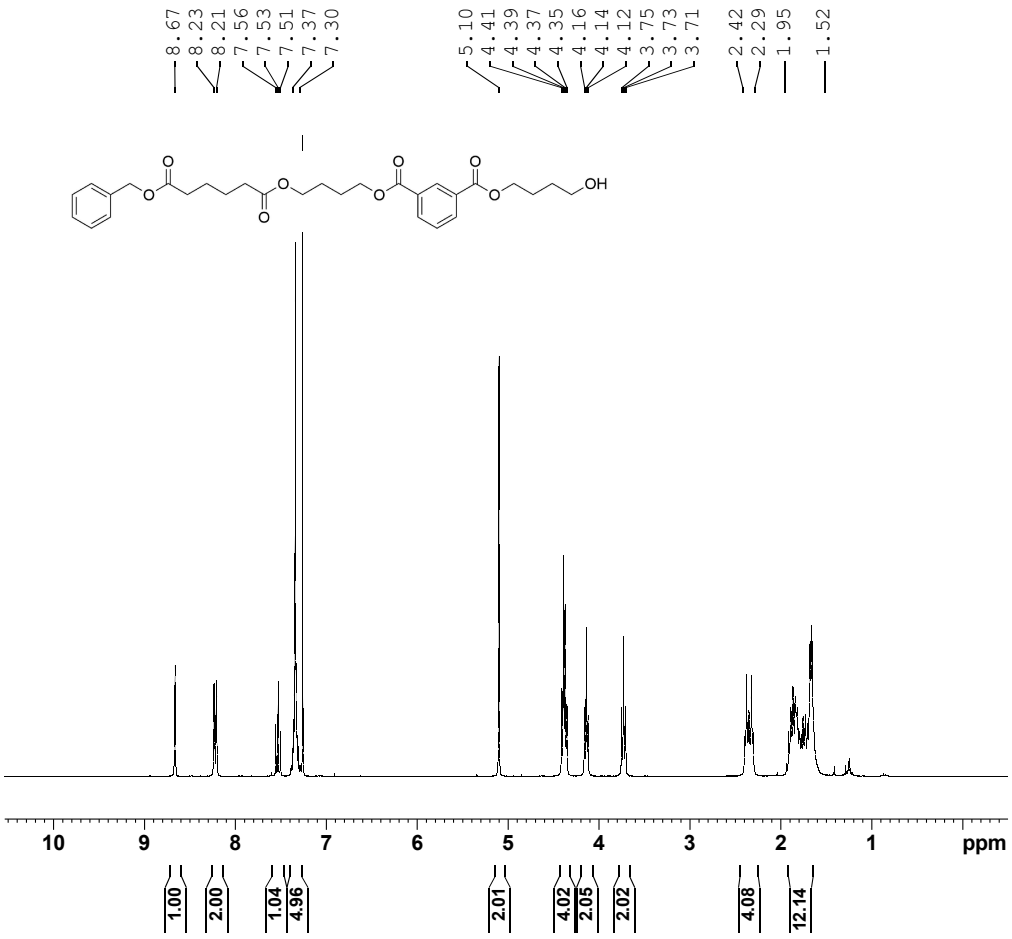

Figure A69- ^{1}H NMR (400 MHz, CDCl3) spectrum obtained for compound **17**.

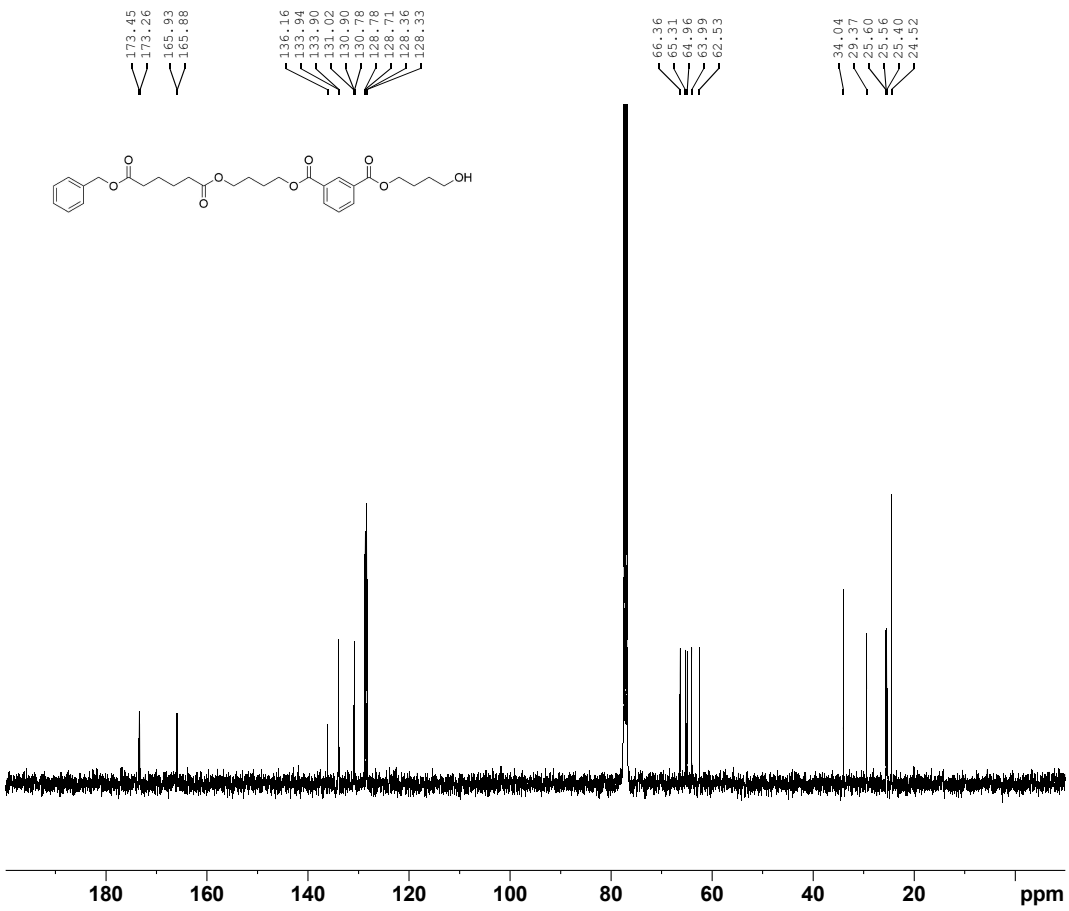

Figure A70- ^{13}C NMR (100 MHz, $CDCl_3$) spectrum obtained for compound **17**.

Elemental Composition Report Page 1

Single Mass Analysis
Tolerance = 5.0 PPM / DBE: min = -10.0, max = 1000.0
Element prediction: Off
Number of isotope peaks used for i-FIT = 4

Monoisotopic Mass, Even Electron Ions
114 formula(e) evaluated with 1 results within limits (up to 5 best isotopic matches for each mass)
Elements Used:
C: 0-100 H: 0-200 O: 0-15

Minimum:				-10.0				
Maximum:		30.0	5.0	1000.0				
Mass	Calc. Mass	mDa	PPM	DBE	i-FIT	Norm	Conf(%)	Formula
529.2446	529.2438	0.8	1.5	11.5	2175.9	n/a	n/a	C29 H37 O9

Figure A71- ASAP(+)-TOF-HRMS elemental composition report obtained for compound **17**.

6-(4-((3-((4-hydroxybutoxy)carbonyl)benzoyl)oxy)butoxy)-6-oxohexanoic acid (18) - Following **Method E, 18** was obtained with quantitative yield as a yellowish oil. ^{1}H NMR ($CDCl_3$, 300 MHz): 8.65 (br s, 1H), 8.21 (d, 2H, ^{3}J = 7.73 Hz), 7.53 (t, 1H, ^{3}J = 7.73 Hz), 4.95-6.14 (br s, 2H), 4.34-4.42 (m, 4H), 4.14 (t, 2H, ^{3}J = 6.18 Hz), 3.73 (t, 2H, ^{3}J = 6.38 Hz), 2.28-2.40 (m, 4H), 1.60-1.94 (m, 12H). ^{13}C NMR ($CDCl_3$, 75 MHz): 178.3, 173.6, 166.0, 165.9, 134.0, 134.0, 130.9, 130.8, 130.7, 128.8, 65.3, 65.0, 64.0, 62.0, 34.0, 33.6, 29.2, 25.5, 25.5, 25.3, 24.4, 24.2. ASAP(+)-TOF-HRMS m/z for $C_{22}H_{30}O_9$ $[M+H]^+$: theoretical 439.1968, found 439.1969.

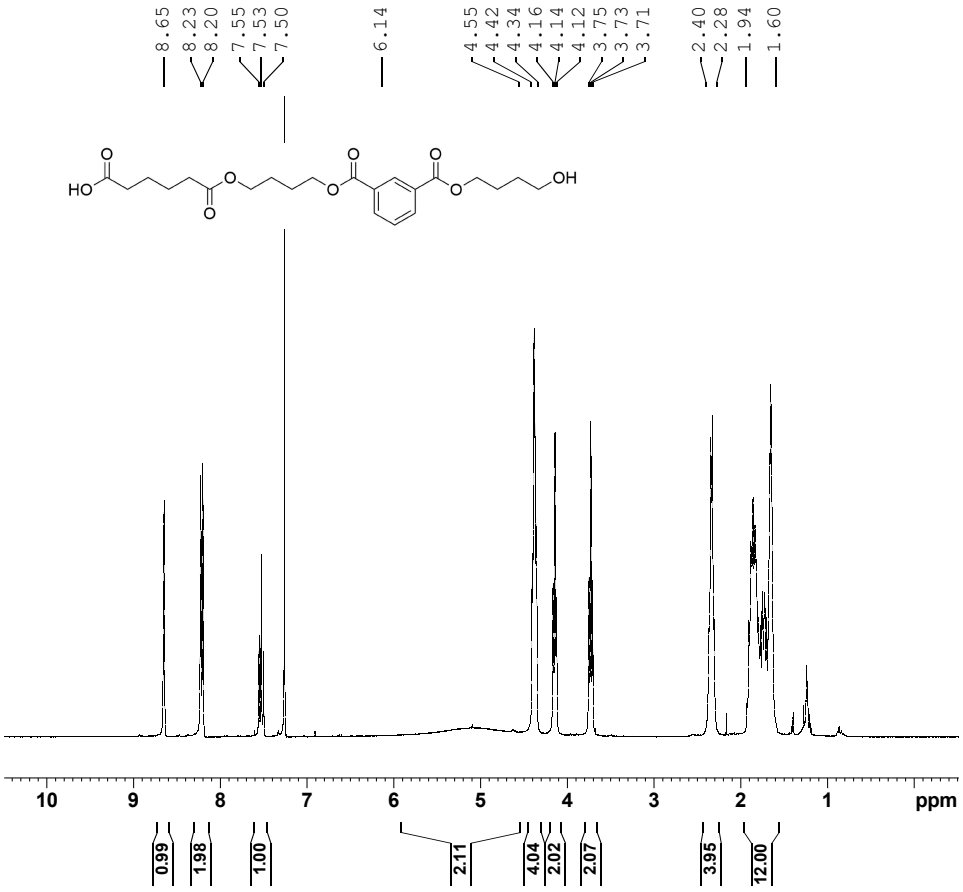

Figure A72- ^{1}H NMR (300 MHz, CDCl3) spectrum obtained for compound **18**.

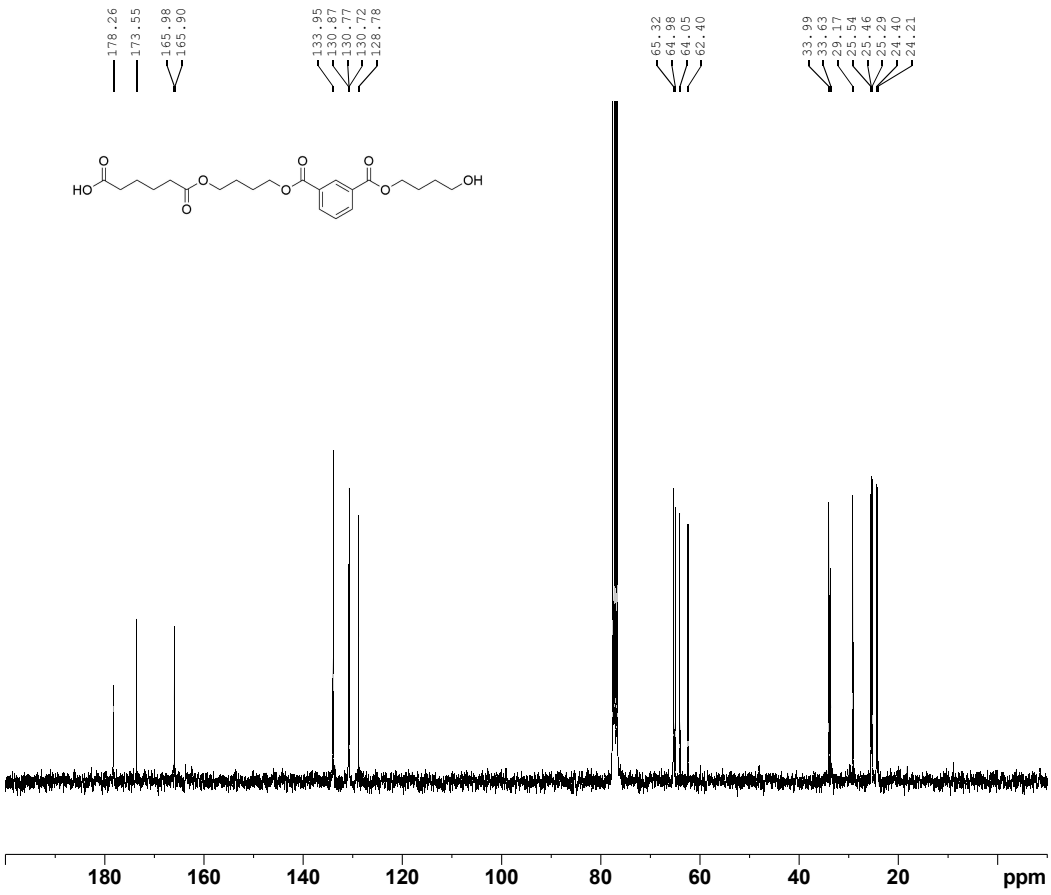

Figure A73- ^{13}C NMR (75 MHz, $CDCl_3$) spectrum obtained for compound **18**.

Elemental Composition Report Page 1

Single Mass Analysis
Tolerance = 5.0 PPM / DBE: min = -10.0, max = 1000.0
Element prediction: Off
Number of isotope peaks used for i-FIT = 4

Monoisotopic Mass, Even Electron Ions
202 formula(e) evaluated with 1 results within limits (up to 5 best isotopic matches for each mass)
Elements Used:
C: 0-100 H: 0-200 N: 0-3 O: 5-13

Minimum:				-10.0				
Maximum:		30.0	5.0	1000.0				
Mass	Calc. Mass	mDa	PPM	DBE	i-FIT	Norm	Conf(%)	Formula
439.1969	439.1968	0.1	0.2	7.5	2761.2	n/a	n/a	C22 H31 O9

Figure A74- ASAP(+)-TOF-HRMS elemental composition report obtained for compound **18**.

3,8,15,20-tetraoxa-1(1,3)-benzenacyclohenicosaphane-2,9,14,21-tetraone (c[2BD+AA+iPA]) - Following **Method F,** the crude was then purified by flash chromatography (cyclohexane/ethyl acetate 90/10 to 30/70, v/v) to afford **c[2BD+AA+iPA]** with 79% yield as a yellowish solid. ^{1}H NMR ($CDCl_3$, 400 MHz): 8.59 (br s, 1H), 8.26 (dd, 2H, ^{3}J = 7.76 Hz, ^{4}J = 1.62 Hz), 7.56 (t, 1H, ^{3}J = 7.76 Hz), 4.39 (t, 4H, ^{3}J = 6.09 Hz), 4.17 (t, 4H, ^{3}J = 6.26 Hz), 2.30-2.38 (m, 4H), 1.77-1.93 (m, 8H), 1.63-1.72 (m, 4H). ^{13}C NMR ($CDCl_3$, 100 MHz): 173.4, 173.4, 165.8, 165.8, 134.3, 134.3, 130.8, 130.8, 130.0, 128.9, 65.1, 65.1, 64.0, 64.0, 34.1, 34.1, 25.6, 25.6, 25.5, 25.5, 24.5, 24.5. ASAP(+)-TOF-HRMS m/z for $C_{22}H_{28}O_8$ $[M+H]^+$: theoretical 421.1862, found 421.1861. Melting point: 65.3 ºC.

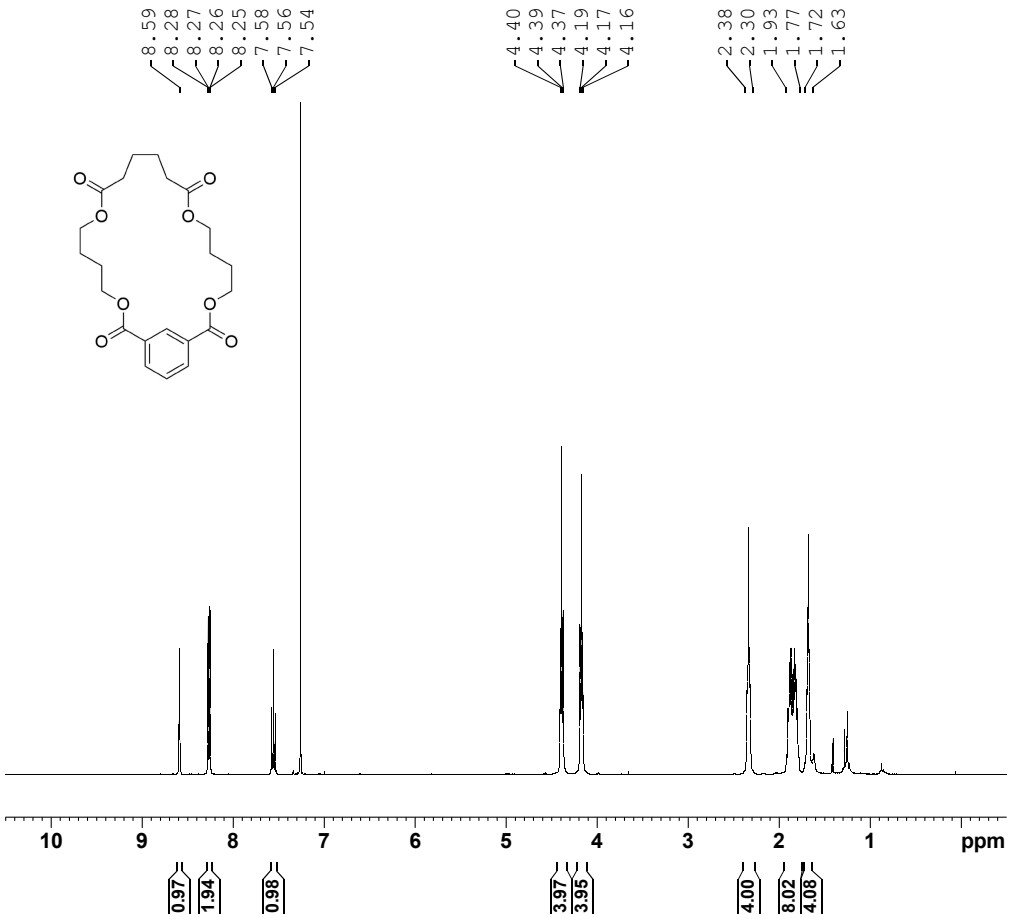

Figure A75- ^{1}H NMR (400 MHz, CDCl3) spectrum obtained for compound **c[2BD+AA+iPA]**.

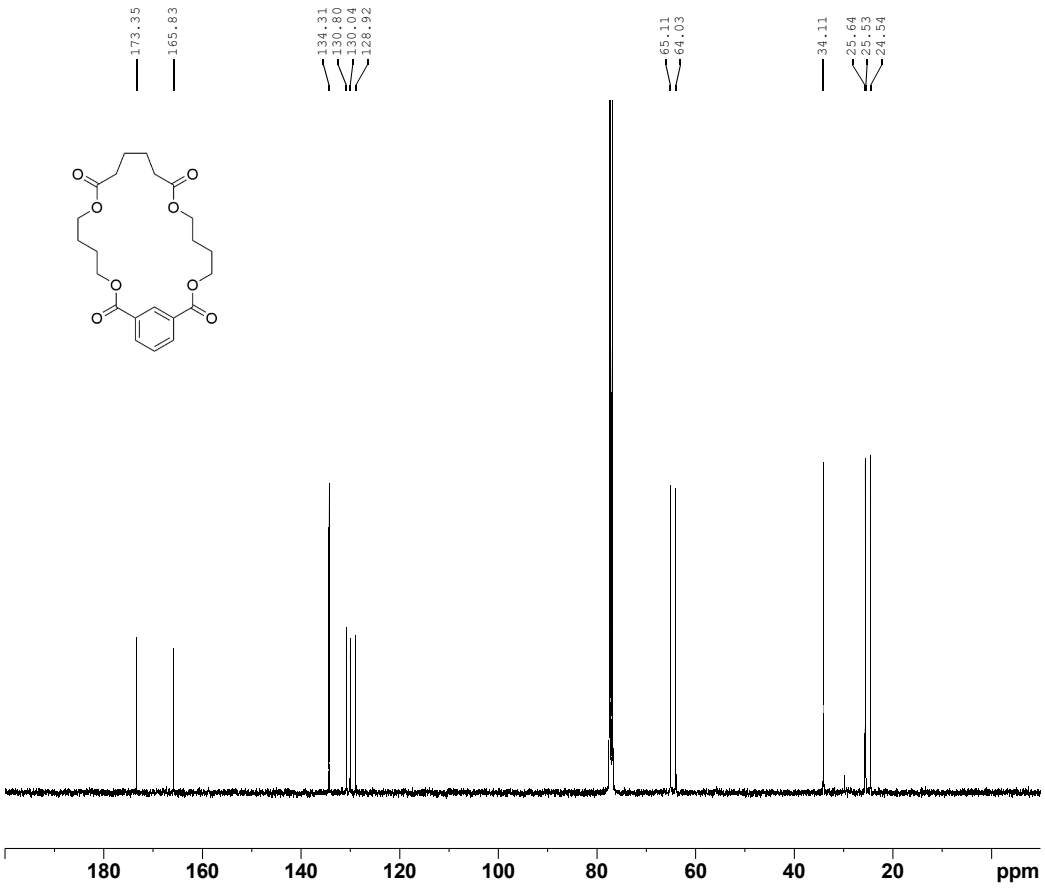

Figure A76- ^{13}C NMR (100 MHz, $CDCl_3$) spectrum obtained for compound **c[2BD+AA+iPA]**.

Elemental Composition Report **Page 1**

Single Mass Analysis
Tolerance = 5.0 PPM / DBE: min = -10.0, max = 1000.0
Element prediction: Off
Number of isotope peaks used for i-FIT = 4

Monoisotopic Mass, Even Electron Ions
70 formula(e) evaluated with 1 results within limits (up to 5 best isotopic matches for each mass)
Elements Used:
C: 0-100 H: 0-200 O: 0-10

DRC78 (SOLIDE) XEVO G2-XS QTOF 13-Nov-2023
20231113_KK_DRC78_01 90 (0.926) Cm (90:91) 1: TOF MS ASAP+
3.45e+006

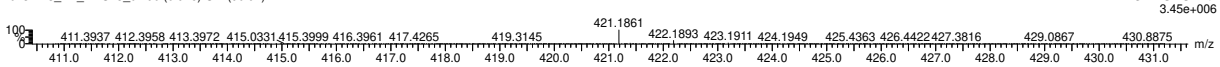

Minimum:				-10.0				
Maximum:		30.0	5.0	1000.0				
Mass	Calc. Mass	mDa	PPM	DBE	i-FIT	Norm	Conf(%)	Formula
421.1861	421.1862	-0.1	-0.2	8.5	1609.6	n/a	n/a	C22 H29 O8

Figure A77- ASAP(+)-TOF-HRMS elemental composition report obtained for compound **c[2BD+AA+iPA]**.

Adipic acid & Propylene glycol series

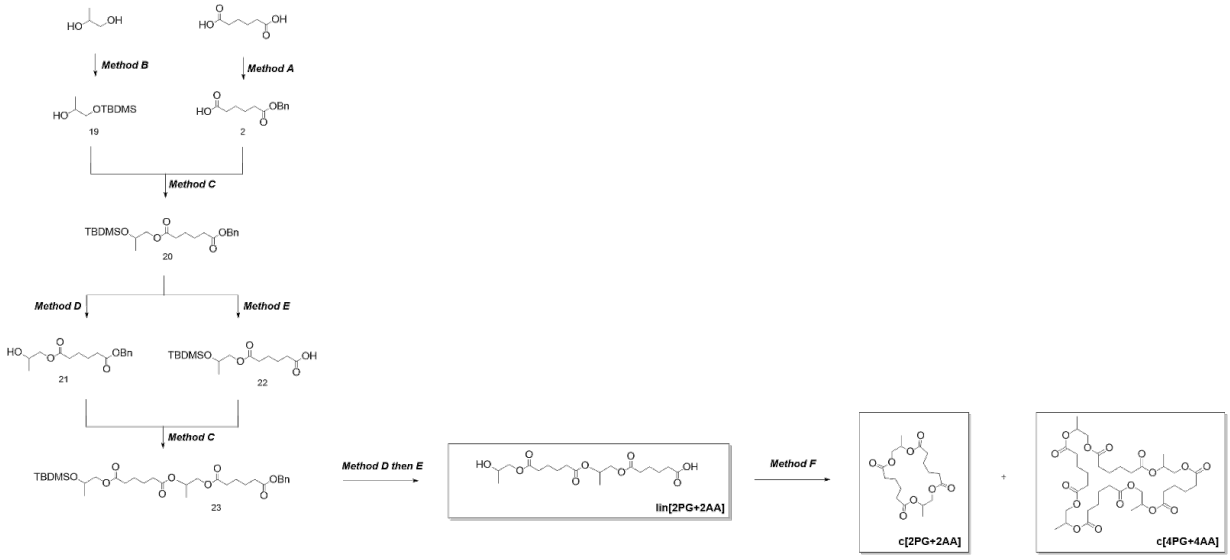

Figure A78 – Synthesis of linear and cyclic oligomer derived from Adipic acid (AA) & propylene glycol (PG).

1-((tert-butyldimethylsilyl)oxy)propan-2-ol (19) - Following **Method B,** the crude was then purified by flash chromatography (cyclohexane/ethyl acetate 90/10 to 70/30, v/v) to afford **19** as a mixture of diastereoisomers with 85% yield as a colorless oil. ^{1}H NMR ($CDCl_3$, 400 MHz): 3.76-3.85 (m, 1H), 3.57 (dd, 1H, ^{2}J = 9.97 Hz, ^{3}J = 3.45 Hz), 3.34 (dd, 1H, ^{2}J = 9.97 Hz, ^{3}J = 7.63 Hz), 2.40-2.54 (br s, 1H), 1.10 (d, 3H, ^{3}J = 6.33 Hz), 0.9 (s, 9H), 0.06 (s, 6H). ^{13}C NMR ($CDCl_3$, 100 MHz): 68.7, 68.1, 26.01, 26.01, 26.01, 18.4, 18.4, -5.2, -5.3. ESI(+)-TOF-HRMS m/z for $C_9H_{22}O_2Si$ $[M+Na]^+$: theoretical 213.1287, found 213.1291.

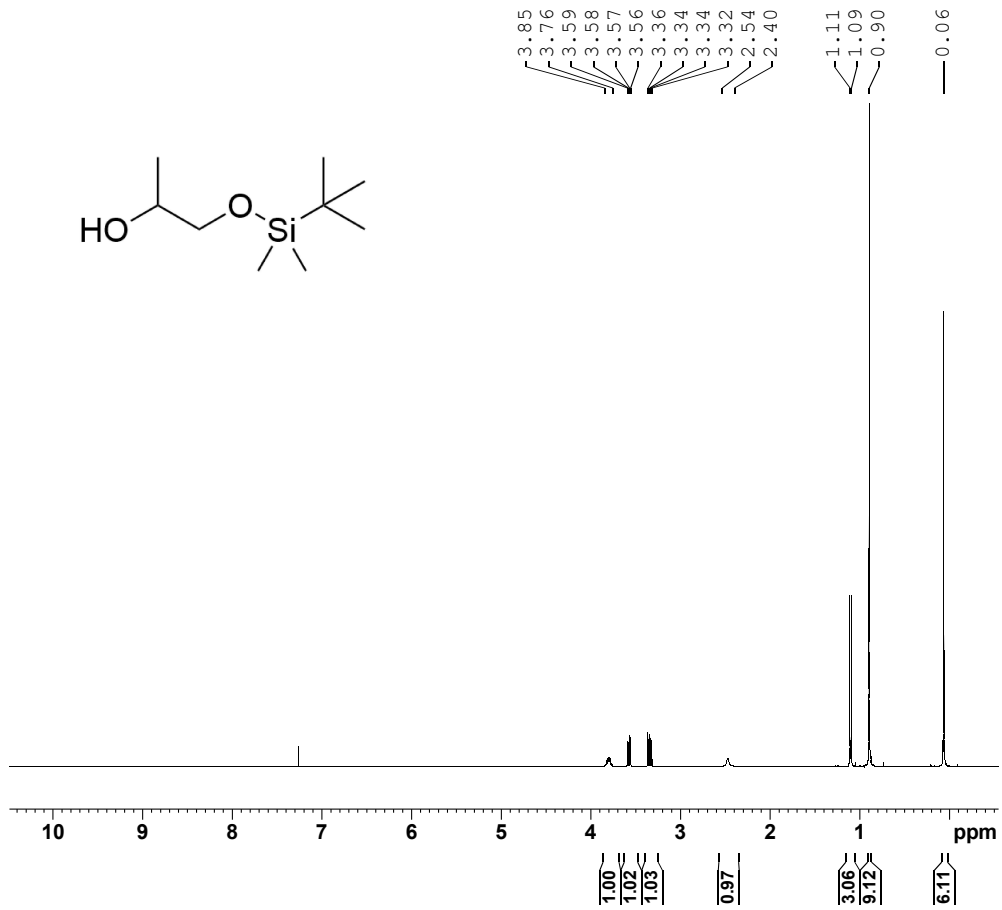

Figure A79- ^{1}H NMR (400 MHz, CDCl3) spectrum obtained for compound **19**.

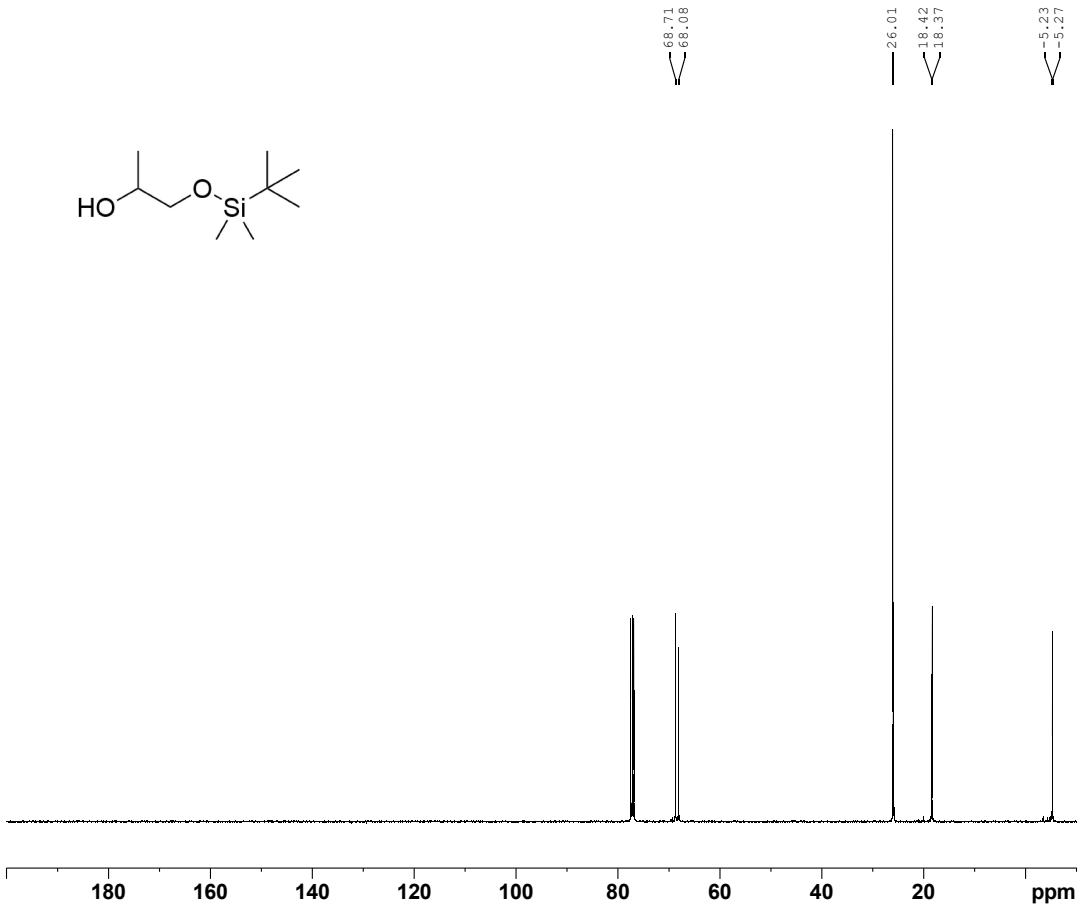

Figure A80- ^{13}C NMR (100 MHz, $CDCl_3$) spectrum obtained for compound **19**.

Elemental Composition Report **Page 1**

Single Mass Analysis
Tolerance = 5.0 PPM / DBE: min = -10.0, max = 1000.0
Element prediction: Off
Number of isotope peaks used for i-FIT = 4

Monoisotopic Mass, Even Electron Ions
206 formula(e) evaluated with 1 results within limits (all results (up to 1000) for each mass)
Elements Used:
C: 0-100 H: 0-200 N: 0-10 O: 0-10 Na: 1-1 Si: 1-1

DRC49 (DCM) - MeOH/H2O (95/5%)
20231006_KK_DRC49_01 81 (0.837) Cm (80:85)

XEVO G2-XS QTOF

06-Oct-2023
1: TOF MS ES+
9.26e+004

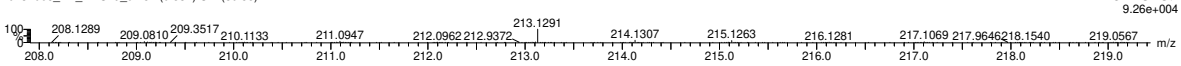

Minimum:				-10.0				
Maximum:		30.0	5.0	1000.0				
Mass	Calc. Mass	mDa	PPM	DBE	i-FIT	Norm	Conf(%)	Formula
213.1291	213.1287	0.4	1.9	-0.5	508.3	n/a	n/a	C9 H22 O2 Na Si

Figure A81- ESI(+)-TOF-HRMS elemental composition report obtained for compound **19**.

benzyl (1-((tert-butyldimethylsilyl)oxy)propan-2-yl) adipate (20) - Following **Method C,** the crude was then purified by flash chromatography (cyclohexane/ethyl acetate 90/10 to 70/30, v/v) to afford **20** as a mixture of diastereoisomers with 91% yield as a colorless oil. ^{1}H NMR ($CDCl_3$, 400 MHz): 7.29-7.40 (m, 5H), 5.11 (s, 2H), 4.89-5.00 (m, 1H), 3.53-3.67 (m, 2H), 2.26-2.43 (m, 4H), 1.59-1.76 (m, 4H), 1.19 (d, 3H, ^{3}J = 6.45 Hz), 0.88 (s, 9H), 0.04 (s, 6H). ^{13}C NMR ($CDCl_3$, 100 MHz): 173.3, 173.0, 136.1, 128.7, 128.7, 128.3, 128.3, 128.3, 71.3, 66.3, 65.7, 34.3, 34.0, 25.9, 25.9, 25.9, 24.5, 24.5, 18.4, 16.5, -5.3-5.3. ASAP(+)-TOF-HRMS m/z for $C_{22}H_{36}O_5Si$ $[M+H]^+$: theoretical 409.2410, found 409.2403.

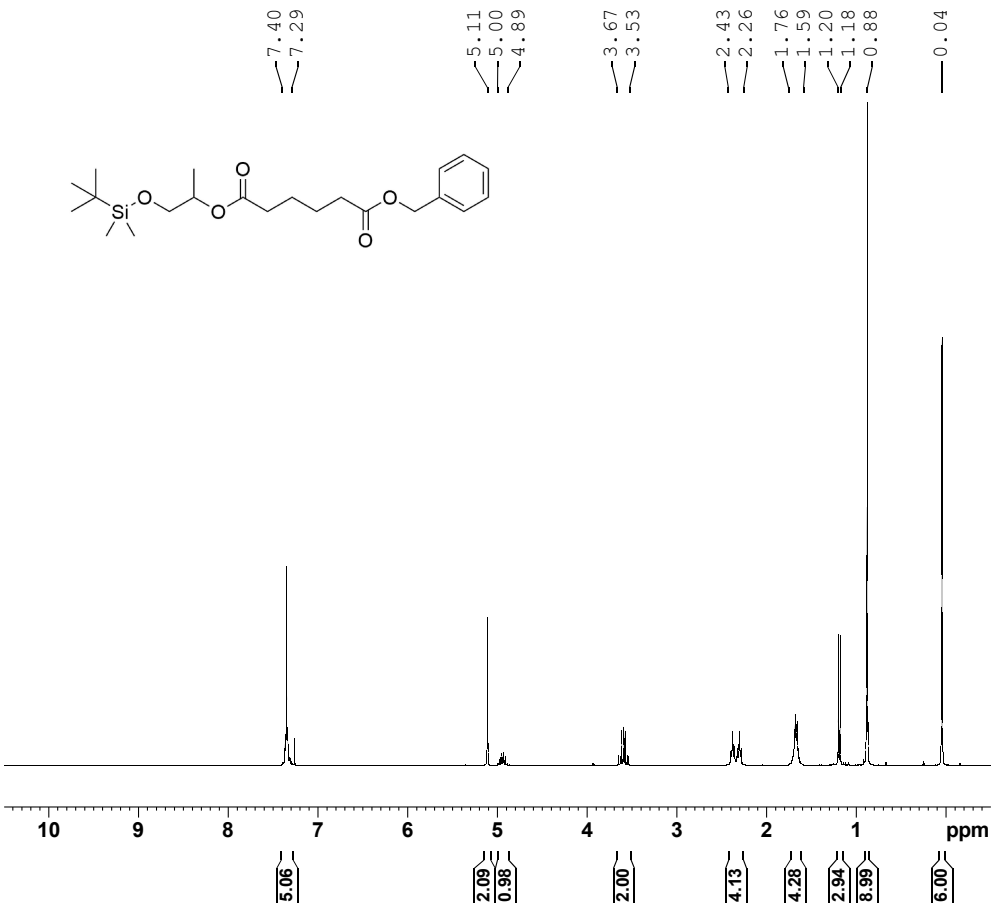

Figure A82- ^{1}H NMR (400 MHz, CDCl3) spectrum obtained for compound **20**.

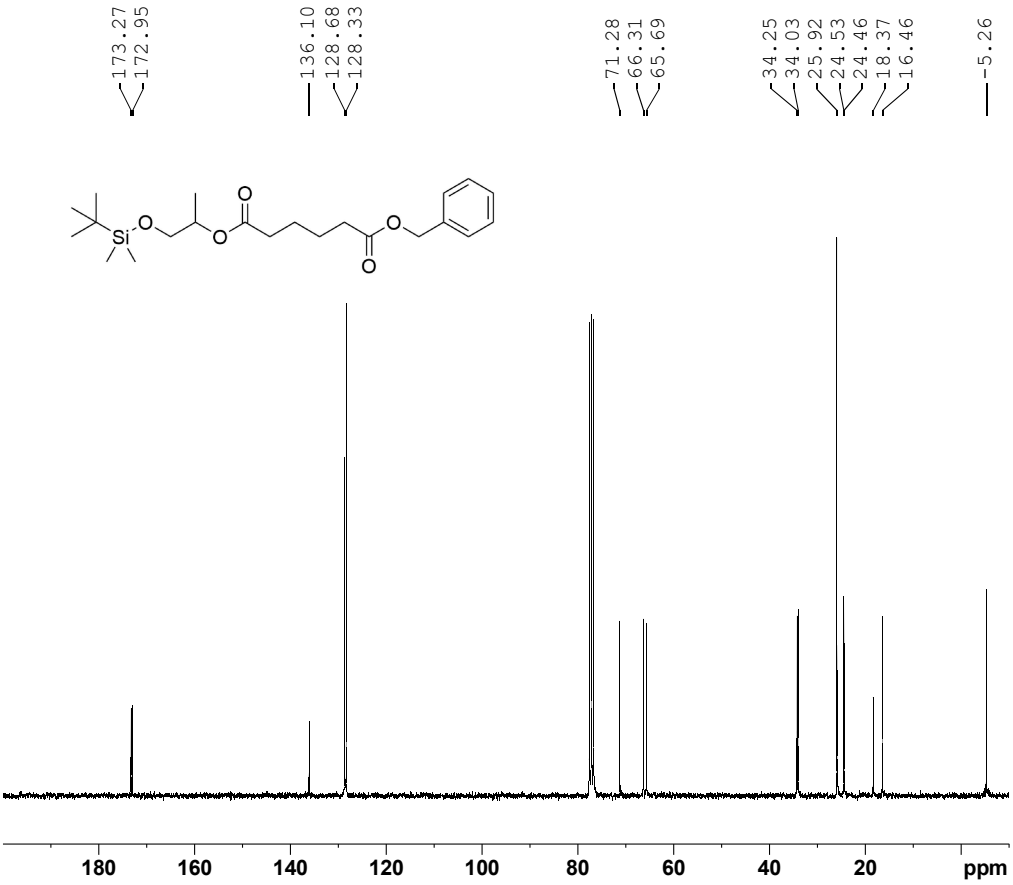

Figure A83- ^{13}C NMR (100 MHz, $CDCl_3$) spectrum obtained for compound **20**.

Elemental Composition Report **Page 1**

Single Mass Analysis
Tolerance = 5.0 PPM / DBE: min = -10.0, max = 1000.0
Element prediction: Off
Number of isotope peaks used for i-FIT = 4

Monoisotopic Mass, Even Electron Ions
66 formula(e) evaluated with 1 results within limits (up to 5 best isotopic matches for each mass)
Elements Used:
C: 0-100 H: 0-200 O: 0-10 Si: 1-1

DRC53 (SOLIDE) XEVO G2-XS QTOF 13-Nov-2023
20231113_KK_DRC53_01 188 (1.904) Cm (184:190) 1: TOF MS ASAP+
7.03e+006

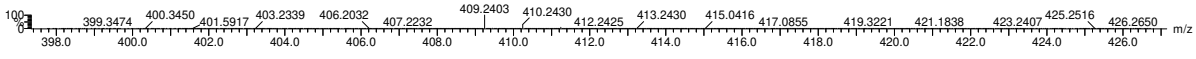

Minimum:				-10.0				
Maximum:		30.0	5.0	1000.0				
Mass	Calc. Mass	mDa	PPM	DBE	i-FIT	Norm	Conf(%)	Formula
409.2403	409.2410	-0.7	-1.7	5.5	2128.4	n/a	n/a	C22 H37 O5 Si

Figure A84- ASAP(+)-TOF-HRMS elemental composition report obtained for compound **20**.

benzyl (1-hydroxypropan-2-yl) adipate (21) - Following **Method D,** the crude was then purified by flash chromatography (cyclohexane/ethyl acetate 90/10 to 60/40, v/v) to afford **21** as a mixture of diastereoisomers with 89% yield as a colorless oil. ^{1}H NMR ($CDCl_3$, 400 MHz): 7.29-7.38 (m, 5H), 5.11 (s, 2H), 4.94-5.04 (m, 1H), 3.56-3.69 (m, 2H), 2.28-2.43 (m, 4H), 1.62-1.74 (m, 4H), 1.22 (d, 3H, ^{3}J = 6.46 Hz). ^{13}C NMR ($CDCl_3$, 100 MHz): 173.4, 173.4, 136.1, 128.7, 128.7, 128.3, 128.3, 128.3, 72.1, 66.4, 65.9, 34.2, 33.9, 24.5, 24.3, 16.3. ASAP(+)-TOF-HRMS m/z for $C_{16}H_{22}O_5$ $[M+H]^+$: theoretical 295.1545, found 295.1543.

Figure A88- ^{1}H NMR (400 MHz, CDCl3) spectrum obtained for compound **21**.

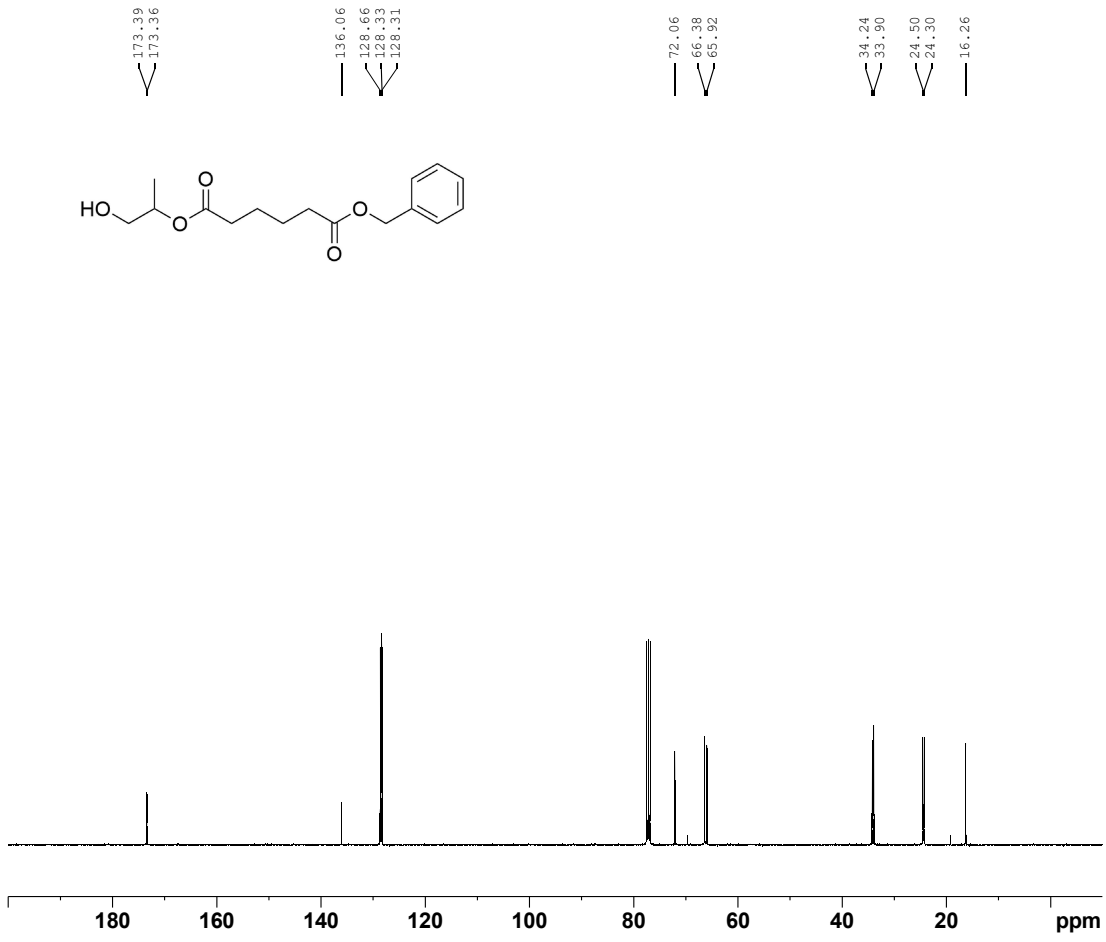

Figure A89- ^{13}C NMR (100 MHz, $CDCl_3$) spectrum obtained for compound **21**.

Elemental Composition Report **Page 1**

Single Mass Analysis
Tolerance = 50.0 PPM / DBE: min = -10.0, max = 1000.0
Element prediction: Off
Number of isotope peaks used for i-FIT = 4

Monoisotopic Mass, Even Electron Ions
31 formula(e) evaluated with 1 results within limits (up to 5 best isotopic matches for each mass)
Elements Used:
C: 0-100 H: 0-200 O: 1-6

DRC56 (SOLIDE) XEVO G2-XS QTOF 13-Nov-2023
20231113_KK_DRC56_01 176 (1.778) Cm (176:177) 1: TOF MS ASAP+ 1.95e+004

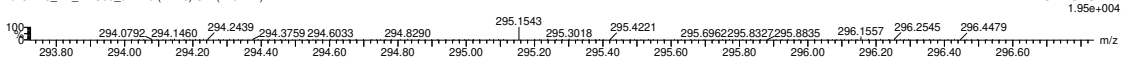

Minimum:				-10.0				
Maximum:		30.0	50.0	1000.0				
Mass	Calc. Mass	mDa	PPM	DBE	i-FIT	Norm	Conf(%)	Formula
295.1543	295.1545	-0.2	-0.7	5.5	784.1	n/a	n/a	C16 H23 O5

Figure A90- ASAP(+)-TOF-HRMS elemental composition report obtained for compound **21**.

6-((1-((tert-butyldimethylsilyl)oxy)propan-2-yl)oxy)-6-oxohexanoic acid (22) - Following **Method E, 22** was obtained as a mixture of diastereoisomers with 97% yield as a colorless oil. ^{1}H NMR ($CDCl_3$, 400 MHz): 4.89-4.99 (m, 1H), 3.54-3.65 (m, 2H), 2.28-2.40 (m, 4H), 1.64-1.71 (m, 4H), 1.19 (d, 3H, ^{3}J = 6.44 Hz), 0.87 (s, 9H), 0.04 (s, 6H). ^{13}C NMR ($CDCl_3$, 100 MHz): 179.3, 173.0, 71.4, 65.7, 34.3, 33.8, 25.9, 25.9, 25.9, 24.5, 24.2, 18.4, 16.5, -5.3, -5.3. ASAP(+)-TOF-HRMS m/z for $C_{15}H_{30}O_5Si$ $[M+H]^+$: theoretical 319.1941, found 319.1934.

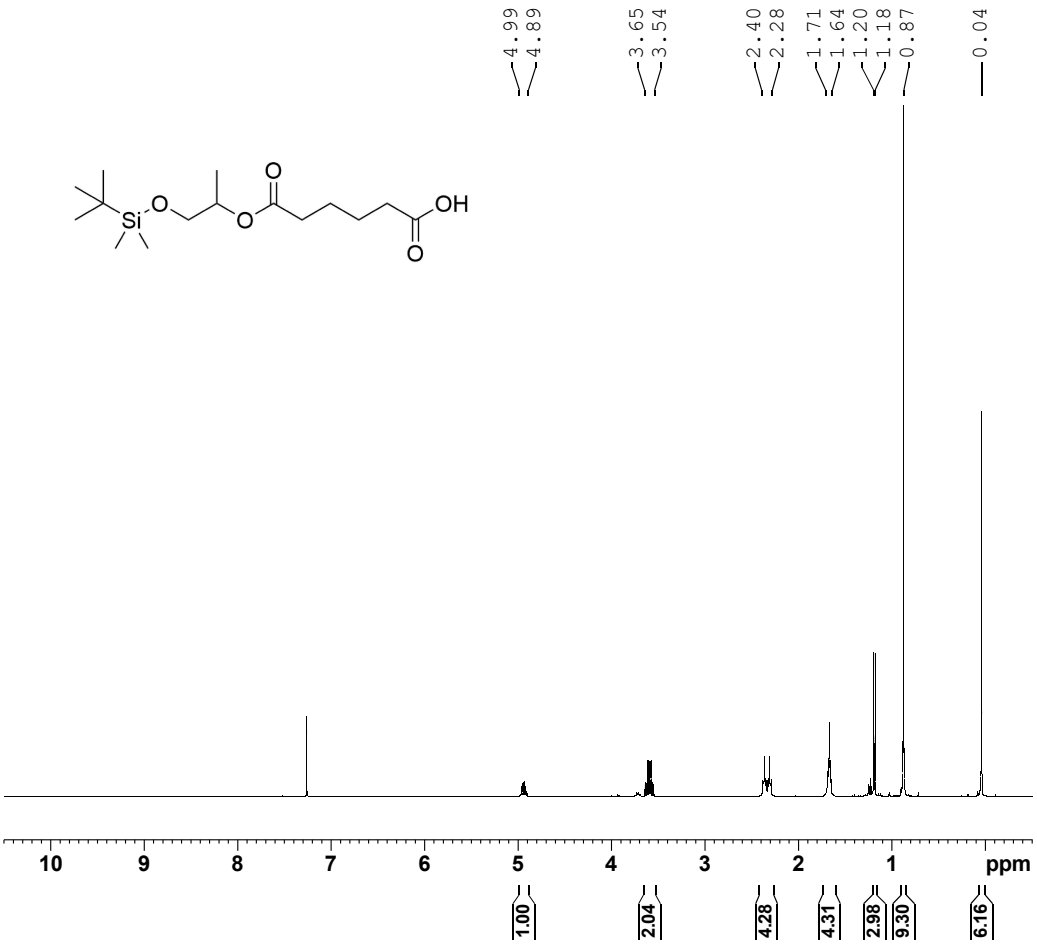

Figure A85- ^{1}H NMR (400 MHz, CDCl3) spectrum obtained for compound **22**.

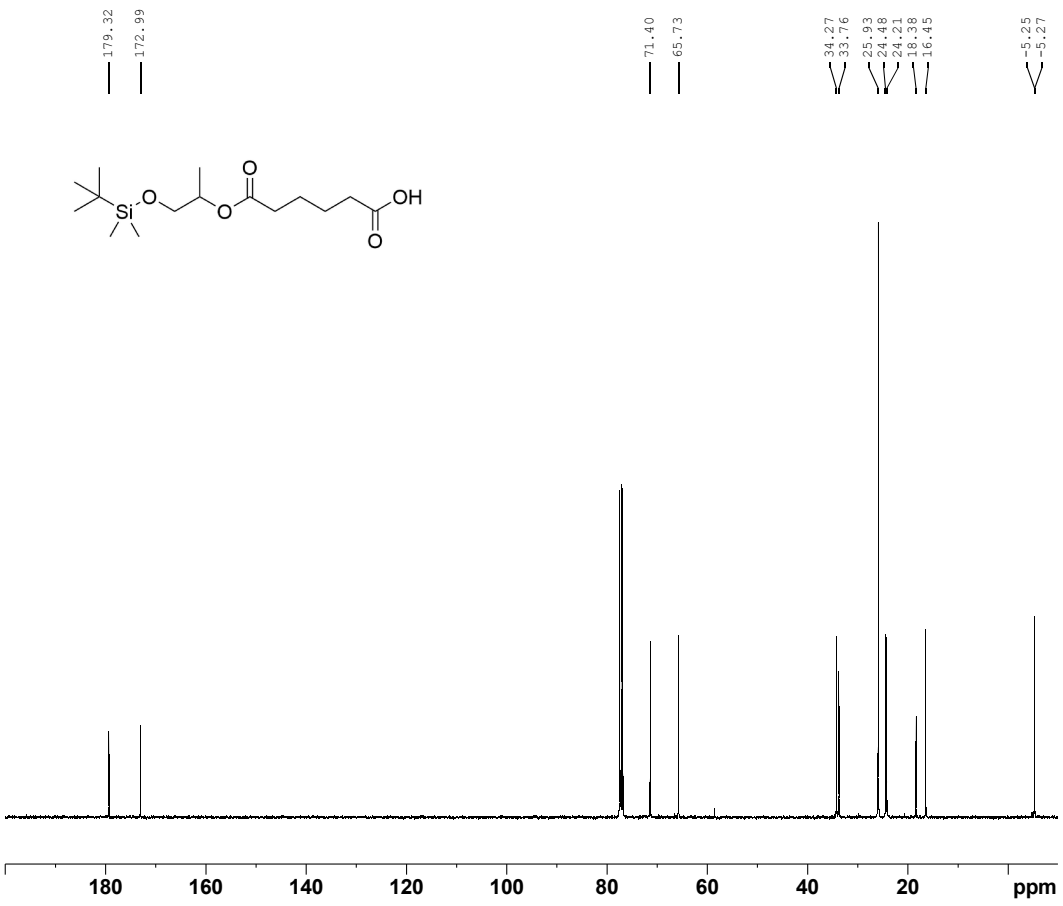

Figure A86- ^{13}C NMR (100 MHz, $CDCl_3$) spectrum obtained for compound **22**.

Elemental Composition Report Page 1

Single Mass Analysis
Tolerance = 5.0 PPM / DBE: min = -10.0, max = 1000.0
Element prediction: Off
Number of isotope peaks used for i-FIT = 4

Monoisotopic Mass, Even Electron Ions
307 formula(e) evaluated with 1 results within limits (up to 5 best isotopic matches for each mass)
Elements Used:
C: 0-100 H: 0-200 N: 0-5 O: 0-10 Si: 1-1

Minimum:				-10.0				
Maximum:		30.0	5.0	1000.0				
Mass	Calc. Mass	mDa	PPM	DBE	i-FIT	Norm	Conf(%)	Formula
319.1934	319.1941	-0.7	-2.2	1.5	2498.3	n/a	n/a	C15 H31 O5 Si

Figure A87- ASAP(+)-TOF-HRMS elemental composition report obtained for compound **22**.

benzyl (2,2,3,3,6-pentamethyl-8,13-dioxo-4,7,14-trioxa-3-silaheptadecan-16-yl) adipate (23) - Following **Method C,** the crude was then purified by flash chromatography (cyclohexane/ethyl acetate 90/10 to 70/30, v/v) to afford **23** as a mixture of diastereoisomers with 72% yield as a colorless oil. ^{1}H NMR ($CDCl_3$, 400 MHz): 7.29-7.38 (m, 5H), 5.09-5.17 (m, 1H), 5.11 (s, 2H), 4.90-4.98 (m, 1H), 4.13-4.19 (m, 1H), 4.00-4.06 (m, 1H), 3.53-3.65 (m, 2H), 2.27-2.41 (m, 8H), 1.60-1.73 (m, 8H), 1.23 (d, 3H, ^{3}J = 6.52 Hz), 1.19 (d, 3H, ^{3}J = 6.41 Hz), 0.88 (s, 9H), 0.04 (s, 6H). ^{13}C NMR ($CDCl_3$, 100 MHz): 173.2, 173.1, 172.9, 172.7, 136.2, 128.7, 128.7, 128.3, 128.3, 128.3, 71.3, 68.3, 66.3, 66.1, 65.7, 34.3, 34.1, 34.0, 33.8, 26.0, 26.0, 26.0, 24.5, 24.5, 24.4, 24.4, 18.4, 16.7, 16.5, -5.2, -5.2. ASAP(+)-TOF-HRMS m/z for $C_{31}H_{50}O_9Si$ $[M+H]^+$: theoretical 595.3302, found 595.3306.

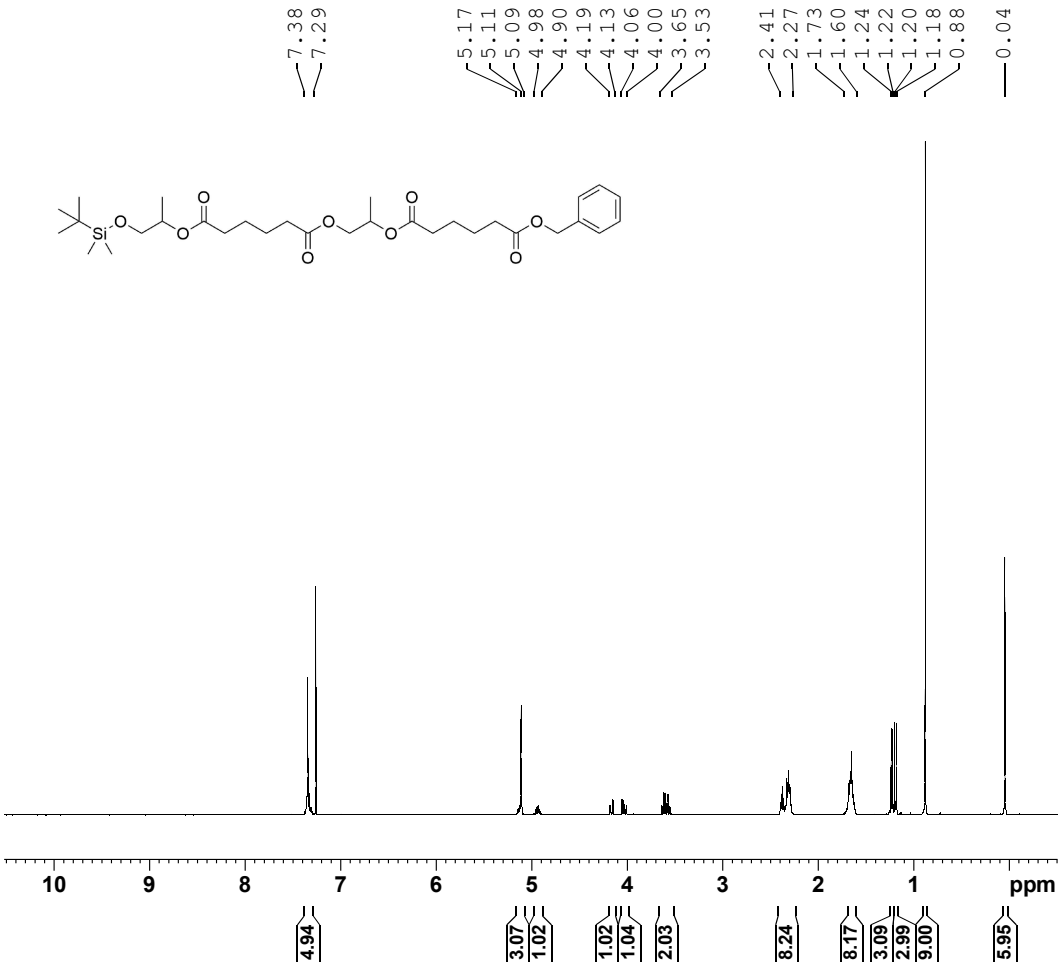

Figure A91- ^{1}H NMR (400 MHz, CDCl3) spectrum obtained for compound **23**.

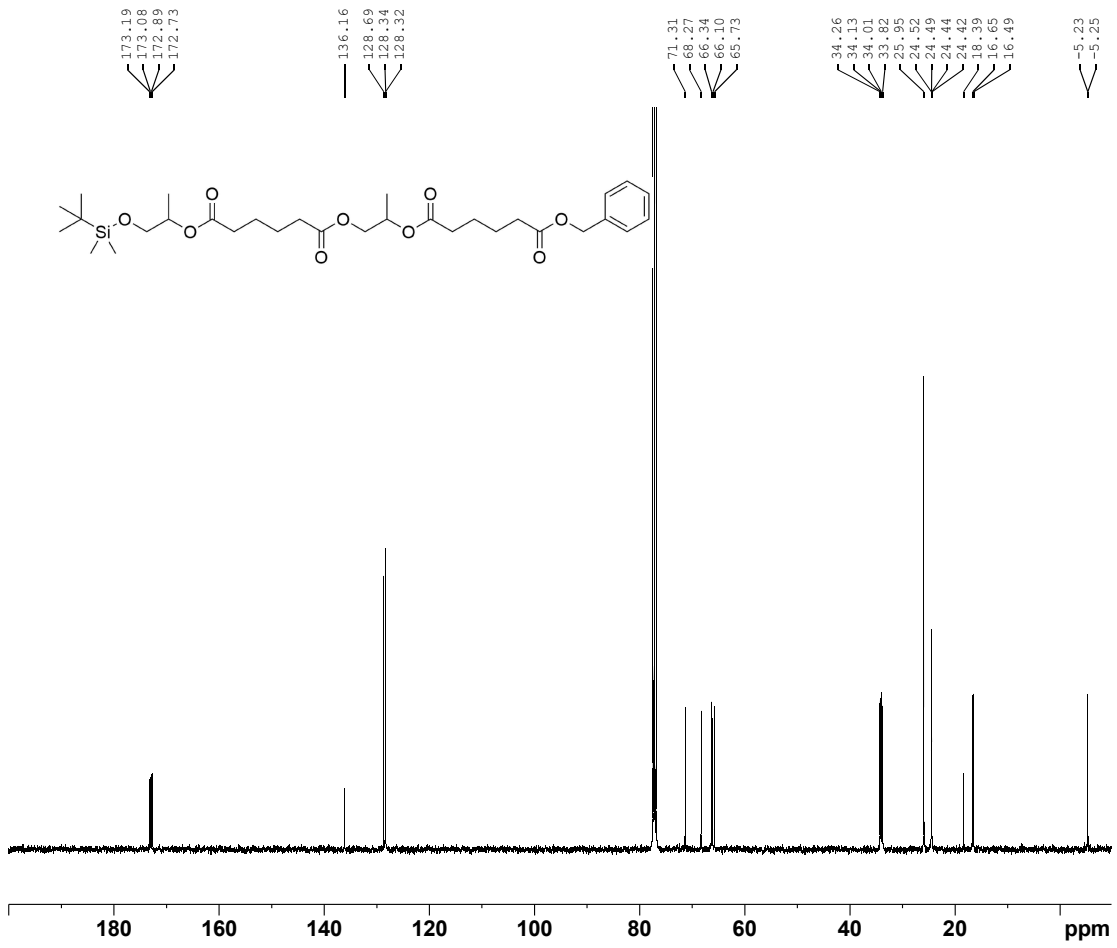

Figure A92- ^{13}C NMR (100 MHz, $CDCl_3$) spectrum obtained for compound **23**.

Elemental Composition Report **Page 1**

Single Mass Analysis
Tolerance = 5.0 PPM / DBE: min = -10.0, max = 1000.0
Element prediction: Off
Number of isotope peaks used for i-FIT = 4

Monoisotopic Mass, Even Electron Ions
83 formula(e) evaluated with 1 results within limits (up to 5 best isotopic matches for each mass)
Elements Used:
C: 0-100 H: 0-200 O: 1-10 Si: 1-1

DRC61 (SOLIDE)
20231113_KK_DRC61_01 166 (1.681) Cm (163:166)

XEVO G2-XS QTOF

13-Nov-2023
1: TOF MS ASAP+
1.48e+006

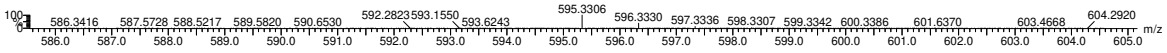

Minimum:				-10.0				
Maximum:		30.0	5.0	1000.0				
Mass	Calc. Mass	mDa	PPM	DBE	i-FIT	Norm	Conf(%)	Formula
595.3306	595.3302	0.4	0.7	7.5	1349.4	n/a	n/a	C31 H51 O9 Si

Figure A93- ASAP(+)-TOF-HRMS elemental composition report obtained for compound **23**.

benzyl (1-((6-((1-hydroxypropan-2-yl)oxy)-6-oxohexanoyl)oxy)propan-2-yl) adipate (24) - Following **Method D,** the crude was then purified by flash chromatography (cyclohexane/ethyl acetate 90/10 to 50/50, v/v) to afford **24** as a mixture of diastereoisomers with 99% yield as a colorless oil. ^{1}H NMR ($CDCl_3$, 400 MHz): 7.29-7.39 (m, 5H), 5.03-5.17 (m, 1H), 5.11 (s, 2H), 4.95-5.03 (m, 1H), 4.14-4.21 (m, 1H), 3.99-4.06 (m, 1H), 3.55-3.70 (m, 2H), 2.27-2.42 (m, 8H), 2.27-2.42 (br s, 1H),1.60-1.72 (m, 8H), 1.23 (d, 3H, ^{3}J = 6.52 Hz), 1.21 (d, 3H, ^{3}J = 6.41 Hz). ^{13}C NMR ($CDCl_3$, 100 MHz): 173.3, 173.2, 173.2, 172.8, 136.1, 128.7, 128.7 128.4, 128.3, 128.3, 72.1, 68.3, 66.4, 66.2, 66.0, 34.3, 34.1, 34.0, 33.7, 24.5, 24.5, 24.4, 24.3, 16.6, 16.3. ASAP(+)-TOF-HRMS m/z for $C_{25}H_{36}O_9$ $[M+H]^+$: theoretical 481.2438, found 481.2434.

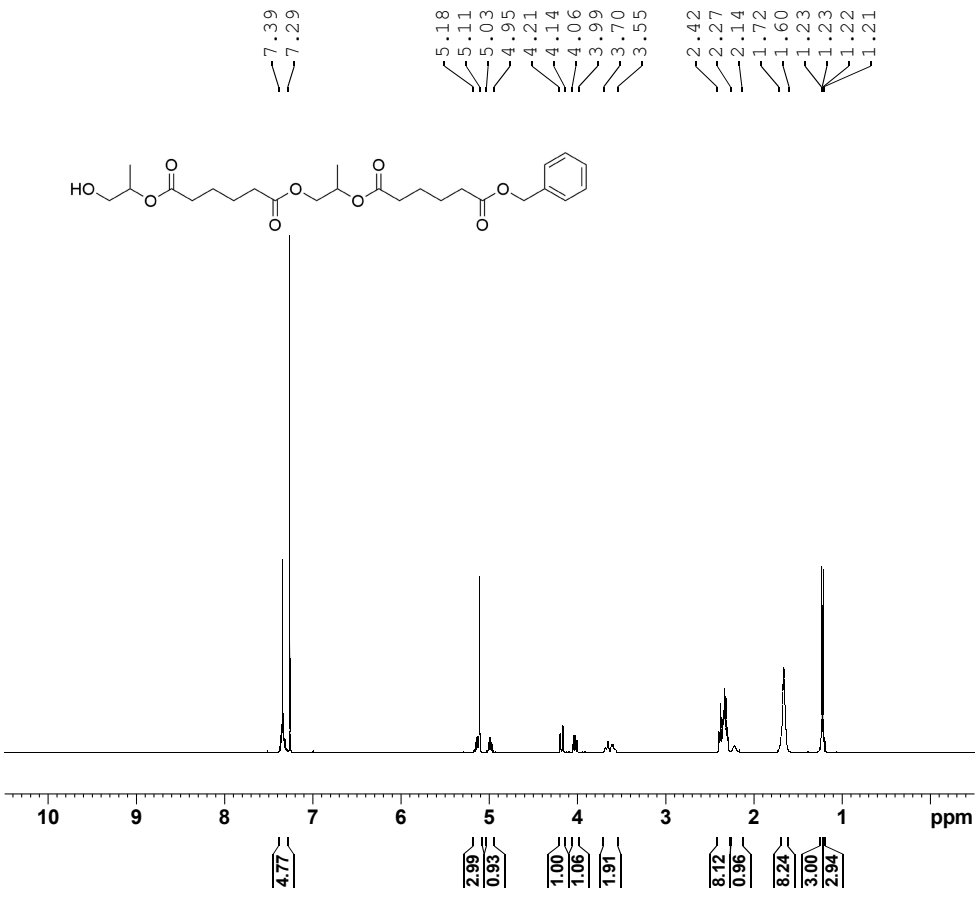

Figure A94- ^{1}H NMR (400 MHz, CDCl3) spectrum obtained for compound **24**.

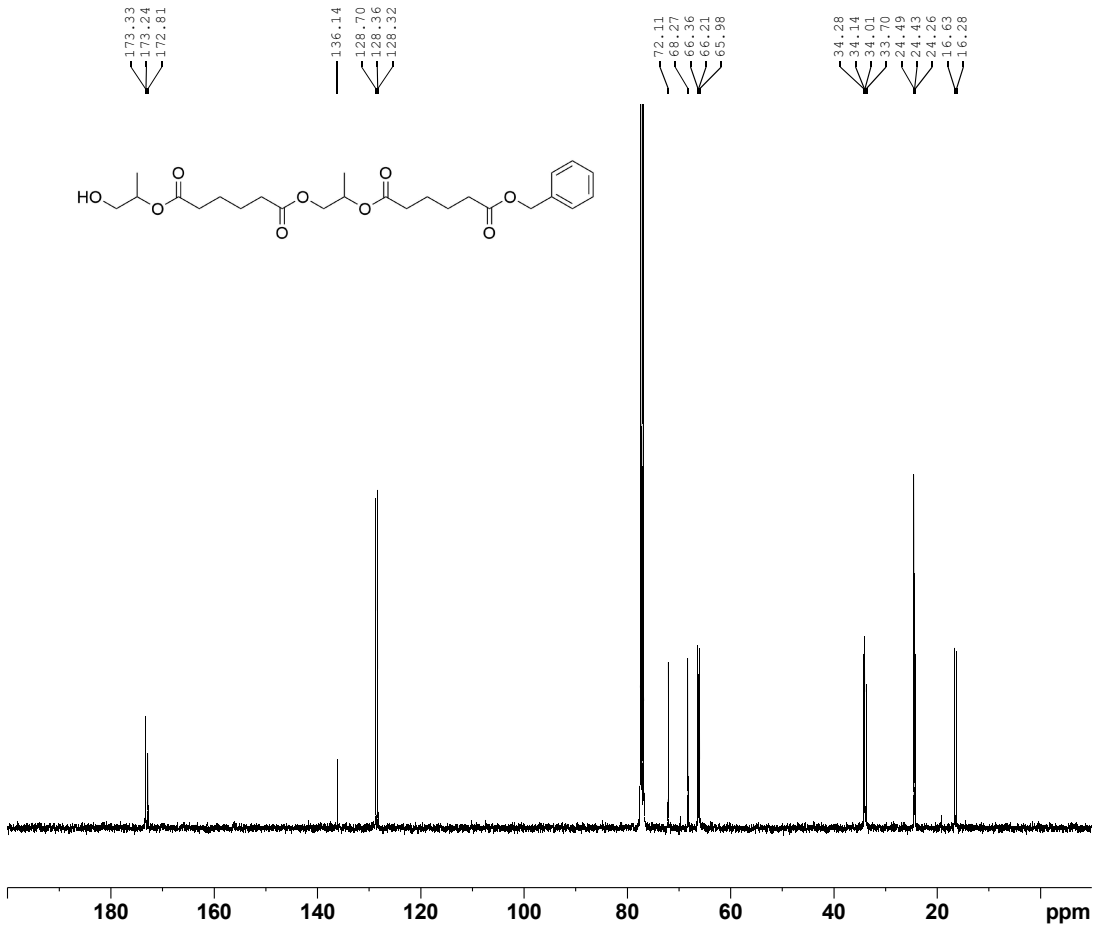

Figure A95- ^{13}C NMR (100 MHz, $CDCl_3$) spectrum obtained for compound **24**.

Elemental Composition Report **Page 1**

Single Mass Analysis
Tolerance = 5.0 PPM / DBE: min = -10.0, max = 1000.0
Element prediction: Off
Number of isotope peaks used for i-FIT = 4

Monoisotopic Mass, Even Electron Ions
69 formula(e) evaluated with 1 results within limits (up to 5 best isotopic matches for each mass)
Elements Used:
C: 0-100 H: 0-200 O: 1-10

DRC64 (SOLIDE) XEVO G2-XS QTOF 13-Nov-2023
20231113_KK_DRC64_01 189 (1.912) Cm (187:189) 1: TOF MS ASAP+
2.61e+006

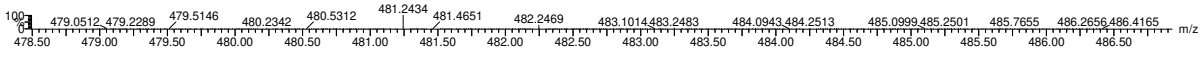

Minimum:				-10.0				
Maximum:		30.0	5.0	1000.0				
Mass	Calc. Mass	mDa	PPM	DBE	i-FIT	Norm	Conf(%)	Formula
481.2434	481.2438	-0.4	-0.8	7.5	1648.5	n/a	n/a	C25 H37 O9

Figure A96- ASAP(+)-TOF-HRMS elemental composition report obtained for compound **24**.

6-((1-((6-((1-hydroxypropan-2-yl)oxy)-6-oxohexanoyl)oxy)propan-2-yl)oxy)-6-oxohexanoic acid (lin[2PG+2AA]) - Following **Method E,** the crude was then purified by flash chromatography (cyclohexane/ethyl acetate 90/10 to 20/80, v/v) to obtain **lin[2PG+2AA]** as a mixture of diastereoisomers with 98% yield as a colorless oil. ^{1}H NMR ($CDCl_3$, 400 MHz): 5.09-5.19 (m, 1H), 4.94-5.03 (m, 1H), 4.15-4.22 (m, 1H), 3.89-4.13 (m, 2H), 3.55-2.74 (m, 1H), 2.26-2.41 (m, 8H), 1.58-1.72 (m, 8H), 1.16-1.27 (m, 6H). ^{13}C NMR ($CDCl_3$, 100 MHz): 177.9, 173.5, 173.3, 173.2, 172.8, 72.0, 69.6, 68.3, 66.2, 61.2, 65.8, 34.2, 34.1, 33.9, 33.7, 33.7, 24.4, 24.4, 24.3, 24.2, 24.2, 19.2, 16.6, 16.2. ASAP(-)-TOF-HRMS m/z for $C_{18}H_{30}O_9$ $[M-H]^-$: theoretical 389.1812, found 389.1807.

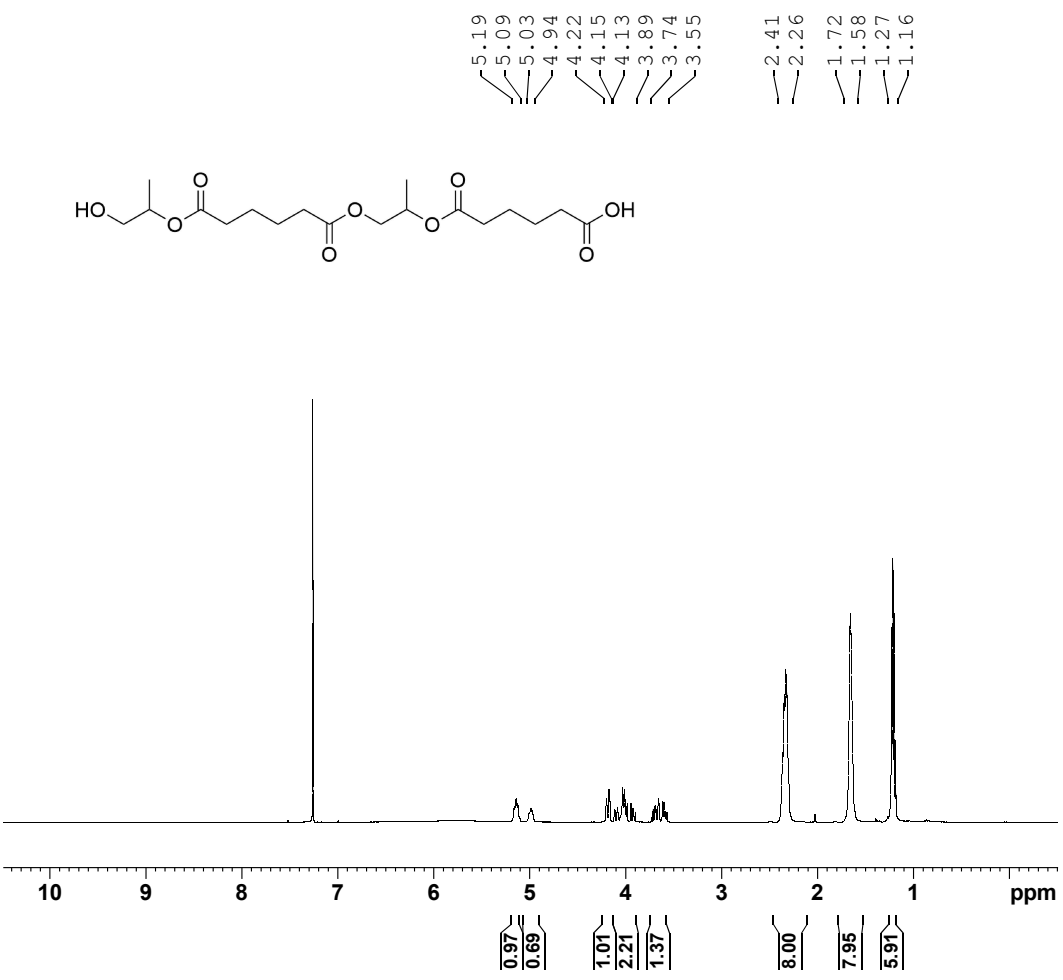

Figure A97- ^{1}H NMR (400 MHz, CDCl3) spectrum obtained for compound **lin[2PG+2AA]**.

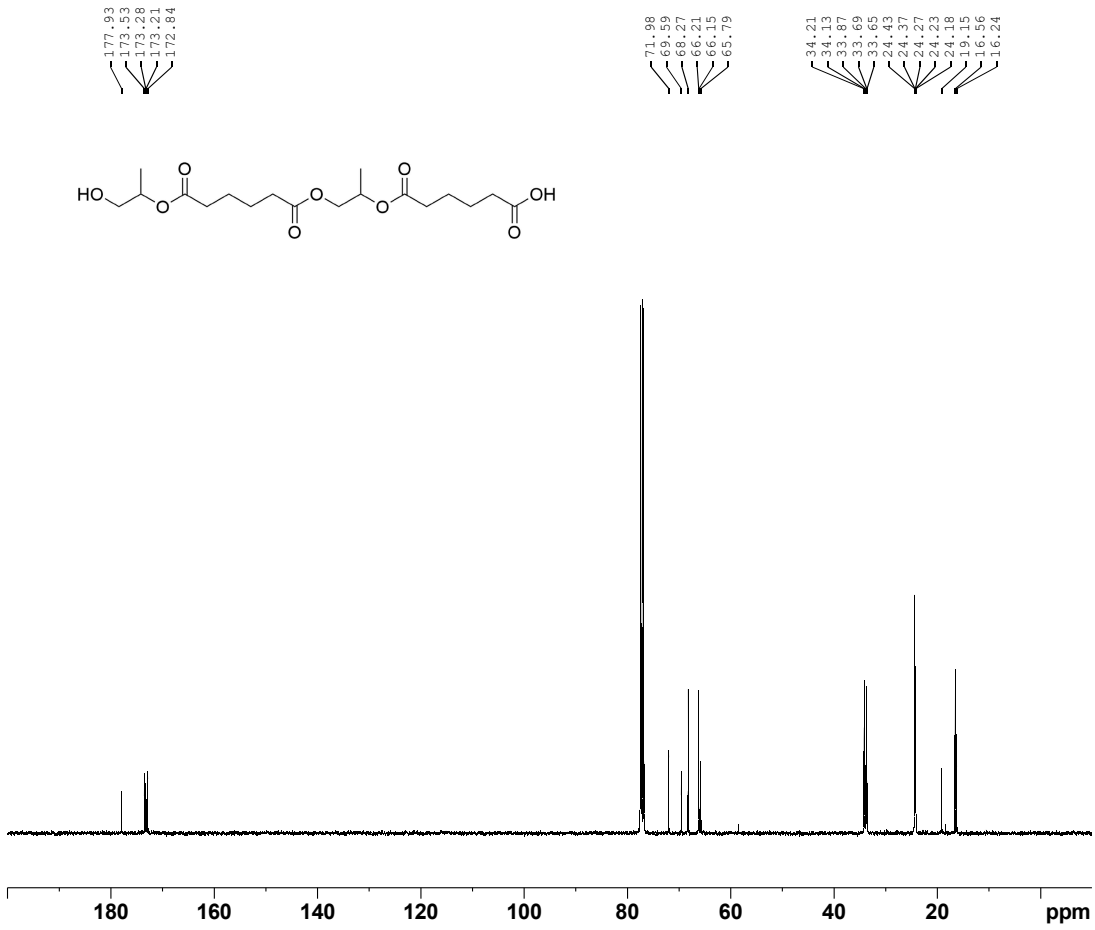

Figure A98- ^{13}C NMR (100 MHz, $CDCl_3$) spectrum obtained for compound **lin[2PG+2AA]**.

Elemental Composition Report **Page 1**

Single Mass Analysis
Tolerance = 5.0 PPM / DBE: min = -10.0, max = 1000.0
Element prediction: Off
Number of isotope peaks used for i-FIT = 4

Monoisotopic Mass, Odd and Even Electron Ions
65 formula(e) evaluated with 1 results within limits (up to 5 best isotopic matches for each mass)
Elements Used:
C: 0-100 H: 0-200 O: 0-10

DRC67 (SOLIDE)
20231106_KK_DRC67_01 265 (2.678) Cm (262:265)

XEVO G2-XS QTOF

06-Nov-2023
1: TOF MS ASAP-
3.63e+006

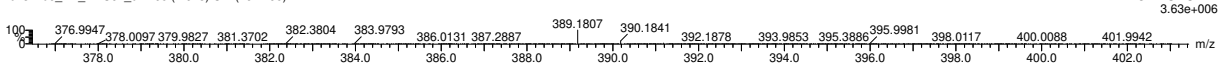

Minimum:				-10.0				
Maximum:		30.0	5.0	1000.0				
Mass	Calc. Mass	mDa	PPM	DBE	i-FIT	Norm	Conf(%)	Formula
389.1807	389.1812	-0.5	-1.3	4.5	1741.4	n/a	n/a	C18 H29 O9

Figure A99- ASAP(-)-TOF-HRMS elemental composition report obtained for compound **lin[2PG+2AA]**.

2,12-dimethyl-1,4,11,14-tetraoxacycloicosane-5,10,15,20-tetraone (c[2PG+2AA]) - Following **Method F,** the crude was then purified by flash chromatography (cyclohexane/ethyl acetate 90/10 to 70/30, v/v) to afford **c[2PG+2AA]** as a mixture of diastereoisomers with 73% yield as a yellowish oil. ^{1}H NMR ($CDCl_3$, 400 MHz): 5.14-5.27 (m, 2H), 4.21-4.37 (m, 2H), 3.86-4.04 (m, 2H), 2.26-2.38 (m, 8H), 1.58-1.75 (m, 8H), 1.17-1.28 (m, 6H). ^{13}C NMR ($CDCl_3$, 100 MHz): 173.0, 173.0, 172.9, 172.8, 172.7, 172.7, 68.3, 68.2, 68.1, 66.3, 66.2, 66.2, 66.1, 34.3, 34.2, 34.1, 34.1, 33.9, 33.9, 33.7, 33.7, 24.5, 24.4, 24.3, 24.3, 24.3, 24.2, 24.1, 16.5, 16.5. ASAP(+)-TOF-HRMS m/z for $C_{18}H_{28}O_8$ $[M+H]^+$: theoretical 373.1862, found 373.1877.

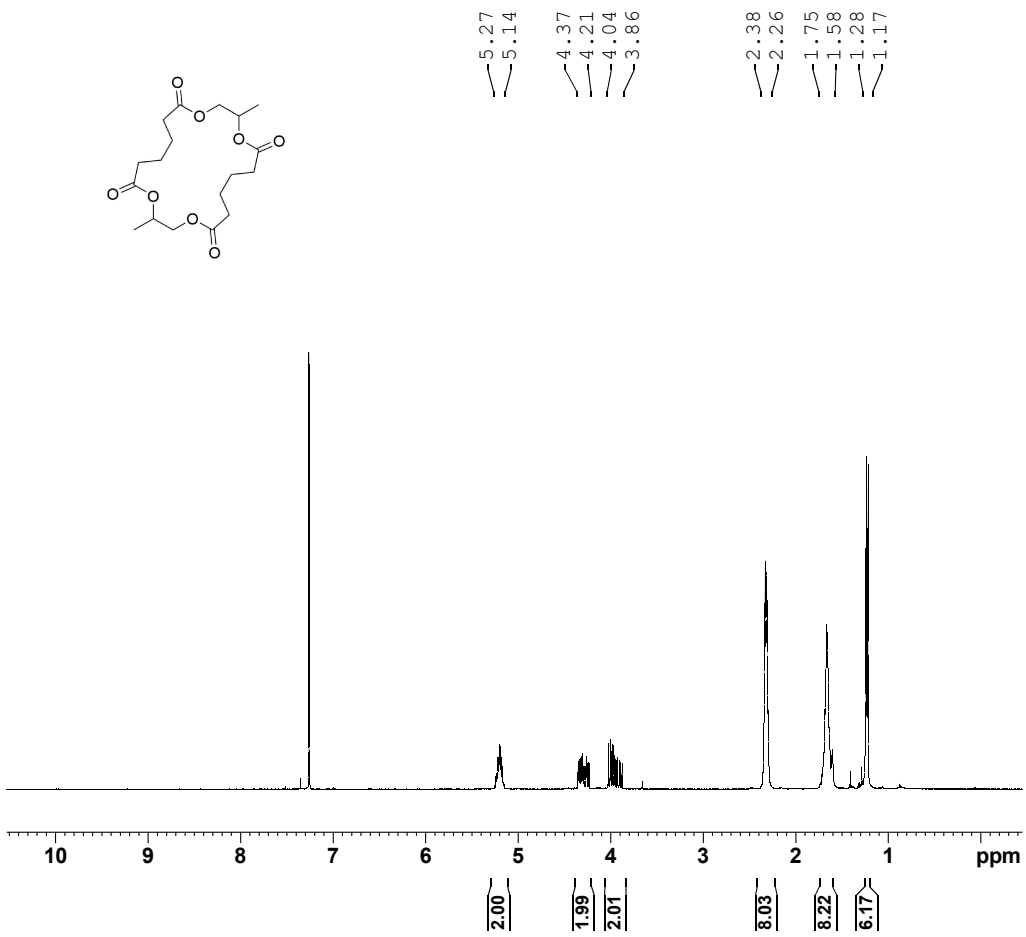

Figure A100- ^{1}H NMR (400 MHz, CDCl3) spectrum obtained for compound **c[2PG+2AA]**.

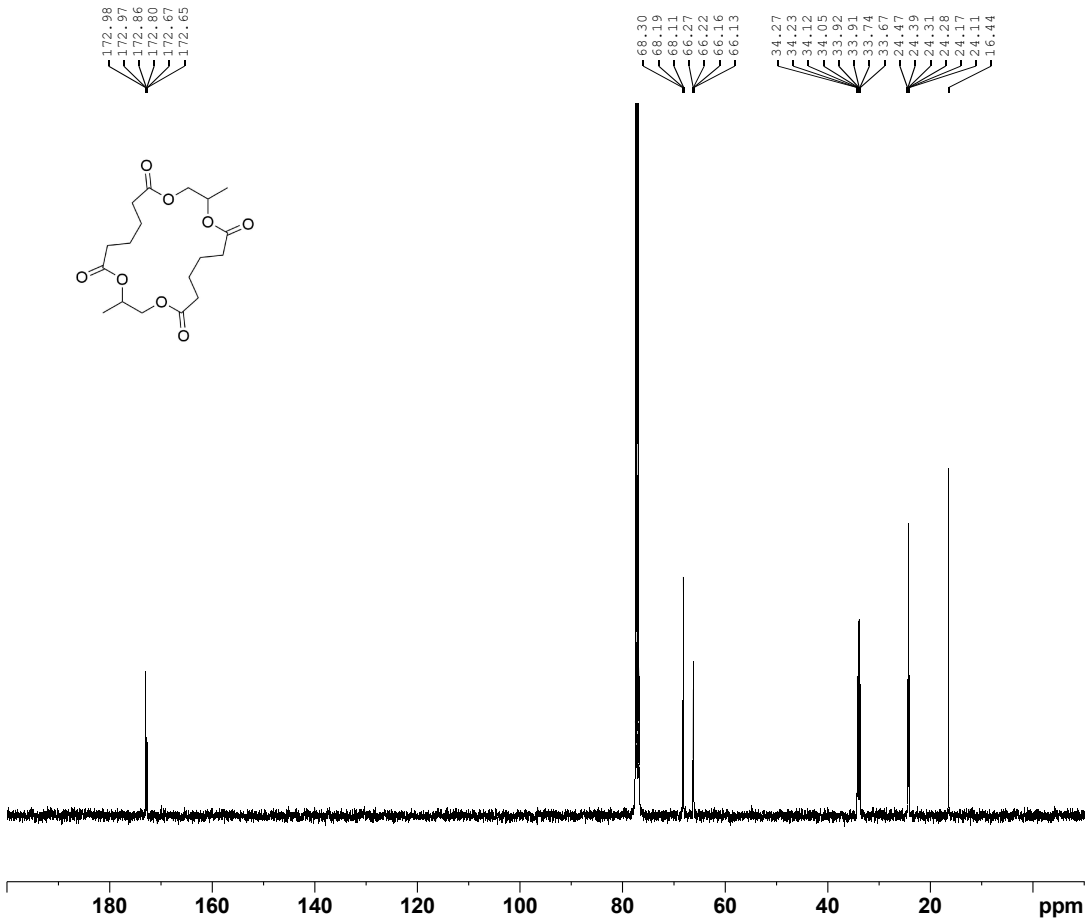

Figure A101- ^{13}C NMR (100 MHz, $CDCl_3$) spectrum obtained for compound **c[2PG+2AA]**.

Elemental Composition Report **Page 1**

Single Mass Analysis
Tolerance = 5.0 PPM / DBE: min = -10.0, max = 1000.0
Element prediction: Off
Number of isotope peaks used for i-FIT = 4

Monoisotopic Mass, Even Electron Ions
28 formula(e) evaluated with 1 results within limits (up to 5 best isotopic matches for each mass)
Elements Used:
C: 0-100 H: 0-200 O: 8-13

DRC79 (SOLIDE)
20231123_KK_DRC79_01 17 (0.197) Cm (14:18)

XEVO G2-XS QTOF

23-Nov-2023
1: TOF MS ASAP+
6.77e+007

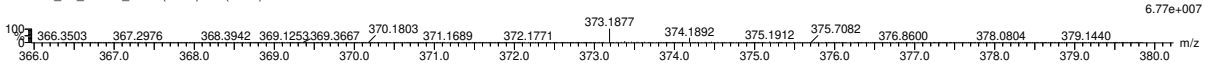

Minimum:				-10.0				
Maximum:		30.0	5.0	1000.0				
Mass	Calc. Mass	mDa	PPM	DBE	i-FIT	Norm	Conf(%)	Formula
373.1877	373.1862	1.5	4.0	4.5	2313.3	n/a	n/a	C18 H29 O8

Figure A102- ASAP(+)-TOF-HRMS elemental composition report obtained for compound **c[2PG+2AA]**.

2,12,22,32-tetramethyl-1,4,11,14,21,24,31,34-octaoxacyclotetracontan-5,10,15,20,25,30,35,40-octaone (c[4PG+4AA]) - Following **Method E,** the crude was then purified by flash chromatography (cyclohexane/ethyl acetate 90/10 to 70/30, v/v) to afford **c[4PG+4AA]** as a mixture of diastereoisomers with 15% yield as a colorless oil. ^{1}H NMR ($CDCl_3$, 400 MHz): 5.09-5.18 (m, 4H), 4.15-4.23 (m, 4H), 3.96-4.06 (m, 4H), 2.23-2.39 (m, 16H), 1.56-1.73 (m, 16H), 1.15-1.28 (m, 12H). ^{13}C NMR ($CDCl_3$, 100 MHz): 173.0, 173.0, 173.0, 173.0, 172.7, 172.7, 172.7, 172.7, 68.2, 68.2, 68.2, 68.2, 66.1, 66.1, 66.1, 66.1, 34.1, 34.1, 34.1, 34.1, 33.8, 33.8, 33.8, 33.8, 24.4, 24.4, 24.4, 24.4, 24.4, 24.4, 24.4, 24.4, 16.6, 16.6, 16.6, 16.6. ASAP(+)-TOF-HRMS m/z for $C_{36}H_{56}O_{16}$ $[M+H]^+$: theoretical 745.3647, found 745.3671. Aspect: Colourless oil.

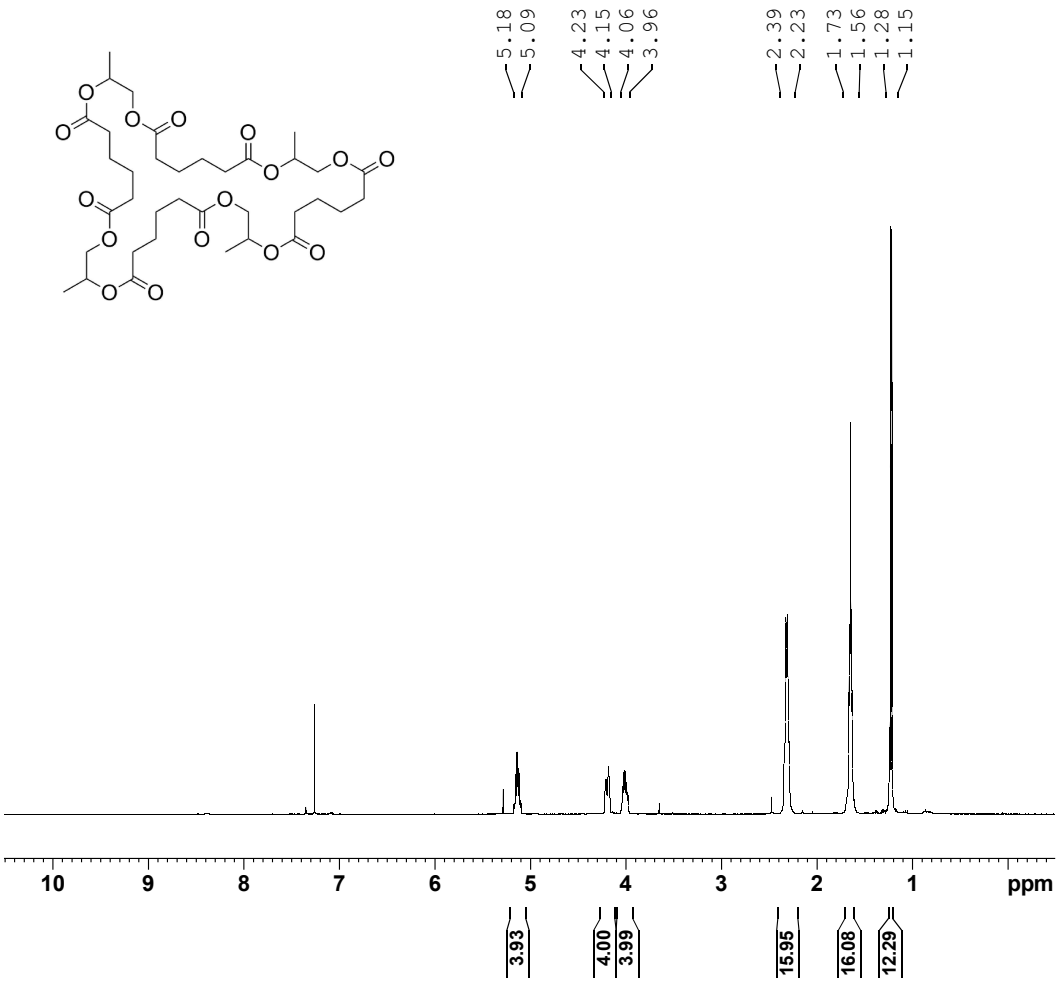

Figure A103- ^{1}H NMR (400 MHz, CDCl3) spectrum obtained for compound **c[4PG+4AA]**.

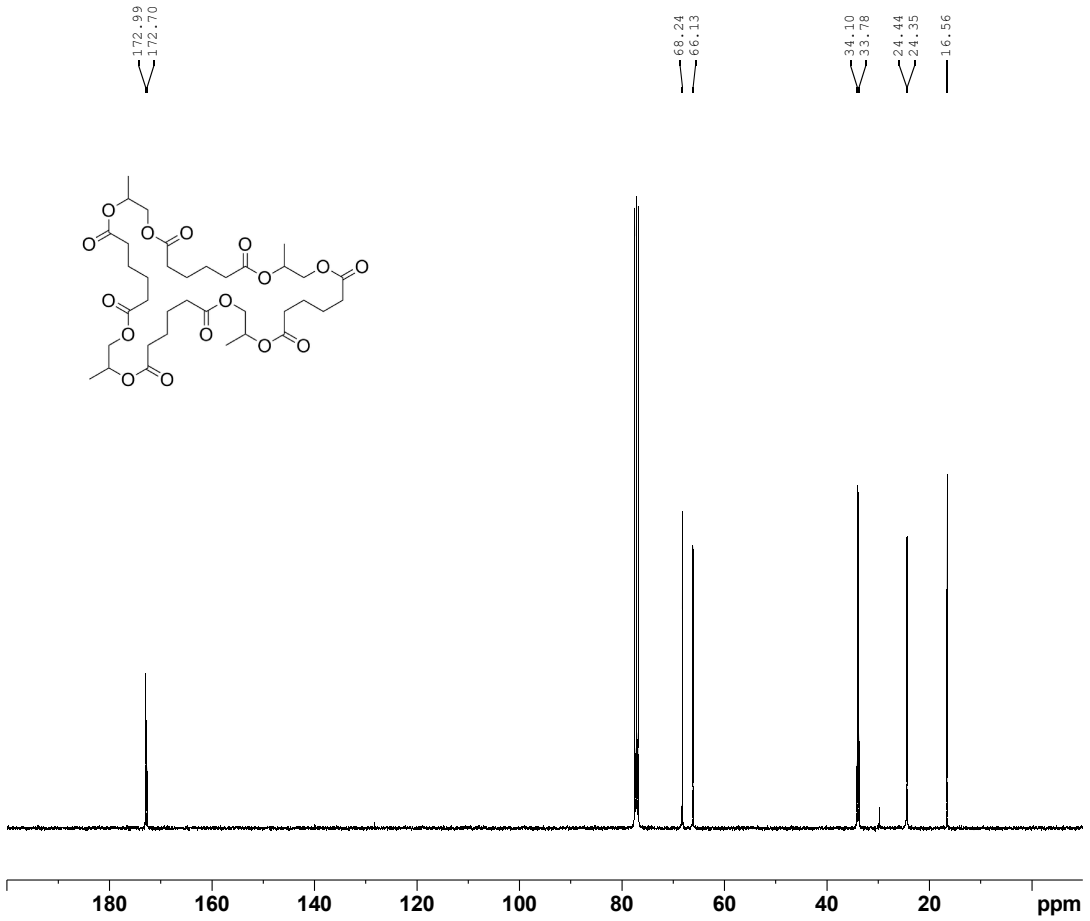

Figure A104- ^{13}C NMR (100 MHz, $CDCl_3$) spectrum obtained for compound **c[4PG+4AA]**.

Elemental Composition Report **Page 1**

Single Mass Analysis
Tolerance = 5.0 PPM / DBE: min = -10.0, max = 1000.0
Element prediction: Off
Number of isotope peaks used for i-FIT = 4

Monoisotopic Mass, Even Electron Ions
8 formula(e) evaluated with 1 results within limits (up to 5 best isotopic matches for each mass)
Elements Used:
C: 0-100 H: 0-200 O: 16-16

DRC79F3 (SOLIDE)
20231123_KK_DRC79F3_01 153 (1.558) Cm (145:153)

XEVO G2-XS QTOF

23-Nov-2023
1: TOF MS ASAP+
9.28e+007

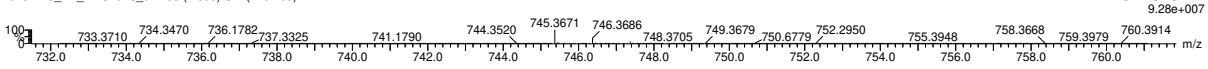

Minimum:				-10.0				
Maximum:		30.0	5.0	1000.0				
Mass	Calc. Mass	mDa	PPM	DBE	i-FIT	Norm	Conf(%)	Formula
745.3671	745.3647	2.4	3.2	8.5	2155.8	n/a	n/a	C36 H57 O16

Figure A105- ASAP(+)-TOF-HRMS elemental composition report obtained for compound **c[4PG+4AA]**.

MSMS identification of oligoesters in migration extracts of samples 1, 2 or 3

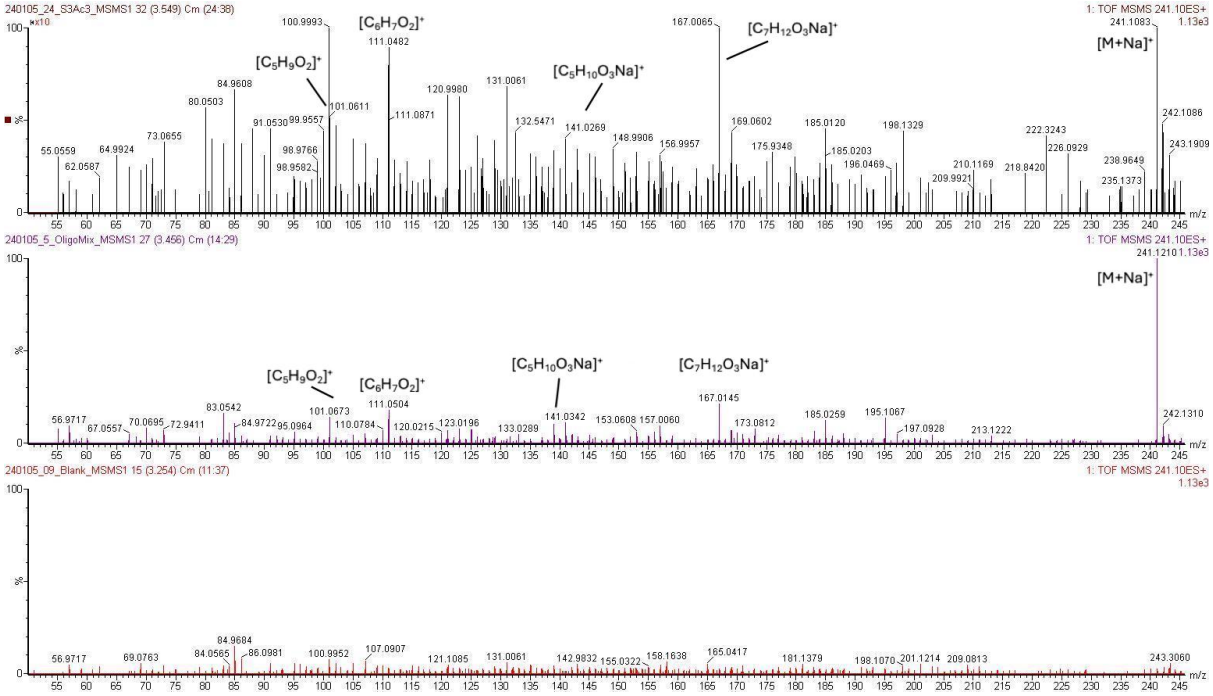

Figure A106- Comparison of the MS/HRMS spectra of *m/z* 241.1046 ion [**lin(BD+AA**) + Na]$^+$ in a S3 migration extract in simulant B (top), a 10 ng kg^{-1} **lin(BD+AA)** solution (middle) and a methanol blank (bottom).

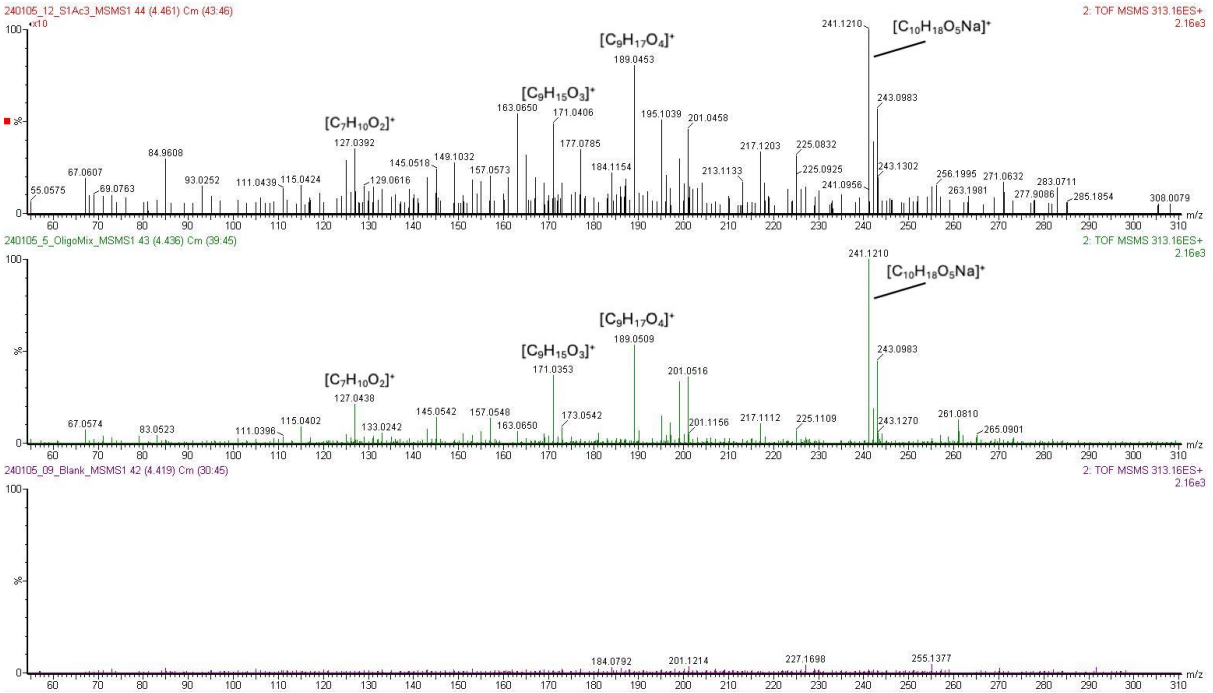

Figure A107- Comparison of the MS/HRMS spectra of m/z 313.1622 ion [**lin(2BD+AA)** + Na]+ in a S1 migration extract in simulant B (top), a 10 ng kg-1 **lin(2BD+AA)** solution (middle) and a methanol blank (bottom). $[M + Na]^+$ ion was too intense and was not fit into the range for ease of visualization.

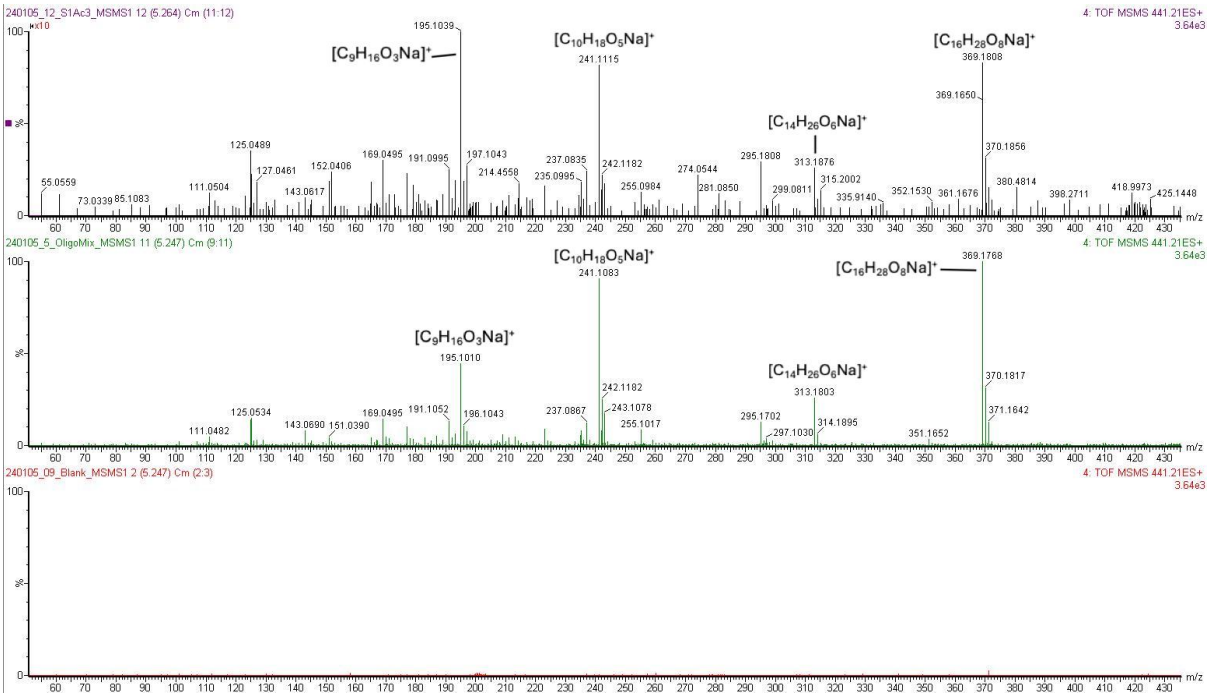

Figure A108- Comparison of the MS/HRMS spectra of m/z 441.2095 ion [**lin(2BD+2AA)** + Na]+ in a S1 migration extract in simulant B (top), a 10 ng kg-1 **lin(2BD+2AA)** solution (middle) and a methanol blank (bottom). $[M + Na]^+$ ion was too intense and was not fit into the range for ease of visualization.

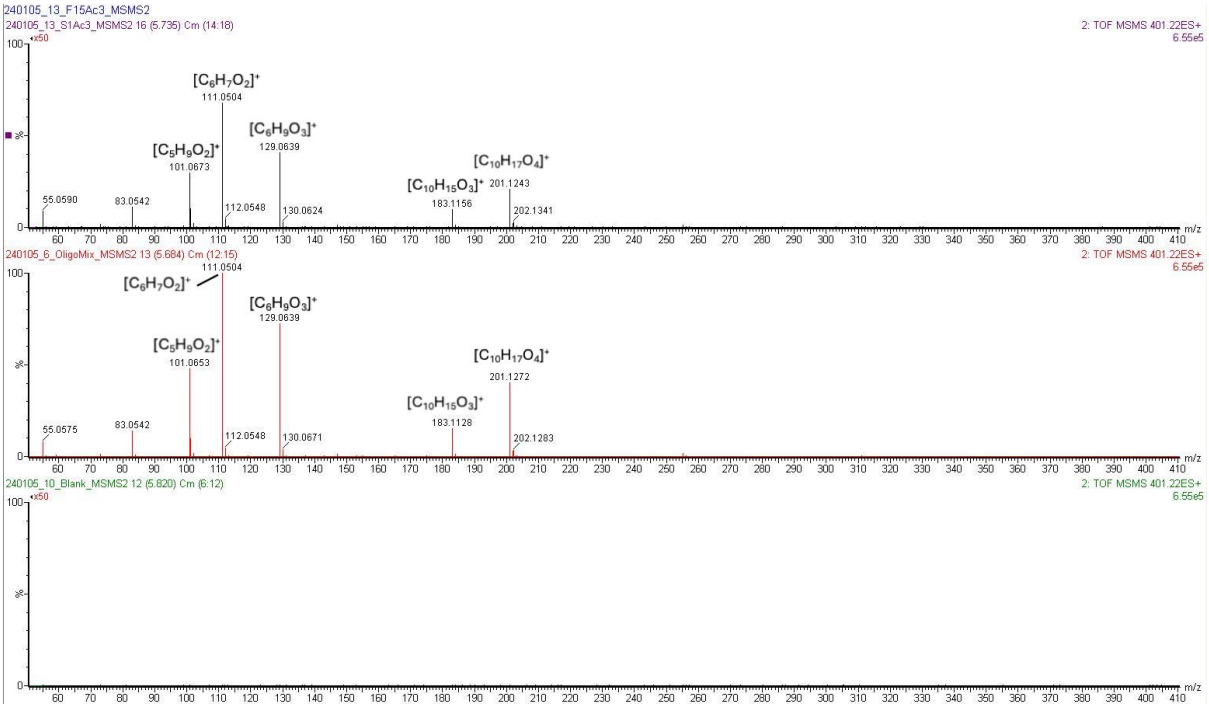

Figure A109- Comparison of the MS/HRMS spectra of *m/z* 401.2170 ion [**c(2BD+2AA)**+H]$^+$ in a S1 migration extract in simulant B (top), a 10 ng kg^{-1} **c(2BD+2AA)** solution (middle) and a methanol blank (bottom).

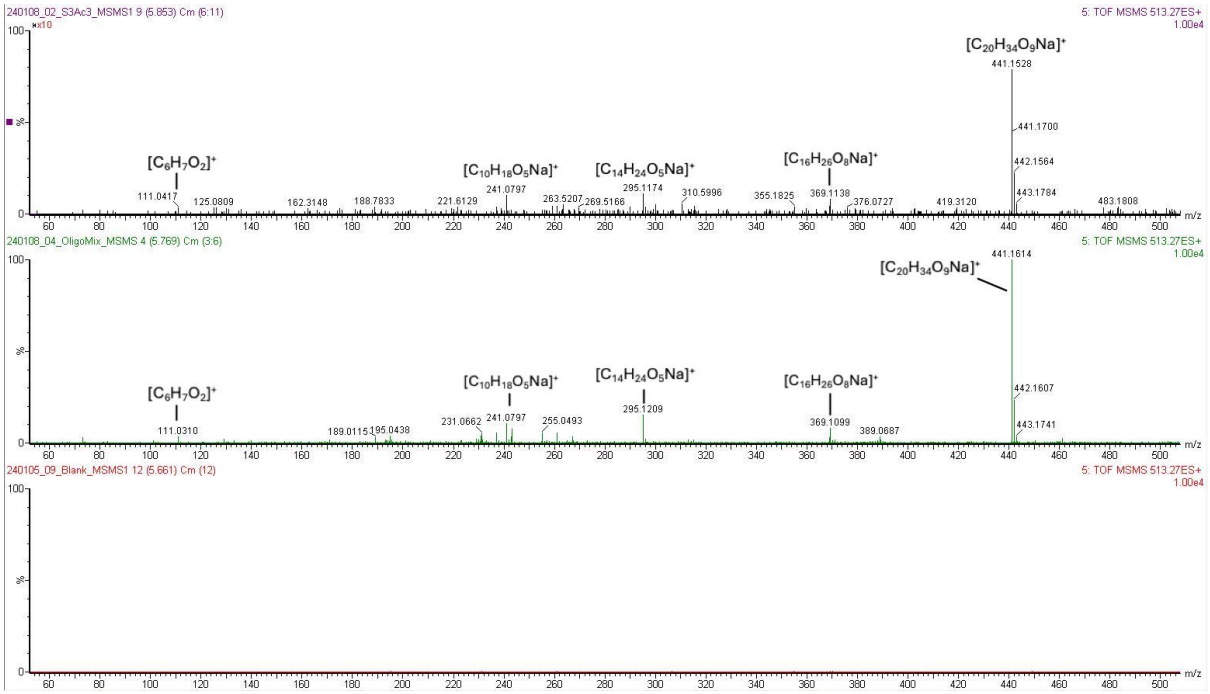

Figure A110- Comparison of the MS/HRMS spectra of *m/z* 513.2670 ion [**lin(3BD+2AA)**+Na]+ in a S3 migration extract in simulant B (top), a 10 ng kg-1 **lin(3BD+2AA)** solution (middle) and a methanol blank (bottom). [M + Na]$^+$ ion was too intense and was not fit into the range for ease of visualization.

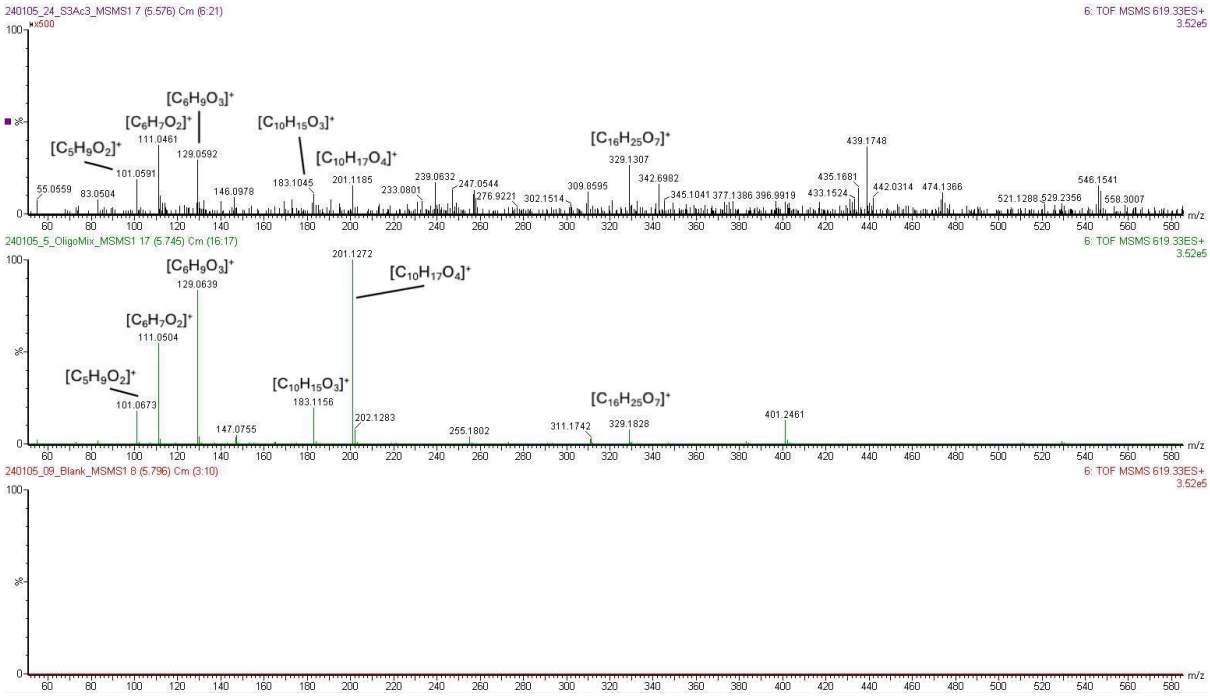

Figure A111- Comparison of the MS/HRMS spectra of *m/z* 619.3324 ion [**lin(3BD+3AA)**+H]+ in a S3 migration extract in simulant B (top), a 10 ng kg-1

lin(3BD+3AA) solution (middle) and a methanol blank (bottom). $[M + H]^+$ ion was too intense and was not fit into the range for ease of visualization.

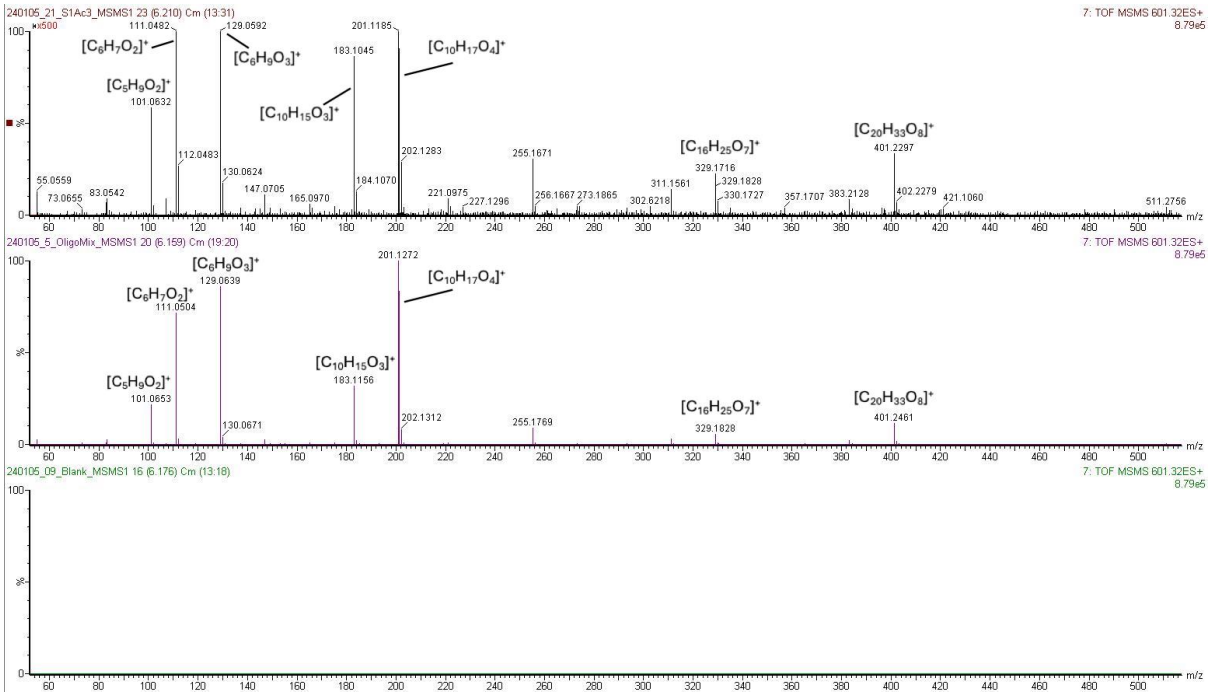

Figure A112- Comparison of the MS/HRMS spectra of *m/z* 601.3219 ion [**c(3BD+3AA)**+H]+ in a S1 migration extract in simulant B (top), a 10 ng kg-1 **c(3BD+3AA)** solution (middle) and a methanol blank (bottom). $[M + H]^+$ ion was too intense and was not fit into the range for ease of visualization.

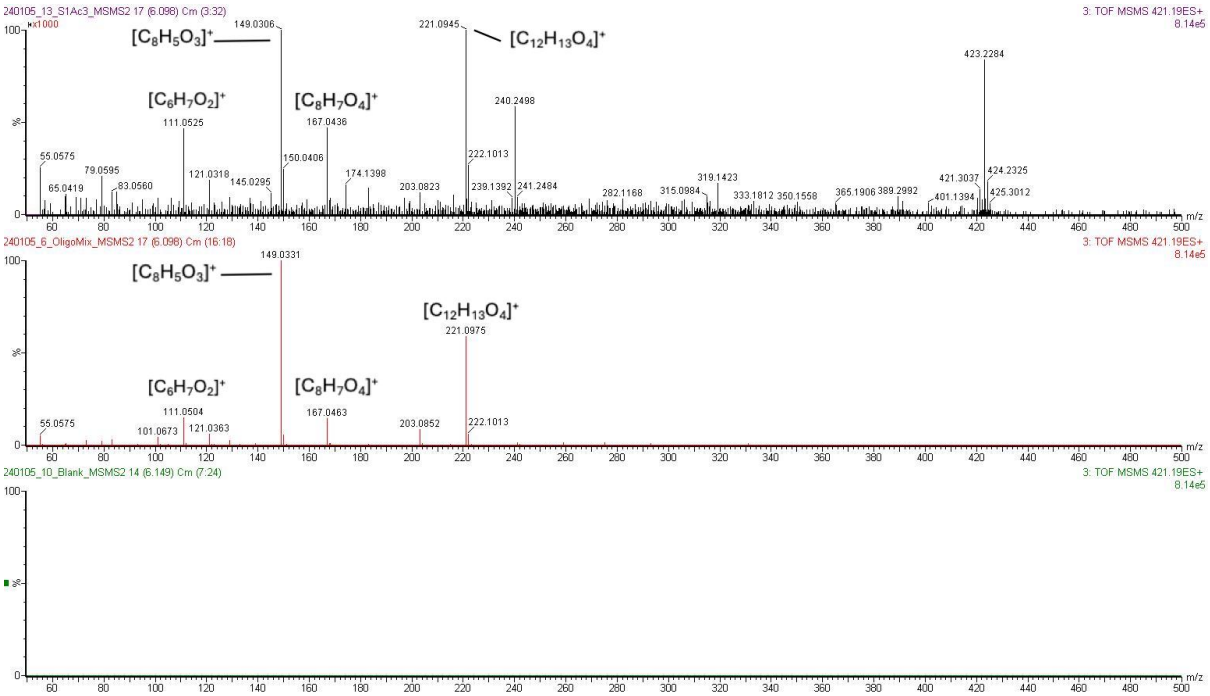

Figure A113- Comparison of the MS/HRMS spectra of *m/z* 421.1857 ion [**c(2BD+AA+iPA)**+H]$^+$ in a S1 migration extract in simulant B (top), a 10 ng kg^{-1} **c(2BD+AA+iPA)** solution (middle) and a methanol blank (bottom).

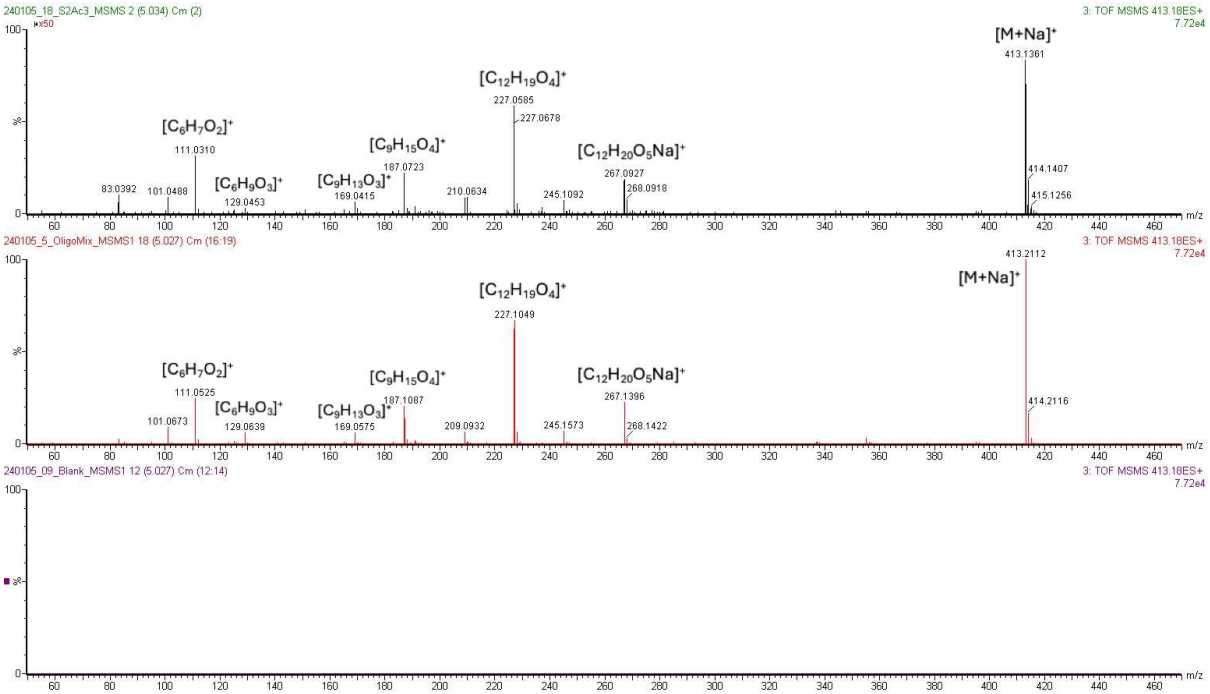

Figure A114- Comparison of the MS/HRMS spectra of *m/z* 413.1782 ion [**lin(2PG+2AA)**+Na]$^+$ in a S2 migration extract in simulant B (top), a 10 ng kg^{-1} **lin(2PG+2AA)** solution (middle) and a methanol blank (bottom).

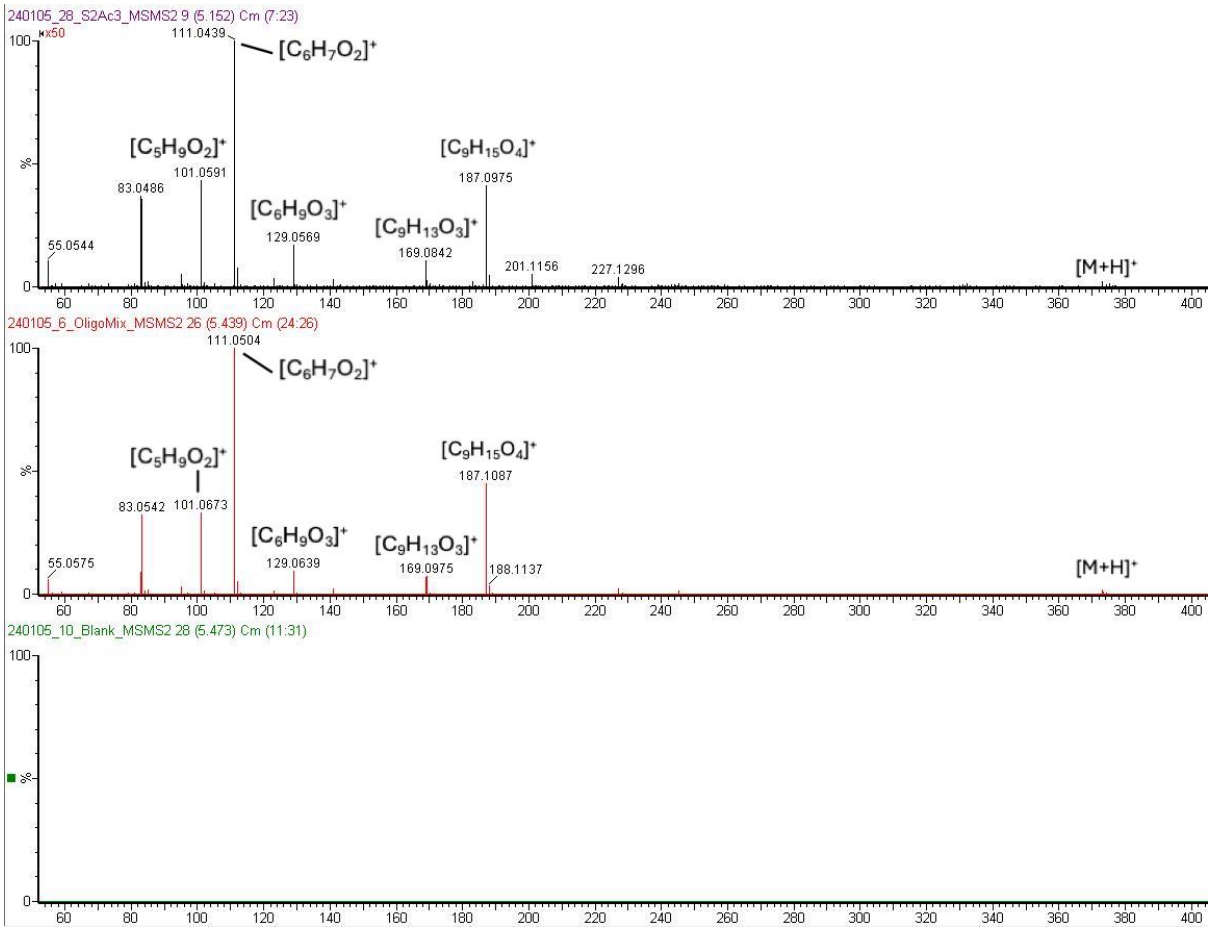

Figure A115- Comparison of the MS/HRMS spectra of *m/z* 373.1857 ion [**c(2PG+2AA)**+H]$^+$ in a S2 migration extract in simulant B (top), a 10 ng kg^{-1} **c(2PG+2AA)** solution (middle) and a methanol blank (bottom).

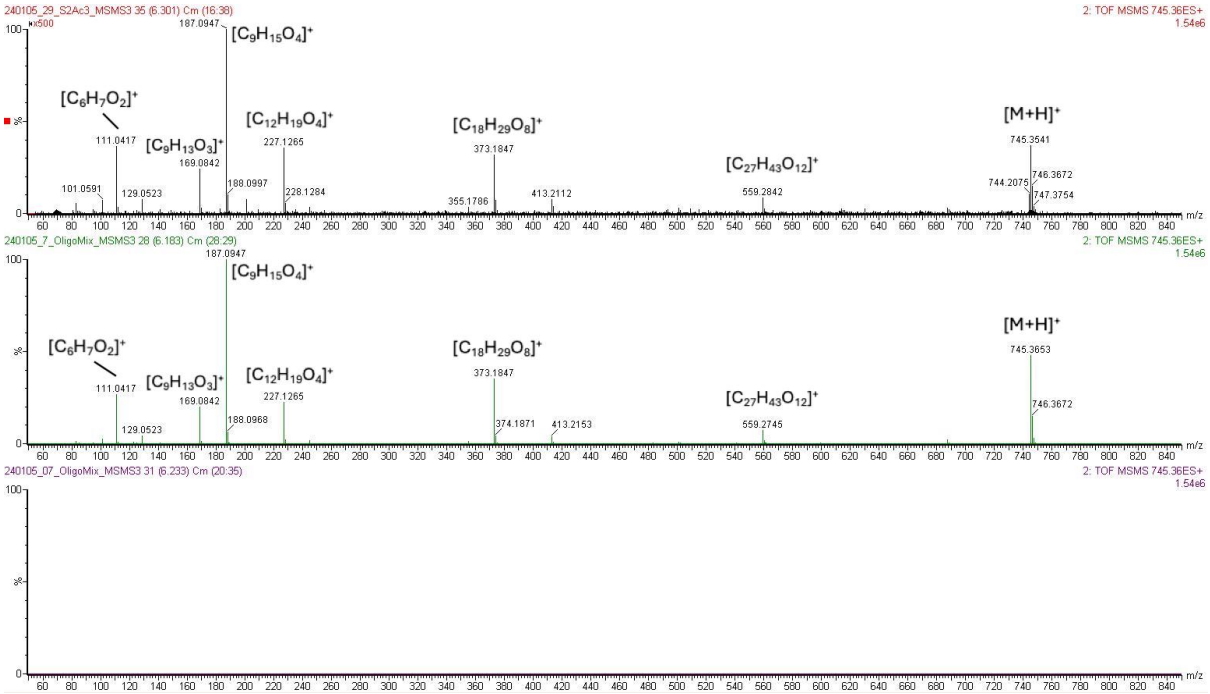

Figure A116- Comparison of the MS/HRMS spectra of *m/z* 745.3641 ion [**c(4PG+4AA)**+H]$^+$ in a S2 migration extract in simulant B (top), a 10 ng kg^{-1} **c(4PG+4AA)** solution (middle) and a methanol blank (bottom).